Ensemble modeling of lake evaporation under climate change

A thesis presented to the School of Health and Science,

Dundalk Institute of Technology in fulfilment of the requirements of the

degree of Doctor of Philosophy

Ruth Sofia La Fuente Pillco

Academic Supervisors: Prof. Eleanor Jennings[1]

Dr. Iestyn Woolway[2]

[1]Dundalk Institute of Technology, Dundalk, Co. Louth, Ireland
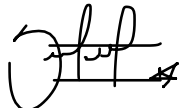
[2]Bangor University, Menai Bridge, Anglesey, Wales

February 2024

Declaration

We, the undersigned declare that this thesis entitled "Ensemble modeling of lake evaporation under climate change" is entirely the author's own work and has not been taken from the work of others, except as cited and acknowledged within the text.

The thesis has been prepared according to the regulations of Dundalk Institute of Technology and has not been submitted in whole or in part for an award in this or any other institution.

Author Name: Ruth Sofia La Fuente Pillco

Author Signature:

Date: 19/02/2024

Supervisor Name: Eleanor Jennings

Supervisor Signature:

Date: 19/02/2024

Funding

Dedicated to my beloved parents, Ruth and Edgar

Acknowledgements

First and foremost, I would like to express my sincere gratitude to my PhD supervisors, Prof. Eleanor Jennings and Dr. Iestyn Woolway, for their guidance, support, and patience from the start to the end of this PhD journey. Thank you both for your dedication and for always finding the time despite the millions of responsibilities that you have. I truly enjoyed our discussions, and I appreciate that you always encouraged me to pursue what was best for my career. Thank you for sharing your invaluable knowledge and for consistently offering support and guidance. I could not have asked for better supervisors.

My heartfelt thanks to my family, especially my parents, Ruth and Edgar, and my brothers, Luis, Marcelo and Gonzalo, for their unconditional love and constant support in my life. I am so grateful and proud to have the most amazing parents and brothers that one could ask. Thank you so much for being who you are and for being an essential part of my life. A very special thanks to my partner Jonas, for his love, care, infinite patience, and support, thanks for being there by my side every step of the way. I also want to thank to my mother-in-law Nancy for her love and support in this journey.

A big shout out to Madjdouline, Shells, Ali, Noe and Job for their unconditional friendship, support, laughs, and silly moments. Thank you for all the great memories we built together in Ireland and in the distance. You rock!

I also would like to thank the GLEON network for granting me the *Lake Expedition 2020* fellowship, which allowed me to participate in a three-year project in team science with a multi-disciplinary team of awesome people. Heather, Jenna, Rosie, MJ, Maartje, Abdou, Elias, Erick, Jem, Paul and Kathie, I enjoyed working with you on this project and learned so much from each one of you. My participation in Lake Expedition 2020 certainly enriched my research, teamwork, and leadership skills, contributing to my development as a scientist. Thank you Lake Expedition 2020 team.

Ensemble modeling of lake evaporation under climate change

Abstract

Approximately 87% of the freshwater on Earth resides in lakes, making them a critical resource for freshwater. Due to the open-water nature of lakes, evaporation is typically the main water loss in most lakes. Therefore, understanding lake evaporation responses to climate change is of paramount importance for the development of mitigation and adaptation strategies. In spite of the complexity of evaporation as a physical process, many studies simulate and quantify lake evaporation using single mechanistic models. The primary objective of this dissertation is to investigate lake evaporation responses to climate change using an ensemble of lake-climate models (i.e., different lake models driven by various climate models) under historic and future climate change scenarios. The dissertation consists of the analyses of local (i.e., lake-specific), regional (i.e., continental), and global lake evaporation simulations over the 20th and 21st centuries (1901-2099) under historic and future scenarios of climate change from the Inter-Sectoral Impact Model Intercomparison Project (ISIMIP) round 2b. Firstly, an evaluation of the differences in lake evaporation estimates among the model ensemble during the historic period was undertaken for a single lake with high socio-economic and political relevance. Furthermore, future lake evaporation projections for this lake are provided by the end of the 21st century. Secondly, the analysis was upscaled to 23 lakes located in Europe, where the association between lake morphometry and evaporation was investigated. Furthermore, historic and future changes in evaporation are reported for these European lakes, along with their implications for water availability. Thirdly, global lake evaporation simulations for 13K 'representative lakes' are assessed for historic and future scenarios of climate change. Spatial patterns among the lake-climate model ensemble are evaluated for distinct lake thermal regions. In addition, the associated uncertainties in future evaporation projections and the changes by the end of the century are calculated. Overall, this dissertation highlights the importance of using a multi-model approach for the prediction of lake evaporation responses to global warming and the need to inform the uncertainties associated with evaporation estimation.

Table of contents

List of figures

List of tables

Notation

Q_{tot}	Heat content of a lake
A_{lake}	Surface area of the lake
S_w	Shortwave radiation
L_w	Longwave radiation
L_{wo}	Outgoing longwave radiation
Q_e	Latent heat flux
Q_h	Sensible heat flux
Q_a	Advected energy
Q_s	Sediment flux
E	Lake evaporation
ρ_o	Density of surface water
L_v	Latent heat of vaporization
T_0	Lake surface water temperature
ρ_z	Density of the overlying air
p	Surface air pressure
R_a	Gas constant for moist air
u_z	Wind speed
z_u	Height at which wind speed was measured
z_t	Height at which temperature was measured
T_z	Air temperature
z_t	Height at which air temperature was measured
q_0	Specific humidity at saturation pressure
λ	Ratio of the molecular weights for dry and moist air
e_{sat}	Saturated vapour pressure
q_z	Specific humidity of the air
z_q	Height at which specific humidity was measured
R_h	Relative humidity
e_s	Saturated vapour pressure from the air
C_{e_z}	Transfer coefficient for height z_q

ε	Emissivity of water
σ	Stefan-Boltzmann constant
P	Precipitation

Chapter 1   Introduction

1.1   The importance of lakes

Currently, there are more than 100 million lakes worldwide (Verpoorter et al. 2014), holding a large portion of the surface freshwater on Earth (Sterner et al. 2020; Wetzel 2001). Lakes support a global heritage of biodiversity (Schallenberg et al. 2013) and provide key ecosystem services that range from drinking water and food to transportation and recreation (Woolway et al. 2020; Havens and Jeppesen 2018; Steinman et al. 2017; Wurtsbaugh et al. 2017; Allan et al. 2015). Because of the various benefits that lakes provide, they are included in the United Nations' Sustainable Development Goals committed to water resources (Goal #6) and the impacts of climate change (Goal #13) (United Nations 2016). In addition, lakes are considered as key indicators of local and regional changes in their watershed, making them crucial to detecting Earth's responses to climate change (Adrian et al. 2009). Accordingly, the Global Climate Observing System (GCOS) has recognised a number of lake variables, including lake temperature, water level and extent, lake ice cover and lake colour, as Essential Climate Variables (ECV's). Therefore, lake research has an important value as an essential element of the United Nations Framework Convention on Climate Change (UNFCCC) and the Intergovernmental Panel on Climate Change (IPCC) (Woolway et al. 2020).

1.2   Lake responses to climate change

Lakes are considered to be sentinels of climate change as they are distributed across a wide range of geographic and climatic regions allowing them to capture different aspects of climate variability. Due to their unique ecosystems, lakes are very sensitive to changes in the climate (Adrian et al. 2009). Some of the most prevalent and concerning physical consequences of climate change on lakes are increasing surface water temperature (O'Reilly et al. 2015; Schneider and Hook 2010), ice cover loss (Sharma et al. 2021; Sharma et al. 2019), changes in evaporation and water budgets (Zhao et al. 2022; Kraemer et al. 2020; Rodell et al. 2018; Wang et al. 2018), lake mixing regimes, stratification (Woolway et al. 2021; Shatwell et al. 2019; Woolway and Merchant 2019; Kraemer et al.

2015), as well as chemical and biological properties (Jennings et al. 2009; Mooij et al. 2005).

Increasing lake surface water temperature is one of the most direct responses of lakes to climate change. Observations from a set of 235 lakes distributed globally suggest that lakes worldwide have warmed at rate of 0.34°C decade^{-1} from 1985 to 2009 (O'Reilly et al. 2015). However, these warming rates are highly variable within regions, with both warming and cooling trends detected at high latitudes (Woolway et al. 2018; O'Reilly et al. 2015). Notably, lakes located in regions with cold winters (e.g. Laurentian Great Lakes and Northern Europe) are warming more rapidly than lakes in regions with warm winters (O'Reilly et al. 2015). These warming trends in lake water temperature, can be explained by an earlier onset of stratification, more prolonged periods of summer stratification (Woolway et al. 2021), reduced ice cover (Sharma et al. 2021), reduced snowmelt (Christianson and Johnson 2020; Sadro et al. 2019), and reduced snowfall (Solomon et al. 2007) that can result in more available energy to warm surface waters or increase evaporation rates (Schmid and Köster 2016) (Fig. 1.1).
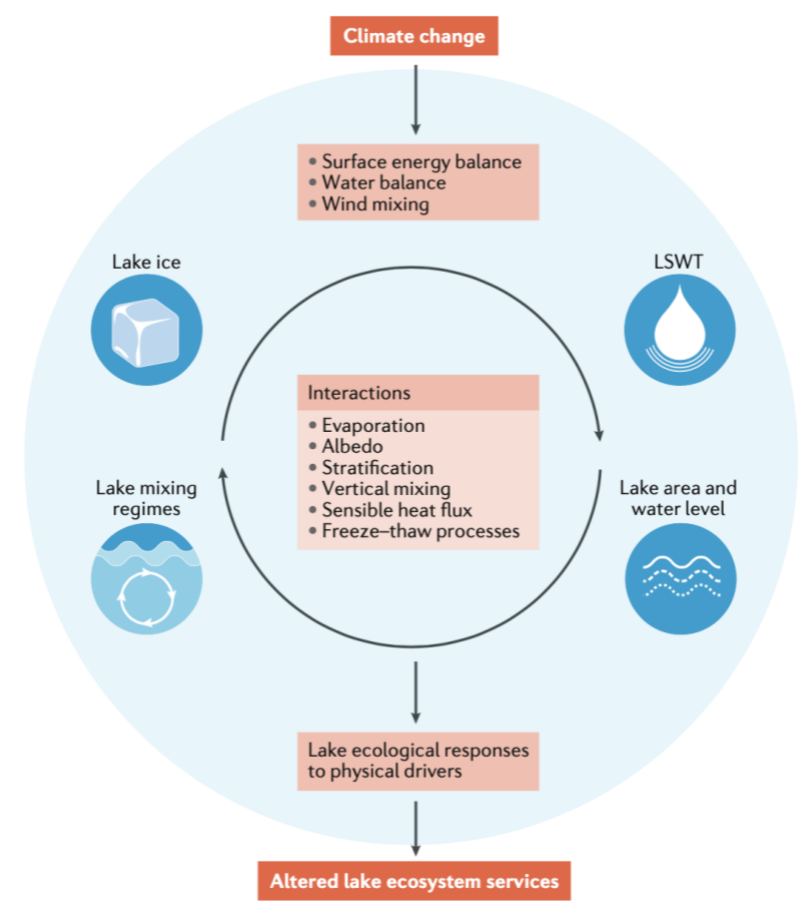
Figure 1.1 Lake responses to climate change. Source: Woolway et al. (2020)

Lakes are experiencing earlier ice break-up, later ice freeze-up and shorter ice duration (Sharma et al. 2021; Woolway et al. 2020; Sharma et al. 2019; Magnuson et al. 2000). Importantly, if greenhouse gas emissions continue to be emitted at the current levels, it has been estimated that thousands of lakes in the Northern Hemisphere will permanently lose ice cover (Sharma et al. 2021), with the number of lakes that experience intermittent ice cover projected to rise from ~15,000 lakes to up to 90,000 lakes by the end of the century (Sharma et al. 2019). However, changes in ice phenology are not linear as some lakes experience faster rates of warming not only in response to climate change variability but also in response to phase shifts of large-scale climate oscillations such as El Niño Southern Oscillation (ENSO), North Atlantic Oscillation (NAO) and the Pacific Decadal Oscillation (PDO) (Van Cleave et al. 2014; Bai et al. 2012).

An upward trend in lake evaporation has been reported both locally and globally (Zhao et al. 2022; Friedrich et al. 2018). Long-term evaporation estimates from a set of 1.4 million lakes have indicated an increase of 3.12 km^3 year^{-1}, with most of this trend

3

being attributed to the increase in evaporation rates (Zhao et al. 2022). Future projections indicate a further rise in evaporation in many regions within a warming world (Zhao et al. 2023; Althoff et al. 2020; Xiao et al. 2018; Helfer et al. 2012). By the end of this century, annual lake evaporation is projected to increase by approximately 16% (Wang et al. 2018). The largest increases in annual evaporation were found at low latitudes, where evaporation rates are already high (Althoff et al. 2020; Zhou et al. 2021; Wang et al. 2018; Helfer et al. 2012), but also in lakes that will transition to becoming ice-free, allowing the potential for evaporation to occur year-round (Li et al. 2022; Woolway et al. 2020; Sharma et al. 2019). Importantly, lake evaporation is projected to show a rapid increase in regions with drying hydroclimate, which will amplify evaporation increase by enlarging the surface vapor pressure deficit (Althoff et al. 2020).

Changes in lake water storage can be attributed to climate change when variations occur coherently across many lakes within extensive geographic regions, ideally absent of other anthropogenic influences (Zhang et al. 2019; Watras et al. 2014). A good example is the Tibetan Plateau, where changes on water storage have been attributed to long-term changes in glacier melt (Stuart-Smith et al. 2021; Shugar et al. 2020), and in precipitation and runoff, in part as a result of climate change, with some exceptions (decreasing water storage) detected in some lakes due to local factors (Zhang et al. 2019; Liao et al. 2013; Zhu et al. 2010). Although the global hydrological cycle is affected by a warming climate (Solomon et al. 2007), the magnitude of variations in water storage attributed to climate change remains uncertain, mostly because human action plays a key role in lake water withdrawal (Wurtsbaugh et al. 2017; Sade et al. 2016; Micklin 2010). However, even in lakes that are not directly influenced by human activity, the effects of climate change can be masked by climate variability and atmospheric teleconnections patterns (Lei et al. 2019; Plewa et al. 2019). In summary, lake water storage projections are limited because of the lack of reliable long-term observations necessary to produce lake water budgets. Therefore, predicting the effects on climate change on the water storage of lakes remains highly uncertain.

The mixing regimes of lakes are projected to change through time, due to climate-induced variations in lake surface water temperature and ice cover. It is projected that ~17% of all lakes are likely to change mixing regimes from dimictic (two mixing periods per year) to monomictic (one mixing period per year) by 2080-2099 (Woolway and

Merchant 2019). Warming winters with warmer lake surface water temperature (O'Reilly et al. 2015) and decreasing ice cover (Sharma et al. 2021; Sharma et al. 2019), will result in lakes no longer inversely stratifying in winter, thus remaining vertically mixed from autumn until spring (Woolway et al. 2021; Woolway and Merchant 2019). In addition, changes in water clarity will also play an important role in the mixing regime of lakes, by affecting the depth at which shortwave radiation is absorbed within a lake (Mesman et al. 2021; Shatwell et al. 2019). While various studies have projected that climate change is likely to shift lake mixing regimes (Zamani et al. 2021) to the right along the polymictic-dimictic-monomictic-oligomictic-meromictic continuum (Woolway et al. 2021; Woolway and Merchant 2019), some lakes will not follow this trend. In some cases, lakes are projected to experience shorter periods of stratification and thus mix more often (Rogozin et al. 2017) due to, for example, regional increases in wind speed or a decline in lake level (i.e., where surface winds can then more easily mix the water column). Therefore, the influence of climate change on lake mixing regimes is complex, and further investigation at a global scale is required.

The chemical and biological properties in lakes can also be altered by changes in climate (e.g. temperature, wind speed, precipitation), as well as changes in the catchment. Secondary effects include possible increases in nutrient loading, changes in the residence time and declining water quality (Jennings et al. 2009; Mooij et al. 2005; Meyer et al. 1999). The effects of any increases in nutrient loading of the lake can be exacerbated by decreased precipitation and water flow which consequently increases the residence time of the lake. Conversely, if precipitation and water flow increase, the residence time of the lake will decrease, flushing out the nutrients and phytoplankton which may result in reduced algal production (Weyhenmeyer 2007; Mooij et al. 2005). However, differences in lake morphometry and site specificity will result in different responses to the relative effect of climate change on lake variables. Nutrient loading will also be strongly affected by catchment management actions (Jennings et al. 2009). Water temperature in lakes has increased at the surface (O'Reilly et al. 2015), while less consistent trends have been detected at other depths (Pilla et al. 2020). These changes in lake water temperature can lead to longer periods of thermal stratification, and therefore, positively influence cyanobacteria blooms (Wagner and Adrian 2009). Nevertheless, dissolved oxygen depletion is undoubtedly one of the most serious consequences with potential detrimental

effects for lake biota at large, community composition, food web structure and the release of phosphorus, and ammonium (Jane et al. 2021; Foley et al. 2012; Larsen et al. 2011). Therefore, climate warming can exacerbate the effects of eutrophication and contribute to the deterioration in the water quality of a lake.

In summary, climate change has important implications for local economies which depend on lakes for drinking water, hydropower generation, irrigation, fish harvesting, tourism and recreation. For these reasons assessment of current and projected status of lakes ecosystems and dynamics under scenarios of climate change, is of paramount importance.

1.3   Research aim and objectives

The growing pressure due to both climate change and population growth on lakes poses a serious threat to their ecosystems. As lakes hold 87% of the surface freshwater available on earth, it is of paramount importance to understand their water dynamics, particularly with regard to losses. Evaporation, as the most significant water loss from lake systems, must receive special attention, since it can considerably affect the stability and the temporal availability of water resources within a basin. However, the unique nature of evaporation from open waters makes it highly sensitive to the choice of model/method for its estimation. Knowledge of the uncertainties associated with these estimates is vital for strategic water management in lakes worldwide. Therefore, the overarching aim of this study is to investigate lake evaporation responses at local and global scales using an ensemble modeling approach (i.e. using multiple independently developed models). The above aim was divided into three specific objectives:

1. To investigate evaporation responses to climate change in a lake with high socio-economic, political and religious value, and to test the performance of the ensemble approach.
2. To examine lake evaporation responses to climate change among lakes within the same geographical region but with different climate conditions and characterised by different morphometric characteristics.

3. Investigate differences in global lake evaporation responses to climate change using an ensemble of models and to quantify the uncertainties in projections of future lake evaporation.

1.4 Thesis structure

This dissertation contains six chapters. The first chapter consists of this introduction and it is followed by a comprehensive literature review in Chapter 2 with focus on lake evaporation research and modeling methodologies such as the ensemble approach. The following chapters, namely Chapters 3-5 consist of the main findings of this dissertation and each contain an introduction, methods, results and discussion in the format of published scientific articles. For example, Chapter 3 consists of a published scientific article in the Journal of Hydrology titled '*Multi-model projections of future evaporation in a sub-tropical lake*' that explores the performance of the ensemble approach in modeling lake evaporation for a lake with high socio-economic, political and religious significance. Chapter 4 consists of a draft article titled '*Increasing warm-season evaporation rates across European lakes due to climate change*', that reports future evaporation projections for a suite of lakes distributed across Europe with differing climate conditions, and morphometric characteristics. Chapter 5 is a submitted article that is currently under review at the Journal of Hydrology titled '*Ensemble modeling of global lake evaporation under climate change*', which investigates the differences in simulated global lake evaporation using an ensemble of models, and provides a quantification of uncertainties in future evaporation projections. Finally, Chapter 6 consists of a synthesis where the main findings of this dissertation, the lessons learned as well as a section that outlines areas of future research (Fig. 1.2).
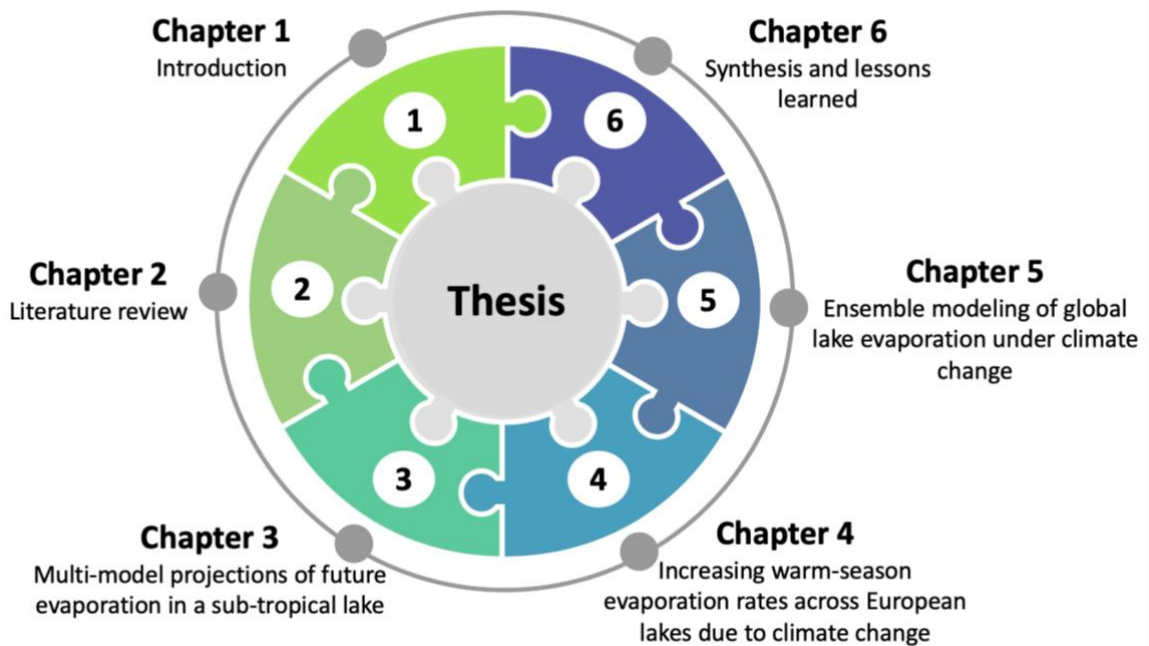
Figure 1.2 Overview of chapters.

1.5 List of publications

The research of this thesis is based on the following publications:

1. **La Fuente, S.**, Jennings, E., Gal, G., Kirillin, G., Shatwell, T., Ladwig, R., Moore, T., Couture, R.-M., Côté, M. and Vinnå, C.L.R. Woolway, R. I. (2022). Multi-model projections of future evaporation in a sub-tropical lake. *Journal of Hydrology*, 2022, p.128729.

2. **La Fuente, S.**, Jennings, E., Lenters, J. D., Verburg, P., Tan, Z., Perroud, M., Janssen, A. B. G., Woolway, R. I. (2024). Ensemble Modeling of global lake evaporation under climate change. *Journal of Hydrology, 2024*, p. 130647.

3. Increasing warm-season evaporation rates across European lakes under climate change - draft manuscript.

In addition, I have contributed to the following collaborations during my PhD:

Published collaborations

1. Kraemer, B.M., Dugan, H., **La Fuente, S.** and Meyer, M.F. (2023). Lake water levels in 'State of the climate in 2022'. *Bulletin of the American Meteorological Society,* 104(9)*, pp. S63-S65.

2. Jansen, J., Woolway, R.I., Kraemer, B.M., Albergel, C., Bastviken, D., Weyhenmeyer, G.A., Marce, R., Sharma, S., Sobek, S., Tranvik, L.J., Perroud, M., Golub, M., Moore, T. N., Vinnå, L.R. **La Fuente, S.**, Grant, L., Pierson, D.C., Thiery, W. and Jennings, E. (2022). Global increase in methane production under future warming of lake bottom waters. *Global Change Biology*, 28(18), pp.5427–5440.

3. Woolway, R.I., Denfeld, B., Tan, Z., Jansen, J., Weyhenmeyer, G.A. and **La Fuente, S.** (2022). Winter inverse lake stratification under historic and future climate change. *Limnology and Oceanography Letters*, 7(4), pp.302–311.

4. Woolway, R.I., Sharma, S., Weyhenmeyer, G.A., Debolskiy, A., Golub, M., Mercado-Bettín, D., Perroud, M., Stepanenko, V., Tan, Z., Grant, L., Ladwig, R., Mesman, J., Moore, T.N., Shatwell, T., Vanderkelen, I., Austin J.A., DeGasperi, C.L., Dokulil, M., **La Fuente, S.**, Mackay, E.B., Schladow, S.G., Watanabe, S., Marcé, R., Pierson, D.C., Thiery, W. and Jennings, E. (2021). Phenological shifts in lake stratification under climate change. *Nature Communications*, 12(1), pp.1–11.

5. Carrea, L., Woolway, R.I., Merchant, C.J., Dokulil, M.T., DeGasperi, C.L., De Eyto, E., Kelly, S., **La Fuente, R.S.**, Marszelewski, W., May, L., Paterson, A.M., Pulkkanen, M., Rusak, J.A., Rusanovskaya, O., Schladow, S.G., Schmid, M., Shimaraeva, S.V., Silow, E.A., Timofeyev, M.A., Verburg, P., Watanabe, S. and Weyhenmeyer, G.A. (2020). Lake surface temperature in 'State of the Climate in 2019'. *Bulletin of the American Meteorological Society,* 101(8), pp. S26-S28.

Chapter 2 Literature review

This chapter provides a review of the current literature on lake evaporation research. The first section consists of a general introduction of the energy budget of lakes and its most important components to introduce lake evaporation. The review then discusses the influence of evaporation on lake ecosystems and it highlights its importance. Climatic and limnological factors that alter evaporation, as well as site-specific characteristics are discussed in the following sections. An introduction to modeling open water evaporation methods is provided in the final section, together with a general overview of ensemble modeling and uncertainty quantification.

2.1 The energy budget of lakes

The heat budget of a lake is the most fundamental component of physical limnology, and is determined by interactions between the atmosphere at the air-water interface (Verburg and Antenucci 2010; Edinger et al. 1968; Dutton and Bryson 1962). It is dictated by heat fluxes at the lake surface, especially shortwave radiation, incoming and outgoing longwave radiation, and the turbulent fluxes of latent and sensible heat (Schmid and Read 2022) (Fig. 2.1). The seasonality of these fluxes is the most important driver for the seasonal mixing processes in lakes. Changes in heat fluxes and the resulting effects on lake thermal structure are the most direct impact of climate change on lakes. The heat content of a lake is determined by the temperature and volume of the water, as well as other water properties that impact water density or specific heat, as expressed in the following equation:

$$\frac{Q_{tot}}{A_{lake}} = S_w + L_w + L_{wo} + Q_e + Q_h + Q_a + Q_s \qquad (2.1)$$

where Q_{tot} is the total heat of the lake, and A_{lake} is the surface area of the lake. Heat fluxes include downward shortwave radiation (S_w) and longwave radiation (L_w), outgoing longwave radiation (L_{wo}), latent (Q_e) and sensible (Q_h) fluxes, advected energy (Q_a), and sediment heat flux (Q_s). Various methods have been used to quantify heat fluxes, from using measurements of temperature and energy fluxes to process-based lake models (Hipsey et al. 2019; Woolway et al. 2015; Fink et al. 2014; Henderson-Sellers 1986).
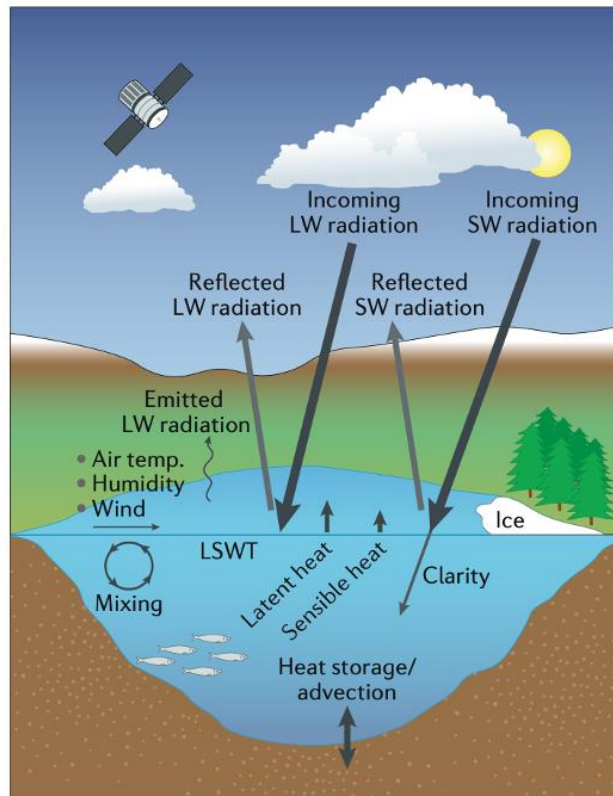
Figure 2.1 Lake surface energy budget and associated atmospheric and in-lake drivers.
Source: Woolway et al. (2020)

2.1.1 Latent and sensible heat fluxes

Latent heat flux represents the energy lost or gained to the lake via a state change from liquid water to vapor (evaporation) or vapor to liquid water (condensation). Latent heat flux changes remove or add water to the lake and are therefore important in the heat budget of the lake. The majority of the latent heat exchange occurs as evaporation, where the magnitude and intensity of the vapor pressure gradient across the air-water boundary is usually expressed as ($\Delta e/\Delta z$) where (Δe) is the vapor pressure difference and (Δz) is the vertical height between the two measurements. Above this layer, wind and vertical mixing remove the water vapor from the boundary layer, thus maintaining the vapor pressure gradient.

Sensible heat is transferred across the water's surface by conduction to or from the air at the air/water boundary. This conduction occurs only in a very thin layer of water or air at the boundary itself and directly depends on the temperature gradient across that boundary, and in contrast to latent heat flux, no state change occurs. Sensible heat transfer

between a lake and the atmosphere takes place by a combination of conduction and convection (Ragotzkie 1978). Similarly to latent heat flux, sensible heat flux can remove or add energy to the lake depending on the prevailing atmospheric drivers and the surface temperature of the lake. The magnitude of sensible heat flux depends strongly on the difference in temperature between air and water and the atmospheric removal.

2.1.2 Shortwave radiation

The main source of energy input at the lake surface is through solar radiation. The sun emits high-intensity radiation in the shorter (visible and ultraviolet) wavelength portion of the spectrum, namely shortwave radiation. It depends on latitude, cloud cover, elevation, and landscape features (i.e. mountains, tree canopies). Some of the incoming radiation is reflected by the lake surface, defined as the shortwave albedo. An albedo value of 1.0 means that 100% of the solar radiation is reflected and a value of zero means that none is reflected. Albedo varies with the angle of incidence (latitude and elevation), time of the year, and surface water conditions (e.g. presence of waves or ice cover). The fraction of solar radiation that is not reflected penetrates below the surface of the lake and it is attenuated by the water column or the lakebed (Ragotzkie 1978). Shortwave radiation penetrates the lake surface, where its radiant energy is absorbed at depth, altering the heat storage of the lake. The availability of this absorbed energy for evaporation cooling depends on lake morphometry. This suggests that approaches that use net radiation as a correction factor, will be of little use in estimating evaporation from open water bodies such as lakes (Granger and Hedstrom 2011).

2.1.3 Longwave radiation

The temperature of the overlying air and water vapor as well as the presence or absence of clouds determine the net longwave radiation flux at the surface of the lake (Ragotzkie 1978). Downwelling longwave radiation is the radiative energy flux from the atmosphere. Its magnitude depends on atmospheric temperature, humidity and cloud cover. Approximately 3% of the downwelling longwave radiation is reflected at the surface of the lake due to longwave albedo, and the remaining energy is absorbed by the lake. Outgoing longwave radiation is the portion of the solar radiation that is emitted from the lake, and it is a function of the surface water temperature. This energy flux represents the

12

largest energy loss term in the heat budget of a lake. Although outgoing longwave radiation increases with water temperature, downwelling longwave radiation also increases with higher air temperature and higher humidity. Given that the water vapor capacity of the air increases as the temperature increases, the net result is that the downwelling radiation tends to increase with temperature more than the outgoing longwave radiation (Ragotzkie 1978). Therefore, total outgoing longwave radiation tends to decrease with increased temperature of air and water.

2.1.4 Lake ice cover

Lake ice formation is dominated by the energy balance at the surface of the lake, and mediated by air temperature, wind speed, and lake surface area, which ensure that vertical heat transfer is sufficient to cool surface water temperatures to 0°C. Precipitation, cloud cover, solar radiation, distance to coastline and regional differences govern the timing of ice formation and ice growth during the winter season (Sharma et al. 2019; Brown and Duguay 2010). Given the transient nature of ice freeze-up and ice break-up processes that occur over periods of days, weeks or even months, changes in these processes can be useful indicators of climate change (Grant et al. 2021; Brown and Duguay 2010).

2.1.5 Lake surface water temperature

Lake surface water temperature is influenced by climatic and in-lake drivers that contribute to the energy budget of the lake. Climate drivers primarily include air temperature, cloud cover, relative humidity, wind speed, incoming longwave radiation and shortwave radiation. The amount of heat entering or leaving the water column is primarily driven by the exchange of radiative (i.e. net longwave radiation and net shortwave radiation), and non-radiative fluxes (i.e. latent and sensible heat) at the air-water interface (Schmid and Köster 2016; Edinger et al. 1968). Aspects of lake morphology, such as surface area, maximum depth and mean depth are also important predictors of surface water temperature (Schmid et al. 2014). In addition to variations in regional weather and lake morphology, additional factors such as latitude, altitude (Vinnå et al. 2021), topographic shading and hydrology of inflows can influence the thermal structure of lakes through influences on lake surface temperature, heat storage and wind

mixing (O'Reilly et al. 2015; Novikmec et al. 2013; Livingstone et al. 2005; Goudsmit et al. 2002).

2.2   The influence of evaporation within lake ecosystems

Due to their typically large open-water areas, lakes can lose substantial amounts of water through evaporation, considerably affecting their water, energy and chemical budgets (Woolway et al. 2020; Riveros-Iregui et al. 2017; Lenters et al. 2005; Schindler 2001). In turn, evaporation is a key physical process governing the functioning of lake ecosystems. Because of its cooling effect on lakes, evaporation can substantially modify water temperature and associated processes with ice formation, stratification (Van Cleave et al. 2014; Lenters et al. 2013; Spence et al. 2013; Mishra et al. 2011), vertical mixing (Ye et al. 2019; MacIntyre et al. 2009) and gas fluxes (Kosten et al. 2010; Read et al. 2012) with likely effects on lake chemistry and biota (Likens et al. 2009; Williamson et al. 2009). Importantly, lake evaporation shares two-way interactions within the lake. These include interactions between evaporation, lake surface temperature, and ice cover (Ye et al. 2019; Van Cleave et al. 2014; Lenters et al. 2013; Spence et al. 2013), feedbacks between salinity and evaporation rates (Riveros-Iregui et al. 2017; Shilo et al. 2015), effects on the regional climate (e.g. lake-effect clouds and precipitation; Thiery et al. 2016; Balsamo et al. 2012), and the coupling of evaporation with changes in lake level and extent (Friedrich et al. 2018; Marsh and Bigras 1988).

Evaporation substantially influences various processes within the lake, however one of the most significant impacts is its role on the fluctuation of water levels (Friedrich et al. 2018; Chen et al. 2017; Lenters et al. 2014). Such changes reflect an alteration in the water balance of lakes that strongly depends on climate variability and anthropogenic management (Yao et al. 2023; Friedrich et al. 2018; Wurtsbaugh et al. 2017; Pekel et al. 2016). Nevertheless, the fluctuation of water level in lakes is not only driven by changes in evaporation, but also by changes in precipitation and its influence on lake inflows. The effect of changing precipitation *(P)* and evaporation *(E)* ratios dictates the fate of the water levels of many lakes, particularly of those that are shallow (Zhou et al. 2021). The concurrent increase in evaporation and decrease in precipitation can result in water level depletion. A decrease in water level can have major implications for access to clean water, affect fishing, transportation of goods, energy generation, water quality and ultimately

end in ecosystem collapse (Semazzi 2011). Given its key role on the P-E dynamics it is thus crucial for water management to understand evaporation variability and its relationship with precipitation.

2.2.1 Climate and limnological factors influencing evaporation

Evaporation is dictated by the magnitude of the vapour pressure gradient between the water surface and the overlying air. This gradient is determined by the temperature of the surface water, the absolute humidity in the atmosphere (vapour pressure), and the amount of turbulent mixing of air at the air-water interface (Woolway et al. 2018; Lenters et al. 2014; Abtew 2001), resulting in high evaporation rates when the water is warm, and the air is cold, dry, windy and the atmospheric boundary layer is unstable (Friedrich et al. 2018; Granger and Hedstrom 2011; Blanken et al. 2000). Thus, some of the most direct atmospheric drivers of lake evaporation are wind speed and absolute humidity (i.e., the basis of eddy covariance measurements).

However, due to the influence of lake surface water temperature on the vapor pressure gradient, other atmospheric and limnological factors which influence the lake heat budget also play a considerable role in evaporation (Friedrich et al. 2018; Lenters et al. 2005; Brutsaert 1982) (Fig. 2.2). As an energy-consuming process, evaporation cools water temperature, thus reducing the surface vapor pressure and the rate of evaporation (i.e., negative feedback). The rate at which this feedback occurs, as well as responses to other energy budget drivers, depend both on the intensity and time-scale of the meteorological forcing and the thermal inertia (e.g. mean depth, ice cover) (Lenters et al. 2014; Van Cleave et al. 2014; Vallet-Coulomb et al. 2001), as well as on the specific properties (e.g. water clarity, salinity) (Heiskanen et al. 2015; Rimmer et al. 2011) of the waterbody. This implies that the meteorological and limnological drivers that influence evaporation go well beyond wind speed and humidity.

Therefore, this not only includes drivers such as net radiation (i.e., main energy source for latent and sensible heat fluxes), but also individual factors such as incoming shortwave radiation (dependent on snow, ice cover and light attenuation), lake heat storage (dependent on atmospheric profiles of temperature, humidity and cloud cover), sediment heat flux and advective sources of energy (i.e., precipitation, groundwater,

surface inflows, and outflows), and finally, changes in lake water level (i.e. changes in water surface temperature and volumetric loss) (Friedrich et al. 2018; Lenters et al. 2014).
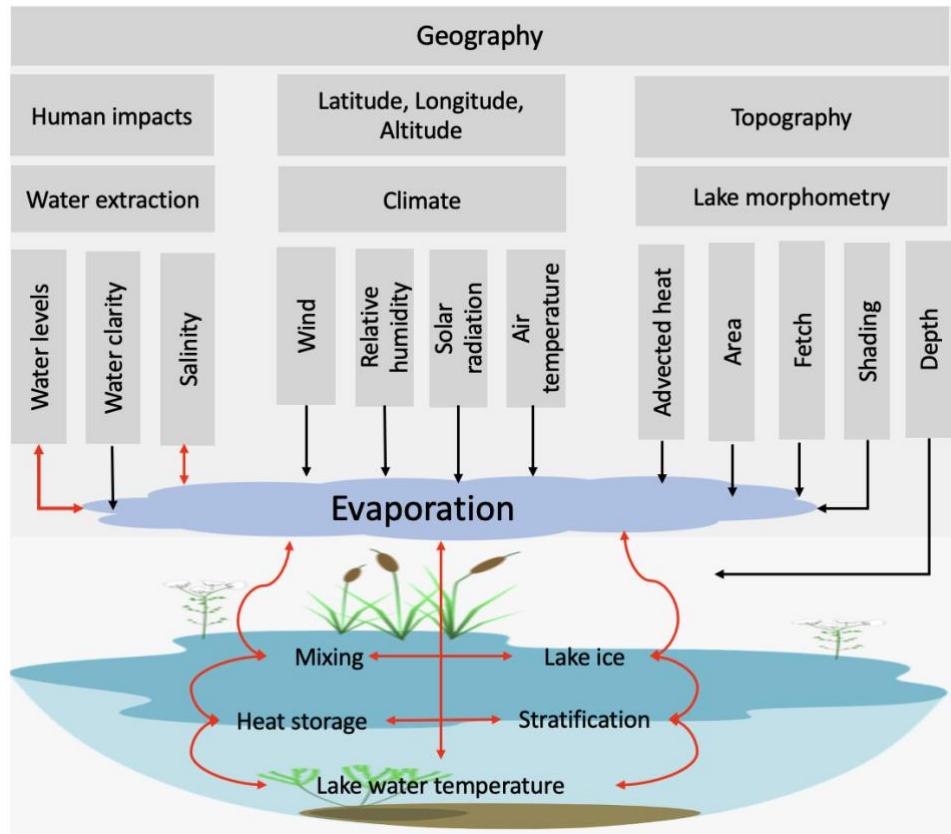
Figure 2.2 Drivers of lake evaporation. Unidirectional arrows indicate one-way interactions, bidirectional arrows indicate two-way interactions.

2.2.2 Site-specific factors altering evaporation

In addition to the climate and limnological drivers, there are a number of lake-specific factors that can modify the fate of evaporation (Fig. 2.2). For example, water clarity (Heiskanen et al. 2015; Thiery et al. 2014), wind sheltering (Hipsey and Sivapalan 2003) and lake depth can substantially modify the timing and/or intensity of lake evaporation, primarily through influences on lake surface temperature, heat storage, and wind mixing (McVicar et al. 2012; Read et al. 2012). As a result of these complex interactions and the dependence of many lake-specific factors, evaporation is highly variable across different lakes (Han and Guo 2023; Wang et al. 2018). Thus, defining the main drivers of lake

evaporation is far from straightforward, and often depends on timescale, lake morphometry, and characteristics of the regional climate.

Importantly, climate drivers such as air temperature, water temperature, humidity, and wind-induced turbulent mixing are heterogenous, particularly on small reservoirs with complex geography (topography, vegetation), and large deep water bodies with strong lake-land boundary layer modifications and horizontal gradients (e.g. surface temperature, ice cover) (Friedrich et al. 2018). This can result in unequal evaporation rates over the lake surface (Friedrich et al. 2018; Spence et al. 2011; Assouline and Mahrer 1993; Mahrer and Assouline 1993; Morton 1983; Weisman and Brutsaert 1973), particularly in lakes with large surface areas. Various methods have been proposed to estimate the horizontal variability of evaporation, using the distance from the upwind shore (Morton 1983; Weisman and Brutsaert 1973), using meso-scale models (Mahrer and Assouline 1993), and remote sensing. For these reasons, land surface data alone are insufficient to parametrize lake evaporation; water surface data are also required (Granger and Hedstrom 2011).

2.3 Modeling lake evaporation

Due to its complex interactions with the surrounding climate, physical properties and characteristics of the lake itself, estimating evaporation from open waters is far from straightforward (Friedrich et al. 2018; Lenters et al. 2005). Eddy covariance is known to be the most direct method to measure evaporation, however it requires a substantial investment in instrumentation and data processing (Guseva et al. 2023; Shevnina et al. 2022; Xiao et al. 2020). In many cases eddy covariance measurements are available for short periods of time and are mostly used for the calibration of process-based models (Schmid and Read 2022). Alternatively, a number of methodologies to estimate evaporation have been developed including pan evaporation, mass balance, energy budget, bulk transfer, combination models, equilibrium temperature and other empirical approaches (Finch and Calver 2008). However, there is no general consensus as to which of these methods yields the best estimate of open-water evaporation (Althoff et al. 2020; Sartori 2000).

Despite its crucial role in the water budget of lakes, and thus in regional water availability, evaporation observations (i.e. eddy covariance measurements) are rare and

not extensively taken (Guseva et al. 2023; Shevnina et al. 2022; Xiao et al. 2020; Granger and Hedstrom 2011; Assouline and Mahrer 1993). In turn, high-frequency monitoring of climate variables and lake water temperature are more widely spread across lakes worldwide. In this sense, combining the empirical evidence (i.e. observations of thermal structure of lakes) with the use of process-based modeling can be vital to understanding lake evaporation responses to climate change. Achieving this goal however, can also be challenging as a number of studies have suggested that open-water evaporation is highly sensitive to the choice of model/method for its estimation (Zhao et al. 2023; Jansen and Teuling 2020; Pillco Zolá et al. 2019; Rosenberry et al. 2007). Therefore, using a single-method or single-model realization may be problematic for capturing evaporation dynamics and variability at local, regional and global scales.

2.4 Ensemble modeling and uncertainty quantification

Almost three decades ago, ensemble modeling was first introduced in atmospheric sciences with applications for forecasting and uncertainty quantification (Parker 2013). It consists of either running the same model multiple times with different settings (e.g. driving data, parameters, initial conditions) or running multiple models on the same study site. The main advantage of using an ensemble approach is that one can combine the wealth of information provided by different independently developed models and provide a range of outputs rather than single estimates (Feldbauer et al. 2022; Grant et al. 2021; Moore et al. 2021; Woolway et al. 2021; Gal et al. 2020; Mesman et al. 2020; Trolle et al. 2014). In this way, one can obtain an approximation of the uncertainties associated with the model simulations. Notably, the performance of the ensemble mean has been reported to outperform any single-model realisation, making ensemble modeling a valuable tool for climate change impact assessments.

Therefore, the use of ensemble (multi-model) approaches has become the norm in climate sciences. However despite its popularity, the application of ensemble approaches to simulate the impacts of climate change on lake systems only started in the last decade with the development of international modeling frameworks such as the LakeMIP (Lake Model Intercomparison Project) (Stepanenko et al. 2010) and the ISIMIP (Inter Sectoral Impact Model Intercomparison Project) lake sector (Golub et al. 2022). As a result, key contributions have focused in the development of tools to facilitate ensemble modeling

in lakes such as the 'LakeEnsemblR' package (Moore et al. 2021) and other individual studies that have tested the multi-model approach in various lake physical properties (Ayala Zamora et al. 2023; Woolway et al. 2021; Gal et al. 2020; Mesman et al. 2020; Trolle et al. 2014).

Chapter 3   Multi-model projections of future evaporation in a sub-tropical lake

Authors: Sofia La Fuente[1*], Eleanor Jennings[1], Gideon Gal[2], Georgiy Kirillin[3], Tom Shatwell[4], Robert Ladwig[5], Tadhg Moore[6], Raoul-Marie Couture[7], Marianne Côté[7], C. Love Råman Vinnå[8], R. Iestyn Woolway[9]

Affiliations:

1. Centre for Freshwater and Environmental Studies, Dundalk Institute of Technology, Dundalk, Ireland
2. Kinneret Limnological Laboratory, Israel Oceanographic & Limnological Research, Migdal, Israel
3. Leibniz-Institute of Freshwater Ecology and Inland Fisheries (IGB), Berlin, Germany
4. Helmholtz Centre for Environmental Research, Department of Lake Research, Magdeburg, Germany
5. Center for Limnology, University of Wisconsin-Madison, Madison, WI, USA
6. Virginia Tech, Department of Biological Sciences, Blacksburg, VA, USA
7. Centre for Northern Studies (CEN), Takuvik Joint International Laboratory, and Department of Chemistry, Université Laval, Quebec City, QC, Canada
8. Eawag, Swiss Federal Institute of Aquatic Science and Technology, Surface Waters - Research and Management, Kastanienbaum, Switzerland
9. School of Ocean Sciences, Bangor University, Menai Bridge, Anglesey, Wales

*Corresponding author: ruthsofia.lafuentepillco@dkit.ie
*Postal address: Centre for Freshwater and Environmental Studies, Dundalk Institute of Technology, Dundalk, Marshes Upper A91 K584, Co. Louth, Ireland

Highlights

1. Lake evaporation projections using a multi-model approach
2. The model ensemble generally captured intra-annual variability and seasonality

3. Projected increase in evaporation and decrease in precipitation this century

3.1 Abstract

Lake evaporation plays an important role in the water budget of lakes. Predicting lake evaporation responses to climate change is thus of paramount importance for the planning of mitigation and adaption strategies. However, most studies that have simulated climate change impacts on lake evaporation have typically utilised a single mechanistic model. Whilst such studies have merit, projected changes in lake evaporation from any single lake model can be considered uncertain. To better understand evaporation responses to climate change, a multi-model approach (i.e., where a range of projections are considered), is desirable. In this study, we present such multi-model analysis, where five lake models forced by four different climate model projections are used to simulate historic and future change (1901-2099) in lake evaporation. Our investigation, which focuses on sub-tropical Lake Kinneret (Israel), suggested considerable differences in simulated evaporation rates among the models, with the annual average evaporation rates varying between 1232 mm year^{-1} and 2608 mm year^{-1} during the historic period (1901-2005). We explored these differences by comparing the models with reference evaporation rates estimated using in-situ data (2000-2005) and a bulk aerodynamic algorithm. We found that the model ensemble generally captured the intra-annual variability in reference evaporation rates, and compared well at seasonal timescales (RMSEc = 0.19, R = 0.92). Using the model ensemble, we then projected future change in evaporation rates under three different Representative Concentration Pathway (RCP) scenarios: RCP 2.6, 6.0 and 8.5. Our projections indicated that, by the end of the 21st century (2070-2099), annual average evaporation rates would increase in Lake Kinneret by 9-22% under RCPs 2.6-8.5. When compared with projected regional declines in precipitation, our projections suggested that the water balance of Lake Kinneret could experience a deficit of 14-40% this century. We anticipate this substantial projected deficit combined with a considerable growth in population expected for this region could have considerable negative impacts on water availability and would consequently increase regional water stress.

Keywords: ensemble modelling, lake evaporation, climate change, Lake Kinneret

3.2 Introduction

Lake evaporation plays a fundamental role in the basic functioning of lakes. Evaporation directly and, in some cases, substantially modifies the hydrologic, chemical, and energy budgets, making it one of the most important physical controls on lake ecosystems (Woolway et al. 2020; Riveros-Iregui et al. 2017; Lenters et al. 2005; Schindler 2001). Not only does lake evaporation play a fundamental role in these budgets through the physical removal of fresh water, but the cooling effect of latent heat flux is also central to the modification of lake temperature, and related processes such as stratification (Van Cleave et al. 2014; Lenters et al. 2013; Spence et al. 2013; Mishra et al. 2011) and vertical mixing (Ye et al. 2019; MacIntyre et al. 2009), with likely impacts on lake chemistry and biota (Wahed et al. 2014; Likens et al. 2009; Williamson et al. 2009). Importantly, lake evaporation also contributes to critical feedbacks within lakes, including interactions between evaporation and lake surface temperature (Kishcha et al. 2021; Ye et al. 2019; Van Cleave et al. 2014; Lenters et al. 2013; Spence et al. 2013), feedbacks between salinity and evaporation rates (Riveros-Iregui et al. 2017; Shilo et al. 2015), and the coupling of evaporation with changes in lake level and extent (Zhan et al. 2019; Friedrich et al. 2018; Li et al. 2013; Marsh and Bigras 1988). While evaporation substantially influences various processes within the lake, fluctuations in water level represent, arguably, one of the most important ones for the ecosystem services that lakes provide. A decline in lake water level can have major implications for access to clean water, collection of food via fishing, the transportation of goods, energy generation, and ecosystem loss (Zohary and Ostrovsky 2011).

Evaporation in lakes is largely governed by the magnitude of the vapor pressure gradient between the lake surface and the overlying atmosphere (Lenters et al. 2014; Lenters et al. 2005; Hostetler and Bartlein 1990). This gradient, and thereafter the transfer of latent heat, is determined primarily by the temperature of the lake surface, the absolute humidity in the atmosphere, and the amount of wind-induced turbulent mixing at the air-water interface (Woolway et al. 2018; Lenters et al. 2014). Some of the most direct atmospheric drivers of lake evaporation are thus wind speed and absolute humidity i.e., the basis of eddy covariance measurements. However, due to the influence of lake surface temperature on the vapor pressure gradient, other atmospheric and limnological factors which influence the lake heat budget also play a considerable role in evaporation

(Friedrich et al. 2018; Lenters et al. 2005; Brutsaert 1982). Overall, the sources of available energy that influence lake evaporation are numerous, including incoming radiation (both solar and longwave), sensible heat flux (via changes in the Bowen ratio), advected heat (snowfall, groundwater, etc.), and changes in heat stored within the lake itself. The energy available for evaporation is also modulated by the amount of outgoing longwave and shortwave radiation, which are dictated by lake surface temperature and shortwave albedo, respectively. In addition to these climatic drivers, numerous lake-specific features, such as water clarity, wind sheltering and lake depth, can modify the timing and/or intensity of lake evaporation, primarily through influences on lake surface temperature, heat storage, and wind mixing (Zhan et al. 2019; McVicar et al. 2012; Read et al. 2012). As a result of these complex interactions and the dependence of many lake-specific factors, evaporation is highly variable between lakes (Zhou et al. 2021; Konapala et al. 2020; Wang et al. 2018; Woolway et al. 2018; Marsh and Bigras 1988).

Given the significance of lake evaporation, as well as its complex interactions with other within-lake processes, predicting its response to climate change is of paramount importance. To accurately simulate lake evaporation responses to historic and future climatic variations, process-based numerical models that can compute complex air-water and within-lake thermodynamic fluxes are needed. A number of such process-based models have been developed in recent decades, including those based on, among other things, eddy-diffusion (Hostetler et al. 1993; Hostetler and Bartlein 1990), bulk formulation (Mironov 2008), energy balance (Hipsey et al. 2019), and turbulence closure (Goudsmit et al. 2002; Burchard et al. 1999). However, most studies that simulate climate change impacts on lake evaporation have utilised only a single mechanistic model (Wang et al. 2018; Lenters et al. 2005; Vallet-Coulomb et al. 2001; Hostetler and Bartlein 1990). Whilst such studies have merit, most lake models implement approximate forms of relationships, either due to incomplete knowledge of some processes or for practical computing purposes. Furthermore, any individual model provides an approximation of reality, for which uncertainty is often not quantified (Moore et al. 2021). An alternate method is to adopt an ensemble approach, where multiple, independently developed models are used. Such coordinated experiments have become the *de facto* standard in climate science including, for example, the Coupled Model Intercomparison Project (Meehl et al. 2005). Ensemble modelling of lake responses to climate change is, however,

in its infancy (Feldbauer et al. 2022; Grant et al. 2021; Moore et al. 2021; Woolway et al. 2021; Gal et al. 2020; Mesman et al. 2020; Trolle et al. 2014).

The overarching aim of this study was to investigate changes in lake evaporation under historic and future climate using a suite of independently developed lake models forced with projections from multiple General Circulation Models (GCMs) to produce an ensemble of lake-climate model projections. Our study was focused on Lake Kinneret (Israel), a lake with high socio-economic, political, and religious value. Also known as the Sea of Galilee, Lake Kinneret provides ~25-30% of the drinking water in Israel (Shilo et al. 2015) and ~100 million m^3 $year^{-1}$ to the Kingdom of Jordan. Analysing the impacts of climate change on evaporation rates in Lake Kinneret is thus of primary importance for adaptation and mitigation strategies. Here, we investigate (i) multi-model projections of lake evaporation during the historical period and evaluate key differences across the model ensemble; (ii) assess the accuracy of the model ensemble relative to a reference evaporation estimated using observed data at seasonal, annual and intra-annual timescales; and (iii) using the model ensemble, we investigate future projections of lake evaporation this century under different climate change scenarios.

3.3   Methods and materials

3.3.1 Study area

Lake Kinneret is a sub-tropical monomictic lake located in the northern region of Israel (Fig. 3.1). The average surface area of the lake is 168.7 km^2 with an average volume of 4100 Mm^3 (Zohary et al. 2014). The mean and maximum depths of Lake Kinneret are 25.6 and 41.7 m, respectively (Shilo et al. 2015), and its average residence time is ~ 8-10 years (Van Emmerik et al. 2013; Rimmer et al. 2009). Climatic conditions in the region can be categorised as warm and dry, with annual average air temperatures of ~21°C (maximum > 36°C), annual average rainfall of 380 mm $year^{-1}$, and surface winds often exceeding ~10 m s^{-1} (Gal et al. 2020; Zohary et al. 2014). The main inflows of Lake Kinneret are the Jordan and Meshushim rivers, and considerable water input comes as runoff and from saline springs as groundwater. The most important outflows from the lake consist of water withdrawals via the National Water Carrier (NWC), the Degania dam and pumping around the lake by local consumers (Gal et al. 2003).
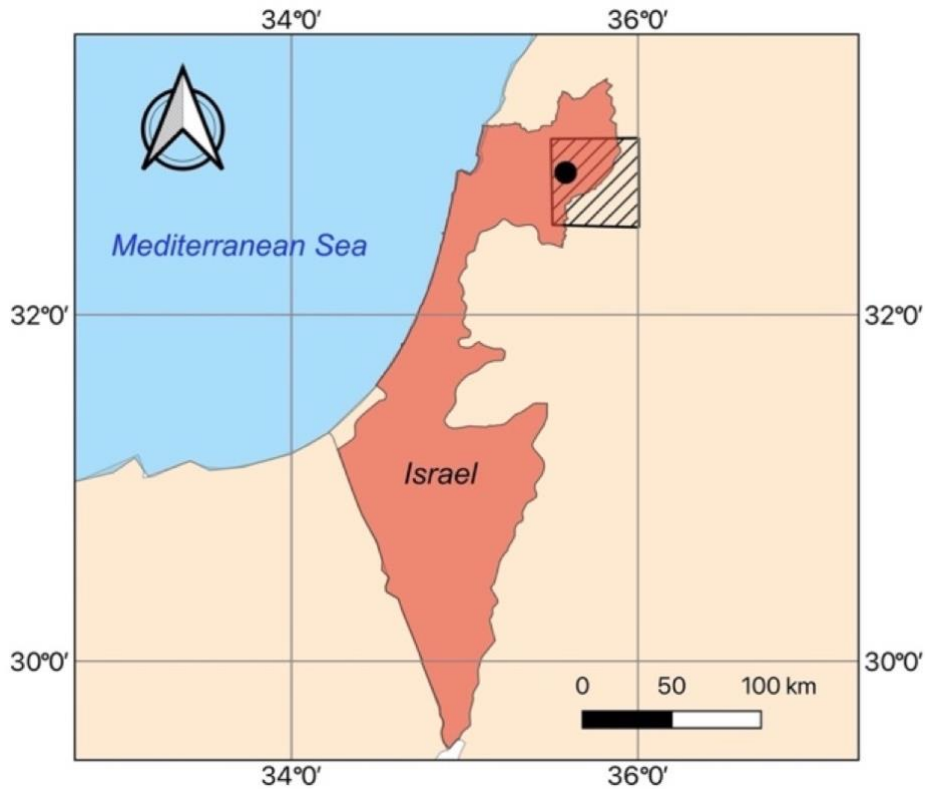
Figure 3.1 Map of Israel with the location of Lake Kinneret shown by the filled black circle. The shaded region represents the spatial domain of the ISIMIP2b input data used to drive the lake models.

3.3.2 Multi-model projections of lake evaporation

Lake projections investigated in this study were a lake-climate model ensemble of 20 model realizations. More specifically, from five lake models driven by four GCMs. The lake models, namely FLake (Mironov 2008), GLM (Hipsey et al. 2019), GOTM (Burchard et al. 1999), MyLake (Saloranta and Andersen 2007), and Simstrat (Goudsmit et al. 2002) (Table 3.1), contributed to the Inter-Sectoral Impact Model Intercomparison Project (ISIMIP) phase 2b Lake Sector (Golub et al. 2022). A description of each lake model used is provided below.

Table 3.1 Summary of the lake models used in this study, including a description of their structure, parameterization and key references.

Lake model (version)	Timestep Simulated/ Reported	Vertical structure / layers reported	Parameterization of turbulent fluxes at air-water interface	Turbulent mixing parameterization	Calibrated parameters	Key references
FLake (ver. 2.0)	Daily	Two-layer self-similar structure / 4	The Monin-Obukhov similarity relations	The water surface temperature is equal to the mixed-layer temperature, this is computed from calculation and constant update of heat fluxes	1. Parameter for profile relaxation time	Mironov (2008)
GLM (ver. 3.0.0)	Daily	Multilayer / 0.5m - max.depth	Algorithm used in Imberger and Patterson (1981)	Energy balance approach for surface layer mixing, eddy diffusivity approach for deep mixing	1. Diffuse attenuation coefficient 2. Longwave (or cloud) scaling factor 3. Wind speed scaling factor	Hipsey et al. (2019)
GOTM (ver. 5.1)	Daily	Multiple / 0.5m - max.depth	Based on Fairall et. al. (1996)	k-ε model	1. e-folding depth for visible; and e-folding depth for non-visible fraction of light 2. Minimum turbulent kinetic energy 3. Surface heat-flux factor 4. Shortwave radiation factor 5. Wind factor	Umlauf and Lemmin (2005); Burchard et al. (2006)
MyLake (ver. 1.12)	Daily	Multilayer / 0.5 m - max.depth	Diffusion coefficient in heat balance	Hondzo and Stefan thermal diffusion model	1. Wind shelter parameter 2. Minimum stability frequency 3. Non-PAR diffuse attenuation coefficient 4. PAR diffuse attenuation coefficient	Saloranta and Andersen (2007)
Simstrat (ver. 2.1.2)	Daily	Multilayer / 0.5m - max depth	Dirichlet condition	k-ε turbulence model with buoyancy and internal seiche parameterization	1. Fraction of wind energy transferred to seiche energy 2. As above during summer and winter 3. Fraction of forcing wind to wind at 10 m 4. Fit parameter scaling absorption of IR radiation from sky	Goudsmit et al. (2002)

3.3.2.1 Lake models description

FLake is a 1-D bulk model based on a two-layer parametric representation of the evolving temperature profile and on the integral budgets of heat and kinetic energy for the layers in question. The structure of the stratified layer between the upper mixed layer and the basin bottom is described using the concept of self-similarity (assumed shape) of the temperature-depth curve (Kirillin 2002). The same concept is used to describe the temperature structure of the thermally active upper layer of bottom sediments and, when present, of the ice and snow cover (Mironov 2008). FLake uses a lake-specific parameterization scheme to compute the fluxes of momentum, and of sensible and latent heat flux at the lake surface based on the Monin-Obukhov similarity relations.

GLM (General Lake Model; Hipsey et al. 2019) is a process-based 1-D hydrodynamic model that provides lake volume-averaged output over the vertical axis. It applies the integral energy assumption to calculate mixed layer depth from external turbulent kinetic energy. Mixing below the mixed layer depth is calculated through a parameterization of the eddy diffusivity coefficient to local gradients of buoyancy and shear. GLM applies a flexible grid structure, which allows the model grid cells to vary in thickness and total number of cells during a simulation. The latent heat flux in GLM is calculated using the algorithm presented in Imberger and Patterson (1981).

GOTM (General Ocean Turbulence Model; Burchard et al. 1999) is a vertical 1-D hydrodynamic water column model that includes key processes related to vertical mixing in marine and fresh waters (Umlauf and Lemmin 2005). It has been adapted for use in hydrodynamic modelling of inland water bodies (Sachse et al. 2014). GOTM is often used as a stand-alone model for investigating boundary layer dynamics in natural waters, but it can also be coupled to biogeochemical models. The surface fluxes of momentum, sensible and latent heat are calculated according to the bulk formulae explained by Fairall et al. (1996). This model has been used to model CO_2 dissolution (Enstad et al. 2008), water quality in lakes (Kong et al. 2022), to predict lake ecosystem state (Andersen et al. 2020) and to hindcast the thermal structure of lakes (Ayala et al. 2020; Moras et al. 2019).

MyLake is a 1-D process-based model used to simulate physical, chemical and biological dynamics in lakes (Saloranta and Andersen 2007). The model simulates thermal stratification, lake ice and snow cover, and phytoplankton dynamics, along with

sediment-water interactions using a simple sediment box model (v.1.12). MyLake uses regularly spaced water layers whose vertical resolution is defined by the user. The turbulent fluxes at the air-water interface are estimated using a diffusion coefficient in the heat balance as explained by Hondzo and Stefan (1993). Different versions of the model have been developed to simulate algal blooms (Salk et al. 2022), CO_2 and CH_4 (Kiuru et al. 2019), internal phosphorus loads (Markelov et al. 2019) and light attenuation dynamics (Pilla and Couture 2021).

Simstrat is a physical deterministic 1-D hydrodynamic model, including vertical mixing induced by internal seiches and surface ice (Gaudard et al. 2019; Goudsmit et al. 2002). This model uses layers of fixed depth (at 0.5 m intervals for lakes with < 50 m maximum depth and at 1 m intervals for lakes > 50 m), and supports multiple options for external forcing, comprising several meteorological variables or surface energy fluxes. Simstrat simulates thermal stratification and ice and snow formation (Gaudard et al. 2019). The surface fluxes are calculated using the Livingstone and Imboden (1989) formulae. Simstrat has been applied in lakes of varying climatic and morphometric conditions (Bärenbold et al. 2022; Råman Vinnå et al. 2021; Mesman et al. 2020; Kobler and Schmid 2019; Thiery et al. 2014).

3.3.2.2 Input data and calibration

Bias-adjusted climate projections from the Coupled Model Intercomparison Project (CMIP5) (Lange 2019) were used to drive each lake model in a one-way direction (i.e. lake-to-atmosphere interactions were not considered). Specifically, the lake models were driven by four GCMs: GFDL-ESM2M, HadGEM2-ES, IPSL-CM5A-LR, and MIROC5 during the 20th and 21st century (1901-2099). Historic simulations were forced using anthropogenic greenhouse gas and aerosol forcings in addition to natural forcing, and covered the period 1901 to 2005. Future projections simulate the evolution of the climate system under three different greenhouse gas emission scenarios Representative Concentration Pathways (RCP): RCP 2.6 (low-emission scenario), RCP 6.0 (medium-high-emission scenario), and RCP 8.5 (high-emission scenario), over the period 2006 to 2099. These pathways encompass a range of potential future global radiative forcing from anthropogenic greenhouse gases and aerosols. The climate data used to drive each lake model included projections of air temperature at 2 m, wind speed at 10 m, surface downwelling shortwave and longwave radiation, precipitation and specific humidity

(Table 3.2). The climate data had a spatial resolution of 0.5 degrees and covered the whole lake surface (Fig. 3.1). Additional input data to the lake models included the hypsographic relationship between depth and surface area (i.e. lake bathymetry), and water transparency (Golub et al. 2022). Salinity feedbacks, water inputs and withdrawals were not considered in the ISIMIP2b simulations. The calibration of the lake models in ISIMIP2b consisted of parameters and coefficients related to processes controlling surface heat and energy fluxes, light attenuation and turbulent kinetic energy and wind (Table 3.1). In addition, different optimization functions were used to minimize the difference between simulated and measured water temperatures. Specific details of model calibration and optimization are given by Golub et al. (2022).

Lake models in ISIMIP2b simulated historic and future projections of lake physical properties including, among other things, daily simulations of lake surface water temperature and latent heat flux. These data were used in this study to estimate evaporation rates in Lake Kinneret as:

$$E = \frac{Q_e}{\rho_o L_v} \hspace{3cm} (3.1)$$

where E is evaporation rate (m s^{-1}), Q_e is the latent heat flux (W m^{-2}), ρ_o is density of surface water (kg m^{-3}), calculated as a function of surface water temperature, T_0 (^{o}C), and $L_v = 2.501 \times 10^6 - 2370\, T_0$ is the latent heat of vaporization (J kg^{-1}).

Table 3.2. Climate forcing variables used as input to drive the lake models used in this study to simulate historical and future evaporation rates in Lake Kinneret.

Variable	Abbreviation	FLake	GLM	GOTM	MyLake	Simstrat
Near-surface relative humidity [%]	hurs		x		x	
Near-surface specific humidity [kg kg^{-1}]	huss	x		x		x
Precipitation [kg m^{-2} s^{-1}]	pr		x	x	x	x
Surface pressure [Pa]	ps			x	x	x

Surface downwelling longwave radiation [W m^{-2}]	rlds	x	x			x
Surface downwelling shortwave radiation [W m^{-2}]	rsds	x	x	x	x	x
Near-surface wind speed at 10m [m s^{-1}]	sfcWind	x	x	x	x	x
Near-surface air temperature [K]	tas	x	x	x	x	x
Eastward near-surface wind [m s^{-1}] (*)	uas			x		x
Northward near-surface wind [m s^{-1}] (*)	vas			x		x

(*) Not included in the bias-correction

3.3.3 Validation of simulated evaporation rates

We compared our simulations of lake evaporation from Lake Kinneret with those estimated from observed data (2000-2005), hereafter referred to as the reference evaporation. Most notably, meteorological data measured on the lake surface, and the algorithms available within the LakeMetabolizer package in R (Winslow et al. 2016; Woolway et al. 2015), were used to estimate the latent heat flux over the observational period, and subsequently the evaporation rates (eq. 3.1), using the bulk aerodynamic algorithm of Zeng et al. (1998). The motivation to use the algorithm of Zeng et al. (1998), as opposed to the many others available (Verburg and Antenucci 2010; Fairall et al. 2003), is that this bulk transfer method has been described as one of the least problematic bulk aerodynamic algorithms used by the scientific community for estimating surface energy fluxes (Brunke et al. 2003) and due to the open-access tools available for its calculation (Winslow et al. 2016; Woolway et al. 2015). In brief, this algorithm applies the Monin-Obukhov similarity theory to the atmospheric boundary layer and states that wind, temperature and humidity profile gradients depend on unique functions of the stability parameter (Text A1).

The latent heat flux, Q_e, used to estimate the reference evaporation was calculated as:

$$Q_e = \rho_z L_v C_{ez} u_z (q_0 - q_z) \qquad (3.2)$$

where $\rho_z = 100p/[R_a(T_z + 273.16)]$ is the density of the overlying air (kg m^{-3}); p is the surface air pressure (hPa); $R_a = 287(1 + 0.608q_z)$ is the gas constant for moist air (J kg^{-1} °C^{-1}; u_z is the wind speed (m s^{-1}) at height z_u (7.8 m) above the water surface; T_z is air temperature (°C) at height z_t (6.3 m) above the water surface; $q_0 = \lambda\, e_{sat}/p$ is the specific humidity at saturation pressure in kg kg^{-1}, with λ representing the ratio of the molecular weights for dry and moist air; e_{sat} is the saturated vapour pressure (hPa), calculated as $e_{sat} = 6.11 exp\left[\frac{17.27 T_0}{237.3 + T_0}\right]$; where T$_0$ (°C) is water surface temperature; $q_z = \lambda e/p$ is the specific humidity of the air (kg kg^{-1}) at height z_q (6.3 m) above the water surface, where $e = R_h e_z/100$ is actual vapour pressure, R_h is the relative humidity (%) and $e_z = 6.11 exp\left[\frac{17.27 T_z}{237.3 + T_z}\right]$ is the saturated vapour pressure (hPa) at z_t. Here, C_{ez} is the transfer coefficient for height z_q, which was calculated after correcting for wind measurement height and atmospheric stability (Zeng et al. 1998) (Fig. A.1). Using the estimated daily C_{ez}, we calculated an average C_{ez} of 1.7×10^{-3} during the study period, which is comparable to those estimated in other lakes (Table A.1). A detailed description of the estimation of reference evaporation is provided in the supplementary material (Text A1). The calculated Q_e was then used to estimate E using eq. 3.1. The estimated reference evaporation was also validated with monthly evaporation from water-solute-heat balances available from the Israel National Water Supply Company (Mekorot) over the common period 2000-2005.

Meteorological data over the 2000-2005 period was collected at a fixed height on-lake weather station (Tabgha) located in the northwest region of Lake Kinneret ~1 km offshore from the Kinneret Limnological Laboratory (35.54° longitude and 32.86° latitude). Air temperature and relative humidity were measured using a Young temperature/relative-humidity sensor probe model 43372C at 6.3 m above water surface. Shortwave radiation (305-2800 nm; W m^{-2}) and downwelling longwave radiation (5-25 nm; W m^{-2}) were measured using a Kipp & Zonen Delft BV pyranometer CM11 and

CG1, respectively at 6.5 m above water surface. Wind speed and direction were measured using a Young wind monitor MA-05106 at 7.8 m above the water surface. Water surface temperature was measured by a Young platinum floating temperature probe model 41342 at a depth of ~0.05 m (Rimmer et al. 2009; Gal et al. 2003). The reported measurement error of the water temperature observations was ± 0.005 °C (Van Emmerik et al. 2013; Rimmer et al. 2009). The sample frequency at the Tabgha station was 10 minutes, and maintenance works were carried out once a month. Precipitation observations were collected from an on-shore weather station located ~2 km from the southern point of the lake.

3.3.4 Statistical methods

To assess the performance of the lake model simulations, we compared reference and simulated evaporation rates over the common period (2000-2005), by estimating the normalized Mean Bias Error (MBE) and the normalized Root Mean Squared Error (RMSEc), and then summarizing the results within a Target Diagram (Jolliff et al. 2009). In addition, the Spearman Rank correlation (R) was used to assess the ability of the models to reproduce seasonal and intra-annual variability patterns from the reference evaporation.

3.3.5 Historic and future projections of precipitation and population

Complementary to our lake evaporation projections, we used historic and future projections of precipitation (P) in the region. These were also available from ISIMIP2b (Frieler et al. 2017). Projections of P and E were used in this study to estimate changes to the net flux of water between the atmosphere and the surface ($P - E$) during the historic and future periods. This net flux was also used to provide insights into potential future changes to the volume of water in Lake Kinneret. The precipitation data consisted of daily values for historic and future scenarios available for the four GCMs and the three RCPs used in projecting future changes in lake evaporation. In addition, we obtained historic and future population projections for the study area that were available from the ISIMIP3b for two Shared Socio-economic Pathways (i.e. SSP-1 comparable to RCP 2.6, and SSP-5 comparable to RCP 8.5) at a 0.5-degree spatial resolution. For Lake Kinneret and the surrounding region, we defined a bounding box of longitude: 34.25° - 36° and latitude:

29.25° - 33.75° when extracting the gridded population data. Concurrent changes in the local population and $P - E$ are used here to provide insights into changes in water stress within the region in the future. Precipitation and population data are freely available from the ISIMIP data repository at https://data.isimip.org.

3.4 Results

3.4.1 Validation of simulated evaporation rates

We compared simulated evaporation rates from our lake-climate model ensemble with the reference evaporation over the period 2000-2005. Our analysis suggests that lake evaporation estimates were sensitive to the choice of lake model. At daily and seasonal timescales, the reference evaporation was generally within the range of those simulated by the model ensemble, which suggests that they adequately capture the intra-annual variability of the reference evaporation. Moreover, the mean of the model ensemble followed closely the seasonal variation in the reference evaporation (Fig. 3.2). To better assess the performance of the individual lake models, we compared the monthly reference and simulated evaporation rates with three performance metrics, namely the Spearman Rank Correlation (R), RMSEc, and MBE (Fig. 3.3; Table 3.3). Our analysis suggested that, among the lake models tested, on the basis of the combined magnitudes of their MBE and RMSEc values (Figure 3.4b), MyLake compared best with the reference evaporation (R = 0.88; RMSEc = 0.14; MBE = -0.04), followed by FLake (R = 0.77; RMSEc = 0.19; MBE = -0.05), GOTM (R = 0.86; RMSEc = 0.23; MBE = 0.18), Simstrat (R = 0.76; RMSEc = 0.31; MBE = 0.27) and GLM (R = 0.77; RMSEc = 0.43; MBE = 0.41). Furthermore, a high correlation and low error (R = 0.92; RMSEc = 0.19; MBE = 0.15) was calculated between the mean of the lake-climate model ensemble and the reference evaporation (Fig. 3.4a). Overall, our comparison suggests that the mean of the models performed better than most of the individual models, and considerably better than the worst performing model (Fig. 3.4). Although, it is important to note that the mean of the ensemble showed slightly higher evaporation rates relative to the reference evaporation, particularly when evaporation rates were low (Fig. 3.4a).
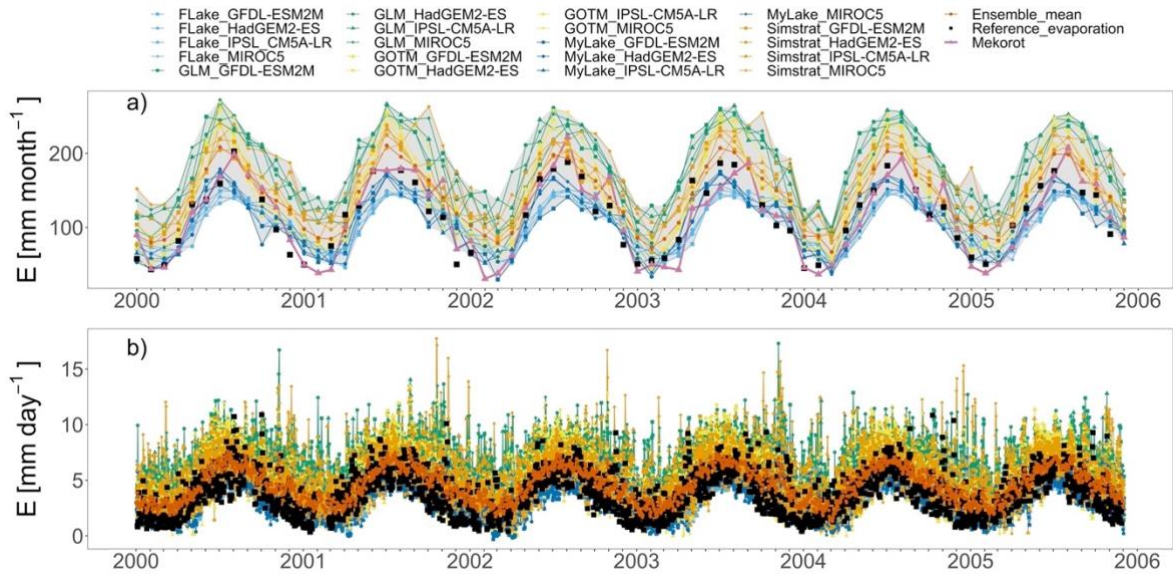
Figure 3.2 Simulated and reference evaporation rates over the historic period (2000-2005) in Lake Kinneret shown at (a) monthly and, (b) daily timescales. Each coloured line represents simulations from an unique lake model forced by an ensemble of GCMs. Pink lines in panel a represent the Mekorot evaporation rates (only available at monthly time steps). Orange lines represent the average of simulated lake evaporation rates from the lake-climate model ensemble. The shaded region in panel a represents the spread (min and max) across the model ensemble.

Table 3.3 Summary of Spearman rank correlation values (R), the Root Mean Square Error (RMSEc) and the Mean Bias Error (MBE) for lake-climate models with respect to reference evaporation over the period 2000-2005.

Lake model	Driving GCM	Spearman rank correlation [R]		RMSEc		MBE	
FLake	GFDL-ESM2M	0.76		0.19		-0.05	
	HadGEM2-ES	0.77	0.77	0.2	0.19	-0.06	-0.05
	IPSL-CM5A-LR	0.77		0.19		-0.04	
	MIROC5	0.76		0.19		-0.05	
GLM	GFDL-ESM2M	0.77		0.43		0.41	
	HadGEM2-ES	0.74	0.77	0.42	0.43	0.4	0.41
	IPSL-CM5A-LR	0.75		0.45		0.43	
	MIROC5	0.81		0.44		0.42	
GOTM	GFDL-ESM2M	0.91	0.86	0.19	0.23	0.14	0.18
	HadGEM2-ES	0.88		0.21		0.14	

	IPSL-CM5A-LR	0.87		0.23		0.18
	MIROC5	0.79		0.3		0.24
MyLake	GFDL-ESM2M	0.87		0.15		-0.05
	HadGEM2-ES	0.85	0.88	0.16	0.14	-0.04
	IPSL-CM5A-LR	0.9		0.13		-0.02
	MIROC5	0.89		0.13		-0.03
Simstrat	GFDL-ESM2M	0.89		0.25		0.23
	HadGEM2-ES	0.88	0.76	0.26	0.31	0.23
	IPSL-CM5A-LR	0.72		0.32		0.28
	MIROC5	0.53		0.41		0.34
Ensemble mean		0.92		0.19		0.15

Note: spanning values -0.04 (MyLake) and 0.27 (Simstrat) appear in the rightmost column.
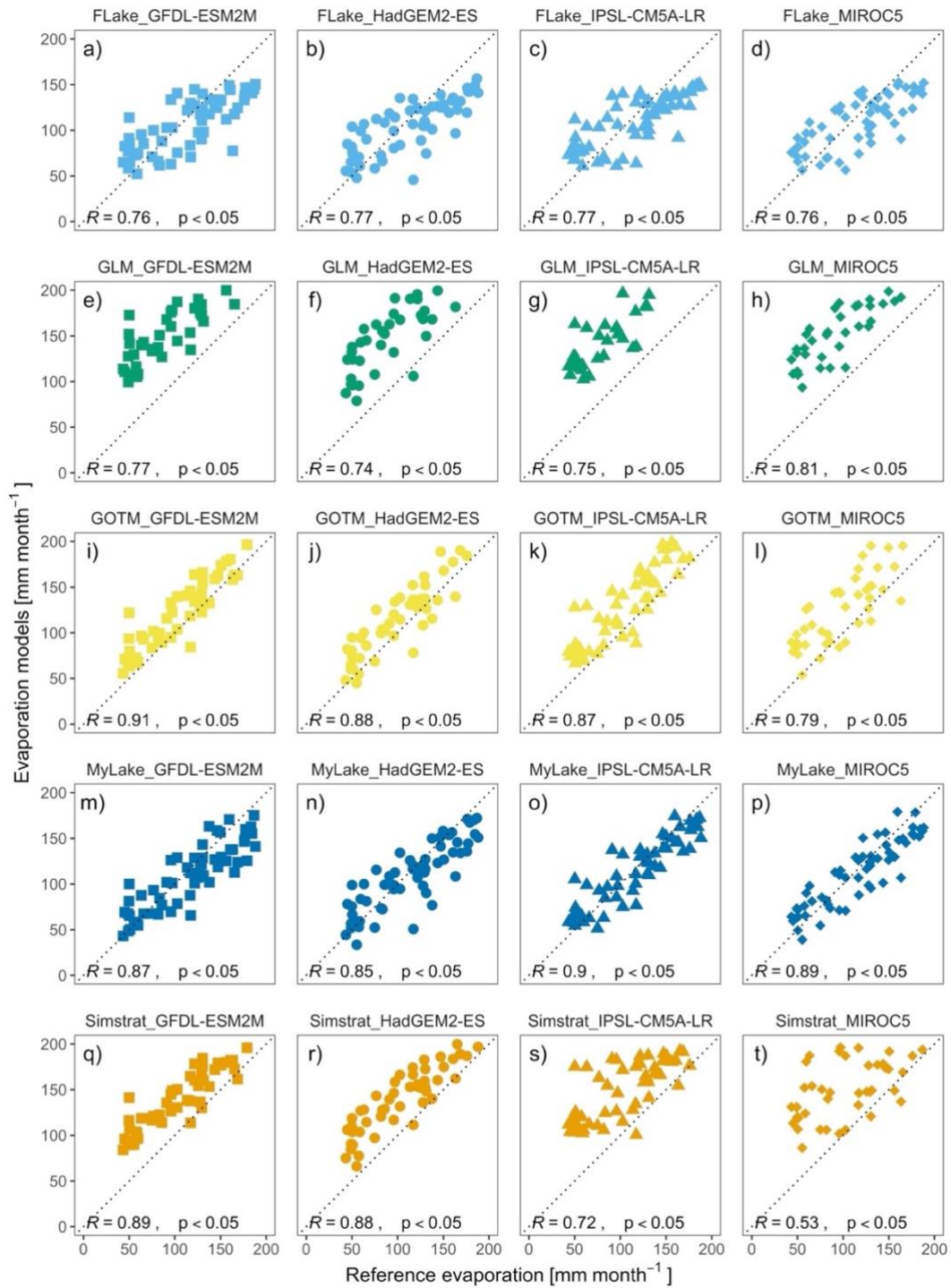
Figure 3.3 Monthly averaged simulated and reference evaporation rates from 2000-2005. Evaporation rates are compared with the Spearman Rank correlation (R), which is shown in the bottom left of each panel. The dashed line represents the 1:1 relationship between simulated and reference evaporation rates. Results are shown for each combination of lake climate models, namely (a-d) FLake, (e-h) GLM, (i-l) GOTM, (m-p) MyLake and (q-t) Simstrat, driven by the four General Circulation Models included in this study.
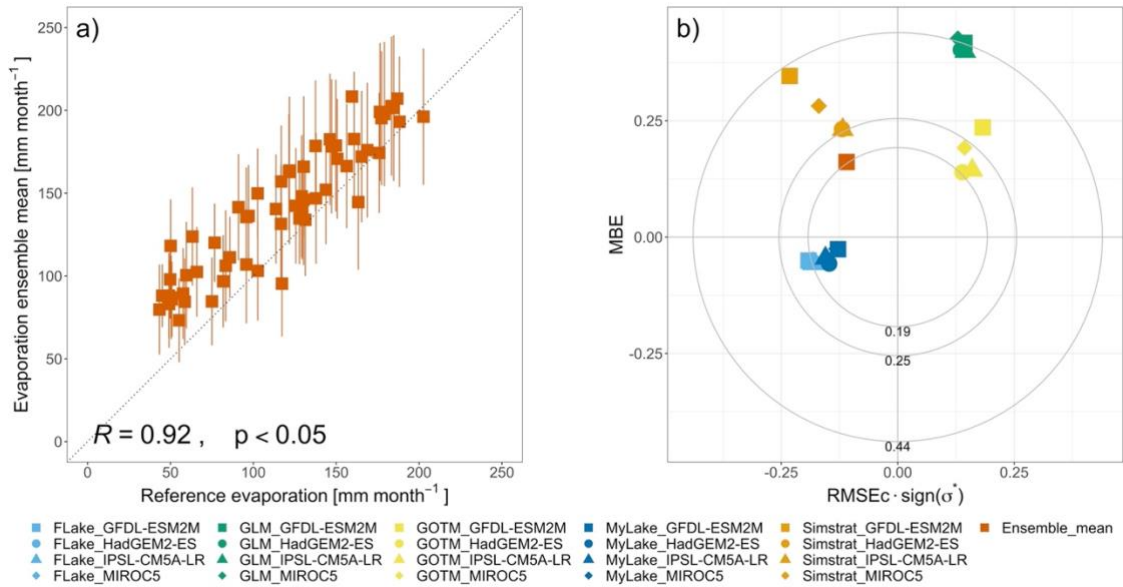
Figure 3.4 Shown are (a) a comparison of reference evaporation rates with the average projections across the lake-climate model ensemble (2000-2005); and (b) a target diagram which summarizes the normalized Mean Bias Error (MBE) and the normalized Root Mean Squared Error (RMSEc) of all simulated evaporation rates across the lake-climate model ensemble. The error bars surrounding the ensemble mean represent the standard deviation of the model ensemble over the 2000-2005 period. The dashed line in panel a represents the 1:1 relationship between the reference evaporation and the ensemble mean.

Moreover, a comparison of reference and simulated evaporation rates at seasonal timescales suggested that some models (e.g., FLake and MyLake) generally underestimated the reference evaporation rates during all seasons except winter, while the opposite was true for other models (e.g., GOTM, GLM and Simstrat), which overestimated evaporation rates in all seasons (Table 3.4). We also calculated the percent error in simulated seasonal evaporation rates, which demonstrated considerable variability in the performance of lake models across seasons. For instance, the models with the lowest percent error across seasons were MyLake (-17% to 21%) and FLake (-24% to 43%). GOTM exhibited errors between 5% and 45%, followed by Simstrat (20% and 99%), and GLM (38% and 111%) (Table 3.4). Overall, our results suggest that for this particular lake, and during the time period of interest, one could argue that MyLake and FLake performed best when simulating the reference evaporation. However, this

could be due to the positive and negative seasonal biases of these lake models being compensated for, and thus resulting in an overall lower bias than GOTM, GLM and Simstrat. Most impressive was the performance of the model ensemble, and particularly the mean, in capturing the seasonality in reference evaporation rates. Importantly, our analysis suggests that some lake models perform better than others during some parts of the year, and that including information from the ensemble is desirable. Finally, a comparison revealed that the reference evaporation closely captured the intra-annual variability of Mekorot evaporation estimates, which is reflected by the high correlation and low error estimated (R = 0.91; RMSEc = 0.10; MBE = -0.02) (see Fig. 3.2a and Fig. A.2), suggesting that our reference evaporation is robust and can be used as a basis for validation of our simulations.

Table 3.4 Comparison of seasonal evaporation rates between the lake models and the reference evaporation over the period 2000-2005. The colour code indicates when the lake model overestimates (blue) and underestimates (red) the reference evaporation. Darker/lighter colours indicate a higher/lower overestimation/underestimation of models.

Lake model	Driving GCM	Seasonal evaporation [mm season^{-1}]				Error [%]							
		Summer (JJA)	Autumn (SON)	Winter (DJF)	Spring (MAM)	Summer (JJA)		Autumn (SON)		Winter (DJF)		Spring (MAM)	
FLake	GFDL-ESM2M	420	384	259	217	-19		-4		42		-27	
FLake	HadGEM2-ES	413	373	259	222	-20	-20	-6	-3	42	43	-25	-24
FLake	IPSL-CM5A-LR	416	389	263	230	-20		-2		45		-22	
FLake	MIROC5	412	396	260	229	-20		-1		43		-23	
GLM	GFDL-ESM2M	703	609	397	433	36		53		118		46	
GLM	HadGEM2-ES	717	605	382	442	39	38	52	54	110	111	49	51
GLM	IPSL-CM5A-LR	726	616	380	462	41		55		109		56	
GLM	MIROC5	712	622	380	456	38		56		109		54	
GOTM	GFDL-ESM2M	639	450	253	299	24		13		39		1	
GOTM	HadGEM2-ES	673	435	243	313	30	29	9	19	33	45	6	5
GOTM	IPSL-CM5A-LR	669	467	277	317	29		17		52		7	
GOTM	MIROC5	696	539	285	313	35		35		57		6	
MyLake	GFDL-ESM2M	456	357	218	238	-12		-10		20		-20	
MyLake	HadGEM2-ES	469	358	229	243	-9	-10	-10	-8	26	21	-18	-17
MyLake	IPSL-CM5A-LR	476	376	221	255	-8		-6		21		-14	

MyLake	MIROC5	469	382	216	251	-9		-4		19		-15	
Simstrat	GFDL-ESM2M	619	487	323	380	20		22		77		28	
Simstrat	HadGEM2-ES	632	489	323	387	22	20	23	34	77	99	31	27
Simstrat	IPSL-CM5A-LR	626	522	391	366	21		31		115		24	
Simstrat	MIROC5	599	636	410	374	16		60		125		26	
Ensemble mean		577	474	298	321	12		19		64		8	
Reference evaporation		517	398	182	296								

3.4.2 Multi-model projections of lake evaporation during the 20th and 21st century

Following the validation of our model ensemble from 2000 to 2005, we investigated long-term historic and future changes in evaporation rates over the period 1900-2099. Specifically, we investigated differences across the lake-climate model ensemble in order to evaluate any discrepancies in projected future change (Fig. 3.5). The future projections showed noticeable differences in lake evaporation anomalies (i.e., the difference between lake evaporation in a given time period relative to the base period [1971-2000] average) across the model ensemble. By the end of this century (2070-2099), our results indicate that, for the high-emissions scenario (RCP 8.5), MyLake and FLake projected the smallest increase in evaporation rates of 320 mm year^{-1} and 329 mm year^{-1}, respectively, whereas GOTM (452 mm year^{-1}), GLM (438 mm year^{-1}) and Simstrat (388 mm year^{-1}) projected the highest change in evaporation rates (Table 3.5). Similar results were found during the historical period where the highest evaporation rates were estimated by GLM, GOTM and Simstrat. Furthermore, our analysis suggests that the magnitude of projected change in evaporation rates differ considerably depending on the GCM used to drive the lake models. Particularly, the average end of century evaporation anomalies across the GCMs (i.e. averaged across all lake models) varied between 109 mm year^{-1} (GFDL-ESM2M) and 227 mm year^{-1} (HadGEM2-ES) under RCP 2.6, between 220 mm year^{-1} (GFDL-ESM2M) and 323 mm year^{-1} (HadGEM2-ES) under RCP 6.0, and between 334 mm year^{-1} (GFDL-ESM2M) and 441 mm year^{-1} (HadGEM2-ES) under RCP 8.5. Thus, the lake simulations using GFDL-ESM2M as input data projected considerably lower evaporation rates this century, and those using HadGEM2-ES projected the greatest change, on average.

Table 3.5 Annual evaporation projections under historical and future scenarios of climate change: RCP 2.6, 6.0 and 8.5 across lake-climate models. The values for the historical period correspond to the average over the period 1971-2000. The values for the RCP scenarios correspond to the average over the period 2070-2099. Lake evaporation simulations are presented for each lake-climate combination. When presenting the change in evaporation, we also calculate the average for each lake model simulated across the GCMs, shown in bold.

Lake model	Driving GCM	Evaporation [mm year⁻¹]				Evaporation change [mm year⁻¹]					
		Historical	RCP 2.6	RCP 6.0	RCP 8.5	RCP 2.6		RCP 6.0		RCP 8.5	
FLake	GFDL-ESM2M	1247	1339	1421	1519	92		173		272	
	HadGEM2-ES	1252	1413	1501	1587	160	**127**	248	**228**	334	**329**
	IPSL-CM5A-LR	1257	1393	1555	1698	136		298		441	
	MIROC5	1261	1383	1455	1529	121		194		268	
GLM	GFDL-ESM2M	2106	2220	2357	2505	114		251		399	
	HadGEM2-ES	2110	2351	2469	2609	241	**169**	359	**278**	500	**438**
	IPSL-CM5A-LR	2106	2277	2338	2578	171		232		472	
	MIROC5	2118	2269	2386	2500	152		268		382	
GOTM	GFDL-ESM2M	2340	2482	2619	2731	141		279		391	
	HadGEM2-ES	2376	2679	2787	2927	303	**204**	410	**313**	551	**452**
	IPSL-CM5A-LR	2433	2621	2686	2898	187		253		465	
	MIROC5	2597	2782	2909	2998	186		312		401	
MyLake	GFDL-ESM2M	1253	1350	1446	1542	96		192		289	
	HadGEM2-ES	1269	1485	1555	1653	216	**147**	287	**220**	385	**320**
	IPSL-CM5A-LR	1262	1406	1460	1610	145		199		348	
	MIROC5	1277	1406	1480	1535	129		203		258	
Simstrat	GFDL-ESM2M	1789	1889	1993	2110	100		204		321	
	HadGEM2-ES	1805	2020	2116	2240	215	**153**	311	**250**	435	**388**
	IPSL-CM5A-LR	1847	1998	2070	2275	151		222		427	
	MIROC5	1970	2118	2231	2339	148		261		369	
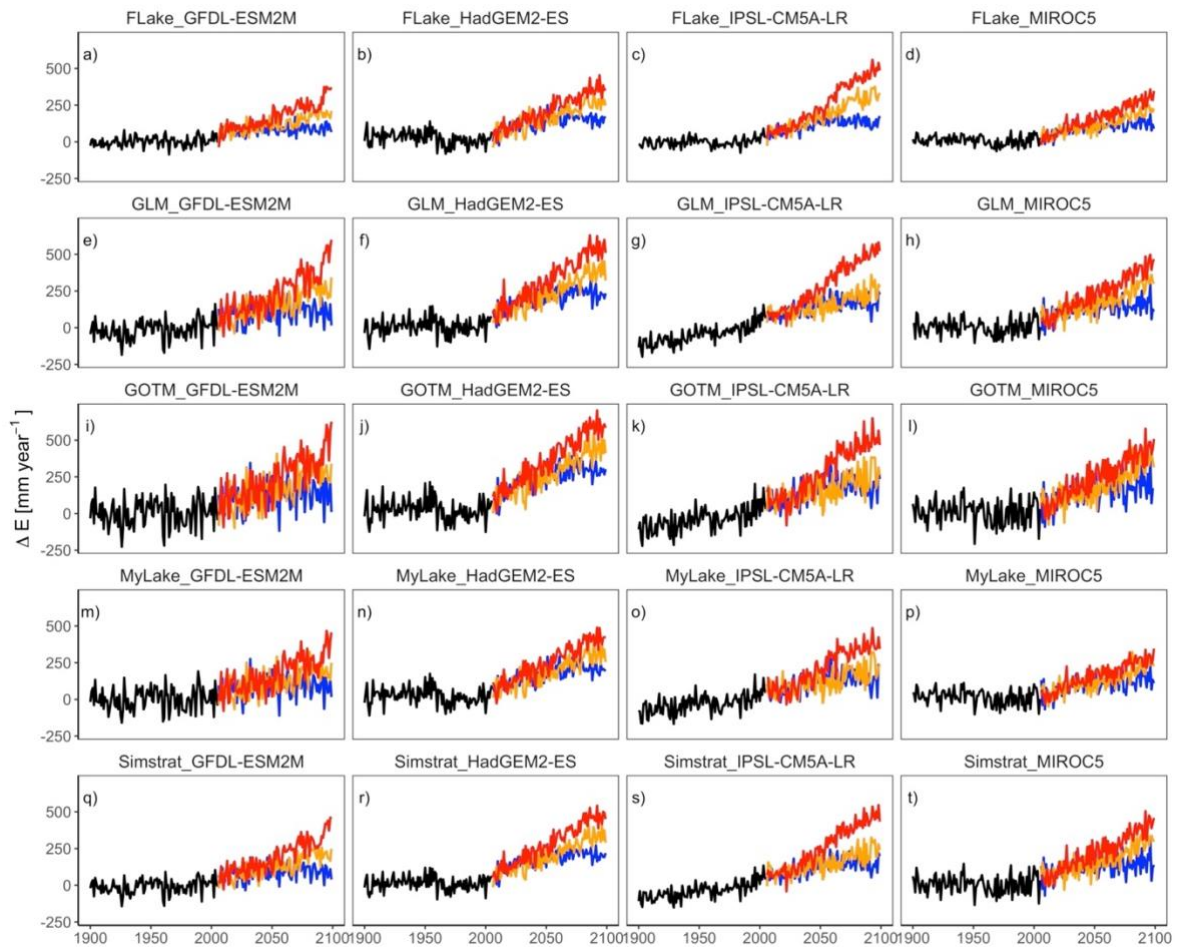
Figure 3.5 Projected changes in annual lake evaporation during the historic (1901-2005) and future (2006-2099) periods. Projections are shown for each of the individual lake-climate models, namely for (a-d) FLake, (e-h) GLM, (i-l) GOTM, (m-p) MyLake and (q-t) Simstrat, driven by the four General Circulation Models included in this study. Black lines represent the historical period, and the coloured lines represent the future period, with the blue, orange and red representing the projected change under RCP (Representative Concentration Pathway) 2.6, 6.0, and 8.5, respectively. Anomalies (ΔE) are quoted relative to the 1971-2000 base-period average.

Given the differences in simulated evaporation rates among the lake-climate model ensemble, it seems relevant to combine the individual ensemble members and to calculate the average and standard deviation among them. The model ensemble indicated an average annual evaporation of 1784±473 mm year^{-1} (quoted uncertainties represent the standard deviation from the model ensemble) during the latter stages of the 20th century

41

(1971-2000 average). During the 21st century (2006 to 2099), the average of the model ensemble demonstrates that evaporation rates are projected to increase considerably in Lake Kinneret (Fig. 3.6). Under RCP 2.6, lake evaporation is projected to increase by 160 ± 70 mm year^{-1} by the end of the 21st century (2070 to 2099). For RCP 6.0, lake evaporation is projected to increase by 258 ± 76 mm year^{-1}. The largest change in lake evaporation is projected under RCP 8.5 with evaporation rates increasing by 385 ± 93 mm year^{-1}. These projected changes correspond to a percent increase of 9%, 14% and 22%, for RCP 2.6, 6.0 and 8.5 respectively, compared to the base-period average (Table 3.6).
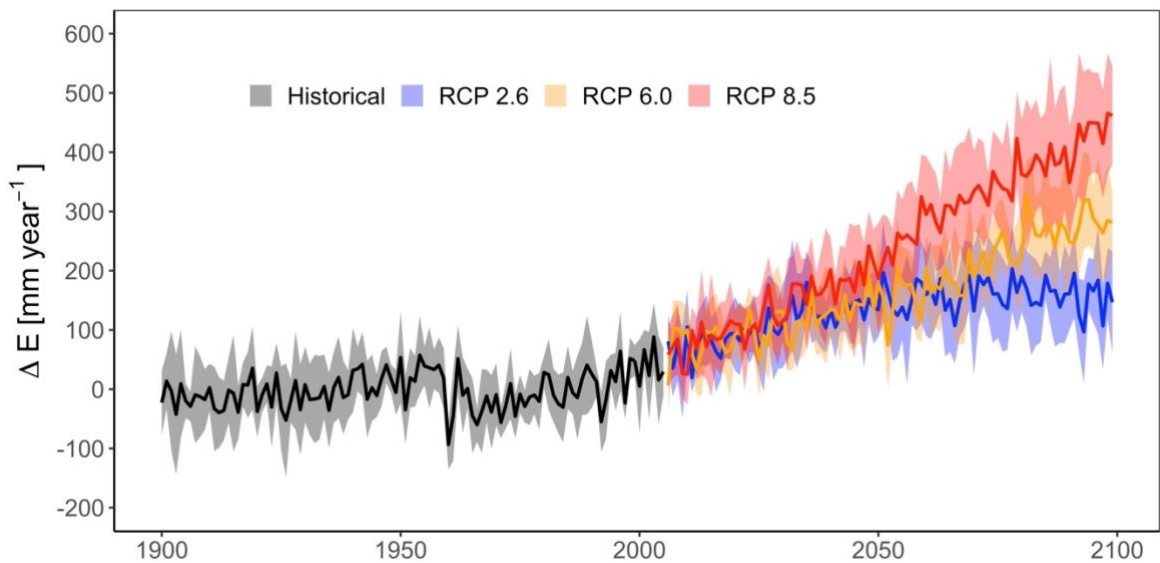
Figure 3.6 Projected changes in annual lake evaporation during the historic (1901-2005) and future (2006-2099) periods in Lake Kinneret. The average of the model ensemble is shown by the thick lines, the standard deviation across the model ensemble is represented by the shaded area. Anomalies (ΔE) are quoted relative to the 1971-2000 base period average for RCP (Representative Concentration Pathway) 2.6, 6.0 and 8.5.

Table 3.6 Annual evaporation projections by the end of the 21st century under future scenarios of climate change: RCP 2.6, 6.0 and 8.5. The evaporation estimates for the historic period correspond to the average over 1971-2000 and the future period corresponds to 2070-2099. Anomalies (Δ) are calculated as future minus historic.

Scenario	Evaporation [mm year⁻¹]	Evaporation change (ΔE) [mm year⁻¹]	Evaporation change (ΔE) [%]
Historical	1784±473	-	-
RCP 2.6	1944±498	160±70	9
RCP 6.0	2042±509	258±76	14
RCP 8.5	2169±530	385±93	22

The magnitude of change in lake evaporation will not be the same throughout the year, but will change differently across seasons (Fig. 3.7). Moreover, similar to our projections of annual evaporation rates, the projected changes in evaporation across seasons will vary across the lake-climate model ensemble. Our future projections of seasonal evaporation show an overall increase compared to the historic period for all seasons and RCP scenarios (Fig. 3.7; Table 3.7). In the historic period (1971-2000) evaporation estimates were between 314±77 mm season⁻¹ in the winter and 621±197 mm season⁻¹ in the summer. We calculated the projected changes in seasonal evaporation by the end of the 21st century (2070-2099) and found that the greatest change occurred in spring, corresponding to an increase of 12% for RCP 2.6, 20% for RCP 6.0 and 30% for RCP 8.5. These changes were followed by an increase in evaporation during autumn, corresponding to an increase of 9% for RCP 2.6, 14% for RCP 6.0 and 20% for RCP 8.5 (Table 3.7). The lowest changes across RCP scenarios were detected in the winter with increases of 8%, 10% and 19% under RCPs 2.6, 6.0 and 8.5 respectively.
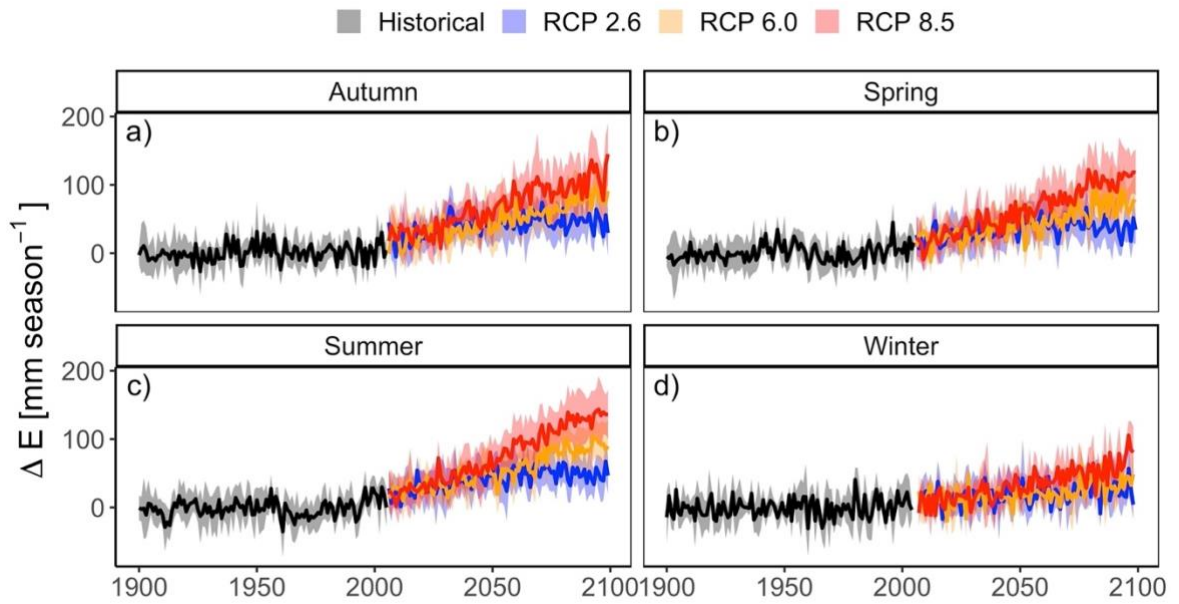
Figure 3.7 Projected changes in seasonal lake evaporation during the historic (1901-2005) and future (2006-2099) periods in Lake Kinneret for (a) Autumn, (b) Spring, (c) Summer, and (d) Winter. The average of the model ensemble is shown by the thick lines, the standard deviation across the model ensemble is represented by the shaded area. Anomalies (ΔE) are quoted relative to the 1971-2000 base period average for RCP (Representative Concentration Pathway) 2.6, 6.0 and 8.5.

Table 3.7 Seasonal evaporation projections by the end of the 21st century under future scenarios of climate change: RCP 2.6, 6.0 and 8.5. The evaporation estimates for the historic period correspond to 1971-2000 and the future estimates correspond to 2070-2099. Anomalies (Δ) are calculated as future minus historic.

Scenarios	Seasonal evaporation change (ΔE) [mm season^{-1}]				Seasonal evaporation change (ΔE) [%]			
	Autumn	Spring	Summer	Winter	Autumn	Spring	Summer	Winter
RCP 2.6	46±27	39±27	50±26	24±25	9	12	8	8
RCP 6.0	72±33	68±32	85±32	32±26	14	20	14	10
RCP 8.5	102±39	101±37	124±36	58±28	20	30	20	19

44

3.4.3 Concurrent changes in precipitation and evaporation

To evaluate the potential impact of the simulated changes in lake evaporation on water level in Lake Kinneret, we analysed the combined impacts of climate change on precipitation and evaporation at annual timescales. Changes in precipitation for our study site were highly variable, with an overall decreasing trend from 2005 until the end of the 21st century for all RCPs (Figure 3.8a). The average precipitation over the historic period was 454 ± 100 mm year^{-1}, but decreased by -28 ± 109 mm year^{-1} (-6%), -98 ± 117 mm year^{-1} (-22%), and -145 ± 102 mm year^{-1} (-32%) by the end of the century under RCP 2.6, 6.0 and 8.5, respectively (Table 3.8). By calculating the difference between precipitation and evaporation (P-E), our analysis showed that the change in multi-model average evaporation was projected to be greater than the change in multi-model average precipitation. These results suggest that changes in lake evaporation will likely be greater than those in precipitation under all RCPs this century. Notably, all RCPs suggested a decrease in P-E until the end of the century (Fig. 3.8b). This change reflected the rapid increase in projected evaporation rates and the concurrent substantial decrease in projected precipitation this century within the study region. Relative to the 1971-2000 base period average (-1330 ± 488 mm year^{-1}), P-E continuously decreased throughout the 21st century. Notably, under RCPs 2.6, 6.0 and 8.5, P-E will decrease by -188 ± 129 mm year^{-1}, -356 ± 148 mm year^{-1}, and -530 ± 145 mm year^{-1}, respectively, by the end of the 21st century (2070-2099) (Fig. 3.8b). These changes represent a percent change in P-E of -14%, -27% and -40% under RCP 2.6, 6.0, and 8.5, respectively (Table 3.8).
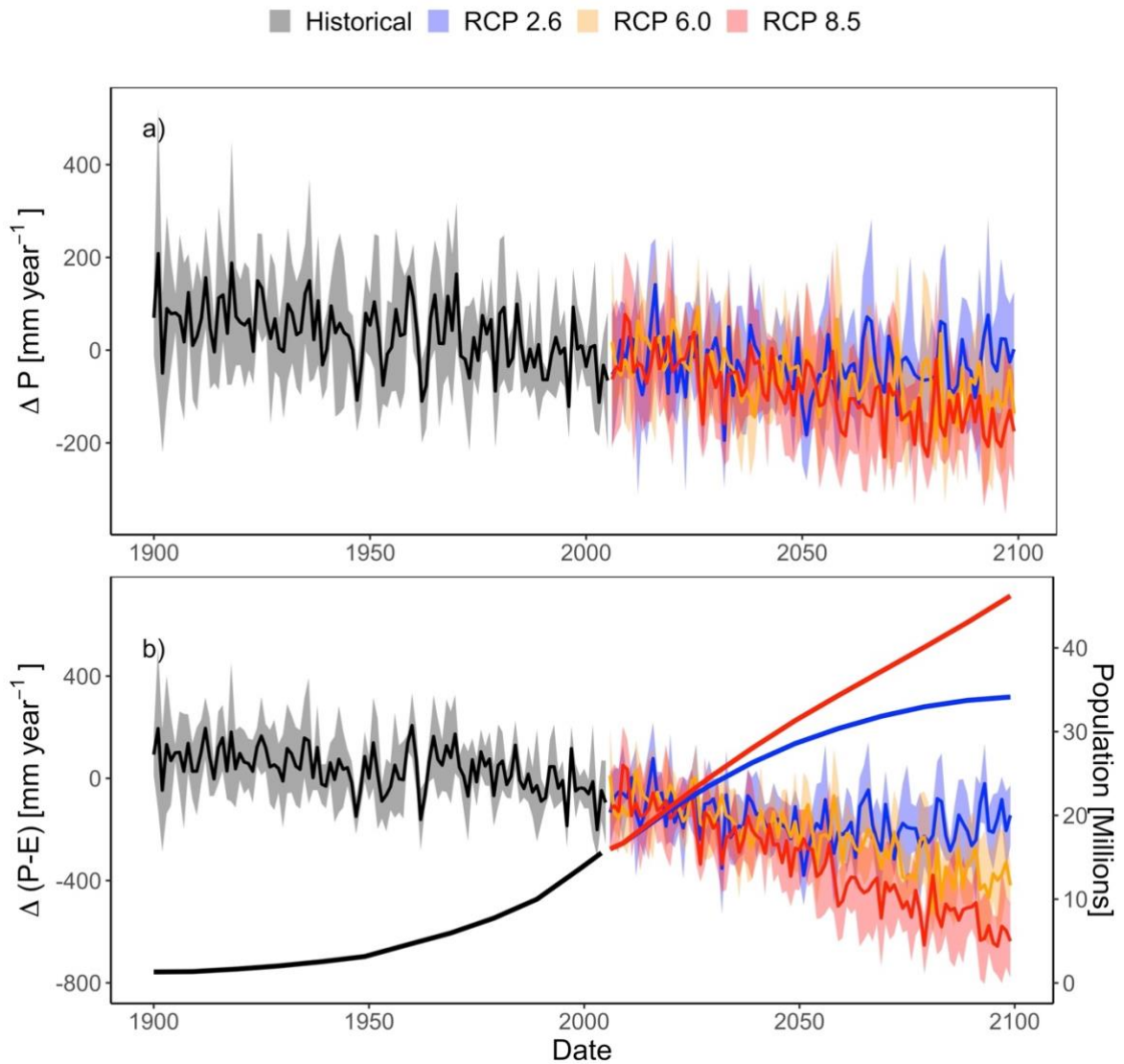
Figure 3.8 Projected changes during the historic (1901-2005) and future (2006-2099)
periods in Lake Kinneret for (a) precipitation and (b) precipitation minus evaporation
(P-E) and population over the study area. The average of the model ensemble is shown
by the thick lines and the standard deviation across the model ensemble is represented by
the shaded area. Anomalies (ΔP and Δ(P-E)) are quoted relative to the 1971-2000 base
period average for RCP (Representative Concentration Pathway) 2.6, 6.0 and 8.5.

The local population within the study region, which was estimated to be around
10 million people during the 1971-2000 base period, is projected to increase during the
twenty-first century (Fig. 3.8b). Projections for the shared socioeconomic pathways SSP-
1 and SSP-5 (i.e. comparable to RCP 2.6 and RCP 8.5, respectively) showed a pronounced

future increase compared to the historical period. In the case of SSP-1/RCP 2.6 there was a steep increase projected for the local population until the mid-21st century (i.e., 2050s), and afterwards a more steady increase towards 2099, with an average population of 33 million. Under SSP-5/RCP 8.5, the future projections demonstrate a very steep increase of population starting from 2005, with an average population of 42 million people by the end of this century. When comparing these increases to the historical period, we estimated a striking increase in population of 248% for the RCP 2.6 scenario, and 337% for the RCP 8.5 (Table 3.8).

Table 3.8 Summary of precipitation (P), precipitation minus evaporation (P-E), and population changes by the end of the 21st century under future scenarios of climate change: RCP 2.6, 6.0 and 8.5. Estimates for the historic period correspond to 1971-2000 and the future estimates correspond to 2070-2099. Anomalies (Δ) are calculated as future minus historic.

Scenario	ΔP [mm year^{-1}]	ΔP [%]	Δ(P - E) [mm year^{-1}]	Δ(P - E) [%]	Population [Million inhabitants]	Population change [%]
Historical	-	-	-	-	10	-
RCP 2.6	-28±109	-6	-188±129	-14	33	248
RCP 6.0	-98±117	-22	-356±148	-27	(*)	(*)
RCP 8.5	-145±102	-32	-530±145	-40	42	337

3.5 Discussion

Projecting future changes in lake evaporation is critical for ecosystem and water resource management, particularly in areas where these resources are already under immense pressure (Prange et al. 2020; Givati et al. 2019). In this study, we provide an assessment of projected changes in evaporation rates in Lake Kinneret, a socioeconomically important lake in the Middle East, using a model ensemble of 20 lake-climate model combinations (5 lake models and 4 GCMs). We found that the ensemble mean of the models tested was superior to most of the individual lake-climate model realizations in describing the reference evaporation rates in Lake Kinneret during the historical period.

This is in agreement with our expectations and in-line with experiences on the use of ensemble modelling within the climate science community (Moore et al. 2021; Trolle et al. 2014), which have often shown that an ensemble approach provides more robust projections of complex systems compared to any single model. By applying 20 lake-climate model combinations to simulate one lake, we were able to understand key differences in model performance and, likewise, to demonstrate the usefulness of an ensemble approach for projecting lake responses to climate change. The lake-climate models generally agreed on the seasonal variability in evaporation rates, and match those shown in the reference evaporation calculated using observational data, with the ensemble mean often showing the best performance. Regarding our future projections, our analysis also demonstrated that it is critical to consider an ensemble of both lake and climate model simulations when projecting future change in lakes, given the spread of the projected changes.

Although we believe that this study bridges an important knowledge gap, there are some limitations that should be considered when interpreting our findings. Firstly, our projections are generated with 1-D process-based lake models, and thus horizontal features in lakes and the intra-lake responses to climate change will not be captured (Laval et al. 2003). In practice, the 1-D lake models used in this study assume that evaporation rates are uniform over the entire lake surface given that input data to the models was available for one location representative of the lake. However, field observations in different regions have shown that the spatial distribution of lake evaporation is highly variable (Lenters et al. 2013; Mahrer and Assouline 1993). Similarly, one might expect within-lake differences in the magnitude of change in lake evaporation rates under climate change, as has already been demonstrated for lake surface temperature (Woolway and Merchant 2018; Mason et al. 2016). The intra-lake variability in evaporation rates could be simulated with 3-D lake models, but these complex models are data intensive and computationally expensive (Amadori et al. 2021), and therefore are not often used for ensemble lake modelling, particularly for investigating future change (Zamani et al. 2021). Furthermore, our comparison of the simulations with reference evaporation from Lake Kinneret, demonstrated some differences in the ability of the lake models to capture some of the variability in evaporation rates. This was particularly evident in winter, when seasonal evaporation rates in this lake are at their lowest. However, evaporation rates at

48

this time of year are unlikely to have a considerable influence on annual evaporation rates in this lake, which are the primary focus of our study. Some of the differences between the simulations and reference evaporation are likely due to the meteorological data used to drive the lake models. Specifically, the GCMs used in this study provide historical and future projections of atmospheric conditions at a relatively coarse (0.5 degree) spatial resolution. The gridded climate data are thus unlikely to capture all of the short-scale spatial variations occurring at the lake surface, particularly given the complex topography in the study region. In addition to these limitations, our model simulations do not consider two-way interactions between the lake and the overlying atmosphere. Furthermore, when evaporation rates are relatively low (e.g., in winter), the percent difference between simulated and reference evaporation will be relatively large.

While we acknowledge the limitations of using GCMs in such regions, these data are undoubtedly the most appropriate to predict future changes in the climate (Busuioc et al. 2001) and, in turn, the studied lake. In an attempt to address the spatial mismatch between observed and simulated meteorological data from the study region, we used bias-corrected GCM output data from ISIMIP2b as input to the lake models (Lange 2019; Frieler et al. 2017). This bias adjustment essentially alters the statistics of climate simulation data for the purpose of making them more similar to observations. To our knowledge, few studies have used GCM data to project future impacts of climate change on Lake Kinneret (Rimmer et al. 2011), with others using weather generators to forecast changes in the near future (Gal et al. 2020). Finally, the results presented in this study, do not consider ongoing climate change adaptations carried by the Israeli government. Despite the limitations described above, the results of our study provide important insights about the future changes in evaporation rates in Lake Kinneret, and is a valuable pilot study for larger scale, across lake, assessments.

The strength of this study is the use of a large ensemble of lake model projections, which has allowed us to identify likely scenarios of future change in lake evaporation within a socioeconomically critical lake. The large ensemble was invaluable in allowing us to not only project future change in evaporation, but also to consider a suite of simulations and, in turn, include uncertainty bounds within our projections. It is our hope that in underscoring the value of including ensemble modelling in lake research, our work motivates continued efforts to employ an ensemble of lake models for better

understanding lake responses to climate change. We see good prospects for continued coordination between lake model development, as well as their inclusion in large climate simulations, particularly given the recent expansion of computing resources facilitates including increasing spatial resolution and correspondingly improved process representation (non-thermodynamic processes in lakes, improved large-scale hydrological processes, etc.). We believe that upscaling the multi-model approach introduced in this study to multiple lakes distributed across climatic gradients and in lakes of varying sizes and physiographic characteristics, could provide important insights into lake evaporation variability and responses to climate change.

The access of water resources for human consumption and ecosystem services highly depends on the spatio-temporal distribution of not only evaporation, but also precipitation, two key components of the water budget of lakes (Konapala et al. 2020). In this study, we estimated the impact of changes in both of these metrics, and consequently on P-E, in Lake Kinneret. We found that in all future climate change scenarios, projected changes in lake evaporation were greater than the projected changes in precipitation, with P-E being predominantly negative, and increasingly so throughout the 21st century. Specifically, by the end of this century, our projections suggest that P-E in Lake Kinneret will decrease by between 14 and 40% under RCP 2.6 and 8.5, respectively. These projected changes largely align with those described by Givati et al. (2019), who projected a future decrease in precipitation in this region, resulting in a 44% decrease in the flow of water from the Jordan River (i.e. the main inflow to Lake Kinneret) by 2050-2079 under RCP 8.5. However, similar dramatic changes in the water budget of Lake Kinneret have already been reported, with observational data demonstrating that precipitation in the Kinneret river basin has reduced considerably since 1985 (Givati et al. 2019). Similarly, streamflow observations from the Jordan River indicate that flow rates have decreased by more than 50% since 2004, provoking historically low levels in Lake Kinneret in 2018 (Tal 2019a).

If the P-E balance of Lake Kinneret changes in-line with our future projections, water availability in the region will likely be severely stressed this century. Notably, in the absence of substantial water inflow changes (e.g., less water extraction for irrigation), a decrease in P-E will likely reduce the total lake volume (Zhou et al. 2021). Our analysis has also demonstrated that a decline in P-E this century will likely occur in parallel with

50

a rapid growth in population. Most notably, the population in the studied region is projected to increase between 248% and 337% by the end of this century under RCP 2.6 and 8.5, respectively. This suggests that a growing population will likely become increasingly dependent on water from Lake Kinneret. Notably, the intensification of water scarcity driven by an increasing deficit in P-E combined with a rapid growth in population, is likely to further enhance the depletion of Lake Kinneret and further enhance the already existing water stress in the region. However, it is also important to note that an increase in water stress within the region might reduce the local population due to possible migration in the future, which is not considered in our assessment. As well as the serious socioeconomic implications of declining water level, influenced by an increasing deficit in P-E, this could lead to critical ecosystem disturbances, such as an increase in salinity with implications for not only physical lake processes (Ladwig et al. 2021) but also the community composition, biomass, and diversity of phytoplankton, zooplankton, macrophytes and fish (Jeppesen et al. 2015), as well as a weakening of key species, the proliferation of invasive species, and a loss of biodiversity (Zohary and Ostrovsky 2011).

Chapter 4 Increasing warm-season evaporation rates across European lakes due to climate change

Authors: Sofia La Fuente[1*], Eleanor Jennings[1], John Lenters[2], Piet Verburg[3], Georgiy Kirillin[4], Tom Shatwell[5], Raoul-Marie Couture[6], Marianne Côté[6], C. Love Råman Vinnå[7], R. Iestyn Woolway[8]

Affiliations:

1. Centre for Freshwater and Environmental Studies, Dundalk Institute of Technology, Dundalk, Ireland
2. University of Michigan, UM Biological Station, Pellston, Michigan, USA
3. National Institute of Water and Atmospheric Research, Wellington, New Zealand
4. Leibniz-Institute of Freshwater Ecology and Inland Fisheries (IGB), Berlin, Germany
5. Helmholtz Centre for Environmental Research, Department of Lake Research, Magdeburg, Germany
6. Centre for Northern Studies (CEN), Takuvik Joint International Laboratory, and Department of Chemistry, Université Laval, Quebec City, QC, Canada
7. Eawag, Swiss Federal Institute of Aquatic Science and Technology, Surface Waters - Research and Management, Kastanienbaum, Switzerland
8. School of Ocean Sciences, Bangor University, Menai Bridge, Anglesey, Wales

*Corresponding author: ruthsofia.lafuentepillco@dkit.ie
*Postal address: Centre for Freshwater and Environmental Studies, Dundalk Institute of Technology, Dundalk, Marshes Upper A91 K584, Co. Louth, Ireland

Keywords: climate change, Europe, inland waters, multi-model, water availability

4.1 Abstract

Lakes represent a vital source of freshwater, accounting for 87% of the Earth's freshwater resources and serving various purposes, including human consumption. As climate

change continues to unfold, understanding the potential evaporative water losses from lakes becomes crucial for effective water management strategies. Here we investigate the impacts of climate change on the evaporation rates of 23 European lakes and reservoirs of varying size. To assess the evaporation trends, we employ a 12-member ensemble of model projections, utilizing three 1-D process-based lake models. These lake models were driven by bias-corrected future climate simulations from four General Circulation Models (GCMs) from the Coupled Model Intercomparison Project Phase 5 (CMIP5), considering historic and Representative Concentration Pathways (RCPs) 2.6, 6.0 and 8.5 over the 1901-2099 period. Our findings reveal a consistent projection of increased warm-season evaporation across all lakes, though the magnitude varies depending on specific factors. By the end of this century (2070-2099), we estimate a 21% and 42% increase in evaporation under the RCP 2.6 and 8.5 scenarios respectively. These projected increases in evaporation rates underscore the significance of adapting strategic management approaches for European lakes to cope with the far-reaching consequences of climate change.

4.2 Introduction

Evaporation plays a pivotal role in the depletion of freshwater resources, contributing to fluctuations in both water level and the surface area of lakes (Woolway et al. 2020; Friedrich et al. 2018; Lenters et al. 2005). Characterized by their changing open-water areas and the occurrence of pronounced vapor pressure gradients at their air-water interface, lakes are prone to significant water loss via evaporation (Zhao et al. 2022; Zhang and Liu 2014; Lenters et al. 2005). The volume of evaporative water loss is influenced by lake surface area and the rate of evaporation (Zhao et al. 2022; Wang et al. 2020; Zhao and Gao 2019). The latter can vary widely among geographical regions and is strongly modulated by regional hydroclimate (Zhou et al. 2021; Wang et al. 2018). Lake evaporation plays a key role in the water and energy budget of lakes and is central to the modification of lake temperature and related processes such as mixing and stratification (Ye et al. 2019; Lenters et al. 2013; Spence et al. 2013; Mishra et al. 2011; MacIntyre et al. 2009). Some of the most direct atmospheric drivers of lake evaporation are wind speed and absolute humidity (Lenters et al. 2014; Van Cleave et al. 2014; McVicar et al. 2012). However, due to the influence of lake surface temperature on the

vapor pressure gradient, other atmospheric and limnological factors also play a considerable role in the evaporation rate (Friedrich et al. 2018; Lenters et al. 2005; Brutsaert 1982). For instance, the energy budget components of a lake's surface that modify evaporation comprise various factors, including incoming and outgoing short- and long-wave radiation as well as the exchange of sensible heat at the air-water interface (Friedrich et al. 2018). Moreover, various distinctive attributes of lakes, including depth, water color and the effect of terrestrial/topographic sheltering can further modulate the extent and timing of lake evaporation, primarily by influencing surface water temperature and the intensity of near-surface turbulence (Wang et al. 2020; McVicar et al. 2012; Read et al. 2012). Indeed, lake evaporation dynamics can significantly alter various aspects within a lake, with the most important effect being on the alteration of water level and surface extent (Friedrich et al. 2018; Xiao et al. 2018; Chen et al. 2017). However, the water balance of most lakes is not only dictated by changes in evaporation but also by changes in precipitation (Woolway et al. 2022; Vystavna et al. 2021). A combined increase in evaporation with a decrease in precipitation can significantly reduce the water quantity of a lake and in turn negatively affect its ecosystem functioning (Finger Higgens et al. 2019; Tal 2019b). For instance, depleting water levels can limit the access to drinking water, food transportation, fisheries, and energy generation, significantly influencing the economy particularly of regions that highly depend on the ecosystem services that lakes provide (Yao et al. 2023; Gownaris et al. 2017; Wurtsbaugh et al. 2017; Gronewold et al. 2013; Bergmann-Baker et al. 1995).

On this basis, simulating and understanding the response of lake evaporation to climate and its relationship with precipitation is crucial for the water management of lakes (Woolway et al. 2020; Friedrich et al. 2018; Lenters et al. 2005). Recent observations have documented an upward trend in lake evaporation both locally and globally, while future projections indicate a further rise in many regions within a warming world (Zhao et al. 2023; La Fuente et al. 2022; Althoff et al. 2020; Xiao et al. 2018; Helfer et al. 2012). By the end of the 21st century, it is projected that global mean annual lake evaporation will increase by approximately 16% (Wang et al. 2018). The largest increases in annual evaporation are projected at low latitudes, where evaporation rates are already high (Zhou et al. 2021; Althoff et al. 2020; Wang et al. 2018; Helfer et al. 2012), but also in lakes that will transition to becoming ice-free, allowing the potential for evaporation to occur

year-round (Li et al. 2022; Woolway et al. 2020; Sharma et al. 2019). Moreover, lake evaporation is expected to increase more rapidly in regions that will experience a drying hydroclimate, which will amplify evaporation increase by enlarging the surface vapor pressure deficit (La Fuente et al. 2022; Althoff et al. 2020). Although there is widespread agreement that lake evaporation is increasing at concerning rates in various regions worldwide, it has been suggested that even within the same geographical area and similar climate conditions, the magnitude of evaporation changes can vary significantly (Wang et al. 2019). This divergence can be attributed to significant lake-specific characteristics, such as hydrological connectivity, water management, and morphometry, which notably influence the hydrological cycle of lakes (Han and Guo 2023; Fergus et al. 2022; Hanson et al. 2021; Wang et al. 2019).

Despite being a major component of the water balance of a lake, evaporation observations are rare due to the cost in logistics and challenges associated with its monitoring (Lenters et al. 2013; Blanken et al. 2011). Alternatively, one can combine empirical evidence (i.e. observations of lake physical properties) with the use of process-based modeling to understand how evaporation is responding to changes in climate (Ayala Zamora et al. 2023; La Fuente et al. 2022). Achieving this goal however, can also be challenging given the high sensitivity of evaporation to the choice of model (La Fuente et al. 2022; Jansen and Teuling 2020; Pillco Zolá et al. 2019; Rosenberry et al. 2007). Therefore, using a single-model realization may be problematic for capturing the strong variability that evaporation exhibits at regional scales. In turn, using an array of diverse lake models is likely to provide a more robust approximation with the underlying assumption that different models provide statistically independent information evenly distributed around the true state (Pennell and Reichler 2011). To address this knowledge gap, here we investigated long-term evaporation responses to climate change using a unique dataset of 23 European lakes of differing area and depth. We used an ensemble of lake-climate models (i.e., three process-based lake models driven by four GCMs) and combined these with water temperature observations and lake bathymetry from the lakes. Specifically, we (i) quantified warm-season lake evaporation rates using an ensemble approach; (ii) investigated regional spatial patterns across European lakes of differing sizes; (iii) analyzed projections of warm-season evaporation and precipitation under different climate change scenarios by the end of the 21st century. We hypothesize that

evaporation rates from lakes within the same geographical region will exhibit a spatial variability in evaporation explained by their morphometric characteristics.

4.3 Methods

4.3.1 Study sites

Our study sites consisted of 23 freshwater lakes situated across Europe. These lakes were selected because they cover a wide range of morphometric characteristics, with their surface area varying between 0.07 and 580 km^2, their mean depth varying between 2 and 153 m, and their latitude between 42°N and 69°N, consisting of mostly temperate and boreal lakes (Fig. 4.1, Table B.1).

4.3.2 Long-term warm-season evaporation simulations, the ISIMIP2b

Our evaporation projections were simulated following the Inter-Sectoral Impact Model Intercomparison Project (ISIMIP) phase 2b lake sector framework. Notably, we used three lake models driven by four GCMs (Golub et al. 2022). The lake models used were FLake (Mironov 2008), MyLake (Saloranta and Andersen 2007), and Simstrat (Goudsmit et al. 2002) (Text B1). ISIMIP2b simulations for the 23 lakes analysed here, were only available for these lake models. FLake, MyLake and Simstrat have been tested and validated in various limnological studies (Huang et al. 2021; Thiery et al. 2014; Stepanenko et al. 2013), making them suitable for this regional assessment. The lake models in ISIMIP2b simulated historic and future projections of lake physical properties including, among other things, daily simulations of lake surface water temperature and latent heat flux at the air-water interface. These two variables were then used to calculate evaporative water loss from latent heat flux using the relationship:

$$E = \frac{Q_e}{\rho_o L_v} \qquad (4.1)$$

where E is evaporation rate (m s^{-1}), Q_e is the latent heat flux (W m^{-2}), ρ_o is density of surface water (kg m^{-3}), calculated as a function of surface water temperature, T$_0$ (°C), and L_v is the latent heat of vaporization (J kg^{-1}) (Henderson-Sellers 1986). As all lakes were

located in the northern hemisphere, the warm-season average evaporation rates were defined as the average over the months Jul-Sep (O'Reilly et al. 2015). In this study, we excluded times during the warm season when lakes experience ice cover. More specifically, we omit all negative values of lake surface water temperature and latent heat flux for each lake, thus excluding them from the analysis (Fig. B.1). Given that the major focus of this study is on the evaporation losses, other physical processes such as ice cover and condensation were not considered.

4.3.3   Input data to the models

To drive the lake models, we used bias-adjusted climate projections from the CMIP5 (Lange 2019). Specifically, the lake models were driven by four GCMs: GFDL-ESM2M, HadGEM2-ES, IPSL-CM5A-LR, and MIROC5, during the 20th and 21st century (1901-2099). These four GCMs were chosen as they best met the requirements of all sectors participating in the ISIMIP, providing the needed scenario length at daily timestep (Frieler et al. 2017). Additionally, these GCMs included a wide range of projected warming rates, with GFDL-ESM2M and HadGEM2-ES being the lower and higher ends of the warming spectrum, respectively (Golub et al. 2022). Historic simulations were forced using anthropogenic greenhouse gas and aerosol forcings in addition to natural forcing and covered the period 1901 to 2005. Future projections simulate the evolution of the climate system under three different greenhouse gas emission scenarios Representative Concentration Pathways (RCP): RCP 2.6 (low-emission scenario), RCP 6.0 (medium-high-emission scenario), and RCP 8.5 (high-emission scenario), over the period 2006 to 2099. These pathways encompass a range of potential future global radiative forcing from anthropogenic greenhouse gasses and aerosols. The climate data used to drive each lake model included projections of air temperature at 2 m, wind speed at 10 m, surface downwelling shortwave and longwave radiation, precipitation and specific humidity (Table B.2). Additional input data to the lake models included the hypsographic relationship between depth and surface area (i.e. lake bathymetry), and water transparency (Golub et al. 2022). The calibration of the lake models in ISIMIP2b consisted of parameters and coefficients related to processes controlling surface heat and energy fluxes, light attenuation and turbulent kinetic energy and wind. In addition, different optimization functions were used to minimize the difference between simulated

57

and measured water temperatures (Table B.3). Specific details of model calibration and optimization are given by Golub et al. (2022).

4.3.4 Analysis

From our 12 unique model projections, we calculated the mean and standard deviation across the model ensemble for each year under both historical and future climatic forcing over the period 1901-2099. To evaluate our lake evaporation simulations, we compared the historic simulations and estimates from the Global Lake Evaporative Volume (GLEV) dataset presented by Zhao et al. (2022) over the common period (1985-2005). Specifically, we selected the studied lakes using their HydroLakes identifier. Most sites, 21 out of the 23 studied sites, were also in the GLEV dataset. Daily ISIMIP2b lake evaporation values were averaged to obtain monthly (for all months) and annual evaporation rates. Then, the ensemble average (i.e., the mean across 12 lake-climate model combinations) for each year over the 1985-2005 period was calculated for each lake, for both ISIMIP2b and GLEV evaporation rates. To assess the ability of the model ensemble to reproduce evaporation from the GLEV dataset, the Spearman Rank correlation (R) between the GLEV values and our averages was calculated for the 21 lakes.

To estimate evaporation changes, daily evaporation rates for the July-September period were averaged to obtain warm-season rates at annual timescales for each lake-climate model combination and scenario. Annual warm-season evaporation anomalies (ΔE) are then calculated as the difference between the values over the period (2070-2099) for each RCP 2.6, 6.0 and 8.5 scenario and those for the control period (1970-1999). Complementary to our evaporation analyses, we used historic and future projections of precipitation for each lake available from ISIMIP2b (Frieler et al. 2017). Daily precipitation data for historic and future scenarios was available for the four GCMs and three RCPs used in evaporation projections. To be consistent with the analysis, we estimated average precipitation over the months Jul-Sep to define the warm-season period. Finally, we calculated the net flux over the lake by using the precipitation and evaporation relationship $(P - E)$ for the historic and future periods. Precipitation data used in this study are freely available at https://data.isimip.org/search/page/2/tree/ISIMIP2b/InputData/query/pr_day/. For these

analyses we used JASMIN, the UK's collaborative data analysis environment (Lawrence et al. 2013).

4.4 Results

4.4.1 Historic warm-season evaporation rates across European lakes

We conducted our analysis to estimate annual warm-season evaporation rates across all 23 lakes for the reference period (1970-1999). The historic simulations showed a significant variation in evaporation rates across the studied lakes ranging from 0.7 mm day^{-1} at Lake Kilpisjarvi in northern Europe, Finland to 3.2 mm day^{-1} at Sau Reservoir in southern Europe, Spain (Figure 4.1, Table B.4). The average evaporation rates across all studied lakes were estimated to be 2.2 ± 0.7 mm day^{-1}. Despite the evident spatial variability that can be attributed to the latitudinal influence on evaporation, we did not observe any clear regional patterns as depicted in Figure 4.1.

When we analyzed historic evaporation rates for each lake individually, we found that the spread across model simulations varied considerably from lake to lake. Notably, we calculated the average minimum and maximum warm-season evaporation rate for all years from 1970-1999 using the 12 lake-climate model realizations for each lake. The spread in the simulations is depicted by the shaded region, and the continuous line represents the ensemble mean (Fig. B.2). We hypothesized that large, deep lakes are likely to exhibit a larger spread in evaporation estimated using 1-D lake models than smaller shallower lakes. Indeed, a greater spread in simulated evaporation was observed for some deep lakes such as Geneva, Neuchatel and Rapbodde, but we observed this also for small shallow lakes such as Langtjern and Nohipalo-Mustjaerv (Fig. B.2). For instance, based on these results we found no relationship between the evaporation variability among the model ensemble simulations and lake morphometry.
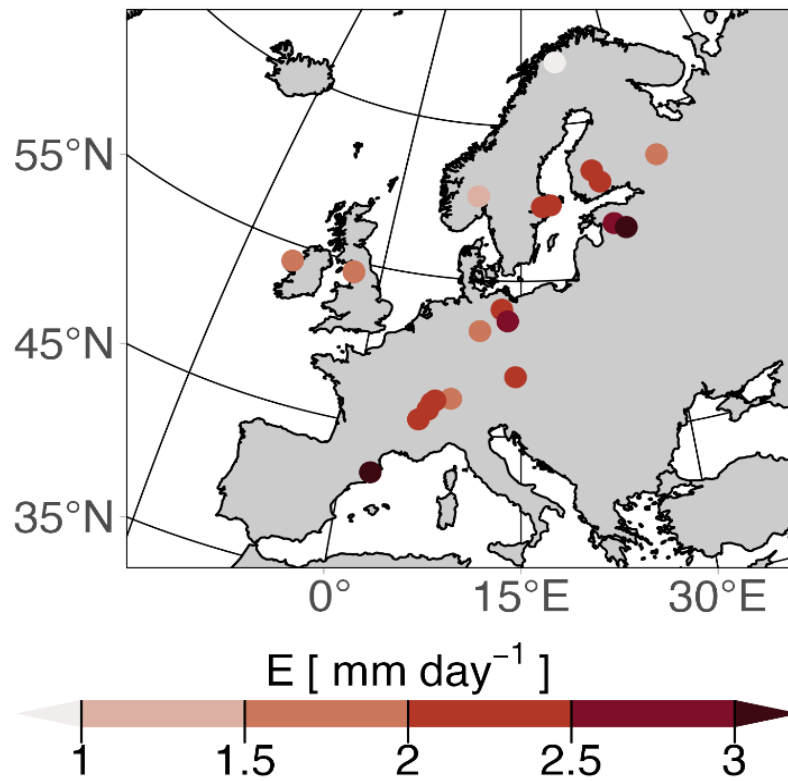
Figure 4.1 Historic (1970-1999) warm-season evaporation rates (mm day^{-1}) for 23 lakes across Europe.

To evaluate our results, we compared our ensemble of historic evaporation simulations and the evaporation from the GLEV dataset over the common period (1985-2005). Our analysis suggested that there was a moderate correlation (R = 0.74; p-value = 0.05) between our estimates and those from the GLEV dataset for the lakes studied. While it is worth acknowledging that a substantial number of our lakes exhibited lower average evaporation rates when compared to the GLEV values (i.e., the average of the model ensemble), it is important to highlight that the evaporation rates of some lakes still fall within the confidence intervals of our ensemble projections (Fig. B.3), whereas in other lakes this was not the case.

4.4.2 Long-term warm-season evaporation projections for the 20th and 21st century

Long-term projections of warm-season evaporation were investigated under historic and future climatic forcing (RCPs 2.6, 6.0 and 8.5) using an ensemble approach. Our historical

projections of warm-season evaporation for the period 1901-2005 revealed a prominent interannual variability (Fig. B.4), with some lakes displaying notable short-term fluctuations in evaporation trends. For example, Sau Reservoir in Spain exhibited both increasing and decreasing patterns during the historical period. Nevertheless, a significant shift occurred across many lakes beginning in the 1980s, marked by a continuous increase in evaporation that persisted until the end of the 20th century (Fig. B.4). Other lakes exhibited less variability in historic evaporation like for example Lake Kilpisjarvi and Lough Feeagh.

During the twenty-first century (2006-2099), all models projected a significant increase in warm-season evaporation across most studied lakes, with the increase intensifying with the warming scenario (Fig. 4.2). We found considerable variability in future projected evaporation across the studied lakes. For example, the increase (ΔE) (i.e., the difference between warm season lake evaporation in each time period relative to the base period [1970-1999] average) estimated under the RCP 8.5 scenario by 2070-2099 for Lake Rimov was 62% with reference to the historic period, approximately five times higher than the 12% increase estimated for Lough Feeagh (Fig. 4.4, Table B.4). At a regional scale, our results revealed a latitude effect on lake evaporation. More specifically, lower latitude lakes exhibited the highest increases in evaporation with some exceptions for lakes located in Sweden and Estonia.

When we estimated the percent increase in evaporation by the end of the century, we found that many lakes located in the southernmost regions exhibited increases higher than 40% under the RCP 8.5 scenario. Other lakes located at higher latitudes exhibited increases in evaporation of approximately 25% (Fig. B.5). Our climate model projections suggest that by 2070-2099, evaporation anomalies across the studied lakes will increase at an average of 0.5 ± 0.9 mm day^{-1} under RCP 2.6, 0.7 ± 0.9 mm day^{-1} under RCP 6.0 and 0.9 ± 1.1 mm day^{-1} under RCP 8.5. Under the RCP 2.6, 6.0 and 8.5 scenarios, evaporation was projected to increase by 21%, 30% and 42%, respectively. Despite the variability found in area and mean depth across the studied lakes, we did not observe a discernible relationship between the projected changes in evaporation and lake morphometry.

4.4.3 *Simultaneous changes in warm-season precipitation and evaporation during the 20th and 21st century*

To evaluate the potential impacts of combined changes in precipitation and evaporation on the water budget of our 23 studied lakes, we estimated the warm-season annual *(P-E)* relationship for all lakes under historic and future scenarios of climate change. Our projections showed that the change in evaporation will likely be greater than the change in precipitation under all scenarios, though with varying magnitude for different lakes (Fig. 4.3). Notably, our results suggested that future precipitation is likely to decrease in the studied lakes, with some exceptions in northern Europe (Fig. B.6). When we calculated *P-E* for the RCP 8.5 scenario we found that all lakes, except Lake Kilpisjarvi in Finland, are projected to experience a deficit in the net water flux ratio *(P-E)* by the end of this century. Similarly, to the spatial variability on our future evaporation projections, a clear latitudinal pattern in *P-E* was detected with lakes located at higher latitudes exhibiting smaller deficits, opposite to lakes in lower latitudes where the deficit reached its highest values (Fig. 4.4, Fig. B.6). For example, Lake Kilpisjarvi in Finland exhibited no change (0 ± 0.7 mm day^{-1}) compared to the -2.1 ± 2.1 mm day^{-1} change in *P-E* estimated for Lake Lower-Zurich in Switzerland (Table B.5). At a regional scale, the *P-E* ratio is projected to decrease by -0.4 ± 1.2 mm day^{-1}, -0.7 ± 1.3 mm day^{-1}, and -1.2 ± 1.6 mm day^{-1} under RCP 2.6, 6.0 and 8.5 respectively.
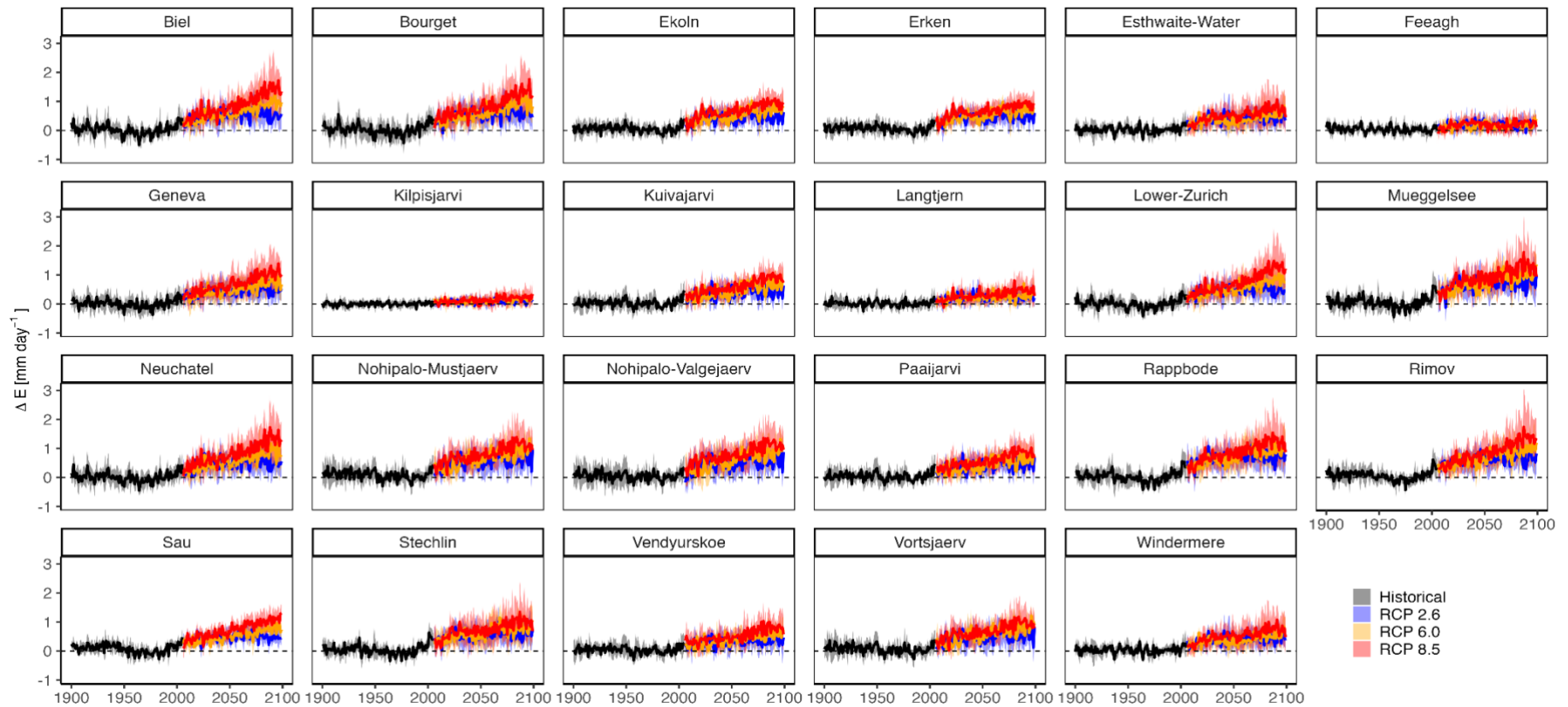
Figure 4.2 Projected changes in annual average warm-season evaporation rates (mm day⁻¹) during the historic (1901-2005) and future (2006-2099) periods for 23 European lakes. The average of the model ensemble is shown by the thick lines, the standard deviation across the model ensemble is represented by the shaded area. Anomalies (ΔE) are quoted relative to the 1970-1999 base period average for RCP (Representative Concentration Pathway) 2.6, 6.0 and 8.5.
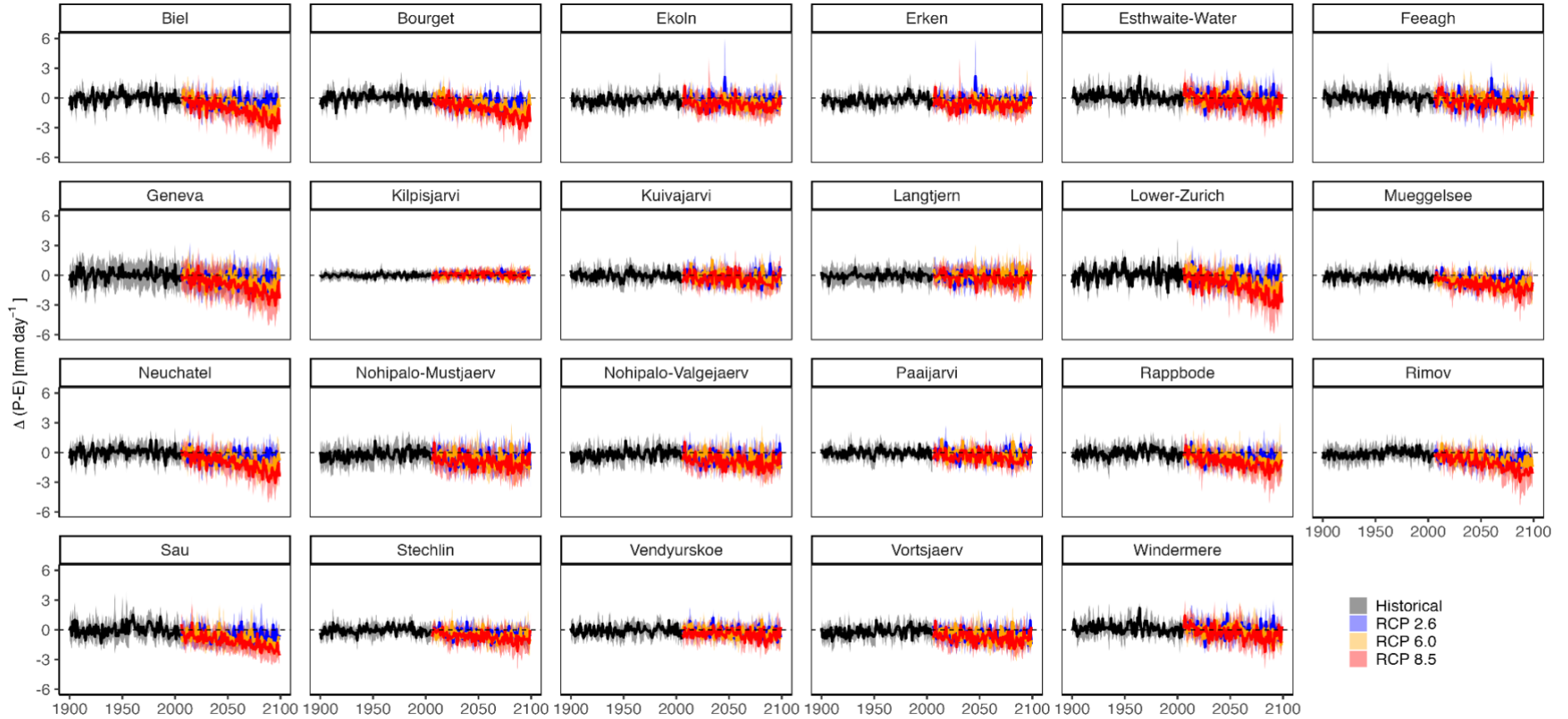
Figure 4.3 Projected changes in average annual warm-season precipitation minus evaporation rates in mm day^{-1} during the historic (1901-2005) and future (2006-2099) periods for 23 European lakes. The average of the model ensemble is shown by the thick lines, the standard deviation across the model ensemble is represented by the shaded area. Anomalies Δ(P-E) are quoted relative to the 1970-1999 base period average for RCP (Representative Concentration Pathway) 2.6, 6.0 and 8.5.
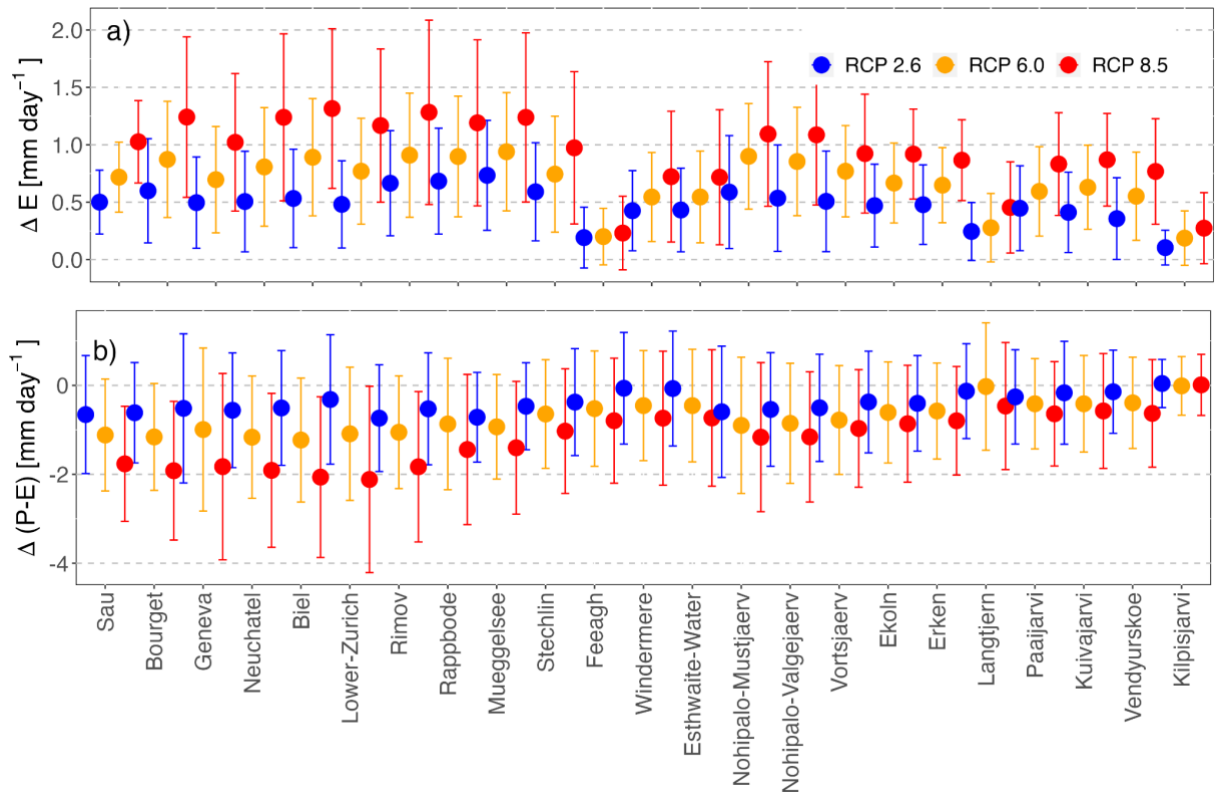
Figure 4.4 Projected changes in warm-season (a) evaporation and (b) precipitation minus evaporation (P-E) rates by the end of this century for 23 European lakes. Anomalies (Δ) are quoted relative to the 1970-1999 base period average for RCP (Representative Concentration Pathway) 2.6, 6.0 and 8.5. The ensemble mean is represented by the dots, and the lines represent the ensemble standard deviation for the warming scenarios.

4.5 Discussion

4.5.1 *Implications for water availability in European lakes and future research*

The availability of water for human consumption and ecosystem services is modulated by spatial and temporal variability in both precipitation and evaporation (Konapala et al. 2020). Here we projected future changes in these key components for 23 lakes across Europe. All model simulations indicated that evaporation is likely to be greater than precipitation under all future climate change scenarios, with the *P-E* relationship being primarily negative throughout the 21st century in most studied lakes. More specifically, we found that under scenarios of climate change most lakes are likely to exhibit deficits

in their water balance. On average, the *P-E* relationship was projected to decrease by -0.4±1.2 mm day^{-1}, and -1.2±1.6 mm day^{-1} under RCP 2.6 and 8.5 respectively. Our results are in alignment with regional assessments reporting that summer precipitation in Europe will experience significant changes following climate change, with southern Europe likely to experience significant drying opposite to northern Europe where precipitation is projected to become even wetter (de Vries et al. 2022). Notably, some of the dramatic effects of climate change on lake water levels were previously observed during the 2000-2003 long-term drought period that lead to a significant decrease of the water levels of European lakes (Wantzen et al. 2008). Notably, other local factors related to human economic activities and ecological management, not considered here, can significantly obscure the effect of evaporation and precipitation on the water storage change of these lakes (Rosen et al. 2023; Wrzesiński and Ptak 2016) and thus result in different outcomes than the projected in this study. If the *P-E* changes in the studied lakes align with our future projections, the water availability in these lakes will be severely affected this century, particularly in southern and central Europe through the depletion of water levels, further exacerbating the already existing water scarcity in these regions during the summer season. While some of these regions may have alternative sources of drinking water for human consumption or irrigation, a decline in lake water levels can lead to dramatic ecological disturbances that could affect the ecosystem functioning of these lakes.

As lake evaporation is increasing at alarming rates due to anthropogenic climate change, there is an urgent need to develop technologies to mitigate the impacts of rising evaporative loss from lakes. Some include physical approaches ranging from the use of floating covers to photovoltaic panels to reduce evaporation and in turn produce solar energy (Jin et al. 2023), chemical approaches with the use of mono layers and biological approaches such as floating plants and wind breakers (Youssef and Khodzinskaya 2019). Importantly, estimating future water availability from lakes can also be achieved by combining climate sciences and water management through the use of water availability models (Shao et al. 2023). Nonetheless, such models are data intensive and can only be applied in lakes with well-established monitoring networks. One of the biggest challenges in the projection of future water availability from lakes remains with the estimation of inflows, outflows from the lake (Riggs et al. 2023), as well as future lake surface area

dynamics (Zhao et al. 2023), both strongly linked to climate variability and anthropogenic management.

4.5.2   *Limitations and uncertainties in ISIMIP2b simulations*

Although we consider that our results bridge an important knowledge gap by providing projections for a range of European lakes, there are certain limitations that should be considered when interpreting the findings. For instance, it is recognised that the use of low spatial (0.5 degree) resolution meteorological data from GCMs is unlikely to capture short-scale processes that regulate the spatial distribution of climate variables (Wang et al. 2004). This is particularly important in regions with complex orography or coastlines, where the local climate variability can significantly alter evaporation occurrence in a lake (Shilo et al. 2015). To address the spatial mismatch between observed and simulated meteorological data, we used bias-corrected GCM data from ISIMIP2b to drive the lake models (Lange 2019; Frieler et al. 2017). This bias-correction methodology particularly adjusts the statistics of GCM data with the purpose of making them more similar to local meteorological observations. Our model ensemble also consisted of 1-D lake models, and therefore, assumed that evaporation rates were uniform over the entire lake surface. Field observations from lakes in different climatic regions have demonstrated the strong spatial variability in lake evaporation, particularly in lakes with large surface areas (Matta et al. 2022; Rodrigues et al. 2021; Rahaghi et al. 2019; Lenters et al. 2013; Mahrer and Assouline 1993). Using sophisticated 3-D models may seem an attractive approach to address this limitation, however such models are data-intensive and computationally expensive (Rocha et al. 2023; Kayastha et al. 2022), making their use impractical for multi-lake ensemble modeling approaches, such as the one presented in this study. The 1-D lake models used here also do not account for two-way interactions between the lake surface and the overlying atmosphere (Wang et al. 2020). These models have, however, been widely used in studies of the effects of future climate change on lake physics (Ayala Zamora et al. 2023; La Fuente et al. 2022; Grant et al. 2021; Woolway et al. 2021; Shatwell et al. 2019). Furthermore, while we estimated the net flux historic and future changes over the studied lakes via *P-E* estimations, we recognize that our approach relates to rainfall only and did not account for key components in the hydrological cycle such as inflow, and outflow (e.g. surface water and groundwater) which can strongly influence

the water budget of a lake. While we recognise these limitations, we consider that our findings still provide valuable insights on a continental scale on the impacts of climate change on the most important components of the water budget of lakes (i.e. evaporation and precipitation) across Europe.

4.5.3 *Warm-season evaporation rates across European lakes*

Quantifying future evaporation changes is critical for the management and protection of European water resources. This is the first study to investigate long-term evaporation responses to climate change specifically focused on European lakes over the 20th and 21st century, using an ensemble of model combinations. The average warm-season evaporation across all studied lakes was 2.2±0.7 mm day^{-1} during the 1970-1999 reference period. The studied lakes covered a wide range of morphometric characteristics, and a latitudinal gradient. A strong spatial variability in lake evaporation was found as expected, with regions with warmer climate exhibiting the highest evaporation rates 3.2 mm day^{-1} (e.g. Sau Reservoir in Spain), whereas the lowest rates were expected in northern frigid regions such as Lake Kilpisjarvi 0.7 mm day^{-1}. However, while we observed a general latitudinal influence on warm season evaporation, there was no clear relationship with lake morphometry. This is in contrast to previous findings, where a clear effect of latitude and lake surface area on evaporation was found (Zhao et al. 2022; Woolway et al. 2018). These discrepancies may be attributable to differences in the source of the wind speed data used in the studies as well as the use of a relatively small number of study lakes to identify a clear morphometric effect on evaporation. As a key driver wind speed can affect lake evaporation considerably, particularly at sub-daily time scales (Granger and Hedstrom 2011). For instance, the significant relationship reported by Woolway et al. (2018) was based on an analysis using over-lake high-frequency wind speed observations, whereas our study used bias-corrected wind speed from a gridded dataset (Lange 2019). For instance, it is likely that observed over-lake measured wind speed will better represent wind speed conditions at the lake than GCM data. In agreement with previous findings (Zhou et al. 2021; Wang et al. 2018), our analysis revealed a substantial increase in warm-season evaporation rates across all studied lakes by the end of this century under our selected scenarios of climate change. Specifically, lake evaporation was projected to increase at an average rate of 0.9±1.1 mm day^{-1} (range

0.2 ± 0.3 mm day^{-1} and 1.3 ± 0.8 mm day^{-1}) under the most pessimistic scenario RCP 8.5. Under the RCP 2.6 scenario, the average evaporation was projected to increase by 0.5 ± 0.9 mm day^{-1} (range 0.1 ± 0.1 mm day^{-1} and 0.7 ± 0.5 mm day^{-1}). This evaporation change represents an average increase of 42% and 21% under the RCPs 8.5 and 2.6, respectively, changes that would have implications for both lake ecosystem function and for drinking water supplies. Similar long-term changes have already been reported for some individual European lakes, where positive historical evaporation trends have been associated with warming surface water temperature (Shatwell et al. 2019; Czernecki and Ptak 2018; Woolway et al. 2017; Fink et al. 2014). We suggest that our findings for multiple lake types and locations across Europe will facilitate the identification of vulnerable lakes to future climatic change and therefore aid local water authorities to take mitigation action.

4.6 Conclusions

Long-term warm-season evaporation changes from 23 lakes across Europe were simulated using an ensemble of lake-climate models, in-situ water temperature observations and lake bathymetry. Our results indicated that most lakes are likely to experience a rapid increase in annual evaporation at an average rate of 0.9 ± 1.1 mm day^{-1} under the most pessimistic scenario RCP 8.5. Under the RCP 2.6 scenario, the average evaporation is projected to increase by 0.5 ± 0.9 mm day^{-1}. These changes represent an average increase of 42% and 21% under the RCPs 8.5 and 2.6, respectively. Importantly, future projections suggest that the water availability of many of the studied lakes will experience a deficit with P-E being predominantly negative throughout the 21st century. These changes in evaporation and precipitation can have a substantial influence on the water availability of lakes and on their ecosystem functioning.

Chapter 5   Ensemble modeling of global lake evaporation under climate change

Authors: Sofia La Fuente[1*], Eleanor Jennings[1], John D. Lenters[2], Piet Verburg[3], Zeli Tan[4], Marjorie Perroud[5], Annette B. G. Janssen[6], R. Iestyn Woolway[7]

Affiliations:

1. Centre for Freshwater and Environmental Studies, Dundalk Institute of Technology, Dundalk, Ireland
2. University of Michigan, UM Biological Station, Pellston, Michigan, USA
3. National Institute of Water and Atmospheric Research, Wellington, New Zealand
4. Pacific Northwest National Laboratory, Richland, Washington, USA
5. Institute for Environmental Sciences, University of Geneva, Geneva, Switzerland
6. Wageningen University & Research, Water Systems and Global Change Group, Wageningen, the Netherlands
7. School of Ocean Sciences, Bangor University, Menai Bridge, Anglesey, Wales

*Corresponding author: ruthsofia.lafuentepillco@dkit.ie

*Postal address: Centre for Freshwater and Environmental Studies, Dundalk Institute of Technology, Dundalk, Marshes Upper A91 K584, Co. Louth, Ireland

5.1 Abstract

Global projections of lake evaporation are typically based on simulations using single mechanistic models. However, because of its complex interactions with various lake physical properties, environmental and anthropogenic drivers, lake evaporation is highly variable and sensitive to the choice of model used. In this study, we present a multi-model analysis to investigate differences across global simulations of lake evaporation during the warm-season using three different lake models driven by outputs from four general circulation models (GCM) (i.e. 12 model combinations in total) for historic and future

scenarios. Our results suggest substantial differences among lake-climate model simulations of lake evaporation. These differences varied throughout the 20th and 21st century, with model driver data explaining 74% of the variance in future projections of warm-season lake evaporation. Our projections indicate that, by the end of the 21st century (2070-2099), global annual lake evaporation rates will increase by 10-27% under Representative Concentration Pathways (RCPs) 2.6-8.5. We highlight the importance of using a multi-model approach for the prediction of future global lake evaporation responses to climate change.

5.2 Introduction

Water is a fundamental and finite resource that is essential to human well-being (United Nations, 2021). However, only ~3% of Earth's water is fresh, and only a small fraction (~1%) can be used as drinking water; the remainder is locked up in glaciers, ice caps, and permafrost, or buried deep underground. Of the fraction of remaining fresh water, more than 87% resides in lakes (Messager et al. 2016; Gleick 1993), making them a critical resource of fresh water for, among other things, human consumption. In lakes, water storage variability is influenced by both anthropogenic and natural factors, primarily by changing water availability within a lake's catchment as well as changes in over-lake precipitation and within-lake processes such as surface and groundwater outflow and open-water evaporation (Cooley et al. 2021; Vystavna et al. 2021; Wurtsbaugh et al. 2017). Importantly, open-water evaporation is a key component of freshwater loss and the resulting variations in lake level and surface extent (Zhao et al. 2022; Friedrich et al. 2018). In fact, due to their large open-water areas and typically strong air-water vapour pressure gradients, lakes can lose a large proportion of their water via evaporation (Zhao et al. 2022; Lenters et al. 2005). Lake evaporation also plays a fundamental role in the energy budget of lakes, and is central to the modification of lake temperature and related processes such as stratification and mixing (Ye et al. 2019; Lenters et al. 2013; Spence et al. 2013; Mishra et al. 2011; MacIntyre et al. 2009). In turn, lake evaporation is crucial for the basic functioning of lakes and is often considered as one of the most important processes influencing their physical environment (Woolway et al. 2020; Friedrich et al. 2018; Lenters et al. 2005).

The volume of evaporative water loss from a lake is governed by its surface area and the rate of evaporation (Zhao et al. 2022; Wang et al. 2020; Zhao and Gao 2019). The latter can vary widely among geographical regions and is highly sensitive to climatic variations (Zhao et al. 2022; Zhou et al. 2021; Wang et al. 2018; Woolway et al. 2018). Some of the most direct atmospheric drivers of lake evaporation are wind speed and absolute humidity (Lenters et al. 2014; Van Cleave et al. 2014; McVicar et al. 2012). However, due to the influence of lake surface temperature on the vapour pressure gradient, other atmospheric and limnological factors also play a considerable role in the evaporation rate (Friedrich et al. 2018; Lenters et al. 2005; Brutsaert 1982). The lake surface energy budget components that influence evaporation are numerous including, among other things, incoming and outgoing short- and long-wave radiation and the exchange of sensible heat at the air-water interface (Friedrich et al. 2018). Several lake-specific features, such as lake depth, water colour, and the influence of terrestrial sheltering (e.g., tall tree canopy) can also modify the magnitude and timing of lake evaporation, primarily through their influences on surface water temperature and the intensity of near-surface turbulence (Wang et al. 2020; McVicar et al. 2012; Read et al. 2012).

Given the importance of lake evaporation, as well as its influence on other within-lake processes, simulating and understanding its response to climate change is of paramount importance. With the use of one-dimensional process-based lake models, previous studies have suggested that global lake evaporation has increased substantially in recent decades, with future projections suggesting a continued increase in many regions within a warming world (La Fuente et al. 2022; Zhou et al. 2021; Wang et al. 2018; Helfer et al. 2012). Specifically, by the end of this century, global mean annual lake evaporation is expected to increase by 16%, and at a rate of ~4% per degree increase in global-mean surface air temperatures (Wang et al. 2018). The largest increases in annual evaporation are expected at low latitudes, where evaporation rates are already high (Zhou et al. 2021; Wang et al. 2018), but also in lakes that will transition to becoming ice-free, allowing the potential for evaporation to occur year-round (Woolway et al. 2020; Sharma et al. 2019). Moreover, lake evaporation is expected to increase rapidly in regions that will experience a drying hydroclimate, which will amplify evaporation increase by enlarging the surface vapor pressure deficit (Farooq et al. 2022; Zhou et al. 2021). The amplified evaporative

loss combined with a decrease in precipitation, will likely reduce lake volumes and, in turn, the quantity of freshwater this century (La Fuente et al. 2022; Zhou et al. 2021).

Previous studies have undoubtedly improved our understanding of lake evaporation responses to climate change. However, most of these studies are based on simulations from a single one-dimensional model (Zhao et al. 2022; Wang et al. 2018). While numerous methods have been developed to estimate evaporation from lakes (Finch and Calver 2008), process-based models have been, in recent years, more frequently used to simulate processes occurring in lakes (Moore et al. 2021). Despite being based on decades of theory, observation, and experimentation, process-based lake models implement approximate forms of relationships, which can depend heavily on tuneable parameters, either due to incomplete knowledge of some processes or for practical computing purposes. Indeed, lake evaporation projections can be sensitive to these limitations and, in turn, to the choice of lake model used (La Fuente et al. 2022; Liu 2022; Pillco Zolá et al. 2019; Rosenberry et al. 2007). An alternative approach, which can combine the wealth of information provided by multiple lake models, is to follow an ensemble approach, that is, to consider outputs from multiple independently developed models. The main advantage of a multi-model approach is that the uncertainty in the individual model predictions can be quantified, allowing the modeller to better assess the likelihood of occurrence of the projections (Moore et al. 2021). In addition, the multi-model ensemble (e.g., average) can often provide a more robust simulation than any single-model realization (La Fuente et al. 2022; Trolle et al. 2014). Previous studies have demonstrated the robustness of ensemble modelling in lakes (Golub et al. 2022; Grant et al. 2021; Moore et al. 2021; Trolle et al. 2014). Importantly, the development of strategies to mitigate the effects of climate change on lakes not only requires robust projections, but also knowledge of uncertainty of model projections. However, the use of ensemble modelling for simulating climate-induced changes in lake evaporation and the quantification of the associated uncertainties have not previously been investigated.

The overarching aim of this study is to investigate differences in global lake evaporation changes using a suite of independently developed lake models forced with multiple General Circulation Models (GCMs) to produce an ensemble of lake-climate model projections. We use an ensemble of three one-dimensional lake models driven by four GCMs (i.e., 12 model realizations) to investigate differences across simulated global

lake evaporation. Here we (i) quantify global lake evaporation rates using a multi-model approach; (ii) evaluate the differences across the model ensemble; (iii) assess future projections of lake evaporation under different climate change scenarios by the end of the 21st century, and related these to projected changes in over-lake precipitation; and (iv) quantify lake model and GCM uncertainty for our future projections of warm-season lake evaporation using the model ensemble.

5.3 Methods

5.3.1 Multi-model projections of global lake evaporation

The simulations used in this study consisted of a lake-climate model ensemble of 12 model realizations (i.e., three lake models, each driven by outputs from four different GCMs). The lake models, namely ALBM (Tan et al. 2015), SIMSTRAT-UoG (Goudsmit et al. 2002) and VIC-LAKE (Bowling and Lettenmaier 2010) (Text C1, Table C.1), contributed to the Inter-Sectoral Impact Model Intercomparison Project (ISIMIP) phase 2b Lake Sector (Golub et al. 2022). The ISIMIP is an international network of climate-impact modelers who contribute to a comprehensive and consistent picture of the world under different scenarios of climate change. Given that, in many cases, sector-specific impact models are constructed independently and lack interaction with other sectors (water, forest, lakes, etc), the ISIMIP aims to address this challenge by forcing a wide range of climate-impact models with the same climate and socio-economic input data, and making the projections publicly available (Frieler et al. 2017). In addition, the lake models used in this study have been tested and validated in a number of limnological assessments (Guo, Zhuang, Yao, Golub, Leung, Pierson, et al. 2021; Guo, Zhuang, Yao, Golub, Leung and Tan 2021; Janssen et al. 2021; Stepanenko et al. 2014; Thiery et al. 2014; Stepanenko et al. 2013; Mishra et al. 2011; Bowling and Lettenmaier 2010), making them suitable for global assessments. For further information on these models, see the supplementary material. The global lake ISIMIP2b simulations are openly accessible and can be found at https://doi.org/10.48364/ISIMIP.931371.

5.3.2 Input data

To drive each of the lake models, bias-corrected climate model projections from ISIMIP2b were used (Text C2, Table C.2), specifically CMIP5 projections from GFDL-ESM2M, HadGEM2-ES, IPSL-CM5A-LR, and MIROC5 for historical and future periods (Lange 2019). These four GCMs were selected as they best met the needs of all sectors participating in the ISIMIP, providing the necessary scenario length at daily temporal resolution (Frieler et al. 2017). In addition these GCMs had a wide range of projected warming rates, with GFDL-ESM2M and HadGEM2-ES representing the lower and higher ends of the warming spectrum, respectively (Golub et al. 2022). Historical simulations used anthropogenic greenhouse gas and aerosol forcing in addition to natural forcing, covering the period 1901 to 2005. Future projections, which represent the evolution of the climate system subject to three different anthropogenic greenhouse gas emission scenarios covering the period 2006 to 2099, RCP 2.6 (the low-emission scenario), RCP 6.0 (the medium-high emission scenario), and RCP 8.5 (the high-emission scenario), were also investigated. The lake models in ISIMIP2b simulated historic and future projections of various lake physical properties, including lake surface water temperature and the latent heat flux at the air-water interface at a 0.5° by 0.5° grid resolution globally, based on the mean depth and surface area of all lakes within a given 0.5° grid. Therefore, these simulations represent an aggregated 'typical lake' for each 0.5° grid (Text C2). These two variables were then used to calculate evaporative water loss from latent heat flux using the relationship:

$$E = \frac{Q_e}{\rho_o L_v} \qquad (5.1)$$

where E is evaporation rate (m s^{-1}), Q_e is the latent heat flux (W m^{-2}), ρ_o is density of surface water (kg m^{-3}), calculated as a function of surface water temperature, T_0 (°C), and $L_v = 2.501 \times 10^6 - 2370\, T_0$ is the latent heat of vaporization (J kg^{-1}) (Henderson-Sellers 1986). In this study, evaporation rates were estimated only for the warm-season and are presented in mm day^{-1}. Warm-season average evaporation rates were defined as the average over the months Jul-Sep for lakes located north of 30°N, and Dec-Feb for lakes located south of 30°S. For lakes located between 30°N and 30°S, we used all months

for estimating average evaporation rates. In this study, we excluded times during the warm season when lakes experience ice cover. More specifically, we omit all negative values of lake surface water temperature and latent heat flux for each lake, thus excluding them from the analysis (Fig. C.1).

5.3.3 Analysis

From our 12 unique model projections we calculated the ensemble mean and standard deviation under both historical and future climatic forcing. More specifically, we calculated the mean and standard deviation of evaporation for (i) a single lake model forced by multiple climate model projections (e.g. the mean of all four GCMs x VIC-LAKE) and (ii) multiple lake models forced by a single climate model (e.g. the mean of all three lake models x GFDL-ESM2M). For this analysis, we used JASMIN, the UK's collaborative data analysis environment (Lawrence et al. 2013). To investigate the across-lake differences in simulated lake evaporation rates, we grouped the studied lakes according to the 'lake thermal region' in which they are located (Gong et al. 2022; Maberly et al. 2020).

To complement our lake evaporation analyses, we used global historic and future projections of precipitation (P) available from ISIMIP2b (Frieler et al. 2017). This precipitation data consisted of daily values for historic and future scenarios available for the four GCMs and three RCPs used in projecting future changes in lake evaporation. Notably, we used the same definition for warm-season evaporation and defined the annual average P over the months Jul-Sep for lakes located north of 30°N, and Dec-Feb for lakes located south of 30°S, and for lakes located in the tropical areas (i.e. between 30°N and 30°S). Then, we calculated the net flux of water between the overlying atmosphere and the surface of each representative lake ($P - E$) during the historic and future periods. Precipitation data used in this study is freely available at https://data.isimip.org/search/page/2/tree/ISIMIP2b/InputData/query/pr_day/.

5.3.4 Uncertainty quantification in future projections of lake evaporation

We used the analysis of variance (ANOVA) to quantify lake and climate model uncertainty on future projections of lake evaporation. First, we calculated the climate change signals (ΔE) (i.e., the difference between lake evaporation in a given time period

relative to the base period [1970-1999] average) for each lake-climate model combination and RCP scenario (i.e. three lake models, four GCMs and three RCPs). In the ANOVA, the total sum of squares (SST) was divided into the effects due to GCM (SSA), lake model (SSB), and the interactions between lake model and GCM (SSI).

$$SST = SSA + SSB + SSI \qquad (5.2)$$

Given the inconsistency in GCM and lake model populations, we performed a subsampling method as explained in Bosshard et al. (2013). For each subsampling iteration (i), we selected three GCMs out of the four to equal the number of lake models, resulting in a total of four GCM trios. Thus, each subsampling iteration had three lake models and three GCMs. Then the variance fraction (η^2) effect was derived as:

$$\eta^2_{GCM} = \frac{1}{I} \sum_{i=1}^{I} \frac{SSA_i}{SST_i} \qquad (5.3)$$

$$\eta^2_{lake\ model} = \frac{1}{I} \sum_{i=1}^{I} \frac{SSB_i}{SST_i} \qquad (5.4)$$

$$\eta^2_{interactions} = \frac{1}{I} \sum_{i=1}^{I} \frac{SSI_i}{SST_i} \qquad (5.5)$$

This analysis was performed for each representative lake and RCP scenario. The variance fraction η^2 corresponds to the contribution of an effect (e.g. lake model) to the total ensemble variance (uncertainty) that can range between 0% and 100%.

5.4   Results

5.4.1 Global warm-season lake evaporation during the historic period

We began our investigation by calculating the historic (1970-1999) warm-season average evaporation rates (i.e., the areal mean of all warm-season evaporation rates during the 30-year period) for lakes worldwide using the lake-climate model ensemble projections. Following the IPCC climate reference regions (Iturbide et al. 2020), our simulations suggested that across the studied sites, the historic warm-season evaporation rates were

typically highest in the tropics, western central Asia, western and central North America and were lowest in the Siberian arctic region and northwest and northeast regions of North America (Fig. 5.1). Ultimately, our simulations showed considerable regional differences during the period of interest (1970-1999). To more clearly evaluate the spatial differences in evaporation rates, we grouped lakes according to the thermal regions in which they are found (Fig. C.2). Our simulations suggested that the highest evaporation rates occurred in the southern warm thermal region, varying between 3.5 and 5.5 mm day^{-1} (these values represent the 25th and 75th percentiles of all simulated warm-season evaporation rates within the thermal region). Similar results were found for the northern warm (between 3.5 and 5.2 mm day^{-1}), and for the northern hot thermal regions (between 3.1 and 5.0 mm day^{-1}). Northern cool and northern frigid thermal regions experienced the lowest warm-season evaporation rates, between 1.6 to 2.8 mm day^{-1}, and 1.1 to 2.2 mm day^{-1}, respectively (Table C.3).

As well as demonstrating clear differences in lake evaporation rates across thermal regions, our global-scale simulations demonstrated noticeable differences in evaporation rates across the lake-climate model ensemble. Most of the differences between models were evident in North America, northern South America, and central Africa (Fig. 5.1). Critically, this suggests that the choice of model used can have a considerable influence on the simulated evaporation rates during the historic period. To explore this effect further, we investigated the differences in the spatial distribution of average lake evaporation across the lake-climate model ensemble and lake thermal regions. The variability in simulated lake evaporation (here denoted by the difference between the quantiles) was more evident across lake models (i.e., the mean of all GCMs) than across GCMs (i.e., the mean of all lake models) (Fig. C.3). Some examples include the evaporation estimates for the tropical hot region ranging between 2±2 mm day^{-1} and 4±1 mm day^{-1} for lake models, whereas almost all GCMs had an evaporation estimate of 3±1 mm day^{-1} for this thermal region. In addition, the northern hot (ALBM: 4±2 mm day^{-1}; VIC-LAKE: 4±1 mm day^{-1}; SIMSTRAT-UoG: 5±1 mm day^{-1}) and southern hot (ALBM: 3±1 mm day^{-1}; VIC-LAKE and SIMSTRAT-UoG 4±1 mm day^{-1}) thermal regions also showed differences across lake models, contrary to the climate models, where all GCMs reported an evaporation rate of 4±2 mm day^{-1} for the northern hot and 4±1 mm day^{-1} for the southern hot region (Tables C.4 and C.5).

5.4.2 Multi-model projections of global lake evaporation during the 21st century

Having investigated historic warm-season lake evaporation rates and the discrepancies across the lake-climate model ensemble, we then investigated projected changes under future climatic forcing (RCPs 2.6, 6.0 and 8.5) from 2006 to 2099. Our projections demonstrated noticeable changes in global lake evaporation anomalies (ΔE) (i.e., the difference between lake evaporation in a given time period relative to the base period [1970-1999] average). All models projected an increase in warm-season lake evaporation by the end of the 21st century. However, the magnitude of change in evaporation rates varied considerably across the model ensemble, particularly at high latitudes. Contrary to the results of the historic period, the evaporation projections from ALBM and SIMSTRAT-UoG were very similar, particularly across latitudinal gradients for the RCP 8.5 scenario (Fig. 5.2 d, h, l, p). The largest discrepancies among lake models were found at higher latitudes, where evaporation projections from VIC-LAKE were consistently higher. In contrast to the other lake models (i.e. ALBM and SIMSTRAT-UoG), VIC-LAKE showed the largest changes in warm-season evaporation at high latitudes (Fig. 5.2). Furthermore, when we compared the differences in lake evaporation anomalies among the GCMs, we found that there was stronger spatial heterogeneity compared to the historic period. A notable example are the GFDL-ESM2M-driven simulations where there were particularly large differences (Fig. 5.2 a-c), such as in eastern North America and Siberia. Moreover, the MIROC5-driven simulations were also highly influenced by the lake model used, especially in North America, eastern Europe and western Siberia (Fig. 5.2 m-o).

The variability in lake evaporation anomalies among GCMs was much greater than among lake models under the RCP 8.5 scenario when compared to the historical period (Fig. C.4). This was most evident when the studied lakes were grouped by thermal region. The most notable examples were found in the tropical hot regions with evaporation anomalies varying between GFDL-ESM2M: 0.4 ± 0.3 mm day^{-1} and HadGEM2-ES: 1.1 ± 0.6 mm day^{-1} for GCMs, and between SIMSTRAT-UoG: 0.7 ± 0.4 mm day^{-1} and ALBM: 0.9 ± 0.8 mm day^{-1} for lake models. In the southern warm region, evaporation anomalies were between GFDL-ESM2M: 0.5 ± 0.4 mm day^{-1} and IPSL-CM5A-LR: 1.3 ± 0.6 mm day^{-1} for the climate models, and between VIC-LAKE: 0.7 ± 0.4

mm day^{-1} and ALBM: 0.9±0.7 mm day^{-1} for lake models. Similar results were found in the northern temperate region GFDL-ESM2M: 0.6±0.3 mm day^{-1} and HadGEM2-ES: 1.5±0.6 mm day^{-1} and between VIC-LAKE: 0.9±0.4 mm day^{-1} and ALBM: 1.2±0.7 mm day^{-1} (Tables C.6, C.7). Global warm-season evaporation maps for RCPs 2.6 and 6.0 are included in the supplementary material (Fig. C.5, C.6). Thus, unlike the results for the historic period (where lake evaporation projections among GCMs were comparable), we found that for the future projections, all GCMs resulted in notoriously different changes in lake evaporation.

When we estimated global average warm-season evaporation changes, it was evident that the influence of GCM models was more important than that of lake models, particularly in the future scenarios (Fig. 5.3). More specifically, when comparing the global average change in evaporation by the end of the century (2070-2099) (i.e. the increase in lake evaporation relative to the base period [1970-1999]), we found that there was a large spread in the projections, particularly for the high-emissions RCP 8.5 scenario. For instance, SIMSTRAT-UoG projected evaporation changes that ranged between 13% and 29%, ALBM evaporation changes varied between 23% and 52%, and VIC-LAKE projections varied between 16% and 33% (Fig. 5.3, Table C.8). Thus, unlike the historic period (where GCM models predicted a similar global average rate of lake evaporation), we found that for the future projections of lake evaporation, the climate models differed considerably from each other in their results.

Due to differences in simulated evaporation rates among the model ensemble, particularly across climate model simulations, using a multi-model average with quoted uncertainties can provide more robust predictions. At a regional scale, we found considerable variability in lake evaporation rates across lake thermal regions. For instance, lake evaporation for the base period (1970-1999) ranged between 1.8±0.5 mm day^{-1} and 4.5±0.28 mm day^{-1} for the northern frigid and southern warm regions respectively (quoted uncertainties represent the standard deviation of the model ensemble). Similarly to the historic period, by the end of the century (2070-2099), evaporation increases varied strongly across thermal regions. Under the most pessimistic scenario RCP 8.5, evaporation increased between 0.3±0.2 mm day^{-1} and 1.2±0.41 mm day^{-1} for the southern temperate and northern warm regions, respectively. These changes represented an increase of 42% for the northern frigid lakes and 12% for the southern

temperate lakes, demonstrating that lakes in the northern hemisphere will experience the largest increases in evaporation compared to the base period (Fig. 5.4, Table C.9).

At a global scale, the model ensemble from this study indicated an average warm-season evaporation rate of 3.2 ± 0.5 mm day^{-1} (quoted uncertainties represent the standard deviation of the model ensemble) during the last decades of the 20th century (1970-1999). During the 21st century (2006-2099) all lake models projected an increase in global lake evaporation. Under the low-emissions scenario (RCP 2.6), global lake evaporation was projected to increase by 0.3 ± 0.1 mm day^{-1} by the end of the 21st century. For the medium-high emissions scenario (RCP 6.0), global lake evaporation was projected to increase by twice as much (i.e., 0.6 ± 0.2 mm day^{-1}). The largest change in global lake evaporation was projected under the high-emissions scenario (RCP 8.5) with evaporation rates increasing by 0.9 ± 0.3 mm day^{-1}, i.e., three times higher than RCP 2.6. These projected changes correspond to an average (although highly variable across the ensemble) percent increase of 10%, 18%, and 27%, for RCP 2.6, 6.0, and 8.5 respectively, compared to the base-period average (Fig. 5.5, Table C.10).

To evaluate the combined effects of warm-season evaporation and precipitation on lakes, we estimated the difference between precipitation and evaporation $(P - E)$ (Fig. C.7). Our analysis revealed that under all RCP scenarios the multi-model average evaporation projections exceeded the multi-model average change in precipitation (Fig. 5.6). For the low-emissions scenario RCP 2.6 some regions in western North America, north South America and the Mediterranean exhibited deficits in P-E. The most pessimistic RCP 8.5 scenario showed a higher deficit in various regions of North America, northern South America, the Mediterranean, western and central Europe, as well as central Asia (Fig. 5.6). Notably, these results reflect the rapid increase in evaporation and the simultaneous decrease in precipitation this century in many lake-rich regions. Relative to the 1970-1999 base period average (0 ± 0.5 mm day^{-1}), P-E continuously decreased throughout the 21st century. For instance, our projections suggest that P-E will decrease by -0.2 ± 0.19 mm day^{-1}, -0.5 ± 0.24 mm day^{-1}, -0.8 ± 0.4 mm day^{-1} under RCPs 2.6, 6.0 and 8.5, respectively by the end of the 21st century (2070-2099) (Fig. 5.6, Table C.11).
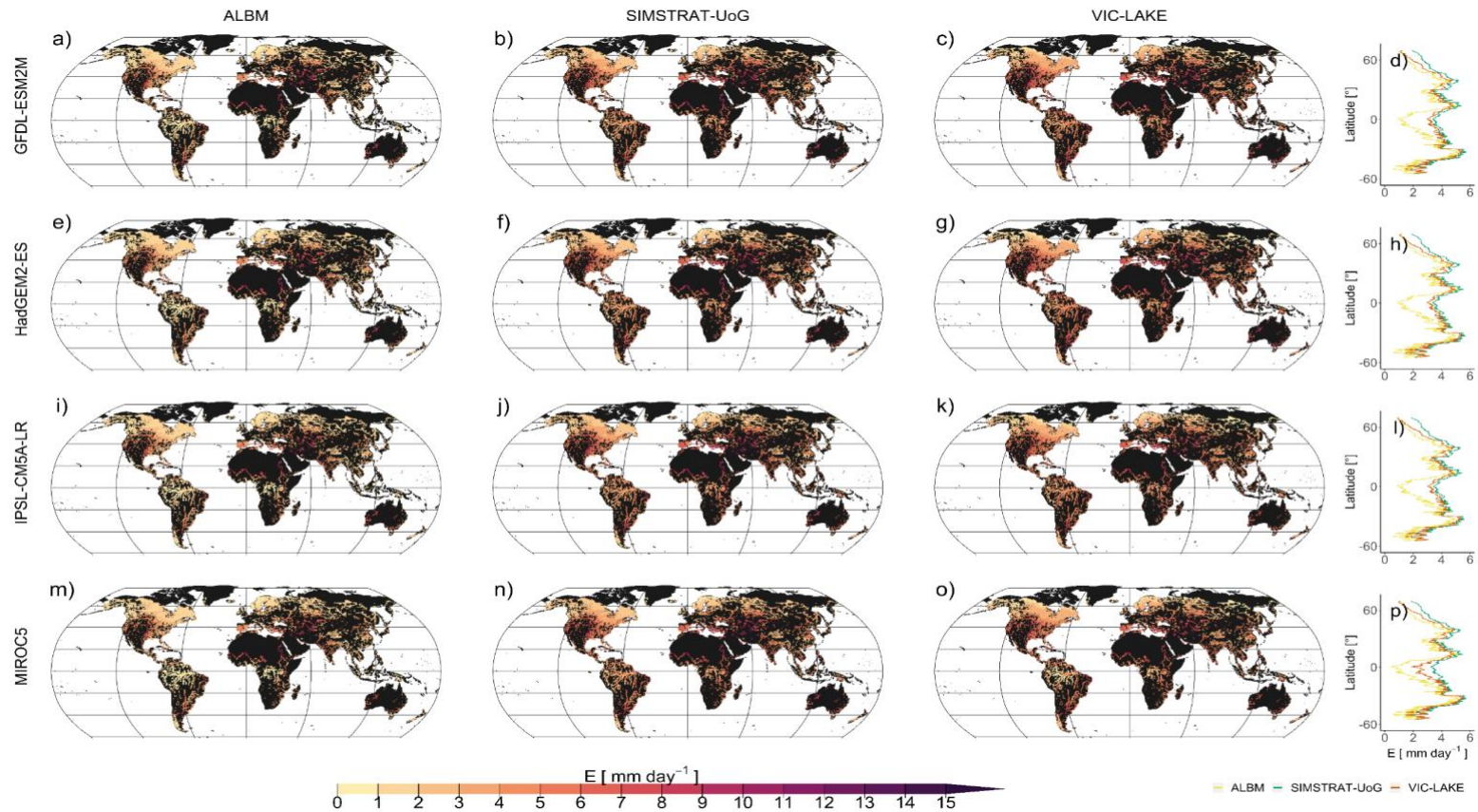
Figure 5.1 Warm-season lake evaporation rates in mm day⁻¹ averaged over the 1970-1999 period for each lake model and General Circulation Model (GCM) combination, shown are: (a, e, i, m) ALBM, (b, f, j, n) SIMSTRAT-UoG, (c, g, k, o) VIC-LAKE. Each lake model was driven by GFDL-ESM2M, HadGEM2-ES, IPSL-CM5A-LR and MIROC5. Latitudinal plots show warm-season evaporation simulations across lake models (d, h, l, p).
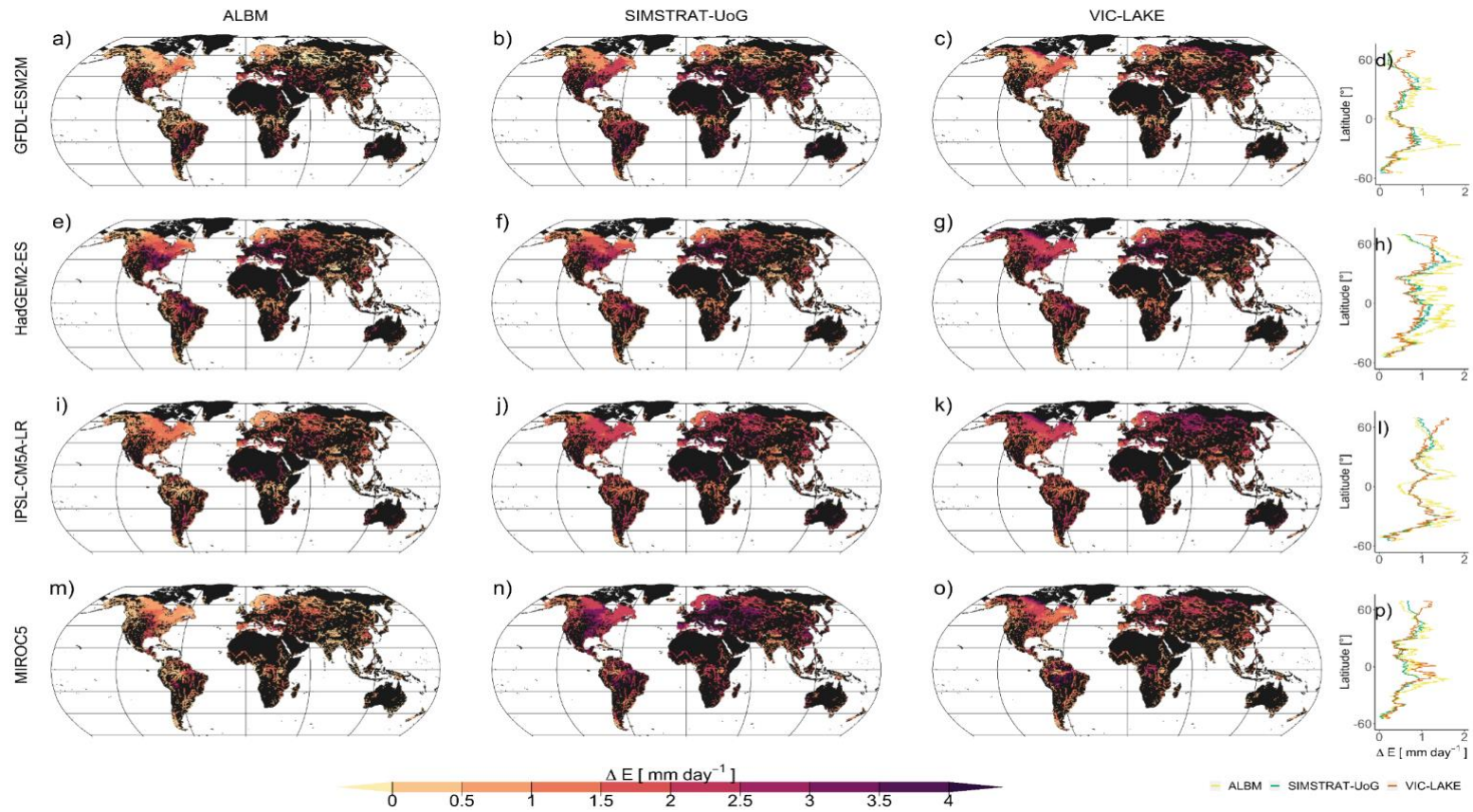
Figure 5.2 Projected changes in warm-season lake evaporation rates in mm day⁻¹ by the end of the 21st century (2070-2099) under Representative Concentration Pathway (RCP) 8.5. Projections are shown for each lake-model combination namely (a, e, i, m) ALBM, (b, f, j, n) SIMSTRAT-UoG and (c, g, k, o) VIC-LAKE. Each lake model was driven by GFDL-ESM2M, HadGEM2-ES, IPSL-CM5A-LR and MIROC5. Latitudinal plots show warm-season evaporation simulations across lake models (d, h, l, p). Anomalies (ΔE) are quoted relative to the 1970-1999 base-period average.
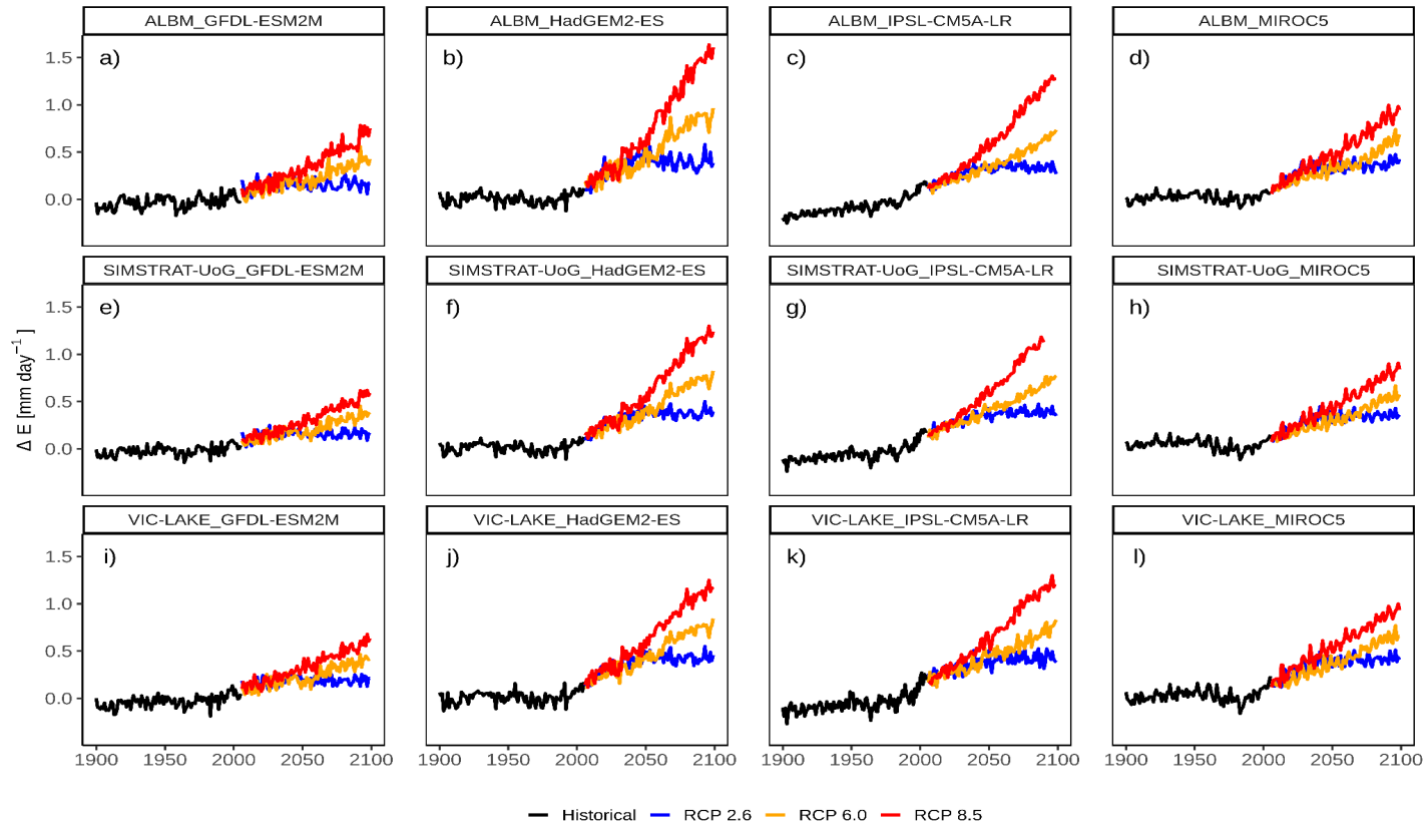
Figure 5.3 Projected changes in global warm-season lake evaporation in mm day-1 during the historic (1901-2005) and future (2006-2099) periods. Projections are shown for each of the individual lake-climate models, namely for (a-d) ALBM, (e-h) SIMSTRAT-UoG and (i-l) VIC-LAKE, driven by the four General Circulation Models included in this study. Black lines represent the historical period, and the coloured lines represent the future period, with the blue, orange and red representing the projected change under RCP (Representative Concentration Pathway) 2.6, 6.0, and 8.5, respectively. Anomalies (ΔE) are quoted relative to the 1970-1999 base-period average.
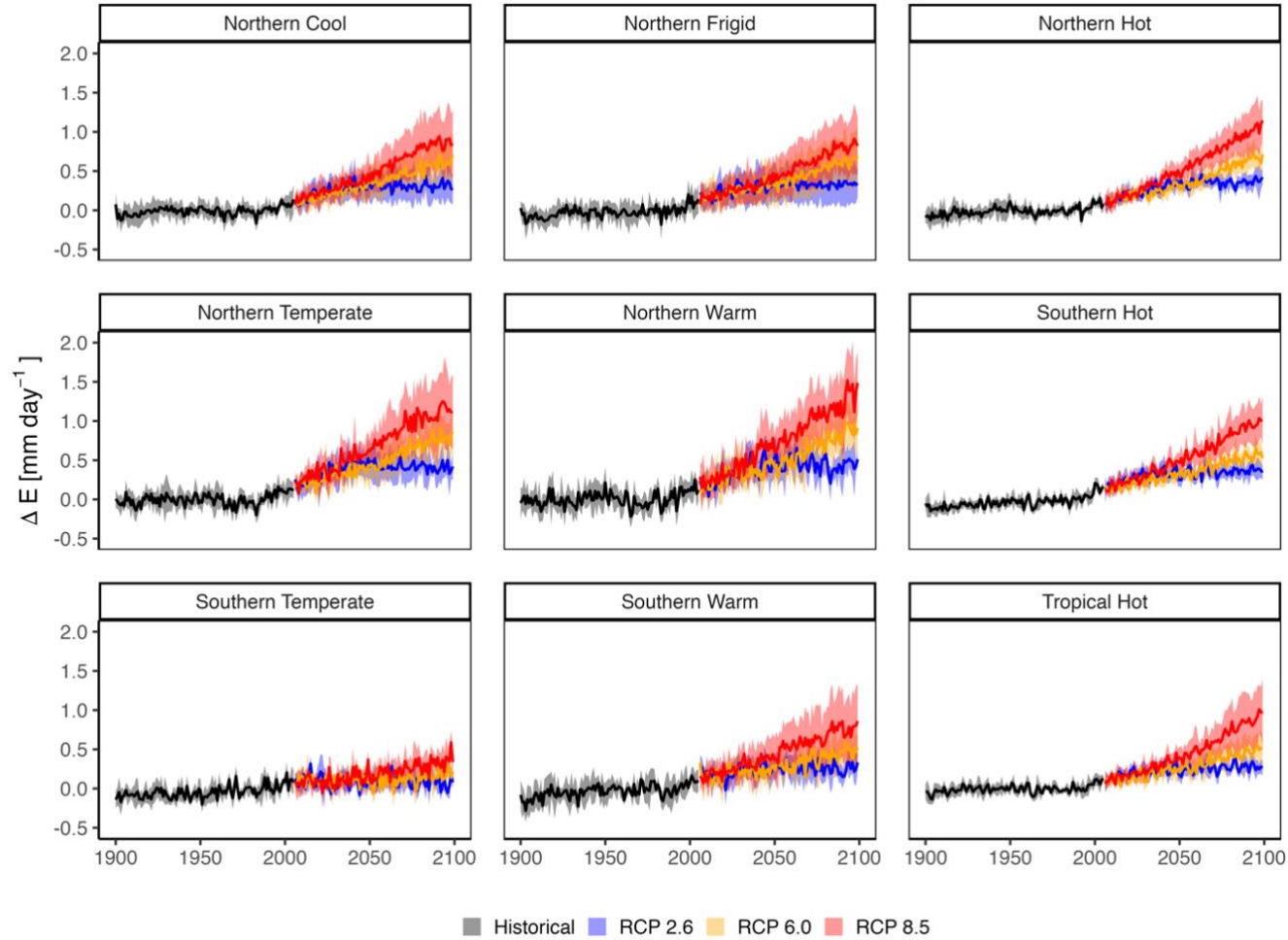
Figure 5.4 Model ensemble projected changes in global warm-season lake evaporation during the historic (1901-2005) and future (2006-2099) periods across lake thermal regions. Anomalies (ΔE) are quoted relative to the 1970-1999 base-period average
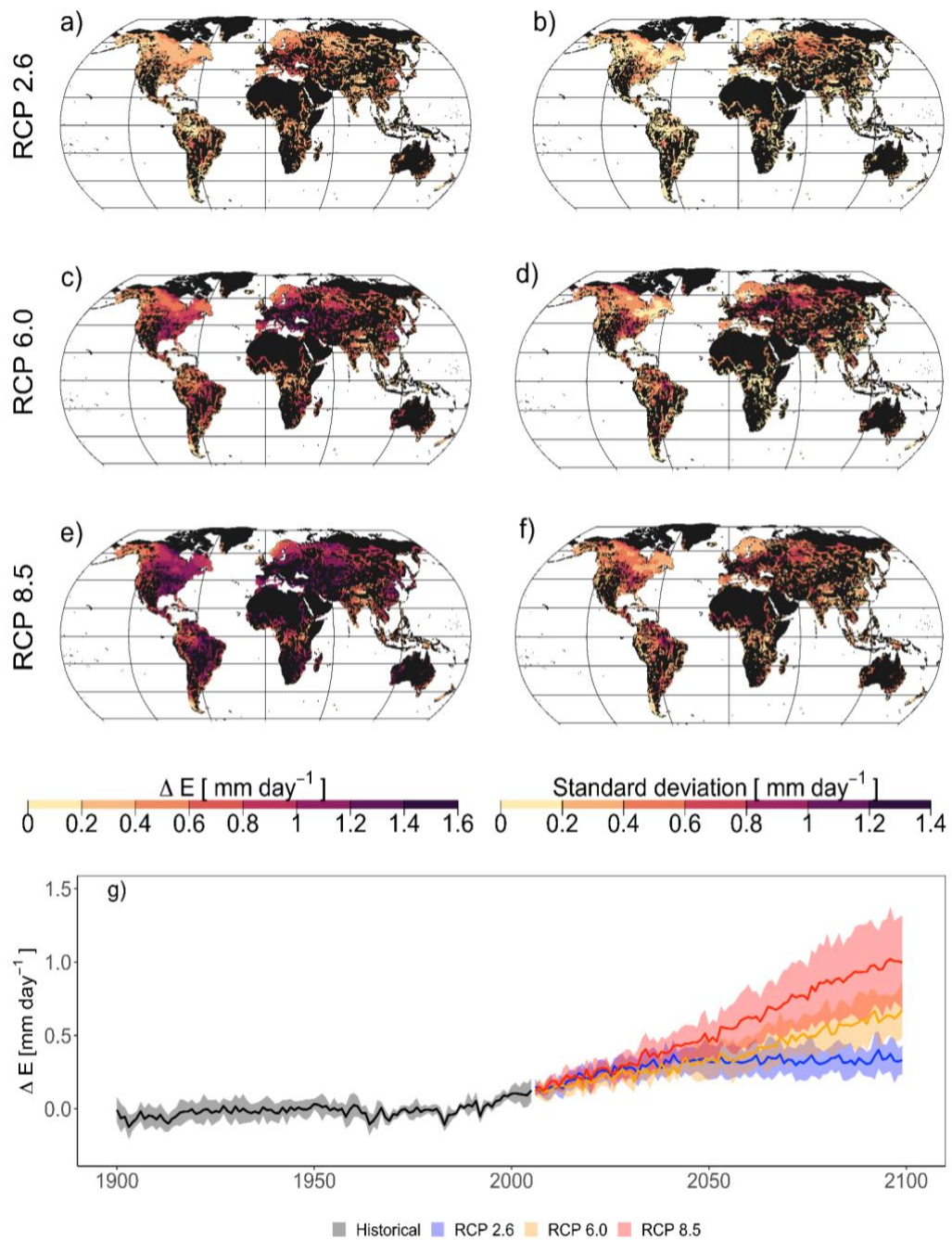
Figure 5.5 Projected changes in warm-season lake evaporation rates in mm day-1 (ΔE) by the end of the 21st century (2070-2099) for Representative Concentration Pathway (a-b) RCP 2.6 ,(c-d) RCP 6.0 and (e-f) RCP 8.5, averaged across lake and climate models. Shown are the mean (left column) and the standard deviation (right column), and (g) model ensemble projected changes in global warm-season lake evaporation during the historic (1901-2005) and future (2006-2099) periods. Anomalies (ΔE) are quoted relative to the 1970-1999 base-period average.
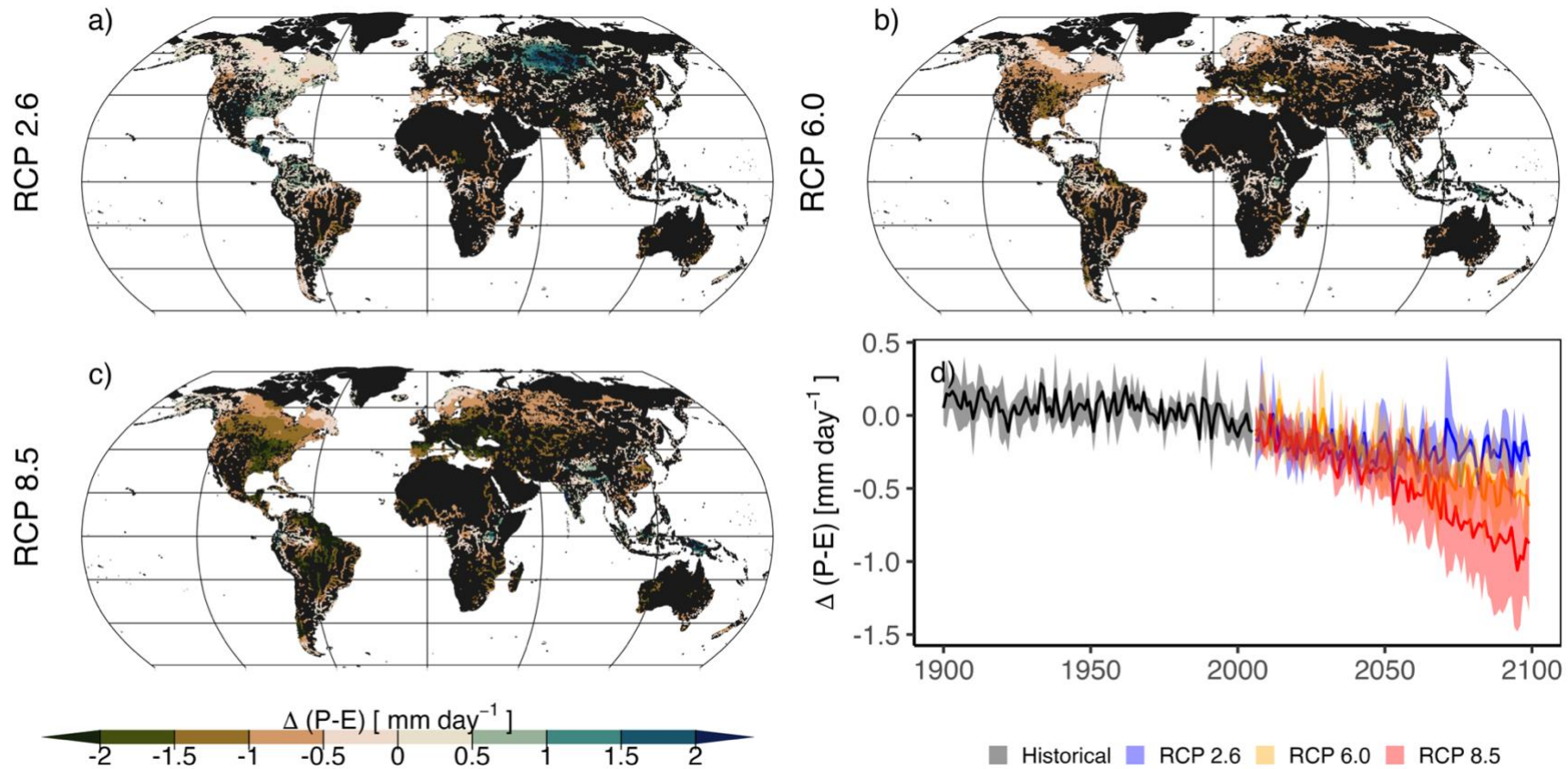
Figure 5.6 Projected changes in warm-season precipitation minus evaporation rates in mm day⁻¹ $\Delta(P - E)$ by the end of the 21st century (2070-2090) for Representative Concentration Pathway (a) RCP 2.6, (b) RCP 6.0 and (c) RCP 8.5, averaged across lake and climate models, and (d) model ensemble projected changes in global warm-season precipitation minus evaporation during the historic (1901-2005) and future (2006-2099) periods. Anomalies $\Delta(P - E)$ are quoted relative to the 1970-1999 base-period average.
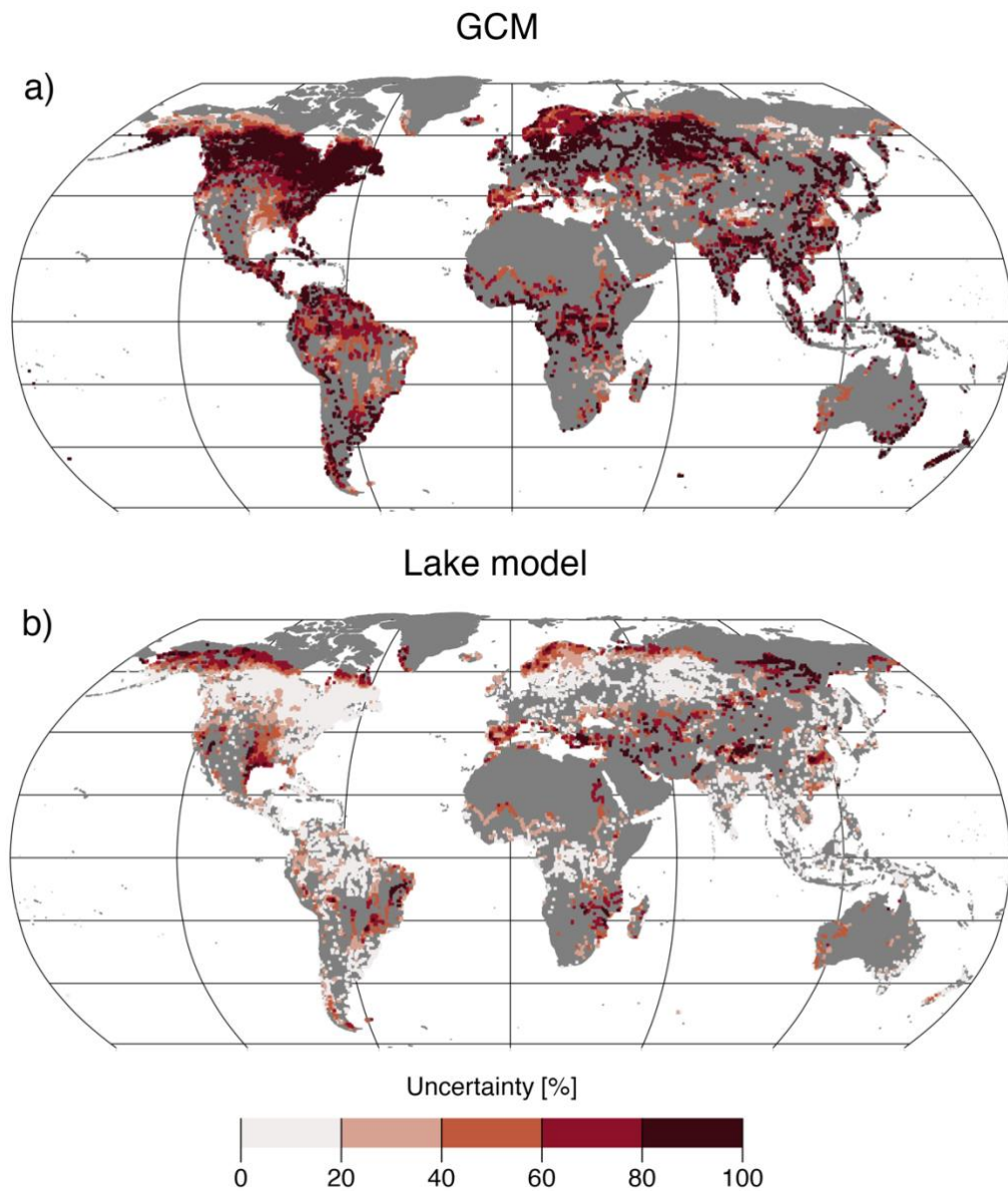
Figure 5.7 Percentage of total uncertainty explained by (a) GCM and (b) lake model in future projections of warm-season lake evaporation over the period 2070-2099 for the Representative Concentration Pathway (RCP) 8.5.
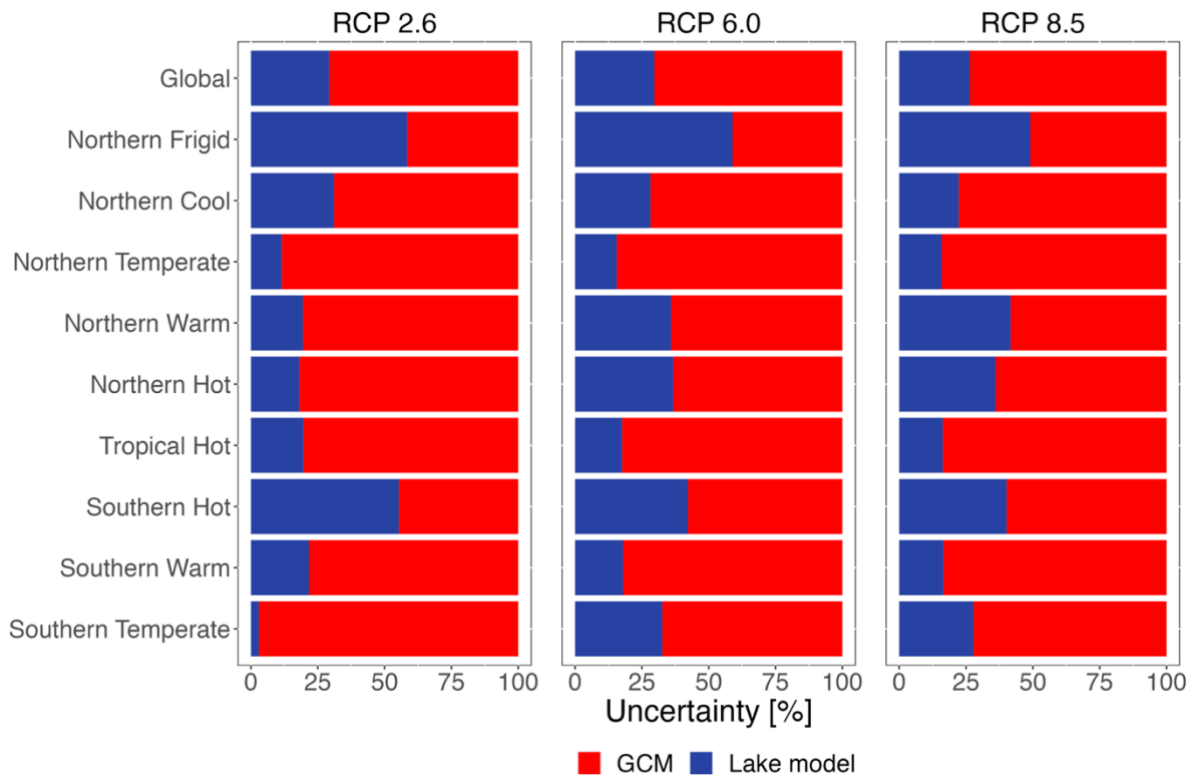
Figure 5.8 Percentage of uncertainty explained by GCM and lake model in projections of warm-season lake evaporation over the 2070-2099 period for the global average, and for the lake thermal regions under Representative Concentration Pathway (RCP) 2.6, 6.0 and 8.5.

5.4.3 Uncertainty in future projections of warm-season evaporation

We quantified the percentage of total variance explained by GCM and lake model for projections of warm-season lake evaporation during the 21st century under RCP 2.6, 6.0 and 8.5 (Fig. C.8, Fig. C.9 and Fig. 5.7). For the aim of this study, we only show the results for GCM and lake model uncertainty and, unlike Bosshard et al. (2013), do not show the interactions between lake model and GCM, which is outside the scope of this study. Figure 5.7 shows the variance explained by both GCM and lake model over the 2070-2099 period for the RCP 8.5 scenario. GCMs accounted for most of the variance (~74%) on global lake evaporation projections (Fig. 5.8), dominating in nearly all regions except some regions of North America, the Tibetan-Plateau, Siberia and West Central Asia (Fig. 5.7). However, it must be noted that the sources of uncertainty varied, particularly when comparing across lake thermal regions (Fig. 5.8), where lake model

variance became greater by the end of this century in the northern regions. We found that for the northern frigid thermal region, GCMs and lake models contributed equally to the variance in lake evaporation estimates at 51% and 49% for the RCP 8.5 scenario, respectively. Increasing trends in variance resulting from the lake models were found in the northern warm, northern hot, and southern temperate regions and to a lesser extent in northern frigid and southern hot regions (Fig. 5.8). GCM variance was mostly dominant in northern temperate, southern warm, and tropical hot regions but was also high in some lakes situated in the southern temperate region. Given that GCM explained most of the variance in future projections of lake evaporation, we further quantified the variability in key meteorological forcings across these models (Fig. C.10). We found that short- and longwave radiation as well as air temperature, showed a stronger variability than relative humidity, precipitation and wind speed. The highest variability was detected in regions of North America and Siberia, where northern cool and temperate lakes were located and to a lesser extent in northern South America.

5.5 Discussion

To the best of our knowledge, this is the first study to evaluate differences in projections of global lake evaporation using an ensemble approach (i.e. a combination of three lake models driven by four GCMs). In line with previous research (La Fuente et al. 2022; Liu 2022; Jansen and Teuling 2020; Pillco Zolá et al. 2019), our comparative analyses suggest that lake evaporation is sensitive to the choice of model used. Differences in spatial patterns of lake evaporation were evident across lake models and GCMs throughout the 20th and 21st century. Moreover, while previous studies using observational data and/or simulations from a single model suggest a latitudinal dependence on lake evaporation, with higher evaporation rates at low latitudes (Zhao and Gao 2019; Wang et al. 2018), our study demonstrates that not only the choice of lake model, but also the choice of driver data (i.e., the climate model) used can play a considerable role in the magnitude of projected evaporation in this climatic region. In fact, in agreement with recent assessments (Zhao et al. 2023), our uncertainty analysis on future projections of lake evaporation suggests that GCM model uncertainty (i.e., variance in estimates of climate models) was greater than lake model uncertainty (i.e., variance in the modeled representation of lake evaporation), explaining 74% of the total variance. Importantly, we

found that the lake model and GCM uncertainty contributions were variable across lake thermal regions, with lakes located in northern thermal regions exhibiting an equal uncertainty contribution from lake model and GCM. Other warm and hot thermal regions exhibited increasing trends in lake model uncertainty contribution during the 21st century, suggesting that uncertainty contribution from lake models and GCMs can be influenced by lake-specific characteristics. Despite the differences in time periods used to estimate evaporation change, our ensemble projections align with those reported by Wang et al. (2018), who estimated a global lake evaporation increase of 16% by 2091-2100 with reference to 2006-2015 under RCP 8.5, comparable to the 27% estimated by our model ensemble by 2070-2099 with reference to the 1970-1999 period. Therefore, our analyses demonstrated that using a single model realization may be problematic for capturing the strong spatial and temporal variability that evaporation rates exhibit at both regional and global scales.

Although we consider our results robust and believe that they bridge an important knowledge gap in climate change assessments, there are some limitations to consider when interpreting our key findings, particularly in terms of the magnitude of projected change from the 12 model realisations. Firstly, similar to both Wang et al. (2018) and Zhou et al. (2021), our simulations represent an aggregated 'typical lake' for each 0.5° longitude-latitude grid, where the modelled representative lake is characterized by the average surface area and depth of all known lakes in that grid. Individual lakes within a 0.5° grid will likely behave differently to the typical lake considered as, for example, lake surface area and depth are known to strongly modulate lake evaporation rates (Zhao et al. 2022; Wang et al. 2020; Zhao and Gao 2019). However, such representations of lakes (i.e., at a gridded scale) are necessary for their inclusion in Earth system models and for global scale projections (Zhou et al. 2021; Vanderkelen et al. 2021; Wang et al. 2018; Subin et al. 2012). Importantly, due to the spatial mismatch between real world lakes and our definition of a 'representative lake' a thorough validation of our results is not feasible and falls beyond the scope of this manuscript. Moreover, as our projections are generated using 1-D process-based lake models, which largely represent average lake conditions (Råman Vinnå et al. 2021; Ulloa et al. 2019), horizontal features within a lake and the intra-lake responses to climate change will not be captured (Calamita et al. 2021; Woolway and Merchant 2018; Mason et al. 2016). In turn, the spatial variability in

evaporation (Lenters et al. 2013; Spence et al. 2013; Mahrer and Assouline 1993), which can be large in some lakes, is not included in our projections. In addition, we highlight that our uncertainty estimations are likely biased due to the unequal number of GCMs and lake models, and thus result in a larger contribution of GCM variance. To address this limitation, we included a subsampling method in our uncertainty analysis, and thus demonstrated that the variance in future lake evaporation projections is mostly dominated by GCM data (Zhao et al. 2023). Furthermore, while this study provides important insights into lake evaporation responses to climate change, we focused solely on the warm season, thus we are neglecting evaporation rates at other times of the year. In some lakes, for example, the high evaporation season occurs during the autumn and winter (e.g., the Laurentian Great Lakes). However, for consistency across a global lake distribution, effects outside the warm seasons were not considered in this study. In addition, our ISIMIP2b simulations assume a constant light attenuation coefficient. While this is common in 1-D global lake simulations (Golub et al. 2022; Grant et al. 2021; Wang et al. 2018), it does mean that changes in water transparency during the 20th and 21st centuries are not considered. Transparency can either increase or decrease in the future, as it has during the historic period (de Farias Mesquita et al. 2020; Heiskanen et al. 2015). These changes in transparency can either amplify or suppress lake evaporation under climate change via its influence on lake surface water temperature (Rose et al. 2016). As it is uncertain how water transparency will change during the 21st century, the ISIMIP2b projections focused solely on the more robust future projections of climate change. While the limitations described above will influence the robustness of our simulations in terms of the projected magnitude of change at local scales (e.g., for individual lakes), we believe that these simulations are extremely useful to answer some of the core questions of this study, notably regarding quantifying differences across a lake and climate model ensemble.

An ensemble mean is typically considered to provide an optimal prediction of lake responses to climate change (La Fuente et al. 2022; Trolle et al. 2014), with the underlying assumption that different models provide statistically independent information evenly distributed around the true state (Pennell and Reichler 2011). Ensemble modelling has become increasingly popular in climate change impact assessments in recent years. However, its application should include, when possible, detailed uncertainty

quantification. This is important due to the high variability that different sources of error and uncertainty (i.e. lake model, climate model, model parameter, initial conditions, etc.) can have on projected historical and future change. Here, we have considered only two sources of uncertainty (i.e., due to lake and climate models), but others could also be important. Specifically, recent studies have highlighted the benefit of using large ensemble simulations (i.e., a set of projections starting from different initial conditions but produced with a single model and identical external forcing (Deser et al. 2020). Given the important role that GCMs play in the uncertainty of lake evaporation, future research could investigate the contribution of key forcings (i.e. wind speed, relative humidity, solar radiation, etc.) to the overall GCM uncertainty, and thus provide valuable information not only for water managers but also for modelers.

The use of large ensembles in lakes is not common, given its computational expense. However, some recent studies have used large ensembles to investigate lake responses to climate change, notably to investigate the contribution of natural vs anthropogenic forcing to changes in lake ice cover (Huang et al. 2022). Similar large ensemble simulations have also been used in terrestrial and marine ecosystems to investigate long-term temperature changes (Schlunegger et al. 2020; Silvy et al. 2020; Mora et al. 2013). Future studies could benefit from investigating lake evaporation responses to climate with the use of large ensembles. In practice no single model can be identified as being the best performing due to the lack of global lake evaporation observations, which limits a detailed validation of these simulations. Our study quantifies the uncertainties associated with our results and thus highlights the advantages of using a multi-model approach. Future studies could benefit from more extensive validation of these global simulations. However, given the cost, accessibility, and technical challenges of obtaining direct measurements of lake evaporation at local, and even more so at global scales, the validation of evaporation estimates is often limited to specific lake sites (Zhao et al. 2022; Wang et al. 2018).

Accurate evaporation quantification is crucial for adaptation and mitigation planning, particularly in regions that rely heavily on the ecosystem services that lakes provide. Indeed, evaporation from lakes is increasing at alarming rates, however it is in fact the P-E (precipitation minus evaporation) relationship that primarily influences the water budget of many lakes. Our results suggest that the increase in evaporation will likely

exceed precipitation, particularly in regions where precipitation is projected to decrease this century. More specifically, all RCP scenarios projected a global decrease in the P-E relationship, with the P-E spatial distribution suggesting that more and more lakes are likely to experience a deficit in their water balance. As two key lake ecosystem threats (i.e. reduced water quantity and water quality deterioration) are directly linked to evaporation, robust model projections with quantified uncertainties are critical to increase the confidence in future projections for decision-making. In a recent assessment of lake Sunapee, Wynne et al. (2023) highlighted the large variability in uncertainty sources for various lake thermal metrics. As a complex physical process related to, among others, surface water temperature and lake heat storage, evaporation is likely to exhibit variability in uncertainty sources across different lake types. Recent studies have highlighted the benefit of investigating climate change impacts in lakes with the use of multiple lake-climate model combinations (Golub et al. 2022; La Fuente et al. 2022; Moore et al. 2021). Indeed, multi-lake-model simulations are increasingly used to provide robust assessments of freshwater ecosystem responses to climatic variations. In addition, multi-model comparisons are powerful methods to explore reliable scientific findings and yield robust policy conclusions (Duan et al. 2019). Our model simulations were part of the ISIMIP framework, and thus open the possibility to link the implications of our results with other relevant sectors (Frieler et al. 2017; Rosenzweig et al. 2017; Warszawski et al. 2014). More specifically, our evaporation simulations can be utilized in studies of regional water availability and water quality, population health, fisheries and marine ecosystems, and agriculture (Zhao et al. 2022; Friedrich et al. 2018; Li et al. 2013; Marsh and Bigras 1988).

5.6 Conclusions

In this study we used an ensemble of lake-climate models to project future global lake evaporation changes under scenarios of climate change. We found substantial differences in projected global lake evaporation across the model ensemble. These differences indicated that a single-model realisation cannot capture the strong spatial and temporal variability that global lake evaporation exhibits. Furthermore, our results projected that global annual lake evaporation rates will increase by 27% under the Representative Concentration Pathway (RCP) 8.5, higher than the 16% increase predicted by earlier studies. Our uncertainty analysis revealed that GCM driver data had a greater contribution

than lake model to the variance in future projections of lake evaporation. Using a multi-model approach is essential for providing robust evaporation projections, and quantifying the uncertainties associated to these projections. The findings of this study have important implications for the water management of lake-rich regions, and provides important insights for the lake modeling community.

Chapter 6   Synthesis and lessons learned

6.1 Summary of findings

Lakes hold a large proportion of the surface freshwater available on Earth, making them critical sources of drinking water for, among other things, human consumption (Gleick 1993). Due to their open-water areas and the vapour pressure gradient at their air-water interface, lakes can experience significant water loss via evaporation (Zhao et al. 2022; Zhang and Liu 2014; Lenters et al. 2005). Therefore, evaporation is the most important component of the hydrological cycle after precipitation, and represents the main water loss for most lakes. Global warming is altering the hydrological cycle and has increased the occurrence of more extreme precipitation, both high and low extremes, as well as enhanced evaporation. These concurrent changes in climate can significantly alter the hydrological cycle of lakes, and thus increase the vulnerability of these natural ecosystems. To alleviate the negative consequences of climate change and increasing water demands on lakes, efficient water management systems are required. Therefore, the ability to adequately monitor and estimate lake evaporation responses to changing climate becomes crucial for adequate and efficient water management (Givati et al. 2019; Prange et al. 2020). Albeit the crucial role of evaporation in the basic functioning of lakes and its influence on water availability, many assessments that quantify the losses from these water bodies often use traditional single-model approaches (Zhao et al. 2022; Wang et al. 2018). Regardless of the limitations of many of the methodologies available for evaporation quantification, very few studies have acknowledged the sensitivity of this physical process to the choice of model/method (La Fuente et al. 2022; Jansen and Teuling 2020; Pillco Zolá et al. 2019; Rosenberry et al. 2007), nor have they reported the uncertainties associated with its estimation (Zhao et al. 2023).

The research presented in this dissertation has been conducted to improve the understanding of lake evaporation responses to climate change and its associated uncertainties through the use of an ensemble (multi-model) modeling approach at local, regional and global spatial scales by addressing the following objectives:

- To investigate evaporation responses to climate change in a lake with high socio-economic, political and religious value, and to test the performance of the ensemble approach. (Chapter 3)

- To examine lake evaporation responses to climate change among lakes within the same geographical region but with different climate conditions and characterised by different morphometric characteristics. (Chapter 4)

- Investigate differences in global lake evaporation responses to climate change using an ensemble of models and to quantify the uncertainties in projections of future lake evaporation. (Chapter 5)
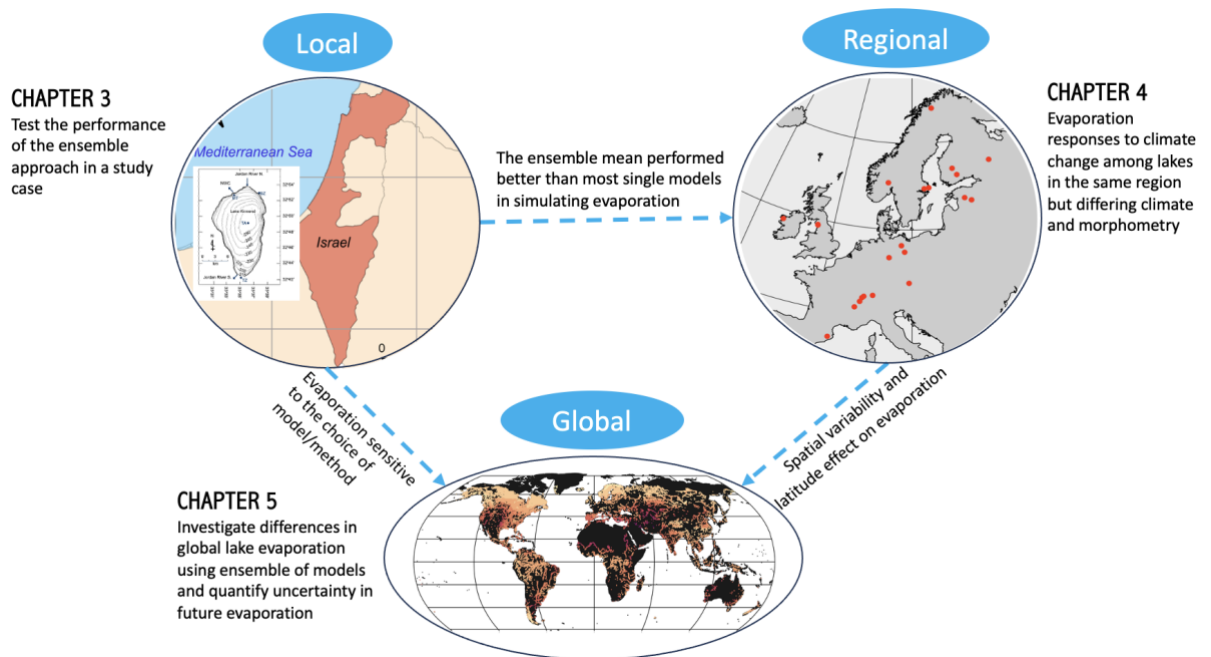
Figure 6.1 Scheme of specific objectives.

Each of these objectives were addressed by Chapters 3 through 5 of this dissertation (Fig. 6.1.). Firstly, Chapter 3 is an assessment of projected changes in evaporation rates in Lake Kinneret, a socioeconomically important lake in the Middle East, using an ensemble of 20 lake-climate model realisations. The results revealed that the ensemble mean of the models tested had a better performance than most of the individual lake-climate model realizations in simulating reference evaporation during the historic period. By using the

ensemble approach, key differences in model performance were better understood and, thus, the usefulness of this approach was demonstrated to project future lake responses to climate change. There was a general agreement on the seasonal variability in evaporation among the lake-climate model ensemble. Importantly, the lake-climate model simulations matched those shown by the reference evaporation calculated using observational data, with the ensemble mean often showing the best performance. Furthermore, this analysis revealed that considering an ensemble of both lake and climate model simulations was critical when projecting future change in lakes, given the spread of the projected changes.

Having tested the robustness of using an ensemble approach, Chapter 4 focused on investigating the spatial variability of long-term evaporation responses to climate change on a set of European lakes with varying climate conditions and morphometry. More specifically, Chapter 4 applied the modeling framework presented on Chapter 3 into 23 lakes distributed across Europe. The analysis carried out in Chapter 4 showed that lake evaporation varied greatly among lakes, but exhibited some latitudinal patterns. Specifically, Chapter 4 indicated that evaporation increased more rapidly in lakes located in the warmer regions of Europe (i.e. south) whereas the lowest changes were detected in cooler regions in the northern region of the continent, elucidating the latitude effect on evaporation. Another important finding of this chapter was related to the relationship between evaporation and lake morphometry. Contrary to previous findings (Zhao et al. 2022; Woolway et al. 2018), the simulated evaporation rates presented in this chapter had no discernible relationship with lake morphometry.

When upscaling the multi-model approach analysis to 13K representative lakes distributed globally as explained in Chapter 5, a high variability in evaporation projections across models was evident. Notably, there were regions where the differences in evaporation projections across models varied from one to three orders of magnitude, demonstrating once again the high dependence of evaporation to the choice of model. Interestingly, this global assessment revealed that the choice of driver data (i.e. GCM) played a pivotal role in evaporation variability, particularly for future projections. This was confirmed by an uncertainty analysis, where GCM data were found to contribute most of the variance on future evaporation estimates. Other regional assessments of future reservoir evaporation in the Contiguous United States have also reported a key role of GCM on evaporation uncertainty (Zhao et al. 2023). While for practical reasons as

described in Chapter 5, the global lake evaporation simulations presented in Chapter 5 could not be validated, both Chapters 3 and 5 highlight that using traditional single-model approaches not only at local but also at global spatial scales may lead to the underestimation or overestimation of the actual evaporation values and thus generate large errors with implications for future water management decisions.

Chapters 3 through 5 also evaluated the combined effects of precipitation (P) and evaporation (E) by calculating the P-E relationship. The results presented in Chapter 3 suggested that the evaporation increase projected in Lake Kinneret is likely to exceed precipitation, meaning that the lake is projected to experience a water deficit under scenarios of climate change. These findings are critical due to the already existing water crisis in the Middle East, which will be further exacerbated by an exponential increase in population estimated for the region. A higher variability in P-E responses to climate change was also found among the European lakes studied in Chapter 4. All models indicated that evaporation is likely to be greater than precipitation under all scenarios, with the P-E ratio being primarily negative throughout the 21st century in most studied lakes. Similarly, the global projections presented in Chapter 5, revealed that under all RCP scenarios the multi-model average evaporation projections exceeded the multi-model average change in precipitation. Notably, these results reflected the rapid increase in evaporation and the simultaneous decrease in precipitation this century in many lake-rich regions.

6.2   Ensemble modeling of lake evaporation

As lakes can lose significant amounts of water due to evaporation (Zhao et al. 2022; Lenters et al. 2005), the differences in evaporation estimates across models that were identified in the ensemble approach in this thesis have important implications for water management (Jansen and Teuling 2020). If the study case of Lake Kinneret presented in Chapter 3 is considered, where evaporation estimates varied considerably among models, some models underestimated the reference evaporation (i.e. estimates of evaporation using in-situ meteorological data) while other models overestimated it (La Fuente et al. 2022). This means that if a water manager was presented with data from only one model and depending on the model used, they could make a decision on whether or not to reduce/increase the outflows/inflows to the lake to preserve ecologically safe lake levels.

Given that direct measurements of evaporation are difficult and expensive to obtain (Lenters et al. 2013; Blanken et al. 2011), the results in this dissertation stress even more that knowledge of the discrepancies among models to estimate evaporation is of great relevance for water management.

A large body of research has successfully implemented ensemble modeling in earth system modeling within the Coupled Model Intercomparison Projects (CMIP) (O'Neill et al. 2016; Taylor et al. 2012), as well as in key components of the global water cycle, including precipitation (Allan 2023; Ahmed et al. 2019), riverflow (Zhou et al. 2023; Gu et al. 2020; Moragoda and Cohen 2020), groundwater (Reinecke et al. 2021), evapotranspiration (Vinukollu et al. 2011), evaporation (Allan 2023; Le and Bae 2020), terrestrial water storage (Ju et al. 2023), sea surface temperature (Tittensor et al. 2021), etc. However, despite the popularity of the ensemble approach in climate sciences, its application in lake systems is still in its infancy. The growing availability of global lake datasets (Khandelwal et al. 2022; Lehner et al. 2022; Meyer et al. 2020; Pekel et al. 2016), expanding monitoring networks (Hanson et al. 2016; Weathers et al. 2013), together with the increasing popularity of well-established process-based models provides great opportunities to improve our fragmentary understanding on the effects of anthropogenic climate change on lakes through the use of multi-model assessments. Indeed, global collaborative efforts such as GLEON and the ISIMIP have resulted in key contributions that have investigated critical physical processes in lakes such as ice phenology (Grant et al. 2021), stratification (Woolway et al. 2021), water temperature and methane emissions (Jansen et al. 2022; Gal et al. 2020), extreme events (Mesman et al. 2020), and phytoplankton (Trolle et al. 2014) (Fig. 6.2). The work presented in this dissertation contributed to the body of research through the investigation of lake evaporation responses to climate change at local, regional and global scales. Not only it bridges an important knowledge gap in a key component of the global hydrological cycle, but it also complements previous research on the lake responses to climate change (Fig. 6.2).

Notably, this research revealed that a high variability in evaporation projections between different models was evident at local, and global scales. For example, the analysis of simulated evaporation in Lake Kinneret revealed differences between the models included in the ensemble. Similarly, our global assessment revealed that there were regions where the differences in evaporation projections between models varied

widely, demonstrating once again the high dependence of evaporation on the choice of model. While the absence of global-scale observed lake evaporation rates did mean that the simulations from the global assessment presented in Chapter 5 could not be compared to reference values, the results of Chapter 3 showed that the use of traditional single-model approaches may lead to the underestimation or indeed overestimation of evaporation rates and thus introduce greater error in estimates that can be potentially used to inform water management. Further, this study highlights that the models used in the ensembles, which have been widely validated and tested in a great diversity of study cases, can be used to simulate regional and global physical processes in lakes.
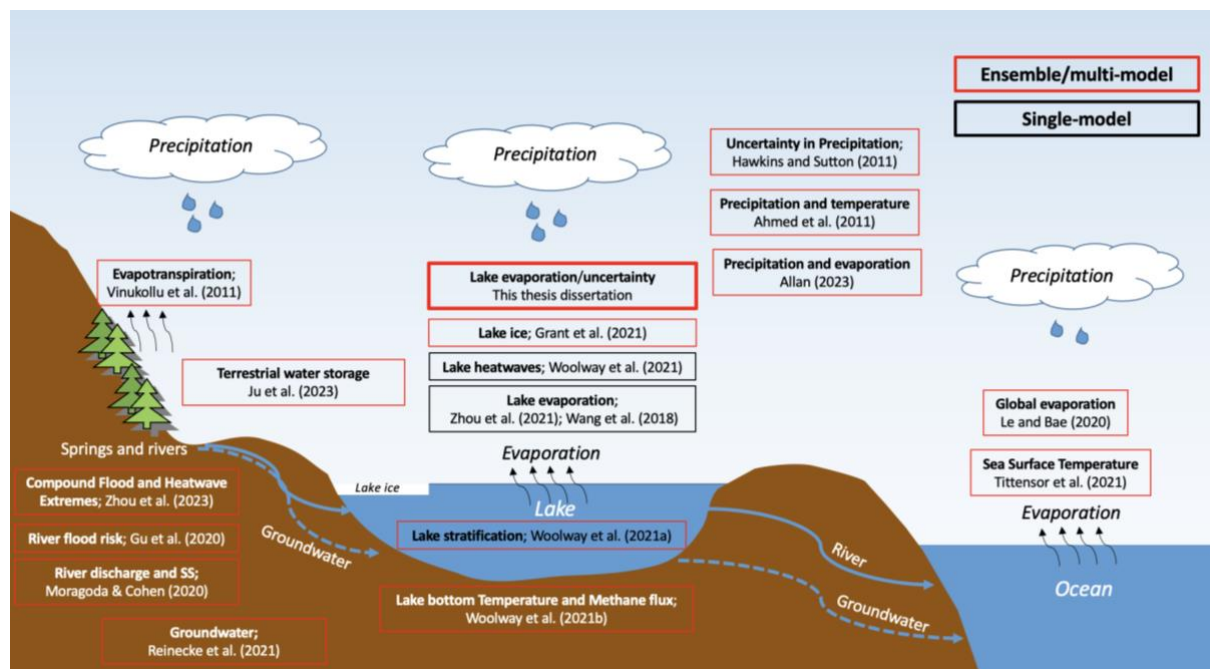
Figure 6.2 Contribution of this dissertation to ensemble/multi-model research in the global water cycle.

6.3 Regional variability in lake evaporation responses to climate change and the role of morphometry

As lakes are rapidly responding to global warming, a number of studies have already reported the effects of climate change on water temperature (Woolway et al. 2017; O'Reilly et al. 2015), ice (Sharma et al. 2019), mixing regimes (Woolway and Merchant 2019), stratification (Woolway et al. 2021) and evaporation (Zhao et al. 2022; Wang et al. 2018). Yet, few studies have analysed these climate effects on lakes at continental

scales despite their utility to define sustainable management strategies and understanding ecological traits (George 2010). Chapter 4 of this dissertation evaluated the regional variability in evaporation from 23 lakes of differing climate and morphometric characteristics distributed across Europe for the first time. To this end, it used a combination of process-based models and observed lake thermal properties. The initial hypothesis of this chapter was that lake morphometric features dictate the fate of evaporation. This assumption was worth investigating as the morphometry of a lake as well as site-specific features can considerably affect its response to a changing climate (Han and Guo 2023; Fergus et al. 2022; Hanson et al. 2021; Wang et al. 2019). However, contrary to research that dominates the literature (Zhao et al. 2022; Woolway et al. 2018), the results suggested that lake morphometry was less relevant in the evaporation variability detected across these European lakes. In turn, an effect of latitude in evaporation across the studied lakes was observed which is comparable with previous findings (Woolway et al. 2018; Woolway et al. 2017; O'Reilly et al. 2015). The discrepancies between these results and earlier research could be due to the different wind speed sources used, as well as to the use of a relatively small number of study lakes to detect a clear morphometric effect. While Woolway et al. (2018) reported a significant relationship between wind speed and evaporation using over-lake high-frequency observations, this dissertation used a gridded dataset (Lange 2019). Therefore, it is likely that the in-situ observations reported by Woolway et al. (2018) were more representative of over-lake conditions than gridded GCM data, thus explaining the discrepancies with earlier research.

6.4   Uncertainties in future projections of lake evaporation

Multi-modeling approaches can be useful to quantify the uncertainty in future projections of lake physical properties through the ensemble spread (Wynne et al. 2023; La Fuente et al. 2022; Moore et al. 2021), and they can also help to attribute the uncertainty to different components of the modeling chain (GCM-Lake Model). This dissertation found that evaporation changes can differ considerably when using different methodologies both at local and global spatial scales. Further, the results demonstrated that using an ensemble modeling approach can be useful for quantifying the uncertainties in the estimations, both at local and global spatial scales. More specifically, Chapter 5 of this dissertation

quantified the uncertainty contribution of both lake model and GCM to future projections of global lake evaporation using an ANOVA method (Bosshard et al. 2013). In agreement with earlier findings (Zhao et al. 2023), the results revealed that the choice of GCM played a pivotal role in the variability of future evaporation estimates. Few studies have previously reported the uncertainties associated with future projections on lake physical properties in single sites (Wynne et al. 2023) and at regional scales (Zhou et al. 2023). This dissertation is the first to report the uncertainties associated with both lake model and GCM on future lake evaporation at a global scale.

Based on simulations for 13K lakes distributed globally, Chapter 5 of this dissertation showed that future evaporation projections were indeed more sensitive to the choice of GCM than to the choice in lake model, which is contrary to the findings presented in Chapter 3 for a single site. Using an ensemble of simulated physical properties for Lake Sunapee, Wynne et al. (2023) demonstrated that surface water variables from lakes were likely more sensitive to GCMs, whereas water column properties were found to be more sensitive to the choice of lake model. While the findings presented in this thesis agreed with Wynne et al. (2023) in that evaporation variance was more sensitive to the GCM forcing data, they also highlight that the uncertainty contribution from either GCM or lake model can vary greatly among sites. For instance, lakes in northern thermal regions showed an equal uncertainty contribution from both the GCM and lake model. Other key contributions of uncertainty analysis in the lake modeling literature have included not only variation between GCMs but also for other sources such as downscaling methods and input from hydrological models (Zhao et al., 2023). Thus while the uncertainty analysis undertaken in this thesis focused only on two sources of uncertainty, other important factors could potentially be explored in future studies (e.g. initial lake model conditions, individual lake model parameterisation, etc).

Uncertainty analyses such as the one presented in this dissertation are vital to improve the current understanding of lake responses to climate change. These types of assessments can help to identify model caveats, guide future development, and ultimately improve projection performance (Wynne et al. 2023; Moore et al. 2021; Janssen et al. 2015). Thus the results presented here not only have important implications for policy relevant advice, but also for modelers. As robust decisions need to be made, reducing the uncertainty in lake modeling can allow for better decisions. However, reducing this type

of uncertainty will only partially solve the problem, as GCM remains to be the primary source of uncertainty. Whilst discussing the caveats of GCMs falls beyond the scope of this dissertation, it is of note that important advances in improving their climate representation have also been reported through the outputs of the CMIP6 project (O'Neill et al. 2016).

6.5 Implications for water availability

This thesis used an ensemble modeling approach and three distinct spatial scales to investigate the impacts of climate change on lake evaporation as well as in precipitation through the *P-E* relationship for the first time. While the local-scale assessment for Lake Kinneret included not only annual but also seasonal analysis, the regional and global assessments of evaporation focused on what was defined as the warm-season. In all cases the projections of *P-E* were primarily negative suggesting that many lakes are likely to experience deficits in their water balance under scenarios of climate change.

In the case of Lake Kinneret, the concurrent evaporation increase and precipitation decrease projected is likely to exacerbate the already existing crisis in the Middle East (La Fuente et al. 2022). In response to these trends, the Israeli government previously decided to replenish the already depleting water levels in Lake Kinneret by building a desalination plant along the Northern Mediterranean shoreline (Tal 2019b). While in this specific case the implementation of a mitigation measure of this magnitude was feasible to cope with the negative effects of climate change, the opposite is expected to happen in many parts of the world, where such mitigation measures would not be economically possible. Similarly, the continental-scale assessment of 23 lakes in Europe in Chapter 4, that was focused on the boreal summer, also revealed a persistent increase in evaporation combined with a decrease in precipitation. Accordingly, recent studies reported that lower than average precipitation will increase in frequency and intensity, resulting in meteorological droughts across Europe (Massari et al. 2022). Thus, if the fate of future evaporation and precipitation from European lakes align with the projections presented in this thesis, it is likely that the increasing trends in evaporation from these lakes during the summer will further amplify the negative impacts of the projected droughts for the region. Finally, the global assessment based on 13K lakes in Chapter 5 showed a larger spatial variability in *P-E* changes, but with a balance that was predominantly negative in

lake-rich regions. This has important implications for water availability, as the projections presented in this dissertation suggest that many lake-rich regions are likely to experience freshwater deficit within a warmer world.

Changing *P-E* ratios have been suggested to cause dramatic changes in the water balance of particularly shallow and seepage lakes, through the depletion of water levels (Hanson et al. 2021). For instance, lakes that were previously permanent have become ephemeral, and ephemeral lakes have become completely dry (Woolway et al. 2022; Finger Higgens et al. 2019). Such changes were not only reported in arid and semi-arid regions (Darehshouri et al. 2022; Wurtsbaugh et al. 2017), but also in northern arctic regions (Finger Higgens et al. 2019). Importantly, water deficits in freshwater from lakes can also amplify the negative effects of droughts in a given region, and thus have major implications for access to clean water, food, energy generation and transportation of goods. As well as the significant socio-economic implications, the depletion of water levels can cause ecosystem disturbances. For example, the removal of freshwater due to evaporation can increase salinity and thus have serious effects not only for physical processes (Ladwig et al. 2021) but also for community composition, biomass, and diversity of phytoplankton, zooplankton, macrophytes and fish (Jeppesen et al. 2015), as well as a weakening of key species, the proliferation of invasive species, and a loss of biodiversity (Zohary and Ostrovsky 2011).

6.6 Future research

The global warming effects on lakes have received less attention in high profile international efforts such as the Intergovernmental Panel on Climate Change (IPCC), United Nations or the Intergovernmental Science-Policy Platform on Biodiversity and Ecosystem Services (IPBES) (Prange et al. 2020). The research presented in this dissertation highlighted the benefits of using a multi-model approach for the simulation of evaporation losses from lakes, and it further demonstrated that using this methodology allows the quantification of uncertainties, which are particularly useful for policy making and for improving projections performance. Nonetheless, certain aspects of this research can be potentially improved and thus can be addressed in future work.

This thesis focused solely on the changes of evaporation rates and not on the overall evaporation volume, a metric which can be more relevant for water management.

These types of studies can be achieved by combining observations from lake water surface area, with evaporation rates to estimate volumetric loss. An alternative approach could be extracting satellite observations (at a global scale) to estimate lake surface dynamics and thus obtain evaporative volumes (Zhao et al. 2022). However, projecting future evaporative volumes remains challenging due to the high variability of lake water surface area (Khandelwal et al. 2022). As a result, there has been little research on future projections of reservoir area at larger spatial scales. Some regional assessments have projected future evaporative volumes from lakes by defining an inflow-area relationship based on observations and using this as a basis to project future lake surface area dynamics (Zhao et al. 2023). However, such assessments require long-term inflow/outflow observations which are mostly limited to reservoirs or lakes with well-established monitoring networks, limiting its applicability at global scales. Recent advancements that combine the Surface Water and Ocean Topography (SWOT) satellite altimeter data with river-lake mass conservation algorithms to estimate river flow at river-lake interfaces (Riggs et al. 2023) seem a promising approach to bridge this knowledge gap.

Water losses due to ice sublimation were also not accounted for in this dissertation. As a large proportion of the world's lakes are located at high latitudes (Messager et al. 2016) and thus freeze during winter (Walsh et al. 1998), sublimation can account for up to 40% of the water losses from lakes in arid regions during the ice-cover period (Huang et al. 2019). Therefore, investigating ice thermodynamics and its role in the heat and mass balance of lakes during the ice-cover period can improve the estimation of seasonal as well as annual water balance from lakes (Cao et al. 2022; Huang et al. 2019).

Future global lake assessments could improve their performance by using locally derived parameter and coefficient values (Golub et al. 2022). While for practical reasons, the global lake evaporation simulations presented in Chapter 5 were not validated, future efforts could potentially make further use of existing modeling frameworks such as the ISIMIP lake sector, to improve the performance of the ensemble of models used to simulate global evaporation. However, compared to the over 100 million lakes distributed worldwide, very few water bodies have sufficient data to allow the parameterisation of lake models globally. Importantly, a large number of these lakes are concentrated in the

northern hemisphere (North America and Europe), showing an evident misrepresentation of tropical, and arctic lakes and therefore a bias in the estimates. Expanding lake monitoring networks to include a wider diversity of lakes would provide opportunities to develop generalized understanding across large ecosystems gradients (Hanson et al. 2016; Hamilton et al. 2015).

6.7 Concluding remarks

This dissertation has contributed to a better understanding of lake evaporation responses to projected climate change. It has demonstrated that by using an ensemble modeling approach, not only can we compare and combine the outputs of different models, but also we can quantify the uncertainties associated with these predictions. Further, this thesis tested the performance of the ensemble modeling approach to simulate lake evaporation in a single site, and investigated the differences in model projections and their uncertainties at a global scale. It further highlighted the implications of increasing lake evaporation to climate change for water availability. The analyses presented in this dissertation provide the first steps to promote the application of ensemble modeling approaches to simulate lake evaporation particularly under scenarios of climate change.

References

Abtew, W. (2001). Evaporation estimation for Lake Okeechobee in south Florida. *Journal of Irrigation and Drainage Engineering*, 127(3), pp.140–121/02/2024 11:02:0047.

Adrian, R., O'Reilly, C.M., Zagarese, H., Baines, S.B., Hessen, D.O., Keller, W., Livingstone, D.M., Sommaruga, R., Straile, D., Donk, E.V., Weyhenmeyer, G.A. and Winder, M. (2009). Lakes as sentinels of climate change. *Limnology and Oceanography*, 54(6part2), pp.2283–2297.

Ahmed, K., Sachindra, D.A., Shahid, S., Demirel, M.C. and Chung, E.-S. (2019). Selection of multi-model ensemble of general circulation models for the simulation of precipitation and maximum and minimum temperature based on spatial assessment metrics. *Hydrology and Earth System Sciences*, 23(11), pp.4803–4824.

Allan, J.D., Smith, S.D., McIntyre, P.B., Joseph, C.A., Dickinson, C.E., Marino, A.L., Biel, R.G., Olson, J.C., Doran, P.J. and Rutherford, E.S. (2015). Using cultural ecosystem services to inform restoration priorities in the Laurentian Great Lakes. *Frontiers in Ecology and the Environment*, 13(8), pp.418–424.

Allan, R.P. (2023). Amplified seasonal range in precipitation minus evaporation. *Environmental Research Letters*, 18(9), p.094004.

Althoff, D., Rodrigues, L.N. and da Silva, D.D. (2020). Impacts of climate change on the evaporation and availability of water in small reservoirs in the Brazilian savannah. *Climatic Change*, 159, pp.215–232.

Amadori, M., Giovannini, L., Toffolon, M., Piccolroaz, S., Zardi, D., Bresciani, M., Giardino, C., Luciani, G., Kliphuis, M. and van Haren, H. (2021). Multi-scale evaluation of a 3D lake model forced by an atmospheric model against standard monitoring data. *Environmental Modelling & Software*, 139, p.105017.

Andersen, T.K., Nielsen, A., Jeppesen, E., Hu, F., Bolding, K., Liu, Z., Søndergaard, M., Johansson, L.S. and Trolle, D. (2020). Predicting ecosystem state changes in shallow lakes using an aquatic ecosystem model: Lake Hinge, Denmark, an example. *Ecological Applications*, 30(7), p.e02160.

Assouline, S. and Mahrer, Y. (1993). Evaporation from Lake Kinneret: 1. Eddy correlation system measurements and energy budget estimates. *Water Resources Research*, 29(4), pp.901–910.

Ayala, A.I., Moras, S. and Pierson, D.C. (2020). Simulations of future changes in thermal structure of Lake Erken: proof of concept for ISIMIP2b lake sector local simulation strategy. *Hydrology and Earth System Sciences*, 24(6), pp.3311–3330.

Ayala Zamora, A.I., Mesman, J.P., Jones, I.D., de Eyto, E., Jennings, E., Goyette, S. and Pierson, D.C. (2023). Climate Change Impacts on Surface Heat Fluxes in a Deep

Monomictic Lake. *Journal of Geophysical Research: Atmospheres*, 2023, p.e2022JD038355.

Bai, X., Wang, J., Sellinger, C., Clites, A. and Assel, R. (2012). Interannual variability of Great Lakes ice cover and its relationship to NAO and ENSO. *Journal of Geophysical Research: Oceans*, 117(C3).

Balsamo, G., Salgado, R., Dutra, E., Boussetta, S., Stockdale, T. and Potes, M. (2012). On the contribution of lakes in predicting near-surface temperature in a global weather forecasting model. *Tellus A: Dynamic Meteorology and Oceanography*, 64(1), p.15829.

Bärenbold, F., Kipfer, R. and Schmid, M. (2022). Dynamic modelling provides new insights into development and maintenance of Lake Kivu's density stratification. *Environmental Modelling & Software*, 147, p.105251.

Bergmann-Baker, U., Brotton, J. and Wall, G. (1995). Socio-economic impacts of fluctuating water levels on recreational boating in the Great Lakes. *Canadian Water Resources Journal*, 20(3), pp.185–194.

Blanken, P.D., Rouse, W.R., Culf, A.D., Spence, C., Boudreau, L.D., Jasper, J.N., Kochtubajda, B., Schertzer, W.M., Marsh, P. and Verseghy, D. (2000). Eddy covariance measurements of evaporation from Great Slave lake, Northwest Territories, Canada. *Water Resources Research*, 36(4), pp.1069–1077.

Blanken, P.D., Spence, C., Hedstrom, N. and Lenters, J.D. (2011). Evaporation from Lake Superior: 1. Physical controls and processes. *Journal of Great Lakes Research*, 37(4), pp.707–716.

Blanken, P.D., Rouse, W.R. and Schertzer, W.M. (2003). Enhancement of evaporation from a large northern lake by the entrainment of warm, dry air. *Journal of Hydrometeorology*, 4(4), pp.680–693.

Bowling, L.C. and Lettenmaier, D.P. (2010). Modeling the effects of lakes and wetlands on the water balance of Arctic environments. *Journal of Hydrometeorology*, 11(2), pp.276–295.

Brown, L.C. and Duguay, C.R. (2010). The response and role of ice cover in lake-climate interactions. *Progress in physical geography*, 34(5), pp.671–704.

Brunke, M.A., Fairall, C.W., Zeng, X., Eymard, L. and Curry, J.A. (2003). Which bulk aerodynamic algorithms are least problematic in computing ocean surface turbulent fluxes?. *Journal of Climate*, 16(4), pp.619–635.

Brutsaert, W. (1982). Evaporation into the atmosphere: Theory. *History, and Applications. D. Reidel.*

Burchard, H., Bolding, K., Kühn, W., Meister, A., Neumann, T. and Umlauf, L. (2006). Description of a flexible and extendable physical–biogeochemical model system for the water column. *Journal of Marine systems*, 61(3–4), pp.180–211.

Burchard, H., Bolding, K. and Villarreal, M.R. (1999). GOTM, a general ocean turbulence model: theory, implementation and test cases. *Space Applications Institute*.

Busuioc, A., Chen, D. and Hellström, C. (2001). Performance of statistical downscaling models in GCM validation and regional climate change estimates: application for Swedish precipitation. *International Journal of Climatology: A Journal of the Royal Meteorological Society*, 21(5), pp.557–578.

Calamita, E., Piccolroaz, S., Majone, B. and Toffolon, M. (2021). On the role of local depth and latitude on surface warming heterogeneity in the Laurentian Great Lakes. *Inland Waters*, 11(2), pp.208–222.

Cao, Y., Fu, C., Wu, Huawu, Wu, Haohao, Zhang, H., Yang, M., Ji, Z., Yu, M. and Dong, L. (2022). Exploring Methods to Estimate Ice Sublimation and Total Water Vapor Flux of Large Lakes in China. *Journal of Geophysical Research: Atmospheres*, 127(21), p.e2022JD037095.

Chen, J., Pekker, T., Wilson, C.R., Tapley, B., Kostianoy, A., Cretaux, J. and Safarov, E. (2017). Long-term Caspian Sea level change. *Geophysical Research Letters*, 44(13), pp.6993–7001.

Choulga, M., Kourzeneva, E., Zakharova, E. and Doganovsky, A. (2014). Estimation of the mean depth of boreal lakes for use in numerical weather prediction and climate modelling. *Tellus A: Dynamic Meteorology and Oceanography*, 66(1), p.21295.

Christianson, K.R. and Johnson, B.M. (2020). Combined effects of early snowmelt and climate warming on mountain lake temperatures and fish energetics. *Arctic, Antarctic, and Alpine Research*, 52(1), pp.130–145.

Cooley, S.W., Ryan, J.C. and Smith, L.C. (2021). Human alteration of global surface water storage variability. *Nature*, 591(7848), pp.78–81.

Czernecki, B. and Ptak, M. (2018). The impact of global warming on lake surface water temperature in Poland-the application of empirical-statistical downscaling, 1971-2100. *Journal of Limnology*, 77(2).

Darehshouri, S., Michelsen, N., Schüth, C., Tajrishy, M. and Schulz, S. (2022). Evaporation from the dried-up lake bed of Lake Urmia, Iran. *Science of The Total Environment*, 2022, p.159960.

Deser, C., Lehner, F., Rodgers, K.B., Ault, T., Delworth, T.L., DiNezio, P.N., Fiore, A., Frankignoul, C., Fyfe, J.C. and Horton, D.E. (2020). Insights from Earth system model initial-condition large ensembles and future prospects. *Nature Climate Change*, 10(4), pp.277–286.

Duan, H., Zhang, G., Wang, S. and Fan, Y. (2019). Robust climate change research: a review on multi-model analysis. *Environmental Research Letters*, 14(3), p.033001.

Dutton, J.A. and Bryson, R.A. (1962). HEAT FLUX IN LAKE MENDOTA 1. *Limnology and Oceanography*, 7(1), pp.80–97.

Edinger, J.E., Duttweiler, D.W. and Geyer, J.C. (1968). The response of water temperatures to meteorological conditions. *Water Resources Research*, 4(5), pp.1137–1143.

Fairall, C.W., Bradley, E.F., Rogers, D.P., Edson, J.B. and Young, G.S. (1996). Bulk parameterization of air-sea fluxes for tropical ocean-global atmosphere coupled-ocean atmosphere response experiment. *Journal of Geophysical Research: Oceans*, 101(C2), pp.3747–3764.

Fairall, C.W., Bradley, E.F., Hare, J., Grachev, A.A. and Edson, J.B. (2003). Bulk parameterization of air–sea fluxes: Updates and verification for the COARE algorithm. *Journal of climate*, 16(4), pp.571–591.

de Farias Mesquita, J.B., Neto, I.E.L., Raabe, A. and de Araújo, J.C. (2020). The influence of hydroclimatic conditions and water quality on evaporation rates of a tropical lake. *Journal of Hydrology*, 590, p.125456.

Farooq, U., Liu, H., Zhang, Q., Ma, Y., Wang, J. and Shen, L. (2022). Spatial variability of global lake evaporation regulated by vertical vapor pressure difference. *Environmental Research Letters*, 17(5), p.054006.

Feldbauer, J., Ladwig, R., Mesman, J.P., Moore, T.N., Zündorf, H., Berendonk, T.U. and Petzoldt, T. (2022). Ensemble of models shows coherent response of a reservoir's stratification and ice cover to climate warming. *Aquatic Sciences*, 84(4), p.50.

Fergus, C.E., Brooks, J.R., Kaufmann, P.R., Pollard, A.I., Mitchell, R., Geldhof, G.J., Hill, R.A., Paulsen, S.G., Ringold, P. and Weber, M. (2022). Natural and anthropogenic controls on lake water-level decline and evaporation-to-inflow ratio in the conterminous United States. *Limnology and Oceanography*, 67(7), pp.1484–1501.

Finch, J. and Calver, A. (2008). Methods for the quantification of evaporation from lakes.

Finger Higgens, R., Chipman, J., Lutz, D., Culler, L., Virginia, R. and Ogden, L. (2019). Changing lake dynamics indicate a drier Arctic in Western Greenland. *Journal of Geophysical Research: Biogeosciences*, 124(4), pp.870–883.

Fink, G., Schmid, M., Wahl, B., Wolf, T. and Wüest, A. (2014). Heat flux modifications related to climate-induced warming of large European lakes. *Water Resources Research*, 50(3), pp.2072–2085.

Foley, B., Jones, I.D., Maberly, S.C. and Rippey, B. (2012). Long-term changes in oxygen depletion in a small temperate lake: effects of climate change and eutrophication. *Freshwater Biology*, 57(2), pp.278–289.

Friedrich, K., Grossman, R.L., Huntington, J., Blanken, P.D., Lenters, J., Holman, K.D., Gochis, D., Livneh, B., Prairie, J. and Skeie, E. (2018). Reservoir evaporation in the Western United States: current science, challenges, and future needs. *Bulletin of the American Meteorological Society*, 99(1), pp.167–187.

Frieler, K., Lange, S., Piontek, F., Reyer, C.P., Schewe, J., Warszawski, L., Zhao, F., Chini, L., Denvil, S. and Emanuel, K. (2017). Assessing the impacts of 1.5 C global warming–simulation protocol of the Inter-Sectoral Impact Model Intercomparison Project (ISIMIP2b). *Geoscientific Model Development*, 10(12), pp.4321- 4345.

Gal, G., Yael, G., Noam, S., Moshe, E. and Schlabing, D. (2020). Ensemble Modeling of the Impact of Climate Warming and Increased Frequency of Extreme Climatic Events on the Thermal Characteristics of a Sub-Tropical Lake. *Water*, 12(7), p.1982.

Gal, G., Imberger, J., Zohary, T., Antenucci, J., Anis, A. and Rosenberg, T. (2003). Simulating the thermal dynamics of Lake Kinneret. *Ecological Modelling*, 162(1), pp.69–86.

Gaudard, A., Råman Vinnå, L., Bärenbold, F., Schmid, M. and Bouffard, D. (2019). Toward an open access to high-frequency lake modeling and statistics data for scientists and practitioners–the case of Swiss lakes using Simstrat v2. 1. *Geoscientific Model Development*, 12(9), pp.3955–3974.

George, G. (2010). *The impact of climate change on European lakes*. Springer.

Givati, A., Thirel, G., Rosenfeld, D. and Paz, D. (2019). Climate change impacts on streamflow at the upper Jordan river based on an ensemble of regional climate models. *Journal of Hydrology: Regional Studies*, 21, pp.92–109.

Gleick, P.H. (1993). Water and conflict: Fresh water resources and international security. *International security*, 18(1), pp.79–112.

Golub, M., Thiery, W., Marcé, R., Pierson, D., Vanderkelen, I., Mercado, D., Woolway, R.I., Grant, L., Jennings, E. and Schewe, J. (2022). A framework for ensemble modelling of climate change impacts on lakes worldwide: the ISIMIP Lake Sector. *Geoscientific Model Development Discussions*, 2022, pp.1–57.

Gong, M., O'Donnell, R., Miller, C., Scott, M., Simis, S., Groom, S., Tyler, A., Hunter, P., Spyrakos, E. and Merchant, C. (2022). Adaptive smoothing to identify spatial structure in global lake ecological processes using satellite remote sensing data. *Spatial Statistics*, 2022, p.100615.

Goudsmit, G., Burchard, H., Peeters, F. and Wüest, A. (2002). Application of k-ε turbulence models to enclosed basins: The role of internal seiches. *Journal of Geophysical Research: Oceans*, 107(C12), pp.23–1.

Gownaris, N.J., Pikitch, E.K., Aller, J.Y., Kaufman, L.S., Kolding, J., Lwiza, K.M., Obiero, K.O., Ojwang, W.O., Malala, J.O. and Rountos, K.J. (2017). Fisheries and water level fluctuations in the world's largest desert lake. *Ecohydrology*, 10(1), p.e1769.

Granger, R. and Hedstrom, N. (2011). Modelling hourly rates of evaporation from small lakes. *Hydrology and Earth System Sciences*, 15(1), pp.267–277.

Grant, L., Vanderkelen, I., Gudmundsson, L., Tan, Z., Perroud, M., Stepanenko, V.M., Debolskiy, A.V., Droppers, B., Janssen, A.B. and Woolway, R.I. (2021). Attribution of

global lake systems change to anthropogenic forcing. *Nature Geoscience*, 14(11), pp.849–854.

Gronewold, A.D., Fortin, V., Lofgren, B., Clites, A., Stow, C.A. and Quinn, F. (2013). Coasts, water levels, and climate change: A Great Lakes perspective. *Climatic Change*, 120(4), pp.697–711.

Gu, X., Zhang, Q., Li, J., Chen, D., Singh, V.P., Zhang, Y., Liu, J., Shen, Z. and Yu, H. (2020). Impacts of anthropogenic warming and uneven regional socio-economic development on global river flood risk. *Journal of Hydrology*, 590, p.125262.

Guo, M., Zhuang, Q., Yao, H., Golub, M., Leung, L.R. and Tan, Z. (2021). Intercomparison of Thermal Regime Algorithms in 1-D Lake Models. *Water Resources Research*, 57(6), p.e2020WR028776.

Guo, M., Zhuang, Q., Tan, Z., Shurpali, N., Juutinen, S., Kortelainen, P. and Martikainen, P.J. (2020). Rising methane emissions from boreal lakes due to increasing ice-free days. *Environmental Research Letters*, 15(6), p.064008.

Guo, M., Zhuang, Q., Yao, H., Golub, M., Leung, L.R., Pierson, D. and Tan, Z. (2021). Validation and Sensitivity Analysis of a 1-D Lake Model Across Global Lakes. *Journal of Geophysical Research: Atmospheres*, 126(4), p.e2020JD033417.

Guseva, S., Armani, F., Desai, A.R., Dias, N.L., Friborg, T., Iwata, H., Jansen, J., Lükő, G., Mammarella, I. and Repina, I. (2023). Bulk transfer coefficients estimated from eddy-covariance measurements over lakes and reservoirs. *Journal of Geophysical Research: Atmospheres*, 128(2), p.e2022JD037219.

Hamilton, D.P., Carey, C.C., Arvola, L., Arzberger, P., Brewer, C., Cole, J.J., Gaiser, E., Hanson, P.C., Ibelings, B.W. and Jennings, E. (2015). A Global Lake Ecological Observatory Network (GLEON) for synthesising high-frequency sensor data for validation of deterministic ecological models. *Inland Waters*, 5(1), pp.49–56.

Han, S. and Guo, F. (2023). Evaporation from six water bodies of various sizes in East Asia: An analysis on size dependency. *Water Resources Research*, 2023, p.e2022WR032650.

Hanson, P.C., Weathers, K.C. and Kratz, T.K. (2016). Networked lake science: how the Global Lake Ecological Observatory Network (GLEON) works to understand, predict, and communicate lake ecosystem response to global change. *Inland Waters*, 6(4), pp.543–554.

Hanson, Z.J., Zwart, J.A., Jones, S.E., Hamlet, A.F. and Bolster, D. (2021). Projected changes of regional lake hydrologic characteristics in response to 21st century climate change. *Inland Waters*, 11(3), pp.335–350.

Havens, K. and Jeppesen, E. (2018). Ecological responses of lakes to climate change. *Water*, 10(7), p.917.

Heikinheimo, M., Kangas, M., Tourula, T., Venäläinen, A. and Tattari, S. (1999). Momentum and heat fluxes over lakes Tämnaren and Råksjö determined by the bulk-aerodynamic and eddy-correlation methods. *Agricultural and forest meteorology*, 98, pp.521–534.

Heiskanen, J.J., Mammarella, I., Ojala, A., Stepanenko, V., Erkkilä, K., Miettinen, H., Sandström, H., Eugster, W., Leppäranta, M. and Järvinen, H. (2015). Effects of water clarity on lake stratification and lake-atmosphere heat exchange. *Journal of Geophysical Research: Atmospheres*, 120(15), pp.7412–7428.

Helfer, F., Lemckert, C. and Zhang, H. (2012). Impacts of climate change on temperature and evaporation from a large reservoir in Australia. *Journal of hydrology*, 475, pp.365–378.

Henderson-Sellers, B. (1986). Calculating the surface energy balance for lake and reservoir modeling: A review. *Reviews of Geophysics*, 24(3), pp.625–649.

Hipsey, M.R., Bruce, L.C., Boon, C., Busch, B., Carey, C.C., Hamilton, D.P., Hanson, P.C., Read, J.S., De Sousa, E., Weber, M. and Winslow, L.A. (2019). A General Lake Model (GLM 3.0) for linking with high-frequency sensor data from the Global Lake Ecological Observatory Network (GLEON). *Geoscientific Model Development*, 12(1), pp.473-523.

Hipsey, M.R. and Sivapalan, M. (2003). Parameterizing the effect of a wind shelter on evaporation from small water bodies. *Water Resources Research*, 39(12).

Hondzo, M. and Stefan, H.G. (1993). Lake water temperature simulation model. *Journal of Hydraulic Engineering*, 119(11), pp.1251–1273.

Hostetler, S. (1991). Simulation of lake ice and its effect on the late-Pleistocene evaporation rate of Lake Lahontan. *Climate Dynamics*, 6(1), pp.43–48.

Hostetler, S. and Bartlein, P. (1990). Simulation of lake evaporation with application to modeling lake level variations of Harney-Malheur Lake, Oregon. *Water Resources Research*, 26(10), pp.2603–2612.

Hostetler, S.W., Bates, G.T. and Giorgi, F. (1993). Interactive coupling of a lake thermal model with a regional climate model. *Journal of Geophysical Research: Atmospheres*, 98(D3), pp.5045–5057.

Huang, L., Timmermann, A., Lee, S.-S., Rodgers, K.B., Yamaguchi, R. and Chung, E.-S. (2022). Emerging unprecedented lake ice loss in climate change projections. *Nature communications*, 13(1), pp.1–12.

Huang, L., Wang, X., Sang, Y., Tang, S., Jin, L., Yang, H., Ottlé, C., Bernus, A., Wang, S. and Wang, C. (2021). Optimizing lake surface water temperature simulations over large lakes in China with FLake model. *Earth and Space Science*, 8(8), p.e2021EA001737.

Huang, W., Cheng, B., Zhang, J., Zhang, Z., Vihma, T., Li, Z. and Niu, F. (2019). Modeling experiments on seasonal lake ice mass and energy balance in the Qinghai–Tibet Plateau: a case study. *Hydrology and Earth System Sciences*, 23(4), pp.2173–2186.

Imberger, J. and Patterson, J. (1981). A dynamic reservoir simulation model-DYRESM, 5. 310–361. In: Proceedings of a Symposium on Predictive Models on Transport Models for Inland and Coastal Waters. Academic New York, p.542.

Iturbide, M., Gutiérrez, J.M., Alves, L.M., Bedia, J., Cerezo-Mota, R., Cimadevilla, E., Cofiño, A.S., Di Luca, A., Faria, S.H. and Gorodetskaya, I.V. (2020). An update of IPCC climate reference regions for subcontinental analysis of climate model data: definition and aggregated datasets. *Earth System Science Data*, 12(4), pp.2959–2970.

Jane, S.F., Hansen, G.J., Kraemer, B.M., Leavitt, P.R., Mincer, J.L., North, R.L., Pilla, R.M., Stetler, J.T., Williamson, C.E. and Woolway, R.I. (2021). Widespread deoxygenation of temperate lakes. *Nature*, 594(7861), pp.66–70.

Jansen, F.A. and Teuling, A.J. (2020). Evaporation from a large lowland reservoir–(dis) agreement between evaporation models from hourly to decadal timescales. *Hydrology and Earth System Sciences*, 24(3), pp.1055–1072.

Jansen, J., Woolway, R.I., Kraemer, B.M., Albergel, C., Bastviken, D., Weyhenmeyer, G.A., Marce, R., Sharma, S., Sobek, S. and Tranvik, L.J. (2022). Global increase in methane production under future warming of lake bottom waters. *Global change biology*, 28(18), pp.5427–5440.

Janssen, A.B., Droppers, B., Kong, X., Teurlincx, S., Tong, Y. and Kroeze, C. (2021). Characterizing 19 thousand Chinese lakes, ponds and reservoirs by morphometric, climate and sediment characteristics. *Water Research*, 202, p.117427.

Janssen, A.B., Arhonditsis, G.B., Beusen, A., Bolding, K., Bruce, L., Bruggeman, J., Couture, R.-M., Downing, A.S., Alex Elliott, J. and Frassl, M.A. (2015). Exploring, exploiting and evolving diversity of aquatic ecosystem models: a community perspective. *Aquatic Ecology*, 49, pp.513–548.

Jennings, E., Allott, N., Pierson, D.C., Schneiderman, E.M., Lenihan, D., Samuelsson, P. and Taylor, D. (2009). Impacts of climate change on phosphorus loading from a grassland catchment: Implications for future management. *Water research*, 43(17), pp.4316–4326.

Jeppesen, E., Brucet, S., Naselli-Flores, L., Papastergiadou, E., Stefanidis, K., Noges, T., Noges, P., Attayde, J.L., Zohary, T. and Coppens, J. (2015). Ecological impacts of global warming and water abstraction on lakes and reservoirs due to changes in water level and related changes in salinity. *Hydrobiologia*, 750(1), pp.201–227.

Jin, Y., Hu, S., Ziegler, A.D., Gibson, L., Campbell, J.E., Xu, R., Chen, D., Zhu, K., Zheng, Y. and Ye, B. (2023). Energy production and water savings from floating solar photovoltaics on global reservoirs. *Nature Sustainability*, 2023, pp.1–10.

Jolliff, J.K., Kindle, J.C., Shulman, I., Penta, B., Friedrichs, M.A., Helber, R. and Arnone, R.A. (2009). Summary diagrams for coupled hydrodynamic-ecosystem model skill assessment. *Journal of Marine Systems*, 76(1–2), pp.64–82.

Ju, J., Wu, C., Li, J., Yeh, P.J.-F. and Hu, B.X. (2023). Global evaluation of model agreement and uncertainty in terrestrial water storage simulations from ISIMIP 2b framework. *Journal of Hydrology*, 617, p.129137.

Kayastha, M.B., Ye, X., Huang, C. and Xue, P. (2022). Future rise of the Great Lakes water levels under climate change. *Journal of Hydrology*, 612, p.128205.

Khandelwal, A., Karpatne, A., Ravirathinam, P., Ghosh, R., Wei, Z., Dugan, H.A., Hanson, P.C. and Kumar, V. (2022). ReaLSAT, a global dataset of reservoir and lake surface area variations. *Scientific Data*, 9(1), p.356.

Kirillin, G. (2002). Modeling of the vertical heat exchange in shallow lakes. Doctoral dissertation, Humboldt-Universität.

Kishcha, P., Starobinets, B., Lechinsky, Y. and Alpert, P. (2021). Absence of surface water temperature trends in Lake Kinneret despite present atmospheric warming: Comparisons with Dead Sea trends. *Remote Sensing*, 13(17), p.3461.

Kiuru, P., Ojala, A., Mammarella, I., Heiskanen, J., Erkkilä, K.-M., Miettinen, H., Vesala, T. and Huttula, T. (2019). Applicability and consequences of the integration of alternative models for CO_2 transfer velocity into a process-based lake model. *Biogeosciences*, 16(17), pp.3297–3317.

Kobler, U.G. and Schmid, M. (2019). Ensemble modelling of ice cover for a reservoir affected by pumped-storage operation and climate change. *Hydrological Processes*, 33(20), pp.2676–2690.

Konapala, G., Mishra, A.K., Wada, Y. and Mann, M.E. (2020). Climate change will affect global water availability through compounding changes in seasonal precipitation and evaporation. *Nature communications*, 11(1), pp.1–10.

Kong, X., Ghaffar, S., Determann, M., Friese, K., Jomaa, S., Mi, C., Shatwell, T., Rinke, K. and Rode, M. (2022). Reservoir water quality deterioration due to deforestation emphasizes the indirect effects of global change. *Water Research*, 2022, p.118721.

Kosten, S., Roland, F., Da Motta Marques, D.M., Van Nes, E.H., Mazzeo, N., Sternberg, L. da S., Scheffer, M. and Cole, J.J. (2010). Climate-dependent CO2 emissions from lakes. *Global Biogeochemical Cycles*, 24(2).

Kourzeneva, E. (2010). External data for lake parameterization in Numerical Weather Prediction and climate modeling. Boreal Environment Research, 15, pp.165-177.

Kraemer, B.M., Anneville, O., Chandra, S., Dix, M., Kuusisto, E., Livingstone, D.M., Rimmer, A., Schladow, S.G., Silow, E. and Sitoki, L.M. (2015). Morphometry and average temperature affect lake stratification responses to climate change. *Geophysical Research Letters*, 42(12), pp.4981–4988.

Kraemer, B.M., Seimon, A., Adrian, R. and McIntyre, P.B. (2020). Worldwide lake level trends and responses to background climate variation. *Hydrology and Earth System Sciences*, 24(5), pp.2593–2608.

La Fuente, S., Jennings, E., Gal, G., Kirillin, G., Shatwell, T., Ladwig, R., Moore, T., Couture, R.-M., Côté, M. and Vinnå, C.L.R. (2022). Multi-model projections of future evaporation in a sub-tropical lake. *Journal of Hydrology*, 615, p.128729.

Ladwig, R., Rock, L.A. and Dugan, H.A. (2021). Impact of salinization on lake stratification and spring mixing. *Limnology and Oceanography Letters*, 8(1), pp.93-102.

Lange, S. (2019). EartH2Observe, WFDEI and ERA-Interim data Merged and Bias-corrected for ISIMIP (EWEMBI), V.1.1, GFZ Data Serv.

Larsen, S., Andersen, T. and Hessen, D.O. (2011). Climate change predicted to cause severe increase of organic carbon in lakes. *Global Change Biology*, 17(2), pp.1186–1192.

Laval, B., Imberger, J., Hodges, B.R. and Stocker, R. (2003). Modeling circulation in lakes: Spatial and temporal variations. *Limnology and oceanography*, 48(3), pp.983–994.

Lawrence, B.N., Bennett, V.L., Churchill, J., Juckes, M., Kershaw, P., Pascoe, S., Pepler, S., Pritchard, M. and Stephens, A. (2013). Storing and manipulating environmental big data with JASMIN. In: 2013 IEEE international conference on big data. IEEE, pp.68–75.

Le, T. and Bae, D.-H. (2020). Response of global evaporation to major climate modes in historical and future Coupled Model Intercomparison Project Phase 5 simulations. *Hydrology and Earth System Sciences*, 24(3), pp.1131–1143.

Lehner, B., Messager, M.L., Korver, M.C. and Linke, S. (2022). Global hydro-environmental lake characteristics at high spatial resolution. *Scientific Data*, 9(1), p.351.

Lehner, B. and Doll, P. (2004). Global lakes and wetlands database. *World Wildlife Fund*, 2004.

Lei, Y., Zhu, Y., Wang, B., Yao, T., Yang, K., Zhang, X., Zhai, J. and Ma, N. (2019). Extreme lake level changes on the Tibetan Plateau associated with the 2015/2016 El Niño. *Geophysical Research Letters*, 46(11), pp.5889–5898.

Lenters, J., Anderton, J.B., Blanken, P., Spence, C. and Suyker, A.E. (2013). Assessing the Impacts of Climate Variability and Change on Great Lakes Evaporation. In: 2011 Project Reports. Brown, D., Bidwell, D., and Briley, L. Available from the Great Lakes Integrated Sciences and Assessments (GLISA) Center: http://glisaclimate.org/media/GLISA_Lake_Evaporation.pdf.

Lenters, J., Blanken, P., Healey, N., Hinkel, K., Ong, J., Peake, C., Potter, B., Riveros-Iregui, D., Spence, C. and Van Cleave, K. (2014). Physical controls on lake evaporation

across a variety of climates and lake types. In: 17th International Workshop on Physical Processes in Natural Waters. p.56.

Lenters, J.D., Kratz, T.K. and Bowser, C.J. (2005). Effects of climate variability on lake evaporation: Results from a long-term energy budget study of Sparkling Lake, northern Wisconsin (USA). *Journal of Hydrology*, 308(1), pp.168–195.

Li, X., Peng, S., Xi, Y., Woolway, R.I. and Liu, G. (2022). Earlier ice loss accelerates lake warming in the Northern Hemisphere. *Nature communications*, 13(1), p.5156.

Li, Y., Wang, N., Li, Z., Ma, N., Zhou, X. and Zhang, C. (2013). Lake evaporation: A possible factor affecting lake level changes tested by modern observational data in arid and semi-arid China. *Journal of Geographical Sciences*, 23, pp.123–135.

Liao, J., Shen, G. and Li, Y. (2013). Lake variations in response to climate change in the Tibetan Plateau in the past 40 years. *International Journal of Digital Earth*, 6(6), pp.534–549.

Likens, G., Benbow, M., Burton, T., Van Donk, E., Downing, J. and Gulati, R. (2009). *Encyclopedia of inland waters*. Elsevier.

Liu, H., Zhang, Y., Liu, S., Jiang, H., Sheng, L. and Williams, Q.L. (2009). Eddy covariance measurements of surface energy budget and evaporation in a cool season over southern open water in Mississippi. *Journal of Geophysical Research: Atmospheres*, 114(D4).

Liu, Z. (2022). Accuracy of methods for simulating daily water surface evaporation evaluated by the eddy covariance measurement at boreal flux sites. *Journal of Hydrology*, 2022, p.128776.

Livingstone, D.M. and Imboden, D.M. (1989). Annual heat balance and equilibrium temperature of Lake Aegeri, Switzerland. *Aquatic Sciences*, 51(4), pp.351–369.

Livingstone, D.M., Lotter, A.F. and Kettle, H. (2005). Altitude-dependent differences in the primary physical response of mountain lakes to climatic forcing. *Limnology and oceanography*, 50(4), pp.1313–1325.

Maberly, S.C., O'Donnell, R.A., Woolway, R.I., Cutler, M.E., Gong, M., Jones, I.D., Merchant, C.J., Miller, C.A., Politi, E. and Scott, E.M. (2020). Global lake thermal regions shift under climate change. *Nature communications*, 11(1), pp.1–9.

MacIntyre, S., Fram, J.P., Kushner, P.J., Bettez, N.D., O'brien, W., Hobbie, J. and Kling, G.W. (2009). Climate-related variations in mixing dynamics in an Alaskan arctic lake. *Limnology and Oceanography*, 54(6part2), pp.2401–2417.

Magnuson, J.J., Robertson, D.M., Benson, B.J., Wynne, R.H., Livingstone, D.M., Arai, T., Assel, R.A., Barry, R.G., Card, V. and Kuusisto, E. (2000). Historical trends in lake and river ice cover in the Northern Hemisphere. *Science*, 289(5485), pp.1743–1746.

Mahrer, Y. and Assouline, S. (1993). Evaporation from Lake Kinneret: 2. Estimation of the Horizontal variability using a two-dimensional numerical mesoscale model. *Water Resources Research*, 29(4), pp.911–916.

Markelov, I., Couture, R., Fischer, R., Haande, S. and Van Cappellen, P. (2019). Coupling water column and sediment biogeochemical dynamics: Modeling internal phosphorus loading, climate change responses, and mitigation measures in Lake Vansjø, Norway. *Journal of Geophysical Research: Biogeosciences*, 124(12), pp.3847–3866.

Marsh, P. and Bigras, S. (1988). Evaporation from Mackenzie delta lakes, NWT, Canada. *Arctic and Alpine Research*, 20(2), pp.220–229.

Mason, L.A., Riseng, C.M., Gronewold, A.D., Rutherford, E.S., Wang, J., Clites, A., Smith, S.D. and McIntyre, P.B. (2016). Fine-scale spatial variation in ice cover and surface temperature trends across the surface of the Laurentian Great Lakes. *Climatic Change*, 138(1), pp.71–83.

Massari, C., Avanzi, F., Bruno, G., Gabellani, S., Penna, D. and Camici, S. (2022). Evaporation enhancement drives the European water-budget deficit during multi-year droughts. *Hydrology and Earth System Sciences*, 26(6), pp.1527–1543.

Matta, E., Amadori, M., Free, G., Giardino, C. and Bresciani, M. (2022). A Satellite-Based Tool for Mapping Evaporation in Inland Water Bodies: Formulation, Application, and Operational Aspects. *Remote Sensing*, 14(11), p.2636.

McVicar, T.R., Roderick, M.L., Donohue, R.J., Li, L.T., Van Niel, T.G., Thomas, A., Grieser, J., Jhajharia, D., Himri, Y. and Mahowald, N.M. (2012). Global review and synthesis of trends in observed terrestrial near-surface wind speeds: Implications for evaporation. *Journal of Hydrology*, 416, pp.182–205.

Meehl, G.A., Arblaster, J.M. and Tebaldi, C. (2005). Understanding future patterns of increased precipitation intensity in climate model simulations. *Geophysical Research Letters* [online], 32(18).

Mesman, J., Ayala, A.I., Adrian, R., De Eyto, E., Frassl, M., Goyette, S., Kasparian, J., Perroud, M., Stelzer, J.A.A. and Pierson, D. (2020). Performance of one-dimensional hydrodynamic lake models during short-term extreme weather events. *Environmental Modelling & Software*, 133, p.104852.

Mesman, J.P., Stelzer, J.A., Dakos, V., Goyette, S., Jones, I.D., Kasparian, J., McGinnis, D.F. and Ibelings, B.W. (2021). The role of internal feedbacks in shifting deep lake mixing regimes under a warming climate. *Freshwater Biology*, 66(6), pp.1021-1035.

Messager, M.L., Lehner, B., Grill, G., Nedeva, I. and Schmitt, O. (2016). Estimating the volume and age of water stored in global lakes using a geo-statistical approach. *Nature communications*, 7(1), pp.1–11.

Meyer, J.L., Sale, M.J., Mulholland, P.J. and Poff, N.L. (1999). Impacts of climate change on aquatic ecosystem functioning and health 1. *JAWRA Journal of the American Water Resources Association*, 35(6), pp.1373–1386.

Meyer, M.F., Labou, S.G., Cramer, A.N., Brousil, M.R. and Luff, B.T. (2020). The global lake area, climate, and population dataset. *Scientific data*, 7(1), pp.1–12.

Micklin, P. (2010). The past, present, and future Aral Sea. *Lakes & Reservoirs: Research & Management*, 15(3), pp.193–213.

Mironov, D.V. (2008). *Parameterization of lakes in numerical weather prediction: Part 1. Description of a lake model.* COSMO Technical Report No 11, Deutscher Wetterdienst. Avaiable from http://www.cosmo-model.org.

Mishra, V., Cherkauer, K.A. and Bowling, L.C. (2011). Changing thermal dynamics of lakes in the Great Lakes region: Role of ice cover feedbacks. *Global and Planetary Change*, 75(3–4), pp.155–172.

Mooij, W.M., Hülsmann, S., Domis, L.N.D.S., Nolet, B.A., Bodelier, P.L., Boers, P.C., Pires, L.M.D., Gons, H.J., Ibelings, B.W. and Noordhuis, R. (2005). The impact of climate change on lakes in the Netherlands: a review. *Aquatic Ecology*, 39(4), pp.381–400.

Moore, T.N., Mesman, J.P., Ladwig, R., Feldbauer, J., Olsson, F., Pilla, R.M., Shatwell, T., Venkiteswaran, J.J., Delany, A.D. and Dugan, H. (2021). LakeEnsemblR: An R package that facilitates ensemble modelling of lakes. *Environmental Modelling & Software*, 143, p.105101.

Mora, C., Frazier, A.G., Longman, R.J., Dacks, R.S., Walton, M.M., Tong, E.J., Sanchez, J.J., Kaiser, L.R., Stender, Y.O. and Anderson, J.M. (2013). The projected timing of climate departure from recent variability. *Nature*, 502(7470), pp.183–187.

Moragoda, N. and Cohen, S. (2020). Climate-induced trends in global riverine water discharge and suspended sediment dynamics in the 21st century. *Global and Planetary Change*, 191, p.103199.

Moras, S., Ayala, A.I. and Pierson, D.C. (2019). Historical modelling of changes in Lake Erken thermal conditions. *Hydrology and Earth System Sciences*, 23(12), pp.5001–5016.

Morton, F.I. (1983). Operational estimates of lake evaporation. *Journal of hydrology*, 66(1–4), pp.77–100.

Nordbo, A., Launiainen, S., Mammarella, I., Leppäranta, M., Huotari, J., Ojala, A. and Vesala, T. (2011). Long-term energy flux measurements and energy balance over a small boreal lake using eddy covariance technique. *Journal of Geophysical Research: Atmospheres*, 116(D2).

Novikmec, M., Svitok, M., Kočický, D., Šporka, F. and Bitušík, P. (2013). Surface water temperature and ice cover of Tatra Mountains lakes depend on altitude, topographic shading, and bathymetry. *Arctic, Antarctic, and Alpine Research*, 45(1), pp.77–87.

O'Neill, B.C., Tebaldi, C., Van Vuuren, D.P., Eyring, V., Friedlingstein, P., Hurtt, G., Knutti, R., Kriegler, E., Lamarque, J.-F. and Lowe, J. (2016). The scenario model

intercomparison project (ScenarioMIP) for CMIP6. *Geoscientific Model Development*, 9(9), pp.3461–3482.

O'Reilly, C.M., Sharma, S., Gray, D.K., Hampton, S.E., Read, J.S., Rowley, R.J., Schneider, P., Lenters, J.D., McIntyre, P.B. and Kraemer, B.M. (2015). Rapid and highly variable warming of lake surface waters around the globe. *Geophysical Research Letters*, 42(24), pp.10–773.

Parker, W.S. (2013). Ensemble modeling, uncertainty and robust predictions. *Wiley interdisciplinary reviews: Climate change*, 4(3), pp.213–223.

Patterson, J. and Hamblin, P. (1988). Thermal simulation of a lake with winter ice cover 1. *Limnology and Oceanography*, 33(3), pp.323–338.

Pekel, J.-F., Cottam, A., Gorelick, N. and Belward, A.S. (2016). High-resolution mapping of global surface water and its long-term changes. *Nature*, 540(7633), pp.418–422.

Pennell, C. and Reichler, T. (2011). On the effective number of climate models. *Journal of Climate*, 24(9), pp.2358–2367.

Pilla, R.M., Williamson, C.E., Adamovich, B.V., Adrian, R., Anneville, O., Chandra, S., Colom-Montero, W., Devlin, S.P., Dix, M.A. and Dokulil, M.T. (2020). Deeper waters are changing less consistently than surface waters in a global analysis of 102 lakes. *Scientific reports*, 10(1), pp.1–15.

Pilla, R.M. and Couture, R. (2021). Attenuation of photosynthetically active radiation and ultraviolet radiation in response to changing dissolved organic carbon in browning lakes: Modeling and parametrization. *Limnology and Oceanography*, 66(6), pp.2278–2289.

Pillco Zolá, R., Bengtsson, L., Berndtsson, R., Martí-Cardona, B., Satgé, F., Timouk, F., Bonnet, M.-P., Mollericon, L., Gamarra, C. and Pasapera, J. (2019). Modelling Lake Titicaca's daily and monthly evaporation. *Hydrology and Earth System Sciences*, 23(2), pp.657–668.

Plewa, K., Perz, A. and Wrzesiński, D. (2019). Links between teleconnection patterns and water level regime of selected Polish lakes. *Water*, 11(7), p.1330.

Prange, M., Wilke, T. and Wesselingh, F.P. (2020). The other side of sea level change. *Communications Earth & Environment*, 1(1), pp.1–4.

Ragotzkie, R.A. (1978). Heat budgets of lakes. In: *Lakes*. Springer, pp.1–19.

Rahaghi, A., Lemmin, U., Cimatoribus, A. and Barry, D. (2019). The importance of systematic spatial variability in the surface heat flux of a large lake: A multiannual analysis for Lake Geneva. *Water Resources Research*, 55(12), pp.10248–10267.

Råman Vinnå, L., Medhaug, I., Schmid, M. and Bouffard, D. (2021). The vulnerability of lakes to climate change along an altitudinal gradient. *Communications Earth & Environment*, 2(1), pp.1–10.

Read, J.S., Hamilton, D.P., Desai, A.R., Rose, K.C., MacIntyre, S., Lenters, J.D., Smyth, R.L., Hanson, P.C., Cole, J.J. and Staehr, P.A. (2012). Lake-size dependency of wind shear and convection as controls on gas exchange. *Geophysical Research Letters*, 39(9).

Reinecke, R., Müller Schmied, H., Trautmann, T., Andersen, L.S., Burek, P., Flörke, M., Gosling, S.N., Grillakis, M., Hanasaki, N. and Koutroulis, A. (2021). Uncertainty of simulated groundwater recharge at different global warming levels: a global-scale multi-model ensemble study. *Hydrology and Earth System Sciences*, 25(2), pp.787–810.

Riggs, R.M., Allen, G.H., Brinkerhoff, C.B., Sikder, M.S. and Wang, J. (2023). Turning lakes into river gauges using the LakeFlow algorithm. *Geophysical Research Letters*, 50(10), p.e2023GL103924.

Rimmer, A., Givati, A., Samuels, R. and Alpert, P. (2011). Using ensemble of climate models to evaluate future water and solutes budgets in Lake Kinneret, Israel. *Journal of Hydrology*, 410(3–4), pp.248–259.

Rimmer, A., Samuels, R. and Lechinsky, Y. (2009). A comprehensive study across methods and time scales to estimate surface fluxes from Lake Kinneret, Israel. *Journal of Hydrology*, 379(1–2), pp.181–192.

Riveros-Iregui, D.A., Lenters, J.D., Peake, C.S., Ong, J.B., Healey, N.C. and Zlotnik, V.A. (2017). Evaporation from a shallow, saline lake in the Nebraska Sandhills: Energy balance drivers of seasonal and interannual variability. *Journal of Hydrology*, 553, pp.172–187.

Rocha, S.M., Molinas, E., Rodrigues, I.S. and Neto, I.E.L. (2023). Assessment of total evaporation rates and its surface distribution by tridimensional modelling and remote sensing. *Journal of Environmental Management*, 327, p.116846.

Rodell, M., Famiglietti, J.S., Wiese, D.N., Reager, J., Beaudoing, H.K., Landerer, F.W. and Lo, M.-H. (2018). Emerging trends in global freshwater availability. *Nature*, 557(7707), pp.651–659.

Rodrigues, I.S., Costa, C.A.G., Raabe, A., Medeiros, P.H.A. and de Araújo, J.C. (2021). Evaporation in Brazilian dryland reservoirs: Spatial variability and impact of riparian vegetation. *Science of The Total Environment*, 797, p.149059.

Rogozin, D., Tarnovsky, M., Belolipetskii, V., Zykov, V., Zadereev, E., Tolomeev, A., Drobotov, A., Barkhatov, Y., Gaevsky, N. and Gorbaneva, T. (2017). Disturbance of meromixis in saline Lake Shira (Siberia, Russia): possible reasons and ecosystem response. *Limnologica*, 66, pp.12–23.

Rose, K.C., Winslow, L.A., Read, J.S. and Hansen, G.J. (2016). Climate-induced warming of lakes can be either amplified or suppressed by trends in water clarity. *Limnology and Oceanography Letters*, 1(1), pp.44–53.

Rosen, V.V., Garber, O.G., Andrushchenko, Y. and Chen, Y. (2023). Examining the Influence of Desalinated Water on Iodine Concentration in Tap Water in Israel. *Journal of Trace Elements and Minerals*, 6, p.100094.

Rosenberry, D.O., Winter, T.C., Buso, D.C. and Likens, G.E. (2007). Comparison of 15 evaporation methods applied to a small mountain lake in the northeastern USA. *Journal of hydrology*, 340(3–4), pp.149–166.

Rosenzweig, C., Arnell, N.W., Ebi, K.L., Lotze-Campen, H., Raes, F., Rapley, C., Smith, M.S., Cramer, W., Frieler, K., Reyer, C.P.O., Schewe, J., Vuuren, D. van and Warszawski, L. (2017). Assessing inter-sectoral climate change risks: the role of ISIMIP. *Environmental Research Letters*, 12(1), p.010301.

Sachse, R., Petzoldt, T., Blumstock, M., Moreira, S., Pätzig, M., Rücker, J., Janse, J.H., Mooij, W.M. and Hilt, S. (2014). Extending one-dimensional models for deep lakes to simulate the impact of submerged macrophytes on water quality. *Environmental Modelling & Software*, 61, pp.410–423.

Sade, R., Rimmer, A., Samuels, R., Salingar, Y., Denisyuk, M. and Alpert, P. (2016). Water management in a complex hydrological basin—application of water evaluation and planning tool (WEAP) to the Lake Kinneret watershed, Israel. In: *Integrated water resources management: concept, research and implementation*. Springer, pp.35–57.

Sadro, S., Melack, J.M., Sickman, J.O. and Skeen, K. (2019). Climate warming response of mountain lakes affected by variations in snow. *Limnology and Oceanography Letters*, 4(1), pp.9–17.

Salk, K.R., Venkiteswaran, J.J., Couture, R., Higgins, S.N., Paterson, M.J. and Schiff, S.L. (2022). Warming combined with experimental eutrophication intensifies lake phytoplankton blooms. *Limnology and Oceanography*, 67(1), pp.147–158.

Saloranta, T.M. and Andersen, T. (2007). MyLake—A multi-year lake simulation model code suitable for uncertainty and sensitivity analysis simulations. *Ecological modelling*, 207(1), pp.45–60.

Sartori, E. (2000). A critical review on equations employed for the calculation of the evaporation rate from free water surfaces. *Solar energy*, 68(1), pp.77–89.

Schallenberg, M., Winton, M.D. de, Verburg, P., Kelly, D.J., Hamill, K.D. and Hamilton, D.P. (2013). Ecosystem services of lakes. *Ecosystem services in New Zealand: conditions and trends. Manaaki Whenua Press, Lincoln*, pp.203–225.

Schindler, D.W. (2001). The cumulative effects of climate warming and other human stresses on Canadian freshwaters in the new millennium. *Canadian Journal of Fisheries and Aquatic Sciences*, 58(1), pp.18–29.

Schlunegger, S., Rodgers, K.B., Sarmiento, J.L., Ilyina, T., Dunne, J.P., Takano, Y., Christian, J.R., Long, M.C., Frölicher, T.L. and Slater, R. (2020). Time of emergence and large ensemble intercomparison for ocean biogeochemical trends. *Global biogeochemical cycles*, 34(8), p.e2019GB006453.

Schmid, M., Hunziker, S. and Wüest, A. (2014). Lake surface temperatures in a changing climate: A global sensitivity analysis. *Climatic change*, 124(1), pp.301–315.

Schmid, M. and Köster, O. (2016). Excess warming of a Central European lake driven by solar brightening. *Water Resources Research*, 52(10), pp.8103–8116.

Schmid, M. and Read, J. (2022). Heat budget of lakes. *Encyclopedia of Inland Waters, second edition, edited by: Mehner, T. and Tockner, K., Elsevier, https://doi. org/10.1016/B978-0-12-819166-8.00011-6*, pp.467–473.

Schneider, P. and Hook, S.J. (2010). Space observations of inland water bodies show rapid surface warming since 1985. *Geophysical Research Letters*, 37(22).

Semazzi, F. (2011). Enhancing safety of navigation and efficient exploitation of natural resources over Lake Victoria and its basin by strengthening meteorological services on the lake. *North Carolina State University Climate Modeling Laboratory Tech. Rep*, 104.

Shao, M., Fernando, N., Zhu, J., Zhao, G., Kao, S.-C., Zhao, B., Roberts, E. and Gao, H. (2023). Estimating Future Surface Water Availability through an Integrated Climate-Hydrology-Management Modeling Framework at a Basin Scale under CMIP6 Scenarios. *Water Resources Research*, 59, p.e2022WR034099.

Sharma, S., Richardson, D.C., Woolway, R.I., Imrit, M.A., Bouffard, D., Blagrave, K., Daly, J., Filazzola, A., Granin, N. and Korhonen, J. (2021). Loss of ice cover, shifting phenology, and more extreme events in Northern Hemisphere lakes. *Journal of Geophysical Research: Biogeosciences*, 126(10), p.e2021JG006348.

Sharma, S., Blagrave, K., Magnuson, J.J., O'Reilly, C.M., Oliver, S., Batt, R.D., Magee, M.R., Straile, D., Weyhenmeyer, G.A. and Winslow, L. (2019). Widespread loss of lake ice around the Northern Hemisphere in a warming world. *Nature Climate Change*, 9(3), pp.227–231.

Shatwell, T., Thiery, W. and Kirillin, G. (2019). Future projections of temperature and mixing regime of European temperate lakes. *Hydrology and Earth System Sciences*, 23(3), pp.1533–1551.

Shevnina, E., Potes, M., Vihma, T., Naakka, T., Dhote, P.R. and Thakur, P.K. (2022). Evaporation over a glacial lake in Antarctica. *The Cryosphere*, 16(8), pp.3101–3121.

Shilo, E., Ziv, B., Shamir, E. and Rimmer, A. (2015). Evaporation from Lake Kinneret, Israel, during hot summer days. *Journal of Hydrology*, 528, pp.264–275.

Shugar, D.H., Burr, A., Haritashya, U.K., Kargel, J.S., Watson, C.S., Kennedy, M.C., Bevington, A.R., Betts, R.A., Harrison, S. and Strattman, K. (2020). Rapid worldwide growth of glacial lakes since 1990. *Nature Climate Change*, 10(10), pp.939–945.

Silvy, Y., Guilyardi, E., Sallée, J.-B. and Durack, P.J. (2020). Human-induced changes to the global ocean water masses and their time of emergence. *Nature Climate Change*, 10(11), pp.1030–1036.

Solomon, S., Qin, D., Manning, M., Chen, Z., Marquis, M., Averyt, K., Tignor, M. and Miller, H. (2007). IPCC fourth assessment report (AR4). *Climate change*, 374.

Spence, C., Blanken, P., Hedstrom, N., Fortin, V. and Wilson, H. (2011). Evaporation from Lake Superior: 2: Spatial distribution and variability. *Journal of Great Lakes Research*, 37(4), pp.717–724.

Spence, C., Blanken, P., Lenters, J.D. and Hedstrom, N. (2013). The importance of spring and autumn atmospheric conditions for the evaporation regime of Lake Superior. *Journal of Hydrometeorology*, 14(5), pp.1647–1658.

Steinman, A.D., Cardinale, B.J., Munns Jr, W.R., Ogdahl, M.E., Allan, J.D., Angadi, T., Bartlett, S., Brauman, K., Byappanahalli, M. and Doss, M. (2017). Ecosystem services in the Great Lakes. *Journal of Great Lakes Research*, 43(3), pp.161–168.

Stepanenko, V., Martynov, A., Jöhnk, K., Subin, Z., Perroud, M., Fang, X., Beyrich, F., Mironov, D. and Goyette, S. (2013). A one-dimensional model intercomparison study of thermal regime of a shallow, turbid midlatitude lake. *Geoscientific Model Development*, 6(4), pp.1337–1352.

Stepanenko, V., Jöhnk, K.D., Machulskaya, E., Perroud, M., Subin, Z., Nordbo, A., Mammarella, I. and Mironov, D. (2014). Simulation of surface energy fluxes and stratification of a small boreal lake by a set of one-dimensional models. *Tellus A: Dynamic Meteorology and Oceanography*, 66(1), p.21389.

Stepanenko, V.M., Goyette, S., Martynov, A., Perroud, M., Fang, X. and Mironov, D. (2010). First steps of a Lake Model intercomparison project: LakeMIP. *Boreal Environment Research*, 15, pp.191-202.

Sterner, R.W., Keeler, B., Polasky, S., Poudel, R., Rhude, K. and Rogers, M. (2020). Ecosystem services of Earth's largest freshwater lakes. *Ecosystem Services*, 41, p.101046.

Stuart-Smith, R., Roe, G., Li, S. and Allen, M. (2021). Increased outburst flood hazard from Lake Palcacocha due to human-induced glacier retreat. *Nature Geoscience*, 14(2), pp.85–90.

Subin, Z.M., Riley, W.J. and Mironov, D. (2012). An improved lake model for climate simulations: Model structure, evaluation, and sensitivity analyses in CESM1. *Journal of Advances in Modeling Earth Systems*, 4(1).

Tal, A. (2019a). Climate change's impact on Lake Kinneret: Letting the data tell the story. *The Science of the total environment*, 685, pp.1272–1275.

Tal, A. (2019b). The implications of climate change driven depletion of Lake Kinneret water levels: the compelling case for climate change-triggered precipitation impact on Lake Kinneret's low water levels. *Science of the Total Environment*, 664, pp.1045–1051.

Tan, Z., Zhuang, Q., Shurpali, N.J., Marushchak, M.E., Biasi, C., Eugster, W. and Walter Anthony, K. (2017). Modeling CO_2 emissions from Arctic lakes: Model development and site-level study. *Journal of Advances in Modeling Earth Systems*, 9(5), pp.2190–2213.

Tan, Z., Yao, H. and Zhuang, Q. (2018). A small temperate lake in the 21st century: Dynamics of water temperature, ice phenology, dissolved oxygen, and chlorophyll a. *Water Resources Research*, 54(7), pp.4681–4699.

Tan, Z., Zhuang, Q. and Walter Anthony, K. (2015). Modeling methane emissions from arctic lakes: Model development and site-level study. *Journal of Advances in Modeling Earth Systems*, 7(2), pp.459–483.

Taylor, K.E., Stouffer, R.J. and Meehl, G.A. (2012). An overview of CMIP5 and the experiment design. *Bulletin of the American meteorological Society*, 93(4), pp.485–498.

Thiery, W., Davin, E.L., Seneviratne, S.I., Bedka, K., Lhermitte, S. and Lipzig, N.P.M. van. (2016). Hazardous thunderstorm intensification over Lake Victoria. *Nature Communications*, 7(1), pp.1–7.

Thiery, W., Stepanenko, V.M., Fang, X., Jöhnk, K.D., Li, Z., Martynov, A., Perroud, M., Subin, Z.M., Darchambeau, F. and Mironov, D. (2014). LakeMIP Kivu: evaluating the representation of a large, deep tropical lake by a set of one-dimensional lake models. *Tellus A: Dynamic Meteorology and Oceanography*, 66(1), p.21390.

Tittensor, D.P., Novaglio, C., Harrison, C.S., Heneghan, R.F., Barrier, N., Bianchi, D., Bopp, L., Bryndum-Buchholz, A., Britten, G.L. and Büchner, M. (2021). Next-generation ensemble projections reveal higher climate risks for marine ecosystems. *Nature Climate Change*, 11(11), pp.973–981.

Trolle, D., Elliott, J.A., Mooij, W.M., Janse, J.H., Bolding, K., Hamilton, D.P. and Jeppesen, E. (2014). Advancing projections of phytoplankton responses to climate change through ensemble modelling. *Environmental Modelling & Software*, 61, pp.371–379.

Ulloa, H.N., Constantinescu, G., Chang, K., Horna-Munoz, D., Sepúlveda Steiner, O., Bouffard, D. and Wüest, A. (2019). Hydrodynamics of a periodically wind-forced small and narrow stratified basin: A large-eddy simulation experiment. *Environmental Fluid Mechanics*, 19(3), pp.667–698.

Umlauf, L. and Lemmin, U. (2005). Interbasin exchange and mixing in the hypolimnion of a large lake: The role of long internal waves. *Limnology and Oceanography*, 50(5), pp.1601–1611.

United Nations. (2016). *The Sustainable Development Goals 2016*. eSocialSciences.

Vallet-Coulomb, C., Legesse, D., Gasse, F., Travi, Y. and Chernet, T. (2001). Lake evaporation estimates in tropical Africa (lake Ziway, Ethiopia). *Journal of hydrology*, 245(1–4), pp.1–18.

Van Cleave, K., Lenters, J.D., Wang, J. and Verhamme, E.M. (2014). A regime shift in Lake Superior ice cover, evaporation, and water temperature following the warm El Niño winter of 1997–1998. *Limnology and Oceanography*, 59(6), pp.1889–1898.

Van Emmerik, T., Rimmer, A., Lechinsky, Y., Wenker, K., Nussboim, S. and Van de Giesen, N. (2013). Measuring heat balance residual at lake surface using Distributed Temperature Sensing. *Limnology and Oceanography: Methods*, 11(2), pp.79–90.

Vanderkelen, I., van Lipzig, N., Sacks, W.J., Lawrence, D.M., Clark, M.P., Mizukami, N., Pokhrel, Y. and Thiery, W. (2021). Simulating the Impact of Global Reservoir Expansion on the Present-Day Climate. *Journal of Geophysical Research: Atmospheres*, 126(16), p.e2020JD034485.

Verburg, P. and Antenucci, J.P. (2010). Persistent unstable atmospheric boundary layer enhances sensible and latent heat loss in a tropical great lake: Lake Tanganyika. *Journal of Geophysical Research: Atmospheres*, 115(D11).

Verpoorter, C., Kutser, T., Seekell, D.A. and Tranvik, L.J. (2014). A global inventory of lakes based on high-resolution satellite imagery. *Geophysical Research Letters*, 41(18), pp.6396–6402.

Vinnå, L.R., Medhaug, I., Schmid, M. and Bouffard, D. (2021). The vulnerability of lakes to climate change along an altitudinal gradient. *Communications Earth & Environment*, 2(1), pp.1–10.

Vinukollu, R.K., Meynadier, R., Sheffield, J. and Wood, E.F. (2011). Multi-model, multi-sensor estimates of global evapotranspiration: Climatology, uncertainties and trends. *Hydrological Processes*, 25(26), pp.3993–4010.

de Vries, H., Lenderink, G., van der Wiel, K. and van Meijgaard, E. (2022). Quantifying the role of the large-scale circulation on European summer precipitation change. *Climate Dynamics*, 59(9–10), pp.2871–2886.

Vystavna, Y., Harjung, A., Monteiro, L.R., Matiatos, I. and Wassenaar, L.I. (2021). Stable isotopes in global lakes integrate catchment and climatic controls on evaporation. *Nature Communications*, 12(1), pp.1–7.

Wagner, C. and Adrian, R. (2009). Cyanobacteria dominance: quantifying the effects of climate change. *Limnology and Oceanography*, 54(6part2), pp.2460–2468.

Wahed, M.S.A., Mohamed, E.A., El-Sayed, M.I., M'nif, A. and Sillanpää, M. (2014). Geochemical modeling of evaporation process in Lake Qarun, Egypt. *Journal of African Earth Sciences*, 97, pp.322–330.

Walsh, S.E., Vavrus, S.J., Foley, J.A., Fisher, V.A., Wynne, R.H. and Lenters, J.D. (1998). Global patterns of lake ice phenology and climate: Model simulations and observations. *Journal of Geophysical Research: Atmospheres*, 103(D22), pp.28825–28837.

Wang, B., Ma, Y., Su, Z., Wang, Y. and Ma, W. (2020). Quantifying the evaporation amounts of 75 high-elevation large dimictic lakes on the Tibetan Plateau. *Science advances*, 6(26), p.eaay8558.

Wang, B., Ma, Y., Wang, Y., Su, Z. and Ma, W. (2019). Significant differences exist in lake-atmosphere interactions and the evaporation rates of high-elevation small and large lakes. *Journal of hydrology*, 573, pp.220–234.

Wang, W., Lee, X., Xiao, W., Liu, S., Schultz, N., Wang, Y., Zhang, M. and Zhao, L. (2018). Global lake evaporation accelerated by changes in surface energy allocation in a warmer climate. *Nature Geoscience*, 11(6), pp.410–414.

Wang, Y., Leung, L.R., McGREGOR, J.L., Lee, D.-K., Wang, W.-C., Ding, Y. and Kimura, F. (2004). Regional climate modeling: progress, challenges, and prospects. *Journal of the Meteorological Society of Japan. Ser. II*, 82(6), pp.1599–1628.

Wantzen, K.M., Rothhaupt, K.-O., Mörtl, M., Cantonati, M., Tóth, L.G.- and Fischer, P. (2008). *Ecological effects of water-level fluctuations in lakes: an urgent issue*. Springer.

Warszawski, L., Frieler, K., Huber, V., Piontek, F., Serdeczny, O. and Schewe, J. (2014). The inter-sectoral impact model intercomparison project (ISI–MIP): project framework. *Proceedings of the National Academy of Sciences*, 111(9), pp.3228–3232.

Watras, C., Read, J., Holman, K., Liu, Z., Song, Y., Watras, A., Morgan, S. and Stanley, E. (2014). Decadal oscillation of lakes and aquifers in the upper Great Lakes region of North America: Hydroclimatic implications. *Geophysical Research Letters*, 41(2), pp.456–462.

Weathers, K., Hanson, P.C., Arzberger, P., Brentrup, J., Brookes, J.D., Carey, C.C., Gaiser, E., Hamilton, D.P., Hong, G.S. and Ibelings, B.W. (2013). The Global Lake Ecological Observatory Network (GLEON): the evolution of grassroots network science. *Limnology and Oceanography Bulletin*, 22(3), pp.71-73.

Weisman, R.N. and Brutsaert, W. (1973). Evaporation and cooling of a lake under unstable atmospheric conditions. *Water resources research*, 9(5), pp.1242–1257.

Wetzel, R.G. (2001). *Limnology: lake and river ecosystems*. Academic Press.

Weyhenmeyer, G.A. (2007). Rates of change in physical and chemical lake variables—are they comparable between large and small lakes?. In: *European Large Lakes Ecosystem changes and their ecological and socioeconomic impacts*. Springer, pp.105–110.

Williamson, C.E., Saros, J.E., Vincent, W.F. and Smol, J.P. (2009). Lakes and reservoirs as sentinels, integrators, and regulators of climate change. *Limnology and Oceanography*, 54(6part2), pp.2273–2282.

Winslow, L.A., Zwart, J.A., Batt, R.D., Dugan, H.A., Woolway, R.I., Corman, J.R., Hanson, P.C. and Read, J.S. (2016). LakeMetabolizer: an R package for estimating lake metabolism from free-water oxygen using diverse statistical models. *Inland Waters*, 6(4), pp.622–636.

Woolway, R.I., Jones, I.D., Hamilton, D.P., Maberly, S.C., Muraoka, K., Read, J.S., Smyth, R.L. and Winslow, L.A. (2015). Automated calculation of surface energy fluxes

with high-frequency lake buoy data. *Environmental Modelling & Software*, 70, pp.191–198.

Woolway, R.I., Verburg, P., Lenters, J.D., Merchant, C.J., Hamilton, D.P., Brookes, J., de Eyto, E., Kelly, S., Healey, N.C. and Hook, S. (2018). Geographic and temporal variations in turbulent heat loss from lakes: A global analysis across 45 lakes. *Limnology and Oceanography*, 63(6), pp.2436–2449.

Woolway, R.I., Kraemer, B.M., Lenters, J.D., Merchant, C.J., O'Reilly, C.M. and Sharma, S. (2020). Global lake responses to climate change. *Nature Reviews Earth & Environment*, 2020, pp.1–16.

Woolway, R.I., Sharma, S., Weyhenmeyer, G.A., Debolskiy, A., Golub, M., Mercado-Bettín, D., Perroud, M., Stepanenko, V., Tan, Z. and Grant, L. (2021). Phenological shifts in lake stratification under climate change. *Nature communications*, 12(1), pp.1–11.

Woolway, R.I., Dokulil, M.T., Marszelewski, W., Schmid, M., Bouffard, D. and Merchant, C.J. (2017). Warming of Central European lakes and their response to the 1980s climate regime shift. *Climatic Change*, 142, pp.505–520.

Woolway, R.I. and Merchant, C.J. (2018). Intralake Heterogeneity of Thermal Responses to Climate Change: A Study of Large Northern Hemisphere Lakes. *Journal of Geophysical Research: Atmospheres*, 123(6), pp.3087–3098.

Woolway, R.I. and Merchant, C.J. (2019). Worldwide alteration of lake mixing regimes in response to climate change. *Nature Geoscience*, 12(4), pp.271–276.

Woolway, R.I., Sharma, S. and Smol, J.P. (2022). Lakes in hot water: the impacts of a changing climate on aquatic ecosystems. *BioScience*, 72(11), pp.1050–1061.

Wrzesiński, D. and Ptak, M. (2016). Water level changes in Polish lakes during 1976–2010. *Journal of Geographical Sciences*, 26, pp.83–101.

Wurtsbaugh, W.A., Miller, C., Null, S.E., DeRose, R.J., Wilcock, P., Hahnenberger, M., Howe, F. and Moore, J. (2017). Decline of the world's saline lakes. *Nature Geoscience*, 10(11), pp.816–821.

Wynne, J.H., Woelmer, W., Moore, T.N., Thomas, R.Q., Weathers, K.C. and Carey, C.C. (2023). Uncertainty in projections of future lake thermal dynamics is differentially driven by lake and global climate models. *PeerJ*, 11, p.e15445.

Xiao, K., Griffis, T.J., Baker, J.M., Bolstad, P.V., Erickson, M.D., Lee, X., Wood, J.D., Hu, C. and Nieber, J.L. (2018). Evaporation from a temperate closed-basin lake and its impact on present, past, and future water level. *Journal of Hydrology*, 561, pp.59–75.

Xiao, W., Zhang, Z., Wang, W., Zhang, M., Liu, Q., Hu, Y., Huang, W., Liu, S. and Lee, X. (2020). Radiation controls the interannual variability of evaporation of a subtropical lake. *Journal of Geophysical Research: Atmospheres*, 125(8), p.e2019JD031264.

Xiao, W., Liu, S., Wang, W., Yang, D., Xu, J., Cao, C., Li, H. and Lee, X. (2013). Transfer coefficients of momentum, heat and water vapour in the atmospheric surface layer of a large freshwater lake. *Boundary-layer meteorology*, 148(3), pp.479–494.

Yao, F., Livneh, B., Rajagopalan, B., Wang, J., Crétaux, J.-F., Wada, Y. and Berge-Nguyen, M. (2023). Satellites reveal widespread decline in global lake water storage. *Science*, 380(6646), pp.743–749.

Ye, X., Anderson, E.J., Chu, P.Y., Huang, C. and Xue, P. (2019). Impact of water mixing and ice formation on the warming of Lake Superior: A model-guided mechanism study. *Limnology and Oceanography*, 64(2), pp.558–574.

Youssef, Y.W. and Khodzinskaya, A. (2019). A review of evaporation reduction methods from water surfaces. In: E3S web of conferences. EDP Sciences, p.05044.

Zamani, B., Koch, M. and Hodges, B.R. (2021). A potential tipping point in the thermal regime of a warm monomictic reservoir under climate change using three-dimensional hydrodynamic modeling. *Inland Waters*, 11(3), pp.315–334.

Zeng, X., Zhao, M. and Dickinson, R.E. (1998). Intercomparison of bulk aerodynamic algorithms for the computation of sea surface fluxes using TOGA COARE and TAO data. *Journal of Climate*, 11(10), pp.2628–2644.

Zhan, S., Song, C., Wang, J., Sheng, Y. and Quan, J. (2019). A global assessment of terrestrial evapotranspiration increase due to surface water area change. *Earth's future*, 7(3), pp.266–282.

Zhang, G., Luo, W., Chen, W. and Zheng, G. (2019). A robust but variable lake expansion on the Tibetan Plateau. *Science Bulletin*, 64(18), pp.1306–1309.

Zhang, Q. and Liu, H. (2014). Seasonal changes in physical processes controlling evaporation over inland water. *Journal of Geophysical Research: Atmospheres*, 119(16), pp.9779–9792.

Zhao, B., Kao, S., Zhao, G., Gangrade, S., Rastogi, D., Ashfaq, M. and Gao, H. (2023). Evaluating Enhanced Reservoir Evaporation Losses From CMIP6-Based Future Projections in the Contiguous United States. *Earth's Future*, 11(3), p.e2022EF002961.

Zhao, G., Li, Y., Zhou, L. and Gao, H. (2022). Evaporative water loss of 1.42 million global lakes. *Nature communications*, 13(1), pp.1–10.

Zhao, G. and Gao, H. (2019). Estimating reservoir evaporation losses for the United States: Fusing remote sensing and modeling approaches. *Remote Sensing of Environment*, 226, pp.109–124.

Zhou, J., Wu, C., Yeh, P.J.-F., Ju, J., Zhong, L., Wang, S. and Zhang, J. (2023). Anthropogenic climate change exacerbates the risk of successive flood-heat extremes: Multi-model global projections based on the Inter-Sectoral Impact Model Intercomparison Project. *Science of The Total Environment*, 889, p.164274.

Zhou, W., Wang, L., Li, D. and Leung, L.R. (2021). Spatial pattern of lake evaporation increases under global warming linked to regional hydroclimate change. *Communications Earth & Environment*, 2(1), pp.1–10.

Zhu, L., Xie, M. and Wu, Y. (2010). Quantitative analysis of lake area variations and the influence factors from 1971 to 2004 in the Nam Co basin of the Tibetan Plateau. *Chinese Science Bulletin*, 55(13), pp.1294–1303.

Zohary, T., Sukenik, A., Berman, T. and Nishri, A. (2014). *Lake Kinneret: ecology and management*. Springer.

Zohary, T. and Ostrovsky, I. (2011). Ecological impacts of excessive water level fluctuations in stratified freshwater lakes. *Inland waters*, 1(1), pp.47–59.

Appendices

Appendix A

Authors: Sofia La Fuente[1*], Eleanor Jennings[1], Gideon Gal[2], Georgiy Kirillin[3], Tom Shatwell[4], Robert Ladwig[5], Tadhg Moore[6], Raoul-Marie Couture[7], Marianne Côté[7], C. Love Råman Vinnå[8], R. Iestyn Woolway[9]

Affiliations:

1. Centre for Freshwater and Environmental Studies, Dundalk Institute of Technology, Dundalk, Ireland

2. Kinneret Limnological Laboratory, Israel Oceanographic & Limnological Research, Migdal, Israel

3. Leibniz-Institute of Freshwater Ecology and Inland Fisheries (IGB), Berlin, Germany

4. Helmholtz Centre for Environmental Research, Department of Lake Research, Magdeburg, Germany

5. Center for Limnology, University of Wisconsin-Madison, Madison, WI, USA

6. Virginia Tech, Department of Biological Sciences, Blacksburg, VA, USA

7. Centre for Northern Studies (CEN), Takuvik Joint International Laboratory, and Department of Chemistry, Université Laval, Quebec City, QC, Canada

8. Eawag, Swiss Federal Institute of Aquatic Science and Technology, Surface Waters - Research and Management, Kastanienbaum, Switzerland

9. School of Ocean Sciences, Bangor University, Menai Bridge, Anglesey, Wales

*Corresponding author: ruthsofia.lafuentepillco@dkit.ie

Text A1. Bulk algorithm for latent heat flux

The turbulent heat fluxes, sensible heat and latent heat, were parameterized by bulk heat transfer algorithms that relate surface layer data to surface fluxes using formulae based on scaling laws and empirical relationships. These procedures involve the calculation of the roughness lengths for momentum, heat and moisture (z_o, z_{oh}, z_{oq}) and the corresponding transfer coefficients (C_{d_z}, C_{h_z}, C_{e_z}) from observed wind speed (u), temperature (T) and humidity (q) profiles, via an iterative routine that involves a friction velocity term, u_{*a} (m s^{-1}), a scaling temperature term, T_* (K), and a scaling humidity term, q_* (g kg^{-1}), as explained in Woolway et al. (2015) and Zeng et al. (1998). Using the above terms, surface fluxes for momentum, sensible heat and latent heat can be calculated as:

$$\tau = C_{d_z}\rho_z u_z^2 = \rho_z u_{*a}^2 \tag{A.1}$$

$$Q_h = \rho_z C_{pa} C_{h_z} u_z (T_o - T_z) = -\rho_z C_{pa} u_{*a} T_* \tag{A.2}$$

$$Q_e = \rho_z L_v C_{e_z} u_z (q_o - q_z) = -\rho_z L_v u_{*a} q_* \tag{A.3}$$

where $\rho_z = 100p/[R_a(T_z + 273.16)]$ is the density of the overlying air (kg m^{-3}); p is the surface air pressure (hPa); $R_a = 287(1 + 0.608q_z)$ is the gas constant for moist air (J kg^{-1} °C^{-1}); u_z is the wind speed (m s^{-1}) at height z_u (7.8 m) above the water surface; $C_{pa} = 1006$ is the specific heat of air at constant pressure (J kg^{-1} °C^{-1}); T_o is the surface water temperature (°C); T_z is air temperature (°C) at height z_t (6.3 m) above the water surface; $L_v = 2.501 \times 10^6 - 2370 \times T_o$ is the latent heat of vaporization (J kg^{-1}); $q_0 = \lambda \, e_{sat}/p$ is the specific humidity at saturation pressure in kg kg^{-1}, with λ representing the ratio of the molecular weights for dry and moist air (=0.622); e_{sat} is the saturated vapour pressure (hPa), calculated as $e_{sat} = 6.11exp\left[\frac{17.27T_0}{237.3+T_0}\right]$; $q_z = \lambda e/p$ is the specific humidity of the air (kg kg^{-1}) at height z_q (6.3 m) above the water surface, where $e = R_h e_z/100$ is actual vapour pressure, R_h is the relative humidity (%) and $e_z = 6.11exp\left[\frac{17.27T_z}{237.3+T_z}\right]$ is the saturated vapour pressure (hPa) at z_t. Here, C_{d_z}, C_{h_z}, and C_{e_z} are the transfer coefficients for heights z_u, z_t, and z_q ,respectively.

The algorithm proposed by Zeng et al. (1998) applies the Monin-Obukhov similarity theory to the atmospheric boundary layer and states that wind, temperature and humidity profile gradients depend on unique functions of the stability parameter, ζ, where $\zeta = zL_w^{-1}$:

$$\phi_m(\zeta) = \frac{\kappa z_u}{u_{*a}} \frac{\partial u}{\partial z} \qquad (A.4)$$

$$\phi_h(\zeta) = \frac{\kappa z_t}{T_*} \frac{\partial T}{\partial z} \qquad (A.5)$$

$$\phi_e(\zeta) = \frac{\kappa z_q}{q_*} \frac{\partial q}{\partial z} \qquad (A.6)$$

where L_w is the Monin-Obukhov length scale (m), κ is the von Karman constant (0.41) and ϕ_m, ϕ_h and ϕ_e are the similarity functions that relate the fluxes of momentum, heat and moisture to the mean profile gradients wind, temperature and humidity, respectively. The Monin-Obukhov length scale is a measure of the reduction of potential energy caused by wind mixing and the growth of atmospheric stratification due to surface fluxes (Brutsaert 1982), and can be calculated as:

$$L_w = \frac{-\rho_z u_{*a}^3 T_v}{\kappa g \left(\frac{Q_h}{c_{pa}} + 0.61 \frac{(T_z + 273.16)Q_e}{L_v} \right)} \qquad (A.7)$$

where $T_v = (T_z + 273.16)(1 + 0.61q_z)$ is the virtual air temperature (K) and $g = 9.780310[1 + 0.00530239\ sin^2\varphi - 0.00000587\ sin^2 2\varphi - (31.55 \times 10^{-8}) \times h]$ is the gravitational acceleration (m s⁻²) where φ is latitude (°) and h is the altitude (m). Atmospheric stability is a function of the Monin-Obukhov length, when L_w is negative the boundary layer is convective and vertical transfer is enhanced (unstable conditions). The opposite is true for stable stratified boundary layers when the heat and latent fluxes are reduced ($L_w > 0$) (Verburg and Antenucci 2010).

According to Zeng et al. (1998), the differential equations for ϕ_m, ϕ_h, ϕ_e can be integrated between the roughness length and measurement height, to obtain wind, temperature and humidity gradients in the atmospheric boundary layer and the corresponding scaling parameters used in calculating the turbulent surface fluxes. In addition, these are used to estimate wind speed, air temperature and humidity at any

reference height (e.g. 10 m) above the lake surface. Using the Monin-Obukhov similarity theory, the flux gradient relations for momentum are:

$$\phi_m(\zeta) = 5 + \zeta \quad \text{for } \zeta > 1 \text{ (very stable)}, \tag{A.8}$$

$$\phi_m(\zeta) = 1 + 5\zeta \quad \text{for } 0 \le \zeta \le 1 \text{ (stable)}, \tag{A.9}$$

$$\phi_m(\zeta) = (1 - 16\zeta)^{-1/4} \quad \text{for -1.574} \le \zeta < 0 \text{ (unstable)}, \tag{A.10}$$

$$\phi_m(\zeta) = \left(0.7\kappa^{2/3}\right)(-\zeta)^{1/3} \quad \text{for } \zeta < -1.574 \text{ (very unstable)}, \tag{A.11}$$

and for sensible heat and humidity, where $\phi_e(\zeta) = \phi_h(\zeta)$, are:

$$\phi_e(\zeta) = \phi_h(\zeta) = 5 + \zeta \quad \text{for } \zeta > 1 \text{ (very stable)}, \tag{A.12}$$

$$\phi_e(\zeta) = \phi_h(\zeta) = 1 + 5\zeta \quad \text{for } 0 \le \zeta \le 1 \text{ (stable)}, \tag{A.13}$$

$$\phi_e(\zeta) = \phi_h(\zeta) = (1 - 16\zeta)^{-1/2} \quad \text{for -0.465} \le \zeta < 0 \text{ (unstable)}, \tag{A.14}$$

$$\phi_e(\zeta) = \phi_h(\zeta) = 0.9\kappa^{4/3}(-\zeta)^{-1/3} \quad \text{for } \zeta < -0.465 \text{ (very unstable)} \tag{A.15}$$

where to ensure continuous functions of $\phi_e(\zeta)$, $\phi_h(\zeta)$ and $\phi_m(\zeta)$, we can match the relations at $\zeta_m = -1.574$ for $\phi_m(\zeta)$ and $\zeta_h = \zeta_e = -0.465$ for $\phi_e(\zeta) = \phi_h(\zeta)$. The flux gradient relations can then be integrated to yield profiles for wind, temperature and humidity, as well as the corresponding scaling terms. The scaling terms can then be used to calculate the surface fluxes for momentum, sensible heat and moisture as well as the corresponding transfer coefficients as:

$$C_{d_z} = \frac{u_{*a}^2}{u_z{}^2} \tag{A.16}$$

$$C_{h_z} = \frac{-u_{*a}T_*}{u_z(T_o - T_z)} \tag{A.17}$$

$$C_{e_z} = \frac{-u_{*a}q_*}{u_z(q_o - q_z)} \tag{A.18}$$

once the Q_e was known, we estimated the lake evaporation using the relation proposed by Henderson-Sellers (1986).
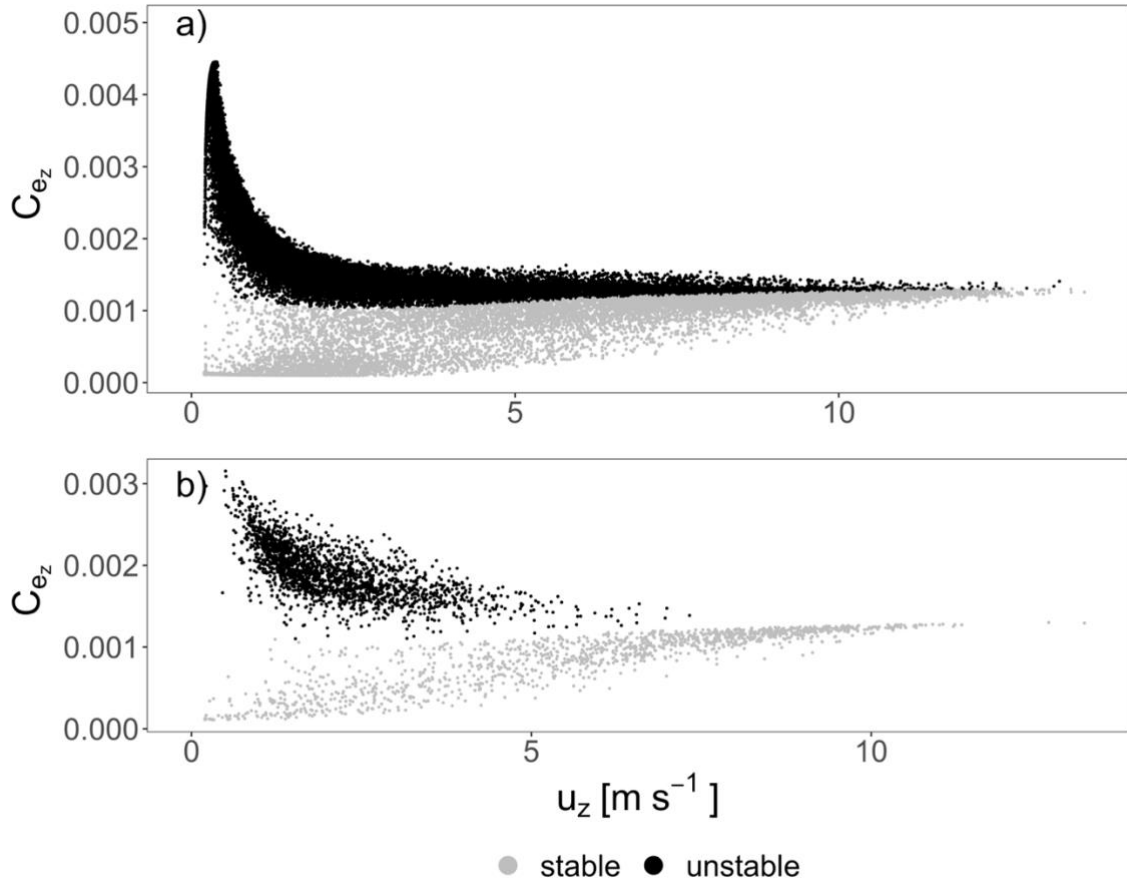
Figure A.1 Transfer coefficient (C_{e_z}) dependence on wind speed (u_z) at (a) sub-daily and (b) daily timestep over the period 2000-2005 for Lake Kinneret. The average C_{e_z} was 1.7×10^{-3} for our study, which is comparable to published studies of four freshwater lakes, particularly those in tropical lakes (e.g., Lake Tanganyika) as shown in Table A.1.
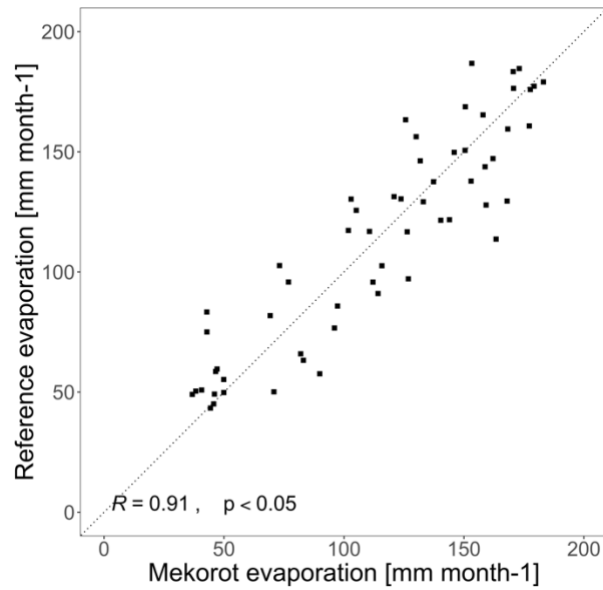
Figure A.2. Monthly averaged evaporation over the period 2000-2005. Mekorot evaporation estimates are compared with our reference evaporation estimates with the Spearman Rank correlation (R). The diagonal line represents the 1:1 relationship between Mekorot and reference evaporation rates.

Table A.1. Examples of transfer coefficient for latent heat flux used in the literature.

Lake	C_{e_z}	Reference
Lake Taihu, China	1.8×10^{-3}	(Xiao et al. 2013)
Lake Valkea-Kotinen, Finland	1.0×10^{-3}	(Nordbo et al. 2011)
Lake Tämnaren, Sweden	1.0×10^{-3}	(Heikinheimo et al. 1999)
Ross Rarnett Reservoir, USA	1.2×10^{-3}	(Liu et al. 2009)
Great Slave Lake, Canada	2.0×10^{-3}	(Blanken et al. 2003)
Lake Tanganyika, East Africa	1.85×10^{-3}	(Verburg and Antenucci 2010)

Appendix B

Text B1. Description of lake models

FLake is a 1-D bulk model based on a two-layer parametric representation of the evolving temperature profile and on the integral budgets of heat and kinetic energy for the layers in question. The structure of the stratified layer between the upper mixed layer and the basin bottom is described using the concept of self-similarity (assumed shape) of the temperature-depth curve (Kirillin 2002). The same concept is used to describe the temperature structure of the thermally active upper layer of bottom sediments and, when present, of the ice and snow cover (Mironov 2008). FLake uses a lake-specific parameterization scheme to compute the fluxes of momentum, and of sensible and latent heat flux at the lake surface based on the Monin-Obukhov similarity relations.

MyLake is a 1-D process-based model used to simulate physical, chemical and biological dynamics in lakes (Saloranta and Andersen 2007). The model simulates thermal stratification, lake ice and snow cover, and phytoplankton dynamics, along with sediment-water interactions using a simple sediment box model (v.1.12). MyLake uses regularly spaced water layers whose vertical resolution is defined by the user. The turbulent fluxes at the air-water interface are estimated using a diffusion coefficient in the heat balance as explained by Hondzo and Stefan (1993). Different versions of the model have been developed to simulate algal blooms (Salk et al. 2022), CO_2 and CH_4 (Kiuru et al. 2019), internal phosphorus loads (Markelov et al. 2019) and light attenuation dynamics (Pilla and Couture 2021).

Simstrat is a physical deterministic 1-D hydrodynamic model, including vertical mixing induced by internal seiches and surface ice (Gaudard et al. 2019; Goudsmit et al. 2002). This model uses layers of fixed depth (at 0.5 m intervals for lakes with < 50 m maximum depth and at 1 m intervals for lakes > 50 m), and supports multiple options for external forcing, comprising several meteorological variables or surface energy fluxes. Simstrat simulates thermal stratification and ice and snow formation (Gaudard et al. 2019). The surface fluxes are calculated using the Livingstone and Imboden (1989) formulae. Simstrat has been applied in lakes of varying climatic and morphometric conditions (Bärenbold et al. 2022; Råman Vinnå et al. 2021; Mesman et al. 2020; Kobler and Schmid 2019; Thiery et al. 2014).

Figure B.1. Workflow for warm-season lake evaporation estimation. JAS: July, August, September.
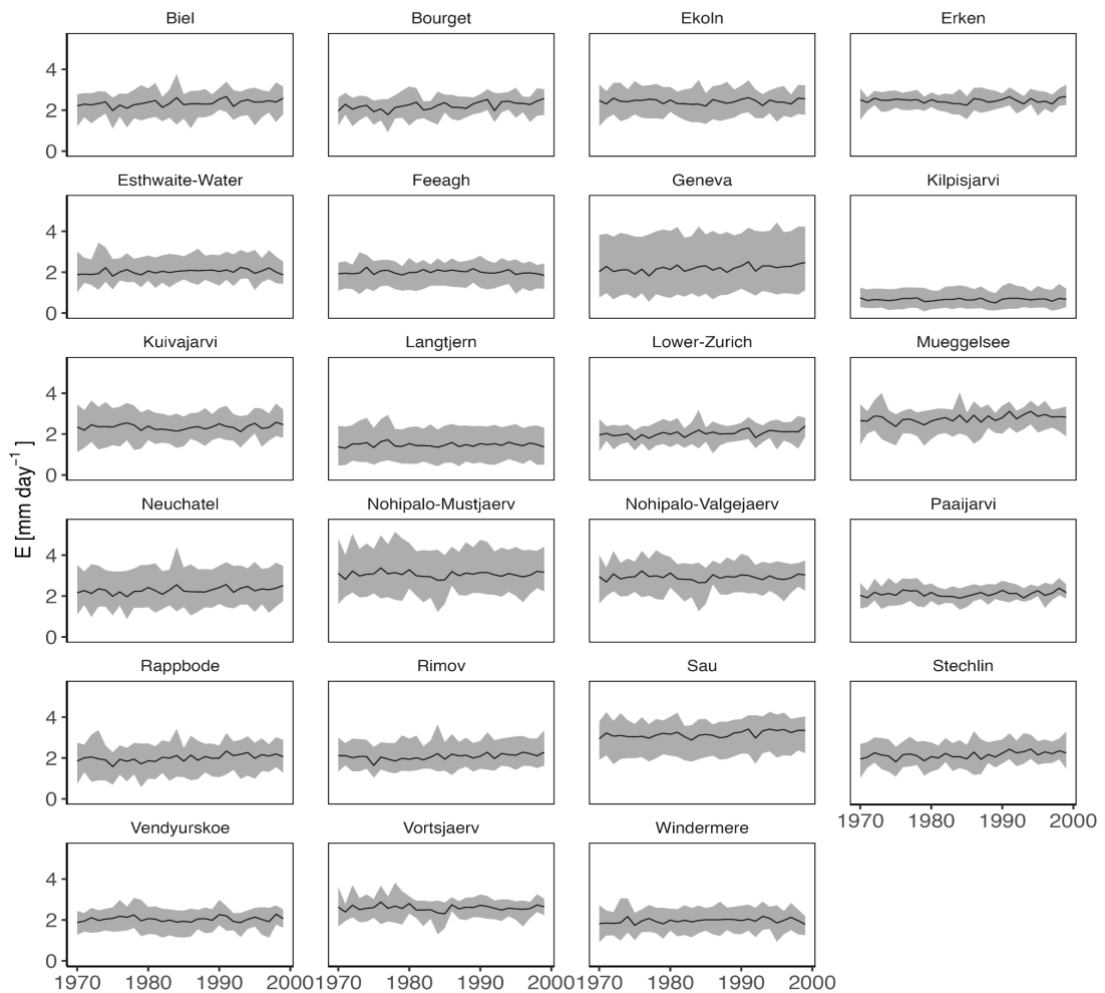
Figure B.2. Historic simulations of warm-season evaporation rates in mm day^{-1} over the 1970-1999 period for European lakes. Ensemble mean is represented by a continuous line and ensemble spread is represented by the shaded area.
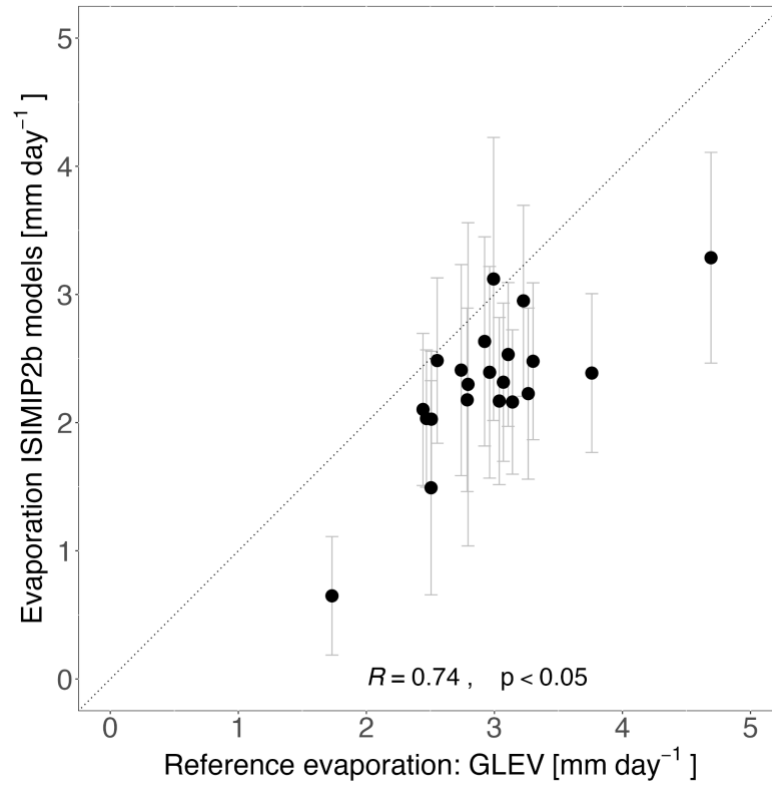
Figure B.3. Comparison of simulated and reference evaporation rates over the period 1985-2005. Each data point represents a comparison of ISIMIP2b simulated evaporation against the lake evaporation from the GLEV dataset (n=21). The data points represent the mean and the confidence intervals across the ISIMIP2b 12 lake-climate model realizations. The dashed line represents the 1:1 relationship between simulated and reference evaporation rates.
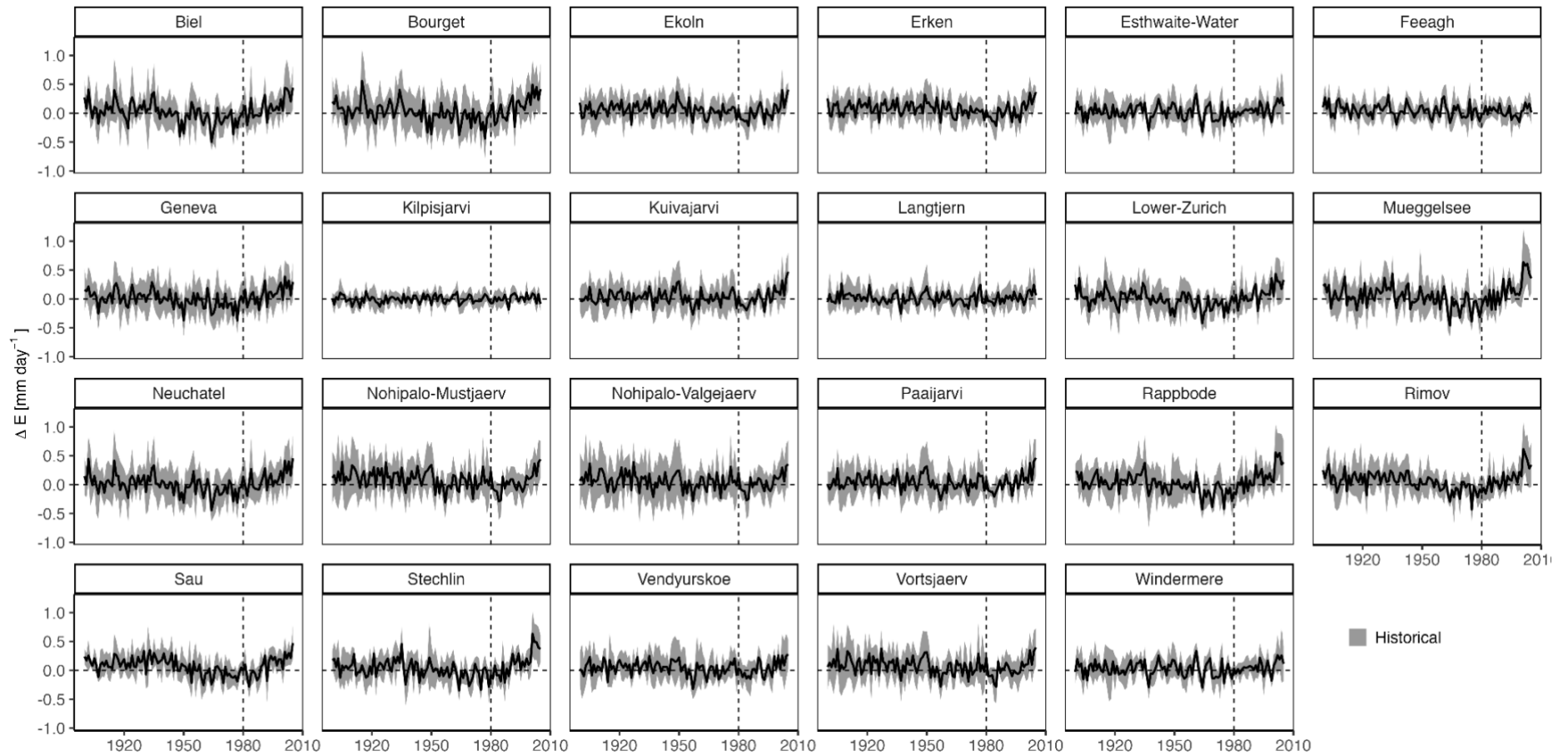
Figure B.4. Average annual warm-season evaporation rates in mm day^{-1} during the historic (1901-2005) period for 23 European lakes. The average of the model ensemble is shown by the thick lines, the standard deviation across the model ensemble is represented by the shaded area. Anomalies (ΔE) are quoted relative to the 1970-1999 base period average.
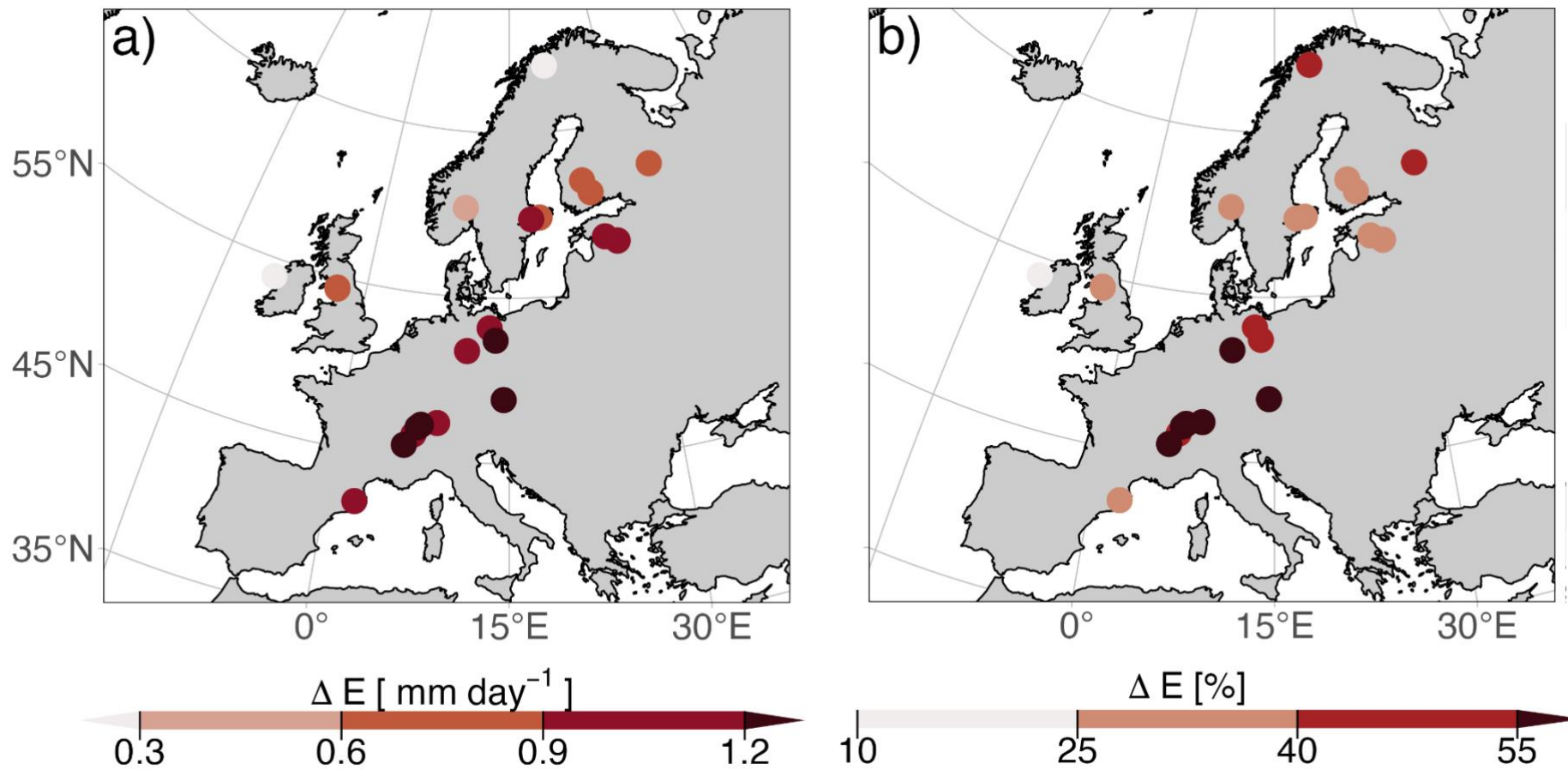
Figure B.5. Average annual warm-season evaporation rates in (a) mm day^{-1} and (b) percentage for 23 European lakes by the end of the 21st century. Anomalies (ΔE) are quoted relative to the 1970-1999 base period average.
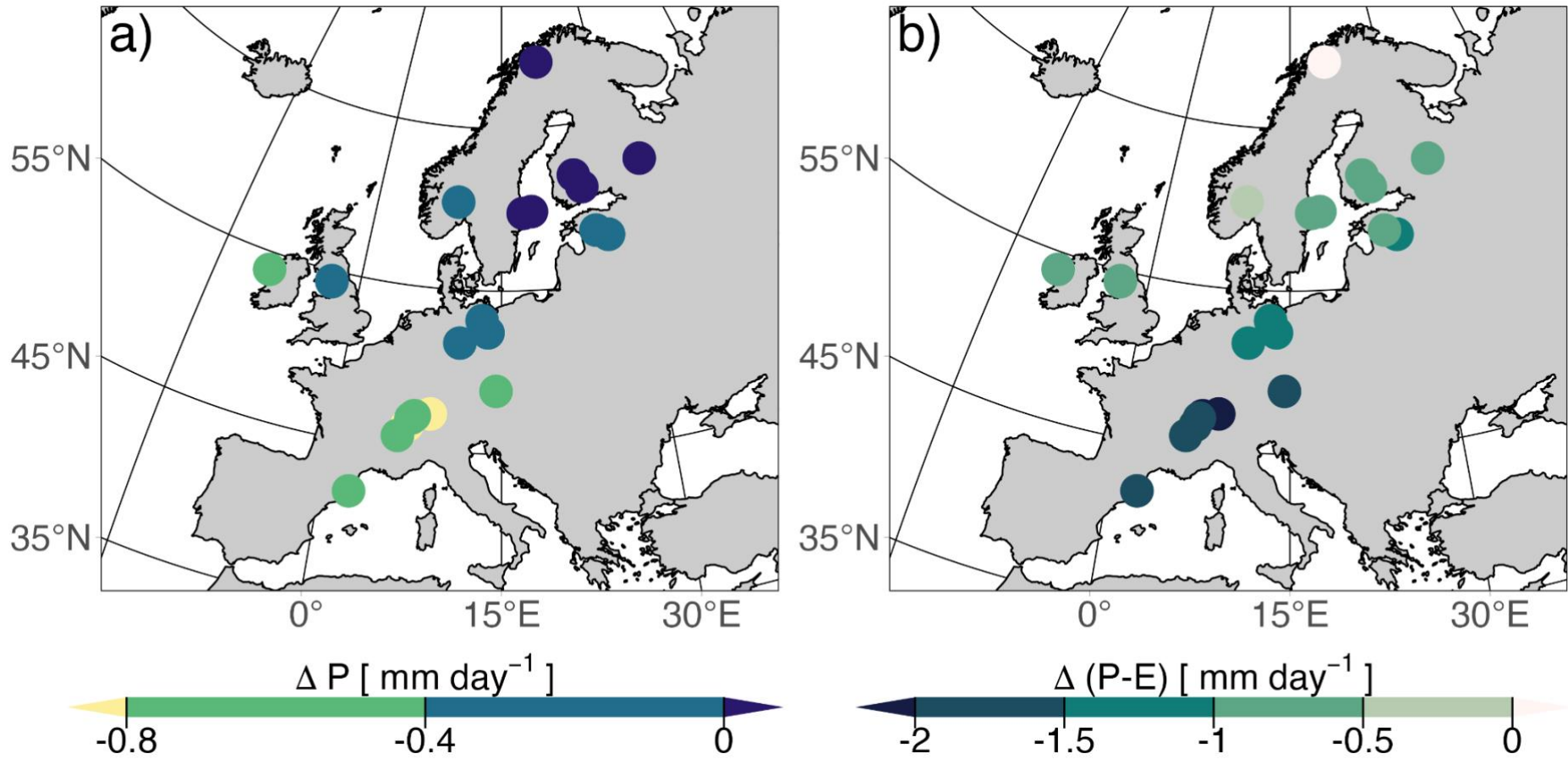
Figure B.6. Average annual warm-season (a) precipitation rates in mm day^{-1} and (b) precipitation minus evaporation rates in mm day^{-1} for 23 European lakes by the end of the 21st century under Representative Concentration Pathway (RCP) 8.5. Anomalies (Δ) are quoted relative to the 1970-1999 base period average.

Table B.1. Summary of characteristics of the 23 studied lakes.

No	Name	Country	Latitude	Longitude	Area [km²]	Mean depth [m]	Max depth [m]	Hydrolakes ID
1	Biel	Switzerland	47.08	7.16	39	30	74	14023
2	Bourget	France	45.76	5.86	44	80	145	14167
3	Ekoln	Sweden	59.75	17.62	20	12	50	102
4	Erken	Sweden	59.84	18.63	24	9	21	12809
5	Esthwaite-Water	UK	54.37	-2.99	1	7	16	1319494
6	Feeagh	Ireland	53.94	-9.58	4	15	44	163604
7	Geneva	Switzerland	46.45	6.59	580	153	310	1261
8	Kilpisjarvi	Finland	69.03	20.77	37	20	57	11270
9	Kuivajarvi	Finland	61.85	24.28	1	6	13	1273488
10	Langtjern	Norway	60.37	9.73	0	2	12	1285001
11	Lower-Zurich	Switzerland	47.28	8.58	67	49	136	14005
12	Mueggelsee	Germany	52.43	13.65	7	5	8	165102
13	Neuchatel	Switzerland	46.91	6.89	217	64	152	1249
14	Nohipalo-Mustjaerv	Estonia	57.93	27.34	0	4	9	1301698
15	Nohipalo-Valgejaerv	Estonia	57.94	27.35	0	6	13	NA
16	Paaijarvi	Finland	61.07	25.13	13	15	85	12603
17	Rappbode	Germany	51.74	10.89	4	29	89	165692
18	Rimov	Czech Republic	48.85	14.49	2	16	44	167991
19	Sau	Spain	41.97	2.39	6	29	65	172244
20	Stechlin	Germany	53.17	13.03	2	23	70	164428
21	Vendyurskoe	Russia	62.1	33.1	10	5	13	NA
22	Vortsjaerv	Estonia	58.31	26.01	270	3	6	1164
23	Windermere	UK	54.31	-2.95	15	21	64	13387

Table B.2. Climate forcing variables used as input to drive the lake models used in this study to simulate historical and future evaporation rates in European lakes.

Variable	Abbreviation	FLake	MyLake	Simstrat
Near-surface relative humidity [%]	hurs		x	
Near-surface specific humidity [kg kg^{-1}]	huss	x		x
Precipitation [kg m^{-2} s^{-1}]	pr		x	x
Surface pressure [Pa]	ps		x	x
Surface downwelling longwave radiation [W m^{-2}]	rlds	x		x
Surface downwelling shortwave radiation [W m^{-2}]	rsds	x	x	x
Near-surface wind speed at 10m [m s^{-1}]	sfcWind	x	x	x
Near-surface air temperature [K]	tas	x	x	x
Eastward near-surface wind [m s^{-1}] (*)	uas			x
Northward near-surface wind [m s^{-1}] (*)	vas			x

Table B.3. Summary of the lake models used in this study, including a description of their structure, parameterization and key references.

Lake model (version)	Timestep Simulated/ Reported	Vertical structure / layers reported	Parameterization of turbulent fluxes at air-water interface	Turbulent mixing parameterization	Calibrated parameters	Key references
FLake (ver. 2.0)	Daily	Two-layer self-similar structure / 4	The Monin-Obukhov similarity relations	The water surface temperature is equal to the mixed-layer temperature, this is computed from calculation and constant update of heat fluxes	1. Parameter for profile relaxation time	Mironov (2008)
MyLake (ver. 1.12)	Daily	Multilayer / 0.5 m - max.depth	Diffusion coefficient in heat balance	Hondzo and Stefan thermal diffusion model	1. Wind shelter parameter 2. Minimum stability frequency 3. Non-PAR diffuse attenuation coefficient 4. PAR diffuse attenuation coefficient	Saloranta and Andersen (2007)
Simstrat (ver. 2.1.2)	Daily	Multilayer / 0.5m - max depth	Dirichlet condition	k-ε turbulence model with buoyancy and internal seiche parameterization	1. Fraction of wind energy transferred to seiche energy 2. As above during summer and winter 3. Fraction of forcing wind to wind at 10 m 4. Fit parameter scaling absorption of IR radiation from sky	Goudsmit et al. (2002)

Table B.4. Annual evaporation projections by the end of the 21st century under future scenarios of climate change: RCP 2.6, 6.0 and 8.5 for each lake. The evaporation estimates for the historic period correspond to the average over 1971-2000 and the future period corresponds to 2070-2099. Anomalies (Δ) are calculated as future minus historic.

Lake	Historic evaporation (E) [mm day^{-1}]	Scenario	Future evaporation (E) [mm day^{-1}]	Evaporation change (ΔE) [mm day^{-1}]	Evaporation change (ΔE) [%]
Biel	2.3±0.5	RCP 2.6	2.9±0.5	0.5±0.4	22
		RCP 6.0	3.2±0.6	0.9±0.5	38
		RCP 8.5	3.7±0.8	1.3±0.7	56
Bourget	2.2±0.4	RCP 2.6	2.8±0.5	0.6±0.5	27
		RCP 6.0	3.1±0.5	0.9±0.5	39
		RCP 8.5	3.5±0.7	1.2±0.7	56
Ekoln	2.4±0.5	RCP 2.6	2.9±0.5	0.5±0.4	19
		RCP 6.0	3.1±0.6	0.7±0.3	27
		RCP 8.5	3.3±0.6	0.9±0.4	38
Erken	2.5±0.3	RCP 2.6	2.9±0.4	0.5±0.3	19
		RCP 6.0	3.1±0.4	0.6±0.3	26
		RCP 8.5	3.3±0.4	0.9±0.4	35
Esthwaite-Water	2±0.5	RCP 2.6	2.5±0.5	0.4±0.4	21
		RCP 6.0	2.6±0.6	0.5±0.4	27
		RCP 8.5	2.7±0.7	0.7±0.6	35
Feeagh	2±0.5	RCP 2.6	2.2±0.5	0.2±0.3	10
		RCP 6.0	2.2±0.5	0.2±0.2	10
		RCP 8.5	2.2±0.5	0.2±0.3	12
Geneva	2.2±1.2	RCP 2.6	2.7±1.2	0.5±0.4	23
		RCP 6.0	2.9±1.3	0.7±0.5	32
		RCP 8.5	3.2±1.5	1±0.6	47
Kilpisjarvi	0.7±0.3	RCP 2.6	0.8±0.4	0.1±0.1	15
		RCP 6.0	0.8±0.4	0.1±0.2	28

		RCP 8.5	0.9±0.5	0.2±0.3	41
Kuivajarvi	2.3±0.5	RCP 2.6	2.8±0.5	0.4±0.3	18
		RCP 6.0	3±0.6	0.6±0.4	27
		RCP 8.5	3.2±0.6	0.9±0.4	37
Langtjern	1.5±0.6	RCP 2.6	1.7±0.7	0.2±0.3	17
		RCP 6.0	1.8±0.7	0.3±0.3	19
		RCP 8.5	1.9±0.8	0.5±0.4	31
Lower-Zurich	2±0.4	RCP 2.6	2.5±0.4	0.5±0.4	24
		RCP 6.0	2.8±0.5	0.8±0.5	38
		RCP 8.5	3.2±0.7	1.2±0.7	57
Mueggelsee	2.8±0.5	RCP 2.6	3.4±0.5	0.7±0.5	25
		RCP 6.0	3.7±0.6	0.9±0.5	34
		RCP 8.5	4±0.8	1.2±0.7	44
Neuchatel	2.3±0.7	RCP 2.6	2.8±0.7	0.5±0.4	24
		RCP 6.0	3.1±0.8	0.8±0.5	37
		RCP 8.5	3.5±0.9	1.2±0.7	54
Nohipalo-Mustjaerv	3.1±0.8	RCP 2.6	3.6±0.9	0.6±0.5	19
		RCP 6.0	4±0.9	0.9±0.5	29
		RCP 8.5	4.2±1	1.1±0.6	36
Nohipalo-Valgejaerv	2.9±0.5	RCP 2.6	3.5±0.6	0.5±0.5	18
		RCP 6.0	3.8±0.6	0.9±0.5	29
		RCP 8.5	4±0.7	1.1±0.6	37
Paaijarvi	2.1±0.3	RCP 2.6	2.6±0.4	0.4±0.4	21
		RCP 6.0	2.7±0.4	0.6±0.4	28
		RCP 8.5	2.9±0.5	0.8±0.4	40
Rappbode	2±0.5	RCP 2.6	2.7±0.6	0.7±0.5	34
		RCP 6.0	2.9±0.6	0.9±0.5	45
		RCP 8.5	3.2±0.8	1.2±0.7	60
Rimov	2.1±0.5	RCP 2.6	2.7±0.6	0.7±0.5	32
		RCP 6.0	3±0.7	0.9±0.5	44
		RCP 8.5	3.4±1	1.3±0.8	62
Sau	3.2±0.7	RCP 2.6	3.7±0.8	0.5±0.3	16

		RCP 6.0	3.9±0.8	0.7±0.3	23
		RCP 8.5	4.2±0.9	1±0.4	32
Stechlin	2.1±0.5	RCP 2.6	2.7±0.6	0.6±0.4	28
		RCP 6.0	2.9±0.6	0.7±0.5	35
		RCP 8.5	3.1±0.8	1±0.7	45
Vendyurskoe	2±0.4	RCP 2.6	2.3±0.3	0.4±0.4	15
		RCP 6.0	2.6±0.4	0.6±0.4	27
		RCP 8.5	2.8±0.4	0.8±0.5	36
Vortsjaerv	2.6±0.4	RCP 2.6	3.1±0.4	0.5±0.4	20
		RCP 6.0	3.4±0.4	0.8±0.4	30
		RCP 8.5	3.5±0.5	0.9±0.5	36
Windermere	2±0.4	RCP 2.6	2.4±0.5	0.4±0.3	22
		RCP 6.0	2.5±0.5	0.5±0.4	28
		RCP 8.5	2.7±0.6	0.7±0.6	37

Table B.5. Annual precipitation minus evaporation (P-E) projections by the end of the 21st century under future scenarios of climate change: RCP 2.6, 6.0 and 8.5 for each lake. The P-E estimates for the historic period correspond to the average over 1971-2000 and the future period corresponds to 2070-2099. Anomalies (Δ) are calculated as future minus historic.

Lake	Historic P-E [mm day^{-1}]	Scenario	Future P-E [mm day^{-1}]	Δ(P-E) [mm day^{-1}]
Biel	1.4±1.1	RCP 2.6	0.9±1.2	-0.5±1.3
		RCP 6.0	0.1±1.3	-1.2±1.4
		RCP 8.5	-0.7±1.7	-2.1±1.8
Bourget	0.9±1	RCP 2.6	0.3±1.1	-0.6±1.1
		RCP 6.0	-0.2±1.1	-1.2±1.2
		RCP 8.5	-1±1.5	-1.9±1.6
Ekoln	-0.3±0.9	RCP 2.6	-0.7±1.1	-0.4±1.1
		RCP 6.0	-0.9±1.1	-0.6±1.1
		RCP 8.5	-1.1±1.3	-0.9±1.3
Erken	-0.3±0.9	RCP 2.6	-0.7±1.1	-0.4±1.1
		RCP 6.0	-0.9±1.1	-0.6±1.1
		RCP 8.5	-1.1±1.2	-0.8±1.2
Esthwaite-Water	1.4±1	RCP 2.6	1.4±1.3	-0.1±1.3
		RCP 6.0	1±1.3	-0.5±1.3
		RCP 8.5	0.7±1.5	-0.7±1.5
Feeagh	2.3±1.1	RCP 2.6	1.9±1.2	-0.4±1.2
		RCP 6.0	1.8±1.3	-0.5±1.3
		RCP 8.5	1.5±1.3	-0.8±1.4
Geneva	1.8±1.5	RCP 2.6	1.3±1.7	-0.5±1.7
		RCP 6.0	0.8±1.8	-1±1.8
		RCP 8.5	0±2	-1.8±2.1
Kilpisjarvi	1±0.5	RCP 2.6	1±0.5	0±0.5
		RCP 6.0	1±0.7	0±0.7
		RCP 8.5	1±0.7	0±0.7
Kuivajarvi	0.1±0.9	RCP 2.6	-0.1±1.1	-0.2±1.2
		RCP 6.0	-0.3±1.1	-0.4±1.1
		RCP 8.5	-0.5±1.3	-0.6±1.3
Langtjern	1.4±1	RCP 2.6	1.3±1	-0.1±1.1
		RCP 6.0	1.4±1.4	0±1.4
		RCP 8.5	0.9±1.4	-0.5±1.4
Lower-Zurich	3.2±1.3	RCP 2.6	2.9±1.4	-0.3±1.5

		RCP 6.0	2.1±1.4	-1.1±1.5
		RCP 8.5	1.1±2	-2.1±2.1
Mueggelsee	-0.8±0.8	RCP 2.6	-1.5±1	-0.7±1
		RCP 6.0	-1.7±1.1	-0.9±1.2
		RCP 8.5	-2.2±1.4	-1.4±1.5
Neuchatel	1.2±1.2	RCP 2.6	0.7±1.3	-0.6±1.3
		RCP 6.0	0.1±1.3	-1.2±1.4
		RCP 8.5	-0.7±1.6	-1.9±1.7
Nohipalo-Mustjaerv	-0.5±1.3	RCP 2.6	-1.1±1.4	-0.6±1.5
		RCP 6.0	-1.4±1.5	-0.9±1.5
		RCP 8.5	-1.6±1.7	-1.2±1.7
Nohipalo-Valgejaerv	-0.3±1.1	RCP 2.6	-0.9±1.2	-0.5±1.3
		RCP 6.0	-1.2±1.4	-0.9±1.4
		RCP 8.5	-1.5±1.4	-1.2±1.5
Paaijarvi	0.3±0.7	RCP 2.6	0±1	-0.3±1.1
		RCP 6.0	-0.2±1	-0.4±1
		RCP 8.5	-0.4±1.2	-0.6±1.2
Rappbode	0.9±1.1	RCP 2.6	0.4±1.2	-0.5±1.3
		RCP 6.0	0.1±1.4	-0.9±1.5
		RCP 8.5	-0.5±1.6	-1.4±1.7
Rimov	0.8±0.9	RCP 2.6	0.1±1.1	-0.7±1.2
		RCP 6.0	-0.3±1.1	-1.1±1.3
		RCP 8.5	-1±1.6	-1.8±1.7
Sau	-1.1±1.2	RCP 2.6	-1.8±1.3	-0.7±1.3
		RCP 6.0	-2.3±1.3	-1.1±1.3
		RCP 8.5	-2.9±1.4	-1.8±1.3
Stechlin	-0.2±0.8	RCP 2.6	-0.7±0.9	-0.5±1
		RCP 6.0	-0.9±1.2	-0.6±1.2
		RCP 8.5	-1.3±1.3	-1±1.4
Vendyurskoe	0.4±0.8	RCP 2.6	0.2±0.9	-0.1±0.9
		RCP 6.0	0±1	-0.4±1
		RCP 8.5	-0.3±1.2	-0.6±1.2
Vortsjaerv	-0.1±1	RCP 2.6	-0.6±1.1	-0.5±1.2
		RCP 6.0	-0.9±1.2	-0.8±1.2
		RCP 8.5	-1.1±1.3	-1±1.3
Windermere	1.5±1	RCP 2.6	1.4±1.3	-0.1±1.3
		RCP 6.0	1.1±1.2	-0.5±1.2
		RCP 8.5	0.8±1.5	-0.7±1.5

Appendix C

Authors: Sofia La Fuente[1*], Eleanor Jennings[1], John D. Lenters[2], Piet Verburg[3], Zeli Tan[4], Marjorie Perroud[5], Annette B.G. Janssen[6], R. Iestyn Woolway[7]

Affiliations:

1. Centre for Freshwater and Environmental Studies, Dundalk Institute of Technology, Dundalk, Ireland
2. University of Michigan, UM Biological Station, Pellston, Michigan, USA
3. National Institute of Water and Atmospheric Research, Wellington, New Zealand
4. Pacific Northwest National Laboratory, Richland, Washington, USA
5. Institute for Environmental Sciences, University of Geneva, Geneva, Switzerland
6. Wageningen University & Research, Water Systems and Global Change Group, Wageningen, the Netherlands
7. School of Ocean Sciences, Bangor University, Menai Bridge, Anglesey, Wales

Text C1. Description of lake models

ALBM (Arctic Lake Biogeochemistry Model) is a one-dimensional (1-D) process-based coupled lake hydrodynamic and biogeochemistry model (Tan et al. 2015). The thermal regimes of lakes are simulated in ALBM using 1-D thermal diffusion equations in both water and sediment columns with atmospheric boundary conditions driven by sensible and latent heat fluxes, incoming longwave radiation, and solar radiation. The surface fluxes in ALBM are estimated using Hostetler and Bartlein, (1990). ALBM was originally developed for Arctic lakes (Tan et al. 2017; Tan et al. 2015) but has been validated and used for other lakes across the globe (Grant et al. 2021; Guo, Zhuang, Yao, Golub, Leung, Pierson, et al. 2021; Woolway et al. 2021; Guo et al. 2020; Tan et al. 2018).

SIMSTRAT-UoG is a physical deterministic 1-D hydrodynamic model (Gaudard et al. 2019; Goudsmit et al. 2002). The model supports multiple options for external forcing, comprising several meteorological variables or surface energy fluxes. SIMSTRAT-UoG simulates thermal stratification and ice and snow formation (Gaudard et al. 2019). Surface energy fluxes in SIMSTRAT-UoG are estimated following Livingstone and Imboden, (1989). SIMSTRAT-UoG has been applied in lakes of varying

climatic and morphometric conditions (Bärenbold et al. 2022; Råman Vinnå et al. 2021; Mesman et al. 2020; Kobler and Schmid 2019; Thiery et al. 2014). Simstrat v.1.0.0 is the version used in this study.

VIC-LAKE is a 1-D lake model derived from the Variable Infiltration Capacity (VIC) Macroscale Hydrologic Model (Bowling and Lettenmaier 2010) and optimized for simulations at a sub-daily timescale. The model is based on a lake energy balance by Hostetler (1991), Hostetler and Bartlein (1990), Patterson and Hamblin (1988). The surface fluxes in VIC-LAKE are estimated using Hostetler and Bartlein, (1990). The VIC-LAKE model also contains an ice module, which dynamically simulates lake ice and snow cover.

Text C2. Input data to lake models

The data used to drive each lake model included projections of air temperature at 2 m, wind speed at 10 m, surface solar and longwave radiation, surface air pressure, and specific humidity, which were available at a daily resolution (Table C.2). Each of the lake models simulated, among other things, the air-water surface energy fluxes at a 0.5° by 0.5° grid resolution globally, based on the mean depth and surface area of all lakes within a given 0.5° grid (i.e., the average depth of all known lakes and the surface area covered). These simulations, therefore, represent an aggregated 'typical lake' for each 0.5° grid, simulating the average lake thermal environment in that location using that grid cell's climate forcing. The locations and grid-scale fractions of lakes within each 0.5° grid were determined by the Global Lakes and Wetlands Database (Lehner and Doll 2004). Lake depth information was aggregated from the original 30 arcsec Global Lake Data Base v2 (GLDBv2) (Choulga et al. 2014; Subin et al. 2012; Kourzeneva 2010) to a 0.5° by 0.5° grid lake depth field. More details can be found in Golub et al. (2022).
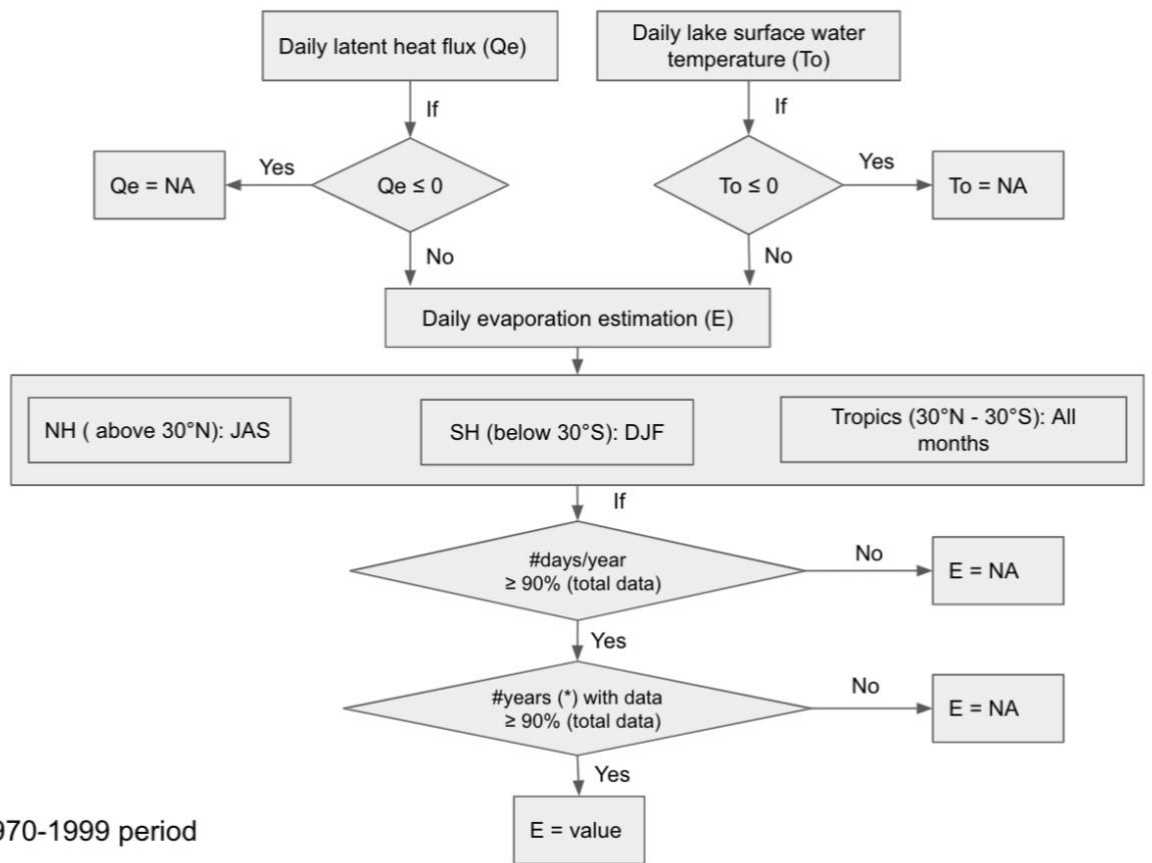
Figure C.1. Workflow for warm-season lake evaporation estimation. JAS: July, August, September. DJF: December, January, February.
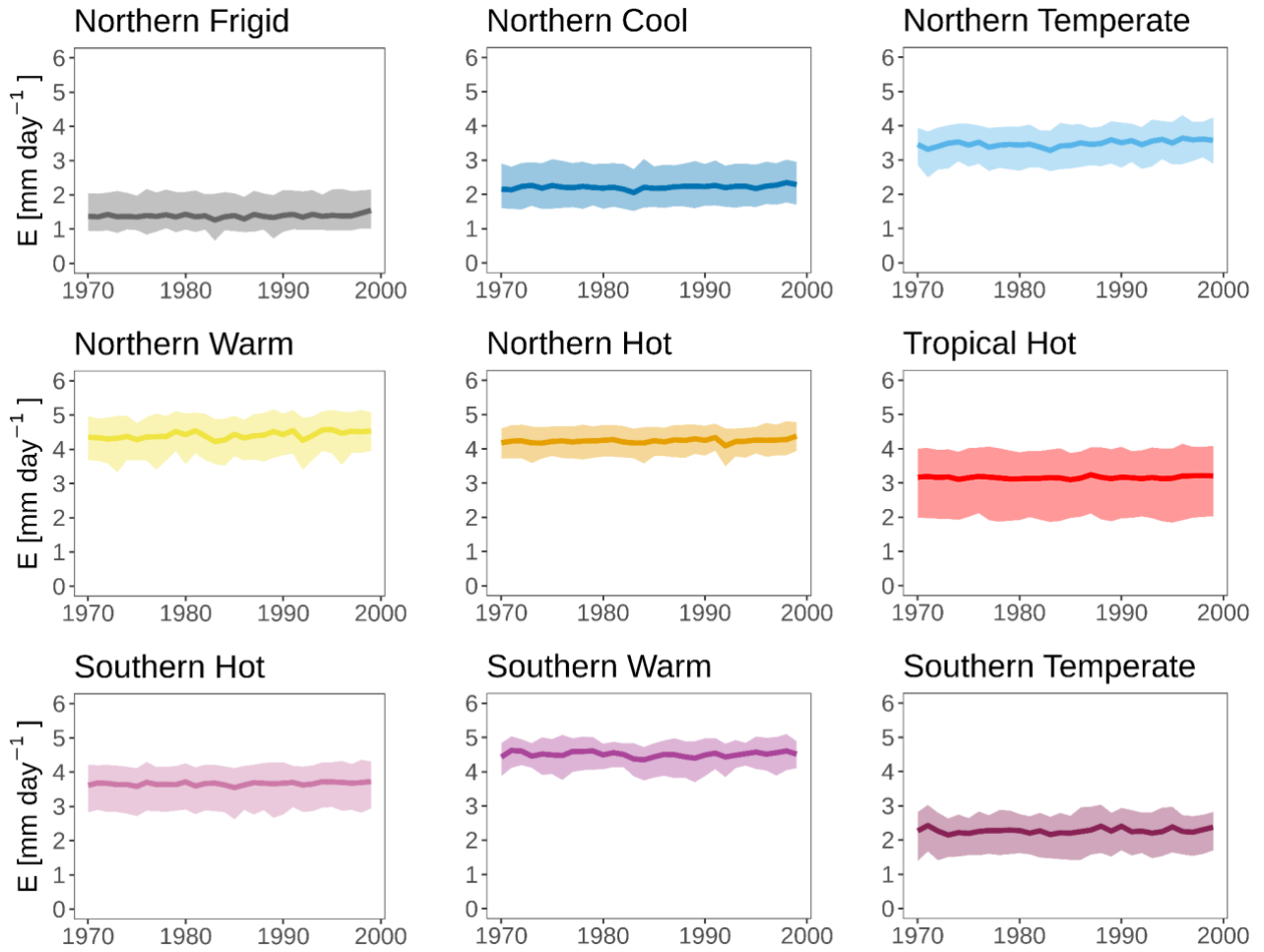
Figure C.2. Annual average warm-season lake evaporation over the 1970-1999 period for different locations representative of each thermal region as defined by Maberly et al. (2020). The thick lines and the shaded region in each panel represent the mean and the spread (min and max) across the model ensemble respectively.
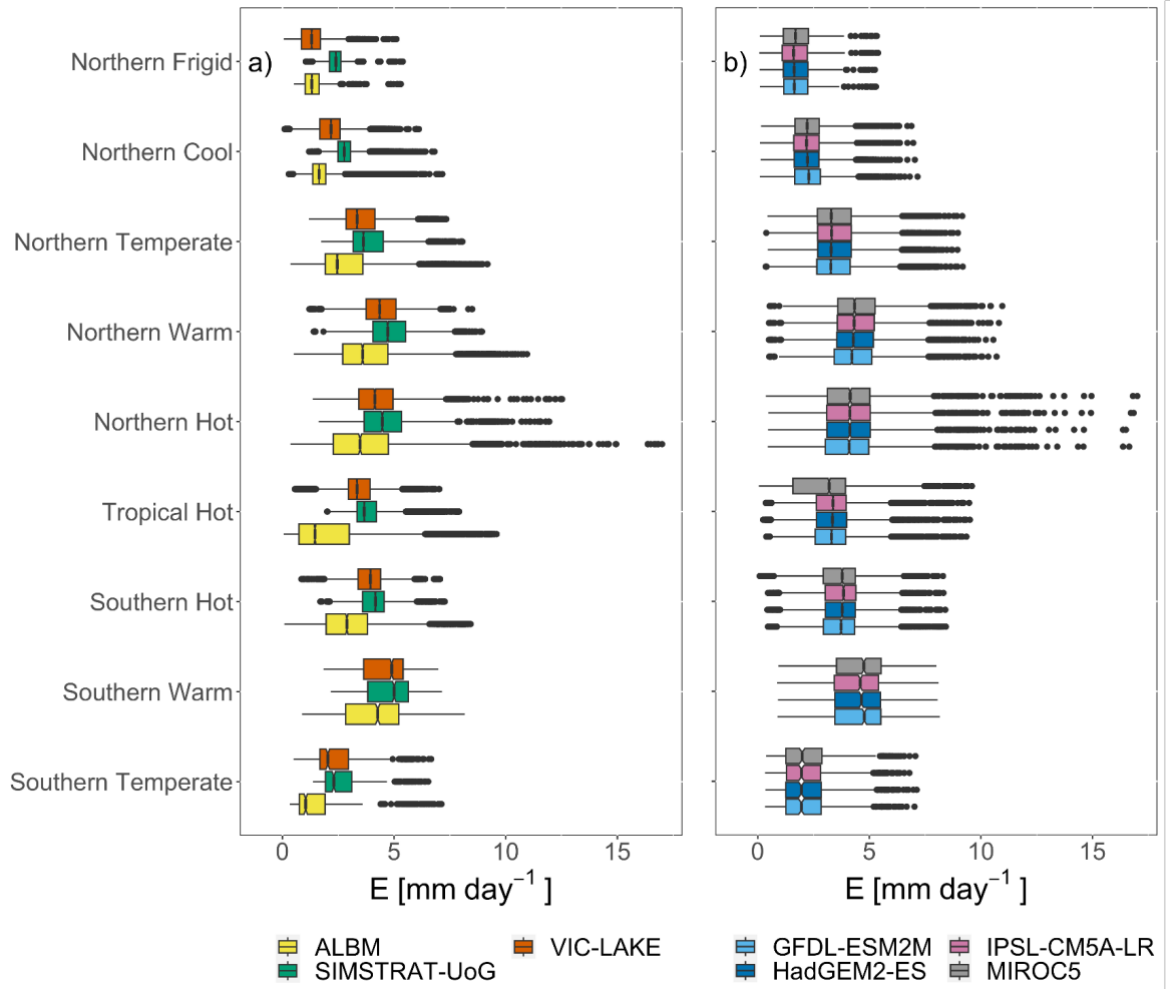
Figure C.3. Boxplots of warm-season lake evaporation rates in mm day⁻¹ averaged over the 1970-1999 period across thermal regions for: a) lake models: ALBM, SIMSTRAT-UoG, and VIC-LAKE, and b) General Circulation Models (GCM): GFDL-ESM2M, HadGEM2-ES, IPSL-CM5A-LR, and MIROC5. Dots represent outliers.
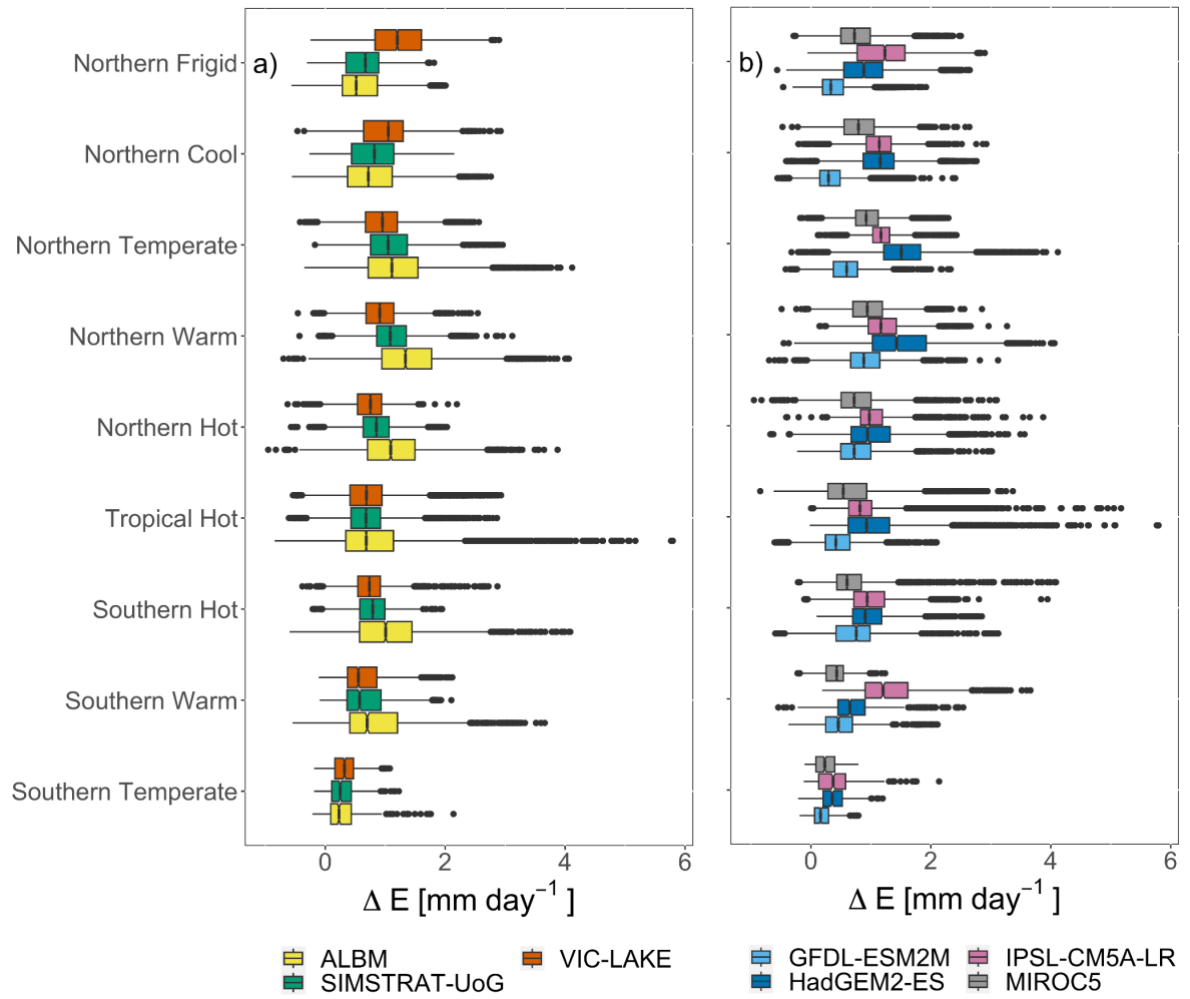
Figure C.4. Boxplots of warm-season lake evaporation anomalies in mm day^{-1} by the end of the 21st century (2070-2099) under Representative Concentration Pathway (RCP) 8.5 across thermal regions for: a) lake models: ALBM, SIMSTRAT-UoG and VIC-LAKE, and b) General Circulation Model (GCM): GFDL-ESM2M, HadGEM2-ES, IPSL-CM5A-LR, and MIROC5. Dots represent outliers. Anomalies (ΔE) are quoted relative to the 1970-1999 base-period average
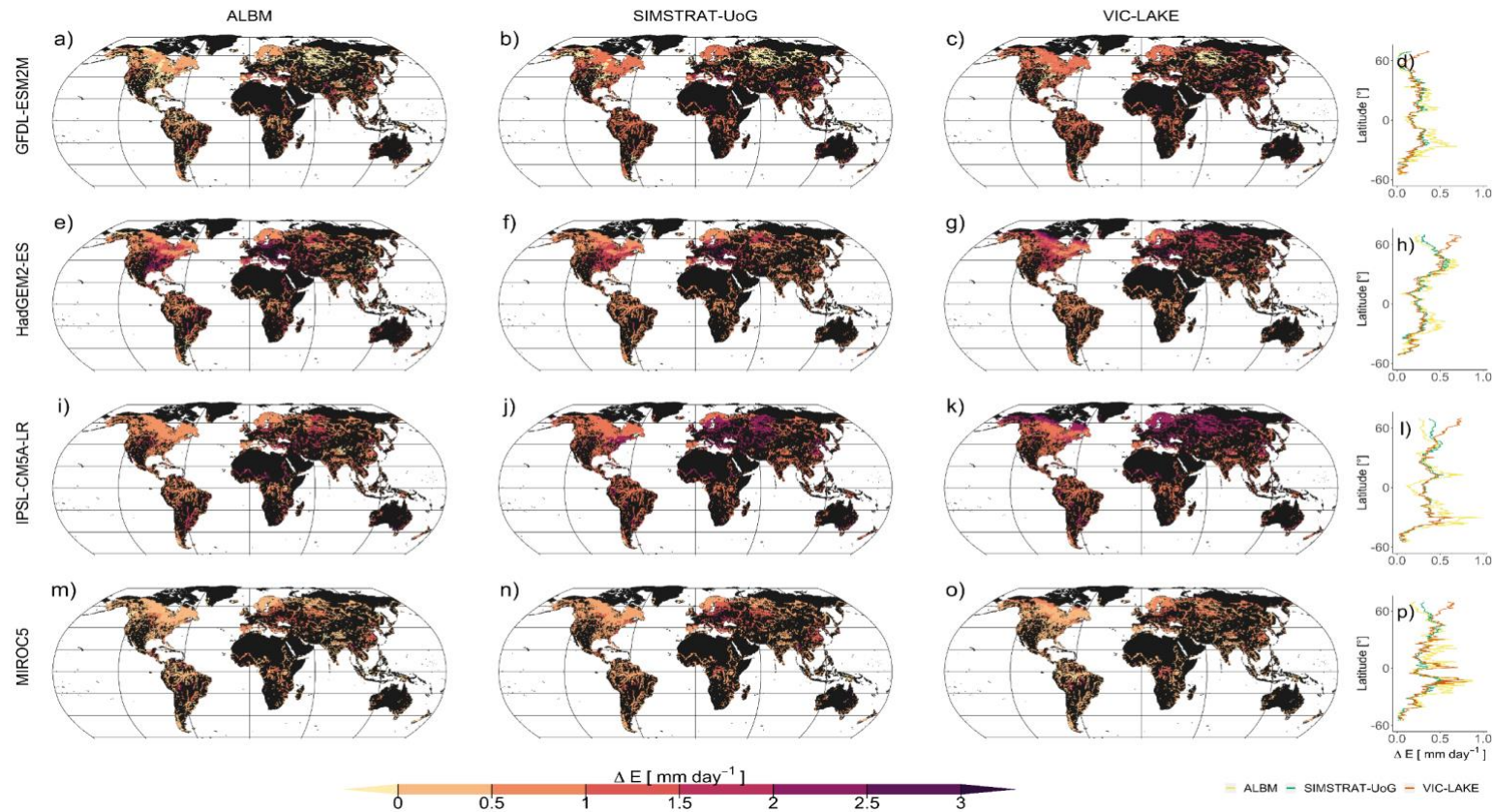
Figure C.5. Projected changes in warm-season lake evaporation rates in mm day^{-1} by the end of the 21st century (2070-2099) under Representative Concentration Pathway (RCP) 2.6. Projections are shown for each lake-model combination namely (a, e, i, m) ALBM, (b, f, j, n) SIMSTRAT-UoG and (c, g, k, o) VIC-LAKE. Each lake model was driven by GFDL-ESM2M, HadGEM2-ES, IPSL-CM5A-LR and MIROC5. Latitudinal plots show warm-season evaporation simulations across lake models (d, h, l, p). Anomalies (ΔE) are quoted relative to the 1970-1999 base-period average.
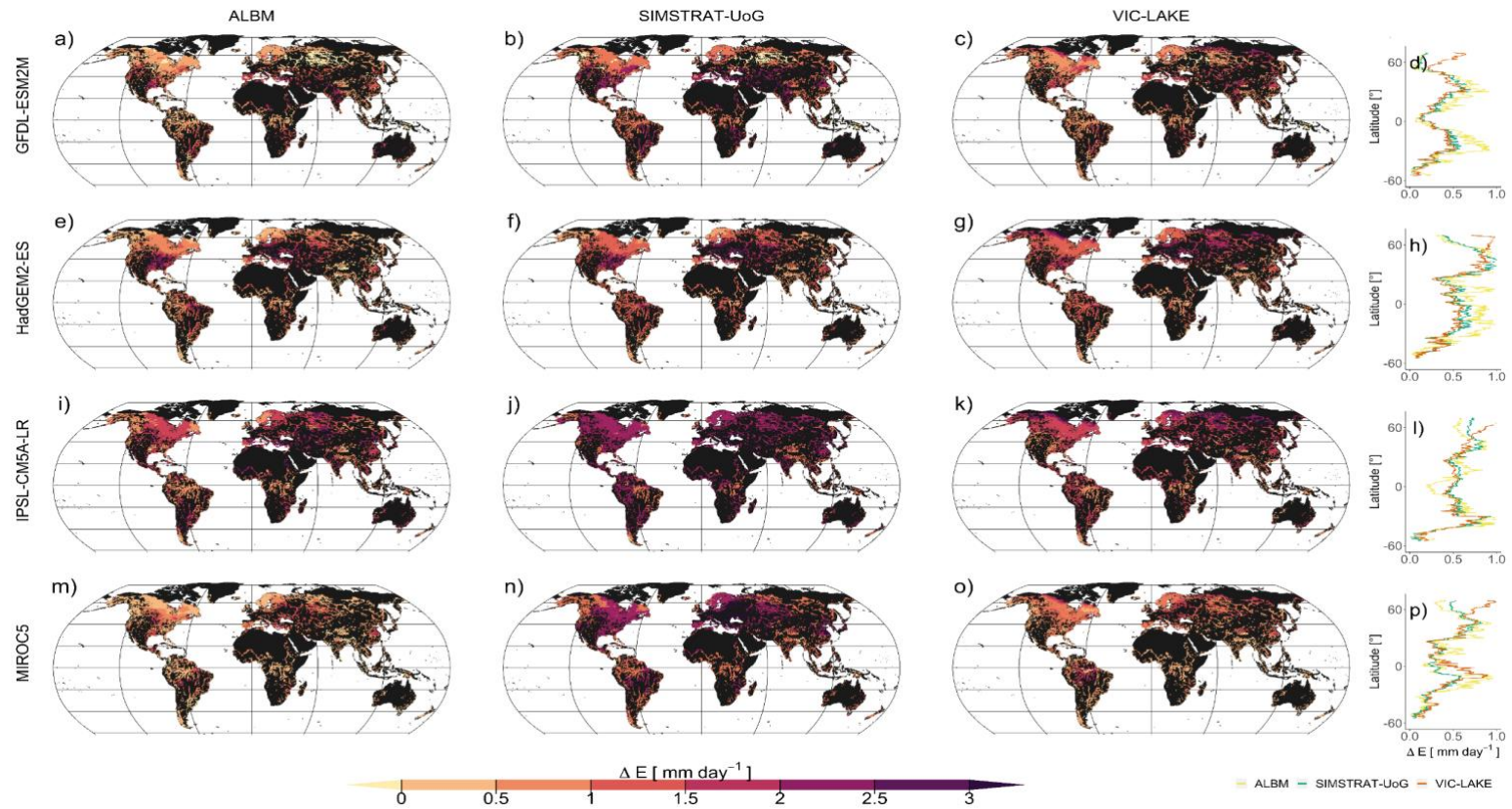
Figure C.6. Projected changes in warm-season lake evaporation rates in mm day^{-1} by the end of the 21st century (2070-2099) under Representative Concentration Pathway (RCP) 6.0. Projections are shown for each lake-model combination namely (a, e, i, m) ALBM, (b, f, j, n) SIMSTRAT-UoG and (c, g, k, o) VIC-LAKE. Each lake model was driven by GFDL-ESM2M, HadGEM2-ES, IPSL-CM5A-LR and MIROC5. Latitudinal plots show warm-season evaporation simulations across lake models (d, h, l, p). Anomalies (ΔE) are quoted relative to the 1970-1999 base-period average.
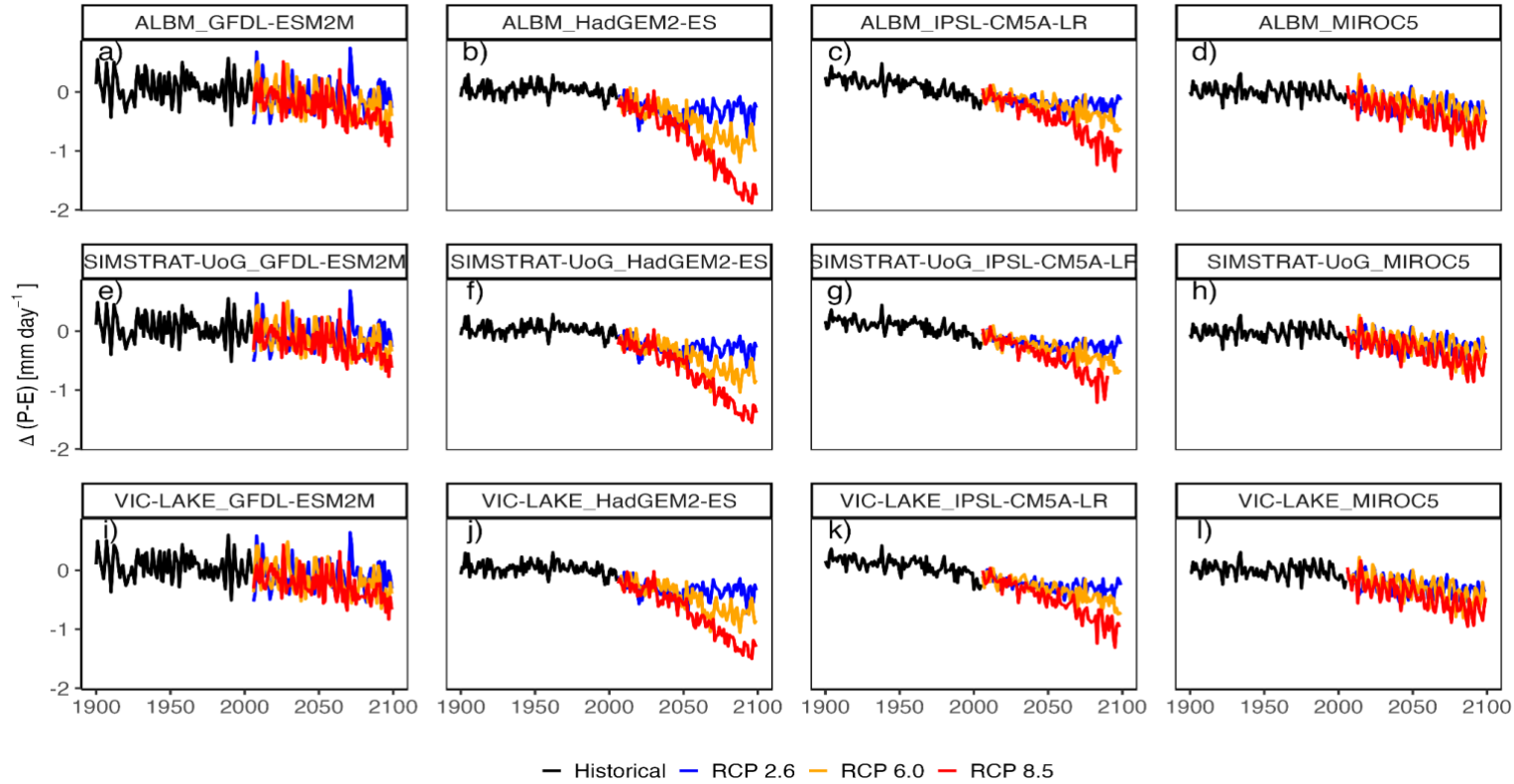
Figure C.7. Projected changes in global warm-season precipitation minus evaporation in mm day^{-1} during the historic (1901-2005) and future (2006-2099) periods. Projections are shown for each of the individual lake-climate models, namely for (a-d) ALBM, (e-h) SIMSTRAT-UoG and (i-l) VIC-LAKE, driven by the four General Circulation Models included in this study. Black lines represent the historical period, and the coloured lines represent the future period, with the blue, orange and red representing the projected change under RCP (Representative Concentration Pathway) 2.6, 6.0, and 8.5, respectively. Anomalies Δ(P-E) are quoted relative to the 1970-1999 base-period average.

Figure C.8. Percentage of total uncertainty explained by (a) GCM and (b) lake model in future projections of warm-season lake evaporation over the period 2070-2099 for the Representative Concentration Pathway (RCP) 2.6.
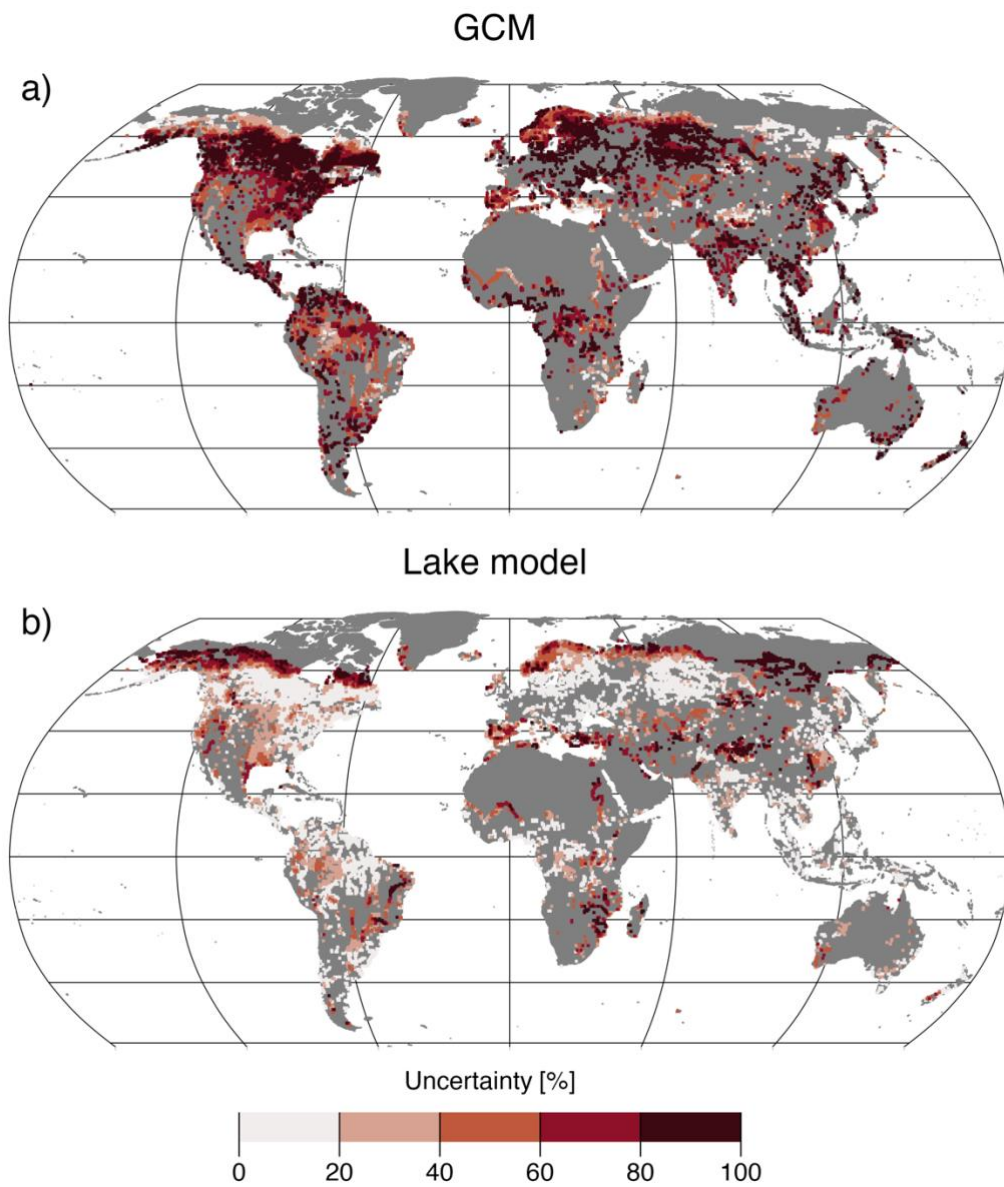
Figure C.9. Percentage of total uncertainty explained by (a) GCM and (b) lake model in future projections of warm-season lake evaporation over the period 2070-2099 for the Representative Concentration Pathway (RCP) 6.0.
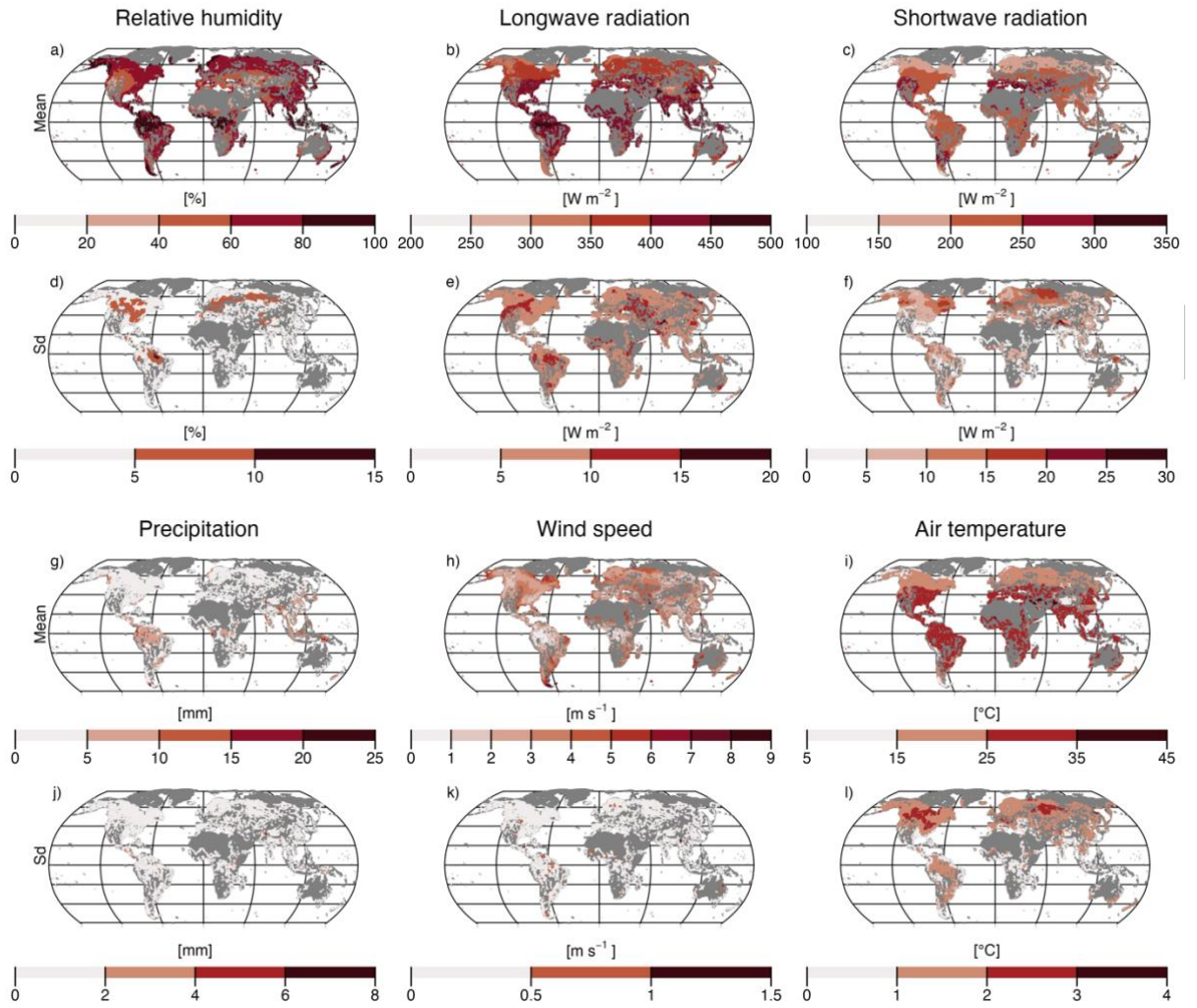
Figure C.10. Mean and standard deviation (Sd) of evaporation drivers: (a, d) relative humidity, (b, e) longwave radiation, (c, f) shortwave radiation, (g, j) precipitation, (h, k) wind speed and (i, l) air temperature over the 2070-2099 under Representative Concentration Pathway (RCP) 8.5.

Table C.1. Summary of the lake models used in this study, including a description of their structure, parameterization and key references

Lake model (version)	Timestep Simulated/ Reported	Vertical structure / layers reported	Parameterization of turbulent fluxes at air-water interface	Turbulent mixing parameterization	Key references
ALBM (ver. 2.0)	Jan-24	Multilayer/51	Based on the method of Hostetler and Bartlein (1990)	Henderson-Sellers thermal diffusion model with wind-driven eddy diffusivity	Tan et al. (2015)
SIMSTRAT-UoG (ver. 1.0.0)	Mar-24	Multilayer / 1-13	Dirichlet condition	k-ε turbulence model with buoyancy and internal seiche parameterization	Goudsmit et al. (2002)
VIC-LAKE (ver. 1.0)	Jun-24	Multilayer /1000	Based on the method of Hostetler and Bartlein (1990)	Henderson-Sellers thermal diffusion model with wind-driven eddy diffusivity	Bowling and Lettenmaier (2010)

Table C.2. Climate forcing variables used as input to drive the lake models used in this study to simulate historical and future warm-season evaporation rates.

Variable	Abbreviation	ALBM	SIMSTRAT-UoG	VIC-LAKE
Near-surface relative humidity [%]	hurs	x		x
Near-surface specific humidity [kg kg^{-1}]	huss		x	
Precipitation [kg m^{-2} s^{-1}]	pr	x	x	x
Snowfall flux [kg m^{-2} s^{-1}]	prsn	x		
Surface pressure [Pa]	ps	x	x	x
Surface downwelling longwave radiation [W m^{-2}]	rlds	x	x	x
Surface downwelling shortwave radiation [W m^{-2}]	rsds	x	x	x
Near-surface wind speed at 10m [m s^{-1}]	sfcWind	x	x	x
Near-surface air temperature [K]	tas	x	x	x
Daily maximum near-surface air temperature [K]	tasmax	x		
Daily minimum near-surface air temperature [K]	tasmin	x		
Eastward near-surface wind [m s^{-1}] (*)	uas		x	
Northward near-surface wind [m s^{-1}] (*)	vas		x	

Table C.3. Summary of average warm-season lake evaporation rates across the model ensemble and lake thermal regions over the 1970-1999 historic period. Standard deviation (Sd), Minimum (Min), Maximum (Max), 25th Percentile (Q25) and 75th percentile(Q75).

Thermal region	Warm-season evaporation rates [mm day^{-1}]						
	Abb	Mean	Sd	Min	Max	Q25	Q75
Northern Frigid	NF	1.7	0.7	0.1	5.4	1.1	2.2
Northern Cool	NC	2.2	0.8	0.1	7.2	1.6	2.8
Northern Temperate	NT	3.5	1.2	0.4	9.2	2.7	4.2
Northern Warm	NW	4.4	1.5	0.5	11.0	3.5	5.2
Northern Hot	NH	4.2	1.8	0.4	17.0	3.1	5.0
Tropical Hot	TH	3.2	1.5	0.1	9.6	2.3	4.0
Southern Hot	SH	3.7	1.2	0.1	8.4	3.0	4.4
Southern Warm	SW	4.5	1.4	0.9	8.2	3.5	5.5
Southern Temperate	ST	2.3	1.4	0.3	7.1	1.3	2.8

Table C.4. Summary of average warm-season lake evaporation rates in mm day^{-1} for climate models and thermal regions over the 1970-1999 historic period.

Climate model	Cluster name	Mean	Sd	Min	Max	Q25	Q75
	Northern Frigid	2	1	0	5	1	2
	Northern Cool	2	1	0	7	2	3
	Northern Temperate	3	1	0	9	3	4
	Northern Warm	4	1	1	11	3	5
GFDL-ESM2M	Northern Hot	4	2	0	17	3	5
	Tropical Hot	3	1	0	9	3	4
	Southern Hot	4	1	0	8	3	4
	Southern Warm	5	1	1	8	3	6
	Southern Temperate	2	1	0	7	1	3
	Northern Frigid	2	1	0	5	1	2
	Northern Cool	2	1	0	7	2	3
	Northern Temperate	3	1	0	9	3	4
	Northern Warm	4	1	1	11	4	5
HadGEM2-ES	Northern Hot	4	2	0	16	3	5
	Tropical Hot	3	1	0	10	3	4
	Southern Hot	4	1	0	8	3	4
	Southern Warm	5	1	1	8	3	5
	Southern Temperate	2	1	0	7	1	3
	Northern Frigid	2	1	0	5	1	2
	Northern Cool	2	1	0	7	2	3
	Northern Temperate	3	1	0	9	3	4
	Northern Warm	4	1	1	11	4	5
IPSL-CM5A-LR	Northern Hot	4	2	0	17	3	5
	Tropical Hot	3	1	0	9	3	4
	Southern Hot	4	1	0	8	3	4
	Southern Warm	4	1	1	8	3	5
	Southern Temperate	2	1	0	7	1	3
	Northern Frigid	2	1	0	5	1	2
	Northern Cool	2	1	0	7	2	3
	Northern Temperate	3	1	0	9	3	4
	Northern Warm	4	1	1	11	4	5
MIROC5	Northern Hot	4	2	0	17	3	5
	Tropical Hot	3	2	0	10	2	4
	Southern Hot	4	1	0	8	3	4
	Southern Warm	5	1	1	8	4	6
	Southern Temperate	2	1	0	7	1	3

Table C.5. Summary of average warm-season lake evaporation rates in mm day^{-1} for lake models and thermal regions over the 1970-1999 historic period.

Lake model	Lake thermal region	Abb.	Warm-season evaporation rates [mm day^{-1}]					
			Mean	Sd	Min	Max	Q25	Q75
ALBM	Northern Frigid	NF	1	0	1	5	1	2
	Northern Cool	NC	2	1	0	7	1	2
	Northern Temperate	NT	3	1	0	9	2	4
	Northern Warm	NW	4	2	1	11	3	5
	Northern Hot	NH	4	2	0	17	2	5
	Tropical Hot	TH	2	2	0	10	1	3
	Southern Hot	SH	3	1	0	8	2	4
	Southern Warm	SW	4	2	1	8	3	5
	Southern Temperate	ST	2	2	0	7	1	2
SIMSTRAT-UoG	Northern Frigid	NF	2	0	1	5	2	3
	Northern Cool	NC	3	1	1	7	2	3
	Northern Temperate	NT	4	1	2	8	3	5
	Northern Warm	NW	5	1	1	9	4	6
	Northern Hot	NH	5	1	2	12	4	5
	Tropical Hot	TH	4	1	2	8	3	4
	Southern Hot	SH	4	1	2	7	4	5
	Southern Warm	SW	5	1	2	7	4	6
	Southern Temperate	ST	3	1	1	7	2	3
VIC-LAKE	Northern Frigid	NF	1	1	0	5	1	2
	Northern Cool	NC	2	1	0	6	2	3
	Northern Temperate	NT	4	1	1	7	3	4
	Northern Warm	NW	4	1	1	9	4	5
	Northern Hot	NH	4	1	1	13	3	5
	Tropical Hot	TH	3	1	1	7	3	4
	Southern Hot	SH	4	1	1	7	3	4
	Southern Warm	SW	5	1	2	7	4	5
	Southern Temperate	ST	2	1	0	7	2	3

Table C.6. Summary of average warm-season lake evaporation (ΔE) for climate models and thermal regions under the Representative Concentration Pathway (RCP) 8.5 over the 2070-2099 period. Anomalies (ΔE) are quoted relative to the 1970-1999 base-period average.

Climate model	Cluster name	Mean	Sd	Min	Max	Q25	Q75
GFDL-ESM2M	Northern Frigid	0.4	0.4	-0.5	1.9	0.2	0.5
	Northern Cool	0.3	0.3	-0.6	2.4	0.1	0.5
	Northern Temperate	0.6	0.3	-0.4	2.3	0.4	0.8
	Northern Warm	0.9	0.4	-0.7	3.1	0.7	1.1
	Northern Hot	0.8	0.4	-0.2	3.0	0.5	1.0
	Tropical Hot	0.4	0.3	-0.6	2.1	0.2	0.6
	Southern Hot	0.8	0.5	-0.6	3.1	0.4	1.0
	Southern Warm	0.5	0.4	-0.4	2.1	0.2	0.7
	Southern Temperate	0.2	0.2	-0.2	0.8	0.1	0.3
HadGEM2-ES	Northern Frigid	0.9	0.5	-0.6	2.6	0.5	1.2
	Northern Cool	1.1	0.4	-0.4	2.8	0.9	1.4
	Northern Temperate	1.5	0.6	-0.3	4.1	1.2	1.8
	Northern Warm	1.5	0.7	-0.5	4.1	1.0	1.9
	Northern Hot	1.0	0.6	-0.7	3.6	0.7	1.3
	Tropical Hot	1.1	0.6	0.0	5.8	0.6	1.3
	Southern Hot	1.0	0.4	0.1	2.8	0.7	1.2
	Southern Warm	0.7	0.4	-0.5	2.5	0.4	0.9
	Southern Temperate	0.4	0.2	-0.2	1.2	0.2	0.5
IPSL-CM5A-LR	Northern Frigid	1.2	0.5	-0.1	2.9	0.8	1.6
	Northern Cool	1.1	0.3	-0.2	2.9	0.9	1.3
	Northern Temperate	1.2	0.3	0.1	2.4	1.0	1.3
	Northern Warm	1.2	0.4	0.1	3.3	1.0	1.4
	Northern Hot	1.0	0.4	-0.4	3.9	0.8	1.2
	Tropical Hot	0.9	0.5	0.0	5.2	0.6	1.0
	Southern Hot	1.0	0.4	-0.1	3.9	0.7	1.2
	Southern Warm	1.3	0.6	0.2	3.7	0.9	1.6
	Southern Temperate	0.4	0.4	-0.1	2.1	0.1	0.6
MIROC5	Northern Frigid	0.8	0.4	-0.3	2.5	0.5	1.0
	Northern Cool	0.8	0.3	-0.5	2.6	0.6	1.1
	Northern Temperate	0.9	0.3	-0.2	2.3	0.7	1.1
	Northern Warm	1.0	0.4	-0.5	2.9	0.7	1.2
	Northern Hot	0.8	0.5	-1.0	3.1	0.5	1.0
	Tropical Hot	0.7	0.6	-0.8	3.4	0.3	0.9
	Southern Hot	0.7	0.5	-0.2	4.1	0.4	0.8
	Southern Warm	0.4	0.2	-0.2	1.2	0.3	0.5
	Southern Temperate	0.2	0.2	-0.1	0.8	0.1	0.4

Table C.7. Summary of average warm-season lake evaporation anomalies (ΔE) for lake models and thermal regions under the Representative Concentration Pathway (RCP) 8.5 over the 2070-2099 period. Anomalies (ΔE) are quoted relative to the 1970-1999 base-period average.

Lake model	Cluster name	Mean	Sd	Min	Max	Q25	Q75
	Northern Frigid	0.6	0.5	-0.6	2.0	0.3	0.9
	Northern Cool	0.8	0.5	-0.6	2.8	0.4	1.1
	Northern Temperate	1.2	0.7	-0.3	4.1	0.7	1.5
	Northern Warm	1.4	0.7	-0.7	4.1	0.9	1.8
ALBM	Northern Hot	1.1	0.6	-1.0	3.9	0.7	1.5
	Tropical Hot	0.9	0.8	-0.8	5.8	0.3	1.1
	Southern Hot	1.0	0.6	-0.6	4.1	0.6	1.4
	Southern Warm	0.9	0.7	-0.5	3.7	0.4	1.2
	Southern Temperate	0.3	0.3	-0.2	2.1	0.1	0.4
	Northern Frigid	0.7	0.4	-0.3	1.8	0.3	0.9
	Northern Cool	0.8	0.4	-0.3	2.2	0.4	1.1
	Northern Temperate	1.1	0.5	-0.2	3.0	0.8	1.4
	Northern Warm	1.1	0.4	-0.4	3.1	0.9	1.4
SIMSTRAT-UoG	Northern Hot	0.9	0.4	-0.6	2.0	0.6	1.1
	Tropical Hot	0.7	0.4	-0.6	2.9	0.4	0.9
	Southern Hot	0.8	0.3	-0.2	1.9	0.6	1.0
	Southern Warm	0.7	0.4	-0.1	2.1	0.4	0.9
	Southern Temperate	0.3	0.3	-0.2	1.2	0.1	0.4
	Northern Frigid	1.2	0.6	-0.2	2.9	0.8	1.6
	Northern Cool	1.0	0.5	-0.5	2.9	0.6	1.3
	Northern Temperate	0.9	0.4	-0.4	2.6	0.7	1.2
	Northern Warm	0.9	0.4	-0.5	2.5	0.7	1.1
VIC-LAKE	Northern Hot	0.7	0.3	-0.6	2.2	0.5	0.9
	Tropical Hot	0.7	0.5	-0.5	2.9	0.4	0.9
	Southern Hot	0.7	0.3	-0.4	2.9	0.5	0.9
	Southern Warm	0.7	0.4	-0.1	2.1	0.4	0.9
	Southern Temperate	0.3	0.2	-0.2	1.1	0.2	0.5

Table C.8. Global warm-season lake evaporation rates for historical (1970-1999) and future (2070-2099) periods across the lake models and General Circulation Models (GCMs) under the Representative Concentration Pathway (RCP) 2.6, 6.0 and 8.5. Presented are global average evaporation, and evaporation change for each lake-climate model combination. Anomalies (ΔE) are quoted relative to the 1970-1999 base-period average.

Lake model	GCM	Evaporation [mm day^{-1}]				Evaporation change (ΔE) [%]		
		Historical	RCP 2.6	RCP 6.0	RCP 8.5	RCP 2.6	RCP 6.0	RCP 8.5
ALBM	GFDL-ESM2M	2.6	2.7	2.9	3.2	6	14	23
	HadGEM2-ES	2.6	3.0	3.4	4.0	15	31	52
	IPSL-CM5A-LR	2.6	2.9	3.2	3.7	13	23	43
	MIROC5	2.6	2.9	3.1	3.4	15	21	31
SIMSTRAT	GFDL-ESM2M	3.7	3.9	4.1	4.2	4	9	13
	HadGEM2-ES	3.7	4.1	4.4	4.8	10	18	29
	IPSL-CM5A-LR	3.8	4.1	4.4	4.8	10	17	28
	MIROC5	3.7	4.1	4.2	4.5	9	13	20
VIC-LAKE	GFDL-ESM2M	3.3	3.4	3.6	3.8	6	11	16
	HadGEM2-ES	3.3	3.7	4.0	4.3	13	22	32
	IPSL-CM5A-LR	3.3	3.7	3.9	4.4	13	20	33
	MIROC5	3.2	3.6	3.8	4.0	13	19	26

Table C.9. Global warm-season lake evaporation rates in mm day-1 for historical (1970-1999) and future (2070-2099) periods across the lake models and General Circulation Models (GCMs) under the Representative Concentration Pathway (RCP) 2.6, 6.0 and 8.5. Anomalies (ΔE) are quoted relative to the 1970-1999 base-period average.

Lake thermal region	Scenario	Evaporation [mm day⁻¹]	Evaporation change (ΔE)	
			[mm day⁻¹]	[%]
Northern Cool	Historical	2.3±0.47	-	-
	RCP 2.6	2.6±0.51	0.3±0.2	13
	RCP 6.0	2.8±0.53	0.6±0.26	24
	RCP 8.5	3.1±0.58	0.8±0.36	35
Northern Frigid	Historical	1.8±0.5	-	-
	RCP 2.6	2.1±0.49	0.3±0.25	18
	RCP 6.0	2.4±0.5	0.6±0.31	32
	RCP 8.5	2.6±0.53	0.7±0.35	42
Northern Hot	Historical	4.2±0.31	-	-
	RCP 2.6	4.6±0.3	0.4±0.12	9
	RCP 6.0	4.8±0.29	0.6±0.16	14
	RCP 8.5	5.1±0.31	0.9±0.27	21
Northern Temperate	Historical	3.5±0.42	-	-
	RCP 2.6	3.9±0.45	0.4±0.19	12
	RCP 6.0	4.2±0.46	0.7±0.25	21
	RCP 8.5	4.6±0.55	1.1±0.42	30
Northern Warm	Historical	4.4±0.42	-	-
	RCP 2.6	4.8±0.44	0.4±0.21	10
	RCP 6.0	5.2±0.44	0.8±0.3	18
	RCP 8.5	5.6±0.47	1.2±0.41	26
Southern Hot	Historical	3.7±0.52	-	-
	RCP 2.6	4±0.47	0.4±0.11	10
	RCP 6.0	4.2±0.49	0.5±0.15	14
	RCP 8.5	4.5±0.45	0.9±0.25	22
Southern Temperate	Historical	2.3±0.46	-	-
	RCP 2.6	2.4±0.46	0.1±0.13	3
	RCP 6.0	2.4±0.47	0.1±0.15	7
	RCP 8.5	2.6±0.5	0.3±0.2	12
Southern Warm	Historical	4.5±0.28	-	-
	RCP 2.6	4.8±0.25	0.3±0.18	6
	RCP 6.0	5±0.27	0.4±0.22	10
	RCP 8.5	5.2±0.37	0.7±0.41	15

	Historical	3.1±0.78	-	-
Tropical Hot	RCP 2.6	3.4±0.77	0.3±0.1	9
	RCP 6.0	3.6±0.79	0.4±0.18	14
	RCP 8.5	3.9±0.78	0.8±0.32	23

Table C.10. Global lake warm-season evaporation projections under historical and future scenarios of climate change. The values for the historical period correspond to the average over the period 1970-1999. The values for Representative Concentration Pathways (RCP) 8.5, 6.0 and 2.6 correspond to the average over the period 2070-2099. Anomalies (ΔE) are quoted relative to the 1970-1999 base-period average.

Lake model	Scenario	Evaporation [mm day⁻¹]	Evaporation change (ΔE) [mm day⁻¹]	[%]
Mean ensemble	Historical	3.2±0.5	-	-
	RCP 2.6	3.5±0.5	0.3±0.1	10
	RCP 6.0	3.8±0.5	0.6±0.2	18
	RCP 8.5	4.1±0.5	0.9±0.3	27

Table C.11. Global lake warm-season precipitation minus evaporation projections under historical and future scenarios of climate change. The values for the historical period correspond to the average over the period 1970-1999. The values for Representative Concentration Pathways (RCP) 8.5, 6.0 and 2.6 correspond to the average over the period 2070-2099. Anomalies Δ(P-E) are quoted relative to the 1970-1999 base-period average.

Lake model	Scenario	P-E [mm day⁻¹]	Δ(P-E) [mm day⁻¹]
Mean ensemble	Historical	0±0.5	-
	RCP 2.6	-0.3±0.52	-0.2±0.19
	RCP 6.0	-0.5±0.53	-0.5±0.24
	RCP 8.5	-0.8±0.58	-0.8±0.4